RISK STRATIFICATION IN ATHEROSCLEROTIC CAROTID STENOSIS

Thesis submitted to Imperial College London
for the degree of Doctor of Philosophy

Joseph Shalhoub

SUPERVISORS

Professor Alun H Davies
Academic Section of Vascular Surgery
Division of Surgery
Department of Surgery & Cancer
Faculty of Medicine
Imperial College London

Dr Claudia Monaco
Cytokine Biology of Atherosclerosis
Kennedy Institute of Rheumatology
Faculty of Medicine
Imperial College London

June 2011

"… candidates for statistical surgery are completely at the surgeon's mercy …
Statistical operations are hard to explain to people. Such operations are rolls of the dice,
a gamble that operating carries fewer risks than the disease."

When the Air Hits Your Brain
Frank T Vertosick Jr, 1996

ABSTRACT

Introduction

Key trials and a Cochrane systematic review in asymptomatic carotid stenosis have highlighted the need to identify a high-risk subgroup of patients with carotid stenosis who may benefit from intervention. Traditionally, this risk stratification has considered structural imaging and clinical factors. However, using only these approaches, still a significant number of patients are missed. Biological attributes are acknowledged as key determinants of thrombo-embolic events. Functional and hybrid structural-functional imaging, and circulating biomarkers allow exploration of plaque biology non-invasively, *in vivo*. The importance of innate immunity in atherosclerosis is now established, with a recent interest in macrophage phenotypic polarisation in atherosclerosis supported by *in vitro* and experimental data, with the hypothesis of an M1 macrophage predominance associated with unstable plaques. The emergence of systems biology has been seen to facilitate understanding of biological pathways and generate hypotheses, although the utility of this approach for the examination of human atherosclerosis tissue has not been fully explored.

Aims

(i) To employ functional imaging to probe carotid atherosclerosis *in vivo*; (ii) to assess the plaque microenvironment in determination of the balance of macrophage populations in unstable compared with stable atherosclerosis; (iii) to investigate whether late phase (LP-) contrast enhanced ultrasound (CEUS) reflects plaque biological features; (iv) to examine the utility of systems biology techniques in distinguishing symptomatic from asymptomatic carotid atherosclerosis tissue, and in hypothesis generation; and (v) to evaluate a putative biomarker for carotid atherosclerosis and plaque vulnerability.

Methods

Patients with carotid stenosis, both symptomatic and asymptomatic, have undergone systematic collection of data, fresh carotid endarterectomy (CEA) specimens, and plasma. Thirty-two patients with 36 carotid stenoses underwent ^{11}C-PK11195 PET/CT. Thirty-seven patients had dynamic (D-) and LP-CEUS carotid imaging. CEA specimens were assessed by immunohistochemical techniques, as well as atheroma cell culture with supernatant multi-analyte profiling (MAP). MAP data was subject to Ingenuity Pathway Analysis. CEA specimens were further examined using systems biology methodologies: transcriptomics with Affymetrix Human Exon 1.0 ST arrays; proteomics and lipidomics by liquid chromatography (LC) coupled to tandem triple quadrupole mass spectrometry (MS); and metabolite profiling

by nuclear magnetic resonance and LC-MS. Furthermore, venous and arterial plasma was quantified for the lysozyme, a putative biomarker in carotid atherosclerosis.

Results

^{11}C-PK11195 PET allowed the non-invasive quantification of intraplaque inflammation in patients with carotid stenoses and, when combined with CTA, provided an integrated assessment of plaque structure, composition and biological activity. ^{11}C-PK11195 PET/CT distinguished between recently symptomatic vulnerable plaques and asymptomatic plaques with a high positive predictive value. D-CEUS and LP-CEUS (at a cut-off of zero) was able to distinguish symptomatic and asymptomatic plaques. Atheroma cell culture and supernatant MAP revealed that symptomatic human atherosclerotic carotid disease is associated with a cytokine and chemokine pattern consistent with the predominance of pro-inflammatory M1-type macrophage polarisation. Furthermore, IFNγ signatures are observed, including the novel finding of CCL20 with its significant elevation in symptomatic atherosclerosis. MAP of supernatants from patients who had undergone ipsilateral carotid LP-CEUS revealed significantly higher levels of IL6, MMP1 and MMP3, as well as greater CD68 and CD31 immunopositivity, in those with high (≥0) compared with low (<0) LP-CEUS signal. This suggests that LP-CEUS was able to reflect plaque biology. Transcriptomic analysis was able to clearly separate stenosing plaque and intimal thickening, as well as unstable and stable atherosclerosis, finding differential expression and alternative splicing of interferon regulatory factor 5 between stenosing plaque and intimal thickening. Proteomic analysis of the salt extract fraction from carotid atherosclerotic plaques identified 2,470 proteins implicated in 33 bio-molecular functions and having their origins previously described in 14 different cellular compartments. There were 159 proteins which, based upon the number of assigned spectra, were significantly different between symptomatic and asymptomatic atherosclerosis. Through lipidomic analysis, 150 lipid species from 9 different classes were identified, of which 24 were exclusive to atherosclerotic plaques. A comparison of 28 carotid endarterectomy specimens revealed differential lipid signatures of symptomatic compared with asymptomatic lesions, as well as stable and unstable plaque areas. Similarly, LC-MS metabolite profiling of organic plaque extract was able to separate symptomatic from asymptomatic atherosclerosis. Arterial and venous plasma lysozyme levels were seen to distinguish individuals with carotid atherosclerosis from matched control subjects. Furthermore, arterial plasma lysozyme levels were significantly higher in patients with symptomatic than asymptomatic carotid stenosis.

Conclusions

These findings support the use of hybrid structural-functional imaging, and the utility and use of a systems biology approach in identifying significantly different and biologically relevant variations in atherosclerosis tissue, and in hypothesis generation for further study. The data presented concurs with recent reports in the literature linking the lipidic/organic component of atherosclerosis with the generation of a pro-inflammatory plaque microenvironment prone to lesion development, instability and the complications thereof. The importance of innate immunity has been highlighted with the demonstration of a predominance of M1 macrophage polarisation and evidence of Th17/IL17 signalling in unstable atherosclerosis. It is hoped that this work will contribute to the ongoing refinement of multi-factorial risk stratification in carotid atherosclerosis.

TABLE OF CONTENTS

ABSTRACT **3**
STATEMENT OF ORIGINALITY **14**
ACKNOWLEDGEMENTS **15**
LIST OF FIGURES **16**
LIST OF TABLES **19**
ABBREVIATIONS **21**
1 INTRODUCTION **26**
1.1 ATHEROSCLEROSIS **27**
1.1.1 Variation across Vascular Beds, Clinical Context and Species *27*
1.2 CEREBROVASCULAR DISEASE **28**
1.2.1 The Burden and Health Economic Impact of Stroke *28*
1.2.2 A Brief History of Carotid Endarterectomy *30*
1.2.3 Intervention for Symptomatic Carotid Stenosis *30*
1.2.4 The Great and Ongoing Debate: Revascularisation for Asymptomatic Carotid Stenosis *31*
1.3 STROKE RISK STRATIFICATION **32**
1.3.1 The 'Obsession' with Degree of Luminal Stenosis *34*
1.4 PLAQUE BIOLOGICAL ATTRIBUTES AND STABILITY **35**
1.4.1 Angiogenesis *35*
1.4.2 Intra-Plaque Haemorrhage *36*
1.4.3 Matrix Degradation *36*
1.4.4 The Language of Atherosclerotic Risk and Vulnerability *37*
1.5 INFLAMMATION AND ATHEROSCLEROSIS **37**
1.5.1 Innate Immunity – A Key Player in Atherosclerosis *39*
1.5.2 Macrophage Heterogeneity in Atherosclerosis *40*
1.5.3 Matrix Metalloproteinases and Tissue Inhibitors of Metalloproteinases in Macrophage Phenotype *43*
1.5.4 Recruitment of Monocyte Subsets to Atherosclerotic Plaques *44*
1.5.5 Macrophage Differentiation in Atherosclerosis *46*
1.5.6 Priming of Macrophages in the Atherosclerotic Plaque *48*
1.5.7 Macrophage Activation Pathways in Atherosclerosis *49*
1.5.8 Toll-Like Receptor Signalling *49*
1.5.9 Toll-Like Receptor Agonists *50*
1.5.10 Toll-Like Receptor Expression in Atherosclerosis *51*

1.5.11 Role of Toll-Like Receptors in Atherosclerosis *52*
1.5.12 NOD-Like Receptors and Inflammasomes and Atherogenesis *54*
1.5.13 Macrophage Deactivation Pathways in Atherosclerosis *56*
1.6 IMAGING IN ATHEROSCLEROSIS **58**
1.7 SYSTEMS BIOLOGY – THE '-OMIC' DISCIPLINES **60**
1.7.1 The Complex Biology of Atherosclerosis *60*
1.7.2 The Utility of Effective Atherosclerosis Research *60*
1.7.3 A Systems Biology Approach *61*
1.7.4 The Variety of Disciplines which Constitute Systems Biology *62*
1.8 BIOMARKERS IN CAROTID ATHEROSCLEROSIS **64**
1.8.1 Lysozyme *64*
1.9 AIMS **65**
2 ASSESSMENT OF CAROTID ATHEROSCLEROSIS BY ^{11}C-PK11195 POSITRON EMISSION TOMOGRAPHY / COMPUTED TOMOGRAPHY **66**
2.1 INTRODUCTION **67**
2.2 METHODS **68**
2.2.1 Study Approvals *68*
2.2.2 Patients *68*
2.2.3 ^{11}C-PK11195 Radiotracer Synthesis *68*
2.2.4 PET/CT Scanning Protocol *69*
2.2.5 Image Reconstruction *70*
2.2.6 Measurement of ^{11}C-PK11195 Uptake *70*
2.2.7 CT Assessment of Carotid Stenosis and Plaque Composition *71*
2.2.8 Ex Vivo Plaque Processing *72*
2.2.9 Autoradiography *72*
2.2.10 Immunohistochemistry *72*
2.2.11 Confocal Fluorescence Microscopy *73*
2.2.12 Statistical Analysis *73*
2.3 RESULTS **73**
2.3.1 Patients *73*
2.3.2 PET/CTA Imaging *75*
2.3.3 Ex Vivo Analysis *79*
2.4 DISCUSSION **81**
2.4.1 Clinical Implications *83*
2.4.2 Limitations *84*

2.4.3 Conclusions *85*

3 ASSESSMENT OF CAROTID ATHEROSCLEROSIS BY DYNAMIC AND LATE PHASE MICROBUBBLE CONTRAST ENHANCED ULTRASOUND **86**

3.1 INTRODUCTION TO CONTRAST ENHANCED ULTRASOUND IN CAROTID ARTERIAL DISEASE **87**

3.1.1 Microbubbles, Non-Linear Behaviour and Mechanical Index *87*

3.1.2 The Current Carotid Ultrasound Examination *88*

3.1.3 The Need to Improve the Current Ultrasound Assessment *89*

3.1.4 Imaging Neovascularisation: The Rationale *89*

3.1.5 Contrast Enhanced Ultrasound to Image Neovascularisation *89*

3.1.6 Microbubbles to Improve Structural Imaging of Plaque *91*

3.1.7 Potential Problems with Contrast Enhanced Ultrasound *91*

3.2 METHODS **92**

3.2.1 Study Approvals *92*

3.2.2 Equipment and Settings *92*

3.2.3 Study Subjects *92*

3.2.4 Unenhanced Duplex Ultrasonography and Gray-Scale Median Score *93*

3.2.5 Contrast Agent, Preparation and Administration *93*

3.2.6 Dynamic Contrast Enhanced Ultrasound *93*

3.2.7 Late Phase Contrast Enhanced Ultrasound *95*

3.2.8 Blinding and Standardisation of Contrast Enhanced Ultrasound Image Acquisition and Data Processing *98*

3.2.9 Statistical Analysis *98*

3.3 RESULTS **99**

3.3.1 Patient Numbers and Characteristics *99*

3.4 DYNAMIC CONTRAST ENHANCED ULTRASOUND **100**

3.5 LATE PHASE CONTRAST ENHANCED ULTRASOUND **101**

3.5.1 Relationship between Late Phase Signal and Symptomatology *101*

3.5.2 Relationship between Late Phase Signal and Time Since Symptoms *102*

3.5.3 Relationship between Late Phase Signal and Gray-Scale Median Score *103*

3.5.4 Relationship between Late Phase Signal and Stenosis *104*

3.5.5 Relationship between Late Phase Signal and Patient Characteristics *104*

3.5.6 Relationship between Late Phase Signal and Dynamic Signal *104*

3.5.7 Multivariate Logistic Regression Analysis *105*

3.6 DISCUSSION **106**

3.6.1 Contrast Enhanced Ultrasound as Compared to Functional and Structural Imaging Modalities 106
3.6.2 Dynamic Contrast Enhanced Ultrasound 107
3.6.3 Late Phase Contrast Enhanced Ultrasound 108
3.6.4 Limitations of Late Phase Contrast Enhanced Ultrasound 110
3.6.5 Conclusion 111
4 MULTI-ANALYTE PROFILING IN CAROTID ATHEROSCLEROSIS 112
4.1 INTRODUCTION 113
4.2 METHODS 114
4.2.1 Ethical Approval and Regulation, Sample and Data Collection, and Definition of Symptomatic Status 114
4.2.2 Carotid Atheromatous Plaque Processing Protocol 114
4.3 CAROTID PLAQUE HISTOLOGY 115
4.3.1 Tissue Embedding 115
4.3.2 Cryosectioning 115
4.3.3 Carotid Plaque Immunohistochemistry 116
4.3.4 Blocking 116
4.3.5 Avidin-Biotin Complex Immunohistochemistry Technique 117
4.3.6 Diaminobenzidine Visualisation 117
4.3.7 Picro-sirius Red Staining 117
4.3.8 Dehydration, Mounting and Coverslip Application 118
4.3.9 Histology Quality Control 118
4.3.10 Image Acquisition and Analysis 118
4.4 CAROTID PLAQUE ENZYMATIC DIGESTION AND CULTURE 120
4.4.1 Plaque Enzymatic Digestion 121
4.4.2 Plaque Cell Culture 122
4.4.3 Storage of Culture Supernatant 122
4.5 MULTI-ANALYTE PROFILING 122
4.5.1 Principles of Multi-Analyte Profiling 122
4.5.2 Milliplex Multi-Analyte Profiling 123
4.5.3 Fluorokine Multi-Analyte Profiling 124
4.5.4 Multi-Analyte Profiling Plate Analysis 124
4.5.5 Cytokines and Chemokines 124
4.5.6 Matrix Metalloproteinases and Tissue Inhibitors of Metalloproteinases 126
4.5.7 Multi-Analyte Profiling Assay Sensitivity 126

4.5.8 Statistical Analysis *127*
4.5.9 Pathway Analysis *127*
4.6 RESULTS **127**
4.6.1 Histological Analysis *128*
4.6.2 Analyte Detection by Multi-Analyte Profiling *130*
4.6.3 Cytokines *136*
4.6.4 Chemokines *137*
4.6.5 Colony Stimulating Factors *137*
4.6.6 Matrix Metalloproteinases *137*
4.6.7 Tissue Inhibitors of Metalloproteinases *137*
4.6.8 Analyte Inter-Relationships and Pathway Analysis *138*
4.7 DISCUSSION **144**
4.7.1 Limitations of the Study *149*
4.7.2 Conclusions *150*
5 THE RELATIONSHIP BETWEEN LATE-PHASE CONTRAST ENHANCED ULTRASOUND AND ATHEROSCLEROTIC PLAQUE BIOLOGICAL FEATURES **151**
5.1 INTRODUCTION **152**
5.2 METHODS **153**
5.2.1 Study Subjects *153*
5.2.2 Conventional Ultrasound, Late-Phase Contrast Enhanced Ultrasound and Analysis *153*
5.2.3 Carotid Endarterectomy Specimen Processing *153*
5.2.4 Histology *154*
5.2.5 Atheroma Cell Culture and Multi-Analyte Profiling *154*
5.2.6 Statistical Analysis *154*
5.3 RESULTS **154**
5.3.1 Histological Analysis *155*
5.3.2 Multi-Analyte Profiling *158*
5.4 DISCUSSION **161**
5.4.1 Study Limitations *163*
5.4.2 Conclusion *163*
6 THE UTILITY OF A SYSTEMS BIOLOGY APPROACH IN EXAMINING CAROTID ATHEROSCLEROSIS BIOLOGY **164**
6.1 INTRODUCTION **165**
6.2 TRANSCRIPTOMICS **165**

6.2.1 Transcriptomic Aims *168*
6.3 TRANSCRIPTOMIC METHODOLOGY **168**
6.3.1 Sample Selection, RNA Extraction and Processing *168*
6.3.2 Transcriptomic Data Analysis *173*
6.4 TRANSCRIPTOMIC RESULTS **174**
6.4.1 Initial Analysis *174*
6.4.2 Stenosing Plaque and Intimal Thickening *175*
6.4.3 Stable and Unstable Atherosclerosis *179*
6.5 TRANSCRIPTOMICS DISCUSSION **180**
6.6 PROTEOMICS **182**
6.7 PROTEOMICS METHODOLOGY **184**
6.7.1 Study Design *184*
6.7.2 Approach to Extraction for Proteomic Analysis *185*
6.7.3 Protein Extraction *186*
6.7.4 Gelatinolytic Zymography *187*
6.7.5 Protein Gel Electrophoresis *187*
6.7.6 Nanoflow Liquid Chromatography Tandem Mass Spectrometry *189*
6.8 SALT EXTRACT PROTEOMICS RESULTS **190**
6.8.1 Analysis Based Upon Symptomatic Status *192*
6.8.2 Analysis Considering Gender *199*
6.8.3 Gelatinolytic Zymography Results and Validation *200*
6.9 DISCUSSION **200**
6.9.1 Gender Differences in Protein Abundance *202*
6.9.2 Limitations *202*
6.10 LIPIDOMICS **203**
6.11 LIPIDOMICS METHODS **204**
6.11.1 Clinical Samples *204*
6.11.2 Workflow Overview *204*
6.11.3 Liquid Extraction Surface Analysis (LESA) Coupled to Nano-ESI-MS *205*
6.11.4 Lipid Extraction *205*
6.11.5 Shotgun Lipidomics *206*
6.11.6 Data Processing *207*
6.11.7 Nomenclature *207*
6.11.8 Statistical Analysis *207*
6.12 LIPIDOMICS RESULTS **208**
6.12.1 Liquid Extraction Surface Analysis (LESA) *208*
6.12.2 Identification of Plaque Lipids *209*

6.12.3 Comparison of Carotid Endarterectomy Samples *210*
6.12.4 Systems-Wide Analysis of Plaque Lipids *215*
6.13 LIPIDOMICS DISCUSSION **217**
6.13.1 Lipids in Atherosclerosis *217*
6.13.2 Systems-Wide Network Analysis *218*
6.13.3 Clinical Relevance *219*
6.13.4 Study Limitations *219*
6.13.5 Conclusions *219*
6.14 INTRODUCTION TO METABOLIC PROFILING **220**
6.14.1 Metabolic Profiling in Atherosclerosis *221*
6.14.2 Objectives *221*
6.15 METABOLIC PROFILING METHODOLOGY **221**
6.15.1 Biological Sample Characteristics and Handling *221*
6.15.2 Metabolite Extraction – Aqueous (Polar) *223*
6.15.3 Metabolite Extraction – Organic *223*
6.15.4 Metabolite Profiling *224*
6.15.5 Nuclear Magnetic Resonance *224*
6.15.6 Nuclear Overhauser Effect Spectroscopy – NOESY *224*
6.15.7 Carr-Purcell-Meiboom-Gill – CPMG *224*
6.15.8 Ultra Performance Liquid Chromatography Mass Spectrometry – UPLC-MS *224*
6.15.9 Unit Variance and Pareto Scaling *225*
6.16 METABOLIC PROFILING RESULTS **225**
6.16.1 Results of NMR PCA *225*
6.17 METABOLITE PROFILING DISCUSSION **227**
7 PLASMA LYSOZYME AS A PUTATIVE BIOMARKER IN CAROTID ATHEROSCLEROSIS **229**
7.1 INTRODUCTION **230**
7.1.1 Aim *230*
7.2 METHOD **230**
7.2.1 Study Subjects *230*
7.2.2 Sample Collection and Processing *231*
7.2.3 Lysozyme Analysis *231*
7.2.4 Statistical Analysis *231*
7.3 RESULTS **231**
7.3.1 Plasma Lysozyme *232*

7.3.2 Carotid Atherosclerotic Plaque Lysozyme *238*
7.4 DISCUSSION **238**
7.4.1 Limitations *240*
7.4.2 Conclusions *240*
8 FINAL DISCUSSION **241**
8.1 CONCLUDING COMMENTS **246**
9 FUTURE WORK **248**
9.1 FUTURE DIRECTIONS FOR CONTRAST ENHANCED ULTRASOUND **249**
9.1.1 Contrast Ultrasound for Stroke Prediction (CUSP) *249*
9.1.2 3-Dimensional Contrast Enhanced Ultrasound *250*
9.1.3 Advances in Microbubble Technology *251*
9.1.4 Combining Diagnosis and Therapeutic Drug Delivery *251*
9.2 FUTURE WORK IN MOLECULAR AND CELLULAR CHARACTERISATION OF ATHEROSCLEROSIS **251**
REFERENCES **253**
APPENDICES **287**
Appendix 1 Grants, Fellowships, Publications and Presentations 287

STATEMENT OF ORIGINALITY

The material presented in this report is the original work of the author. Where results or diagrams have been reproduced from the work of others, the source is clearly stated.

ACKNOWLEDGEMENTS

I would like to take this opportunity to thank the many people who have been so generous with their time and expertise in allowing me to complete this thesis. First and foremost to my supervisors Professor Alun Davies and Dr Claudia Monaco whom I thank for their patience, guidance and scientific input.

To all the members of the Academic Section of Vascular Surgery, particularly Mr Ian Franklin, Mr Chung Lim, Miss Amanda Shepherd, Mr Muzaffar Anwar, Mr Tristan Lane and Miss Hayley Moore. And all those in Cytokine Biology of Atherosclerosis (also known as 'Team Claudia') including, Dr Louise Full, Mrs Amanda Cross, Miss Nagore Astola, Mr Mika Falck-Hansen, Dr Jennifer Cole, Dr Leena Viiri, Mrs Ilona Krysynska-Jiaja, Mr Mike Goddard and Miss Anusha Seneviratne.

For their help with the PET/CT study, I thank Dr Oliver Gaemperli, Professor Paolo Camici and Dr Ornella Rimoldi. The contrast enhanced ultrasound study would not have been possible without the work of Professor Edward Leen, Dr David Owen and Mr Ankur Thapar. I thank Miss Nazeeha Hasan and Dr Pankaj Sharma for their contribution towards the transcriptional profiling, and Professor Manuel Mayr, Dr Athanasios Didangelos and Dr Christin Stegemann for their expertise in proteomics and lipidomics. To Mr Panagiotis Vorkas, Dr Elizabeth Want, Professor Elaine Holmes and Professor Jeremy Nicholson for their metabolomics input, and Dr Vahitha Abdul-Salam and Dr Robert Edwards for their help with the lysozyme analysis. I acknowledge Dr Louise Brown for her expert statistical support.

My sincere thanks to the many patients who participated in the studies.

And finally, to my parents, my sister Rita, my brother Michael, and my wife Ruth.

LIST OF FIGURES

Figure 1	Intra- and extra-cranial arterial circulation	29
Figure 2	Summary of biological attributes contributing to atheromatous plaque instability	35
Figure 3	Summary of known interaction between immune cells, through cytokines	38
Figure 4	The relationship between M1, M2 and MOX macrophage phenotypes	42
Figure 5	Multi-step paradigm of macrophage activation	44
Figure 6	The interaction between TLR and inflammasome signalling	50
Figure 7	The influence of PPARγ on macrophage phenotype	57
Figure 8	The rise of atherosclerosis research	61
Figure 9	The synthetic 'workflow' of a cell	62
Figure 10	A 'top-down' approach to biology	63
Figure 11	Summary of the key disciplines in systems biology	63
Figure 12	Schematic showing the TSPO location on the outer mitochondrial membrane of activated cells of the mononuclear lineage and downstream signalling	67
Figure 13	Semiquantitative plaque calcification scoring system.	71
Figure 14	^{11}C-PK11195 PET / CT imaging of an asymptomatic carotid atheroma	76
Figure 15	^{11}C-PK11195 PET / CT imaging of symptomatic carotid atherosclerosis	76
Figure 16	^{11}C-PK11195 PET / CT imaging of a symptomatic carotid atheroma – close-up	77
Figure 17	Quantification ^{11}C-PK11195 PET / CT imaging parameters	77
Figure 18	Axial co-registration of ^{11}C-PK11195 PET and CT images	78
Figure 19	Discriminatory value of carotid plaque ^{11}C-PK11195 PET / CT	79
Figure 20	^{3}H-PK11195 autoradiography, CD68 and TSPO immunohistochemistry and double immunofluorescence confocal microscopy	80
Figure 21	*In vivo* and *in vitro* PK11195	81
Figure 22	Dynamic contrast enhanced ultrasound time-intensity curve and parameters	94
Figure 23	Dynamic contrast enhanced ultrasound image analysis and quantification	95
Figure 24	Late phase contrast enhanced ultrasound image analysis	97
Figure 25	Normalised plaque peak dynamic echo intensity	100
Figure 26	Normalised plaque late phase intensity	102
Figure 27	Normalised plaque late phase and declines with time since symptoms	103
Figure 28	Gray-scale median score	103
Figure 29	There is a trend towards positive correlation between normalised plaque late phase and dynamic peak signals	104
Figure 30	Combined LP-CEUS and D-CEUS score	105

Figure 31 Carotid plaque processing protocol 115
Figure 32 Image acquisition of stained histological sections comparing conventional and motorised stage microscope - camera setups 119
Figure 33 Image analysis for quantification of histological staining 120
Figure 34 Carotid atheroma cell culture work-flow 121
Figure 35 Plaque cap thickness on picro-sirius red staining 129
Figure 36 CD68 and CD31 percentage area immunopositivity 129
Figure 37 Plaque culture supernatant levels of cytokines in distinguishing symptomatic from asymptomatic plaques 134
Figure 38 Plaque culture supernatant levels of chemokines in distinguishing symptomatic from asymptomatic plaques 135
Figure 39 Plaque culture supernatant levels of matrix metalloproteinases in distinguishing symptomatic from asymptomatic plaques 136
Figure 40 Analyte inter-relationships 139
Figure 41 Network analysis 142
Figure 42 Key canonical pathways in human carotid atherosclerosis 143
Figure 43 A schematic summarising the soluble analytes with differential protein production between symptomatic and asymptomatic carotid atherosclerosis, reflecting a predominance of pro-inflammatory M1-macrophage polarisation 144
Figure 44 The MSP/RON Pathway 145
Figure 45 The relationship between normalised plaque late phase echo intensity and CD68, CD31 and minimum plaque cap thickness 157
Figure 46 LP-CEUS and B-mode ultrasound comparison with plaque CD68 imunohistochemistry 158
Figure 47 IL6, MMP1 and MMP3 production is significantly higher from plaques with a LP-CEUS signal ≥0 161
Figure 48 Carotid endarterectomy specimen processing for transcriptomic profiling .169
Figure 49 Agilent bioanalyser output for assessment of RNA quality 170
Figure 50 Relationship between Nanodrop and Agilent bioanalyser data 172
Figure 51 Relative Log expression signal 174
Figure 52 Sample pairs derived from the same carotid endarterectomy specimen were not seen to cluster 174
Figure 53 Hierarchical clustering analysis of stenosing plaque and intimal thickening paired samples 175
Figure 54 Separation of stenosing plaque and intimal thickening on 2-dimensional principal components analysis 176

Figure 55 Separation of stenosing plaque and intimal thickening on 3-dimensional principal components analysis 176
Figure 56 Differential expression and splicing of interferon regulatory factor 5 (IRF5) comparing stenosing atherosclerosis and intimal thickening..... 178
Figure 57 Separation of stable and unstable atherosclerosis on 3-dimensional principal components analysis 179
Figure 58 Interferon regulatory factor 5 in the pattern recognition receptor pathway . 180
Figure 59 Salt extract protein gel electrophoresis 188
Figure 60 Salt extract protein gel band excision prior to trypsination 189
Figure 61 Comparison of assigned spectra in sample and replay of tandem mass spectrometry 190
Figure 62 Separation based on proteomic analysis of symptomatic and asymptomatic carotid atherosclerosis by 2-dimensional principal components analysis.... 199
Figure 63 Salt extract gelatinolytic zymography – comparison with MMP9 spectra by tandem mass spectrometry 200
Figure 64 Macroscopic classification of unstable ruptured regions and stable areas within carotid plaques 204
Figure 65 Liquid extraction surface analysis (LESA) compared to lipid extracts 208
Figure 66 Cholesteryl ester species abundance differentially and exclusively found within atherosclerotic plaque compared with control artery 210
Figure 67 Principal components analysis for lipid profiles of symptomatic and asymptomatic patients 211
Figure 68 Principal components analysis of lipidomic data based upon top 10 differentially expressed species 213
Figure 69 Principal components analysis of lipidomic data based upon lipid classes . 214
Figure 70 Systems-wide relationships between lipids involved in atherosclerosis 216
Figure 71 Processing of carotid atherosclerotic plaque for metabolic profiling with storage of tissue for future mass spectroscopy imaging 223
Figure 72 Representative NMR and UPLC-MS spectra 225
Figure 73 Results of NMR PCA 226
Figure 74 Results of organic UPLC-MS PCA 227
Figure 75 An example of MALDI mass spectroscopy imaging 228
Figure 76 Arterial plasma lysozyme for carotid stenosis versus controls 233
Figure 77 Venous plasma lysozyme for carotid stenosis versus controls 234
Figure 78 Arterial plasma lysozyme levels and symptomatic status 236
Figure 79 Contrast Ultrasound for Stroke Prediction (CUSP) study design 249
Figure 80 3-dimensional contrast enhanced ultrasound 250

LIST OF TABLES

Table 1 Cytokines and chemokine gene expression in human macrophage polarisation 40

Table 2 A comparison of human and murine monocyte subsets 45

Table 3 The inverse relationship between the relative spatial resolution and sensitivity for contrast agent detection of common imaging techniques 59

Table 4 Characteristics of the symptomatic and asymptomatic patient groups 74

Table 5 ^{11}C-PK11195 PET / CT imaging results 75

Table 6 Contrast enhanced ultrasound imaging and acquisition parameters 92

Table 7 Characteristics of the symptomatic and asymptomatic patient groups 100

Table 8 Ultrasound features of carotid plaque in patients with and without symptoms 101

Table 9 Correlation coefficient matrix.....106

Table 10 Multivariate logistic regression model for symptomatic status 106

Table 11 Candidate cytokines and chemokines for exploration using multi-analyte profiling and their roles.....125

Table 12 Candidate matrix metalloproteinases and tissue inhibitors of metalloproteinases for exploration using multi-analyte profiling and their roles.....126

Table 13 Multi-analyte profiling assay sensitivity for MMP and TIMP analysis.....126

Table 14 Subject characteristics.....128

Table 15 Analyte detection – cytokines and chemokines 131

Table 16 Analyte detection – MMPs and TIMPs 132

Table 17 Biological networks in human carotid atherosclerosis 141

Table 18 Characteristics of the high and low LP-CEUS signal groups 155

Table 19 Analysis of immunohistochemistry 156

Table 20 Analysis of cytokine and chemokine multi-analyte profiling.....159

Table 21 Analysis of matrix metalloproteinase and tissue inhibitor of metalloproteinase multi-analyte profiling 160

Table 22 Summary of transcriptomic studies in human atherosclerosis.....167

Table 23 Extracted RNA assessed by Nanodrop and Agilent bioanalyser 171

Table 24 Characteristics of the individuals included in the transcriptomic study 173

Table 25 Summary of proteomic and metabolite profiling studies in human atherosclerosis.....184

Table 26 Clinical characteristics of symptomatic and asymptomatic patients.....185
Table 27 Categorisation of the 2470 identified salt extract proteins 191
Table 28 Indentified proteins whose abundance within salt extracts is significantly different between symptomatic and asymptomatic carotid atherosclerosis.198
Table 29 Lipid species found exclusively in atherosclerotic plaques.....209
Table 30 Clinical characteristics of patients whose plaques were divided into ruptured (unstable) and non-ruptured (stable) areas.....212
Table 31 Characteristics of the individuals included in the metabolite profiling study 222
Table 32 Characteristics of the study groups.....232
Table 33 Receiver operator characteristic analysis results 233
Table 34 Arterial plasma lysozyme and its relationship with demographic, clinical and pharmacotherapeutic parameters 235
Table 35 Characteristics of the six patients with high arterial plasma lysozyme levels 237
Table 36 Carotid atherosclerotic plaque lysozyme analysis 238

ABBREVIATIONS

2D	2 dimensional
3D	3 dimensional
3DRP	3 dimensional re-projection
A2RA	angiotensin 2 receptor antagonist
ABC	avidin biotin complex / ATP-binding cassette transporter
ACAS	Asymptomatic Carotid Atherosclerosis Study
ACEi	angiotensin converting enzyme inhibitor
ACN	acetonitrile
ACSRS	Asymptomatic Carotid Stenosis and Risk of Stroke
ACST	Asymptomatic Carotid Surgery Trial
ALIU	arbitrary linear intensity units
AMU	atomic mass units
ANOVA	analysis of variance
ANT	adenine nucleotide translocator
apo	apolipoprotein
ARFI	acoustic radiation force impulse
ASA	acetyl salicylic acid (aspirin)
AUC	area under curve
BFI	B-flow imaging
BMT	best medical therapy
CAS	carotid artery stenting
CCL	chemokine (C-C) motif ligand
CD	cluster of differentiation
cDNA	complimentary DNA
CE	cholesteryl ester
CEA	carotid endarterectomy
CEUS	contrast enhanced ultrasound
CI	confidence interval
COPD	chronic obstructive pulmonary disease
CP	canonical pathway / Carr-Purcell
CPMG	Carr-Purcell-Meiboom-Gill
CRP	C-reactive protein
CSF	colony stimulating factor
CT	computed tomography
CTA	computed tomography angiography
CVA	cerebrovascular accident
CX3CL	chemokine (C-X3-C) motif ligand
CXCL	chemokine (C-X-C) motif ligand
D	dimensional
D2O	deuterium oxide
DAB	3,3'-diaminobenzidine
DAMP	danger associated molecular pattern
DAPI	4’,6-diamidino-2-phenylindole
dB	decibel
DC	dendritic cell
D-CEUS	dynamic contrast enhanced ultrasound
DCM	dicholoromethane

DE	dimensional electrophoresis
DESI	desorption electrospray ionisation
DICOM	Digital Imaging and Communications in Medicine
DM	diabetes mellitus
DMEM	Dulbecco's modified Eagle medium
DNA	deoxyribonucleic acid
DPX	distyrene, plasticiser, xylene
ECG	electrocardiograph
ECM	extracellular matrix
ECST	European Carotid Surgery Trial
EDTA	ethylenediaminetetraacetic acid
ELISA	enzyme linked immunosorbent assay
ENA	epithelial cell-derived neutrophil-activating peptide
ESI	electrospray ionisation
ESVS	European Society for Vascular Surgery
EVA-3S	Endarterectomy Versus Angioplasty in Patients with Severe Symptomatic Carotid Stenosis
EVG	elastic Van Gieson
FBS	foetal bovine serum
FDG	fluorodeoxyglucose
FDR	false discovery rate
FSE	fast spin echo
fwhm	full width at half maximum
GCP	Good Clinical Practice
G-CSF	granulocyte colony stimulating factor
GC-MS	mass spectrometry coupled to gas chromatography
GDI	guanosine 5’-diphosphate dissociation inhibitor
GE	General Electric
GLC	gas liquid chromatography
GM-CSF	granulocyte macrophage colony stimulating factor
GSK	GlaxoSmithKline
GSM	grey scale median
GST	glutathione S-transferase
H&E	haematoxylin and eosin
HDL	high density lipoprotein
HEV	high endothelial venules
HILIC	hydrophilic interaction chromatography
HPLC	high performance liquid chromatography
HRP	horseradish peroxidase
hsCRP	high sensitivity C-reactive protein
HSP	heat shock protein
HTN	hypertension
HU	Hounsfield units
HUVEC	human vascular endothelial cell
ICA	internal carotid artery
ICAROS	Imaging in Carotid Angioplasty and Risk of Stroke
ICH	International Conference on Harmonisation
IDO	indoleamine 2,3-dioxygenase
IFN	interferon
IHC	immunohistochemistry

IL	interleukin
IMM	inner mitochondrial membrane
IMS	industrial methylated spirit
IMT	intima media thickness
IP	interferon (gamma) induced protein
IRF	interferon regulatory factor
I-TAC	IFN-inducible T-cell α chemoattractant
ITS	insulin, transferrin, selenite
IUPAC	International Union of Pure and Applied Chemistry
K_d	dissociation constant
LC	liquid chromatography
LC-MS	mass spectrometry coupled to liquid chromatography
LDL	low density lipoprotein
LESA	liquid extraction surface analysis
LP	late phase
lPC	lyso-phosphatidylcholine
LP-CEUS	late phase contrast enhanced ultrasound
lPE	lyso-phosphatidylethanolamine
lPS	lyso-phosphatidylserine
LPS	lipopolysaccharide
MACS	magnetic cell sorting
MALDI	matrix-assisted laser desorption/ionisation
MAP	multi-analyte profiling
MAPK	mitogen activated protein kinase
MCP	monocyte chemotactic protein
M-CSF	macrophage colony stimulating factor
MDSE	motion-sensitised driven-equilibrium
MFI	mean fluorescent intensity
MHC	major histocompatibility complex
MHRA	Medicines and Healthcare products Regulatory Agency
MI	mechanical index
MIP	macrophage inflammatory protein
MLD	minimal lumen diameter
MMP	matrix metalloproteinase
MR	magnetic resonance
MRI	magnetic resonance imaging
MS	mass spectrometry
MSI	mass spectrometry imaging
MS/MS	tandem mass spectrometry
MSP	macrophage stimulating protein
MT	membrane type
MTT	3-(4,5-dimethyl-2-yl)-2,5-diphenyltetrazolium
MyD88	myeloid primary differentiation response gene 88
m/z	mass per charge ratio
NA	not applicable
NASCET	North American Symptomatic Carotid Endarterectomy Trial
NCBI	National Center for Biotechnology Information
NF	nuclear factor
NHS	National Health Service
NK	natural killer

NL	negative loss
NLR	NOD-like receptor
NMR	nuclear magnetic resonance
NNT	number needed to treat
NOD	nucleotide-binding oligomerisation domain
NOESY	nuclear Overhauser effect spectroscopy
NPV	negative predictive value
NS	non-significant
NSB	non-specific binding
OCT	optimised cutting temperature
ODS	octadecylsilane
OMM	outer mitochondrial membrane
OPLSDA	orthogonal partial least squares discriminant analysis
OSEM	ordered subset expectation maximisation
P	phosphorylated
PAGE	polyacrylamide gel electrophoresis
PAMP	pathogen associated molecular pattern
PAP7	peripheral benzodiazepine receptor associated protein 7
PBR	peripheral benzodiazepine receptor
PBS	phosphate buffered saline
PC	plaque calcification / phosphatidylcholine / principal component
PCA	principal components analysis
PCC	Pearson correlation coefficient
PCR	polymerase chain reaction
PE	phycoerythrin / phosphatidylethanolamine
PET	positron emission tomography
PI	precursor ion
PLSDA	partial least squares discriminant analysis
ppm	parts per million
PPV	positive predictive value
PRAX1	peripheral benzodiazepine receptor associated protein 1
PRR	pattern recognition receptor
PS	phosphatidylserine
P/S	penicillin / streptomycin
psi	pounds per square inch
QALY	quality-adjusted life year
QC	quality control
QqQ	triple quadrupole
Q-TOF	quadrupole-time of flight
R	receptor
RANTES	regulated on activation normal T cell expressed and secreted
RD	reference diameter
RIN	RNA integrity number
RNA	ribonucleic acid
ROC	receiver operating characteristic
ROI	region of interest
RON	receptor d'origine nantais
RP	reverse phase
RPM / rpm	revolutions per minute
RPMI	Roswell Park Memorial Institute medium

RREC	Riverside Research Ethics Committee
SAF	serum amyloid A activating factor
SBTI	soya bean trypsin inhibitor
scc	side chain cleavage
SD	standard deviation
SDS	sodium dodecyl sulphate
SELDI	surface-enhanced laser desorption/ionisation
SEM	standard error of mean
SLE	systemic lupus erythematosus
SM	sphingomyelin
SMC	smooth muscle cell
SNP	single nucleotide polymorphism
SNR	signal to noise ratio
SOD	superoxide dismutase
SPECT	single positron emission computed tomography
SPSS	Statistics Package for the Social Sciences
SSI	supersonic shear imaging
STAT	signal transducer and activator of transcription
SUV	standardised uptake value
T	tesla
TAG	triacylglycerol
TBR	target-to-background ratio
TBS	tris(hydroxymethyl)aminomethane buffered saline
TE	echo time
TGF	transforming growth factor
Th	T helper
TIA	transient ischaemic attack
TIMP	tissue inhibitor of metalloproteinase
TIP DC	tumour necrosis factor and inducible nitric oxide synthase-producing dendritic cell
TLR	toll-like receptor
TNF	tissue necrosis factor
TOF	time of flight
TSPO	translocator protein 18kDa
TSE	turbo spin echo
UPLC	ultra performance liquid chromatography
US	ultrasound
USPIO	ultrasmall superparamagnetic particles of iron oxide
UTMD	ultrasound targeted microbubble destruction
UV	ultraviolet / unit variance
VDAC	voltage-dependent anion channel
VEGF	vascular endothelial growth factor

1 INTRODUCTION

1.1 ATHEROSCLEROSIS

1.1.1 Variation across Vascular Beds, Clinical Context and Species

Atherothrombotic vascular disease is the leading cause of mortality worldwide, accounting for a fifth of all deaths (Lopez et al. 2006). The manifestations of the disease are often sudden and dramatic, including myocardial infarction and sudden death (Oalmann et al. 1980). Atherosclerosis is a systemic condition affecting arteries throughout the body. Similar mechanisms apply in the formation of atheromatous plaques in arteries supplying all major organ systems. These include:

- Coronary arterial disease, leading to ischaemic heart disease, myocardial infarction, cardiomyopathy and cardiac failure;
- Renovascular disease, leading to hypertension and renal impairment;
- Peripheral arterial disease, leading to intermittent claudication and critical limb ischaemia;
- Mesenteric arterial disease, leading to gut claudication and acute ischaemic bowel; and
- Cerebrovascular disease, leading to transient ischaemic attacks (TIAs), amaurosis fugax and cerebrovascular accidents (CVAs, strokes).

Although similar mechanisms have been described in the formation of these atheromatous lesions throughout the arterial tree, the process by which the arterial disease in the carotid artery causes focal neurological symptomatology is somewhat different to the mechanisms by which end organ dysfunction is precipitated in the other listed organ systems. In the non-cerebral arterial tree, it is an acute plaque event leading to platelet aggregation, thrombosis and vessel occlusion which is responsible for organ dysfunction.

In addition to the differences seen in the various vascular beds, atheroma studies in humans show that plaque rupture may occur without the formation of an occlusive thrombus, highlighting the importance of understanding why some plaque disruptions (even mild disruptions or erosions) result in occlusive thrombus, whilst extensive disruption (*i.e.* plaque rupture) can occur with little consequence (Schwartz et al. 2007).

Furthermore, much work on atherosclerosis has been undertaken in murine models. However, the relevance of the natural history of atheromata in these models to the final events seen in human lesions is not yet known (Schwartz et al. 2007).

1.2 CEREBROVASCULAR DISEASE

The World Health Organisation defines stroke as 'a syndrome characterised by rapidly developing symptoms and signs of focal (at times global) loss of cerebral function lasting for 24 hours or longer or leading to death with no apparent cause other than that which is vascular in origin'.

1.2.1 The Burden and Health Economic Impact of Stroke

Stroke is the third most common cause of death and the single greatest cause of adult disability in the developed world (2009) with, according to the Office for National Statistics, 150,000 individuals suffering a stroke in the UK per annum. Following a stroke, 20 to 30% of patients die within one month, approximately one third are left with a long-term disability, and 12% requiring institutional care at one year. Stroke has a greater disability impact than any other chronic disease, with over 300,000 people living with moderate to severe disabilities owing to stroke (Adamson et al. 2004).

Data from the National Audit Office shows that stroke represents a huge economic burden and each year costs the NHS approximately £2.8 billion and industry £1.8 billion in lost productivity and disability. Furthermore, these costs are predicted to continue to rise.

Approximately 15% of patients who have a stroke will have had a pre-warning in the form of a transient ischaemic attack (TIA), which is defined as an acute neurological event that resolves completely within 24 hours from onset. For events affecting the (internal) carotid artery territory, the transient neurological symptoms include contra-lateral hemiparesis, hemiparasthaesia, transient monocular blindness (amaurosis fugax), hemi-neglect and cortical dysfunction (aphasia, agraphia and apraxia).

Approximately 80-90% of all strokes are ischaemic in nature and atherosclerosis affecting the major extracranial (internal and common carotid arteries) and intracranial (anterior, middle and posterior cerebral arteries) blood vessels is causal in approximately 30% of cases, with the ratio of extracranial to intracranial lesions being greater than 2:1. In a further 30% of cases, embolus originating from the heart is implicated and in the remaining 40% the cause is unknown.

In the setting of the cerebral circulation, there is redundancy in the vascular supply owing to the anastomotic ring of the Circle of Willis, which is fed by the two internal carotid arteries and the two vertebral arteries (Figure 1). Occlusion of one of these four feeding vessels

should not result in critical cerebral ischaemia. As such, one or more of the vessels feeding the Circle of Willis have been found to be occluded on imaging without clinical consequence, and without radiological evidence of infarction on tomographic imaging.

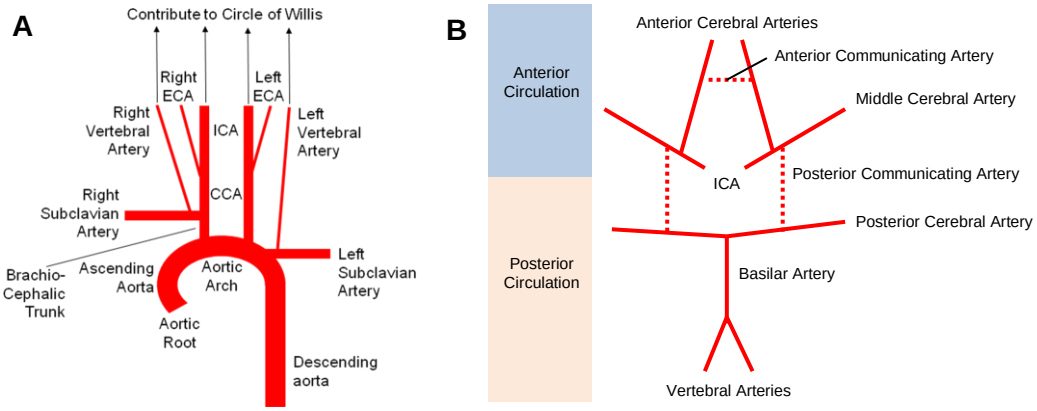


Figure 1 Intra- and extra-cranial arterial circulation

A schematic representation of the supra-aortic extra-cranial arterial anatomy (A) and Circle of Willis (B) highlighting the anterior circulation, derived from the internal carotid arteries (ICA), and the posterior circulation derived from the vertebral arteries. The anastomotic ring is completed by the anterior communicating and paired posterior communicating arteries, which are shown as dashed lines in B. CCA, common carotid artery; ECA, external carotid artery.

On the basis of anatomic or angiographic studies, several Circle of Willis variations exist in more than 50% of the human population (Macchi et al. 1996; Hoksbergen et al. 2000; Merkkola et al. 2006; Papantchev et al. 2007). Insufficient cross-perfusion could be expected mainly in cases with multiple variations, which were found in 30% of the patients in Macchi's series (Macchi et al. 1996) and in 23% of the patients in Hoksbergen's series (Hoksbergen et al. 2000; Urbanski et al. 2008). In such situations, occlusion of one carotid artery may result in critical focal cerebral ischaemia, and the consequences thereof.

There are occasions where there is an overall reduction in the blood flow into the Circle of Willis by virtue of significant stenosis or occlusion to a number of these inflow arteries. This leads to non-focal ‘low flow’ neurological episodes. This situation is uncommon.

More common and significant is the embolisation of plaque material from stenosed internal carotid arteries into the end organ branches of the Circle, particularly the middle cerebral artery, which is responsible for clinically important focal neurological syndromes.

Therefore, it is important to learn lessons from the mechanisms which are responsible for atherosclerosis throughout the body's arterial tree. We can, to a certain extent, extrapolate what is seen in the non-cerebral vascular tree to the situation which arises in carotid artery stenosis. However, this needs to be done so with a degree of caution. Carotid arterial disease is a unique situation and, where possible, research to be applied to atherosclerotic carotid stenosis should be studied in carotid atherosclerosis and applied directly, as opposed to inferred wholly from what is seen in plaques from elsewhere in the body.

1.2.2 A Brief History of Carotid Endarterectomy

The first open carotid revascularisation procedure reported was performed in 1954 by Harry Hubery Grayson ("Felix") Eastcott at St Mary's Hospital, London (Eastcott et al. 1954). The indication for surgery in this landmark case was, what was described as, crescendo transient ischaemic attack, and involved the resection of the diseased arterial segment and vascular reconstruction by direct anastomosis. The first carotid endarterectomy (CEA) was reported by Michael DeBakey, the first of 1,155 cases undertaken over 11 years from 1954 (Debakey et al. 1965). However, some controversy exists over the claim of the first carotid endarterectomy, with reports that this was achieved – but not published – by Stanley Crawford (Crawford et al. 1966; Robertson 1998).

1.2.3 Intervention for Symptomatic Carotid Stenosis

Discussions regarding intervention for carotid stenosis have centred largely on symptomatic status. Intervention, in the form of CEA, for symptomatic carotid stenosis has been supported by two major trials: the European Carotid Surgery Trial (ECST) (ESCT 1998) and the North American Symptomatic Carotid Endarterectomy Trial (NASCET) (NASCET 1991), both of which showed a long term significant reduction in stroke and death rates with CEA. Furthermore, in the context of symptomatic disease, benefit was related to the degree of stenosis. At two years, NASCET demonstrated an absolute risk reduction with CEA of 8.4% and 15.0% for 50-69% and 70-99% stenosis, respectively (NASCET 1991). ECST, likewise, showed that risk was reduced by 5.7% and 21.2% at 5 years (ESCT 1998; Rothwell et al. 2003b). The evidence has been re-evaluated by an expert working party of the European Society for Vascular Surgery (ESVS), with intervention stated to be indicated in symptomatic patients with stenosis greater than 70% (Liapis et al. 2009). The caveat is now in place that CEA is recommended for individuals with stenosis of greater than 50% where the peri-operative risk of stroke and death is less than 6%, and surgery should be undertaken within 2 weeks of symptoms (Naylor 2007; Liapis et al. 2009).

1.2.4 The Great and Ongoing Debate: Revascularisation for Asymptomatic Carotid Stenosis

Two key trials investigating CEA in asymptomatic carotid disease have been completed. The Asymptomatic Carotid Atherosclerosis Study (ACAS) randomised 1,662 patients with asymptomatic carotid stenosis of 60-99% to either CEA or medical therapy. ACAS found that CEA afforded a significant reduction in TIA and stroke, but not major stoke and death (ACAS 1995). The benefit of CEA was not seen in women. The Asymptomatic Carotid Surgery Trial (ACST) randomised almost twice as many patients as ACAS (3,120 patients), also with asymptomatic 60-99% carotid stenosis, to either immediate or deferred CEA. ACST reported a significant reduction in all strokes at 5 years of 6.4% versus 11.8% in the immediate versus deferred CEA groups, respectively (Halliday et al. 2004). This represented a 5.4% net benefit with CEA which, when subgroup analysis based upon gender was undertaken, revealed a non-significant 4.1% absolute risk reduction in women and a significant 8.2% benefit in men. Three years was required to counterbalance the operative risk in women (Halliday et al. 2004). The ESVS recommends surgical intervention in males aged less than 75 years with an asymptomatic stenosis of 70-99% where the peri-operative stroke and death risk is less than 3%. The benefit conferred by intervention in women with asymptomatic carotid stenosis is less clear, therefore CEA is recommended in younger, fit females (Liapis et al. 2009). Alongside this, there has been an improvement in best medical therapy (BMT) which should reduce the benefit derived from CEA. However, surgery is becoming safer with peri-operative stroke and death rates in CEA falling, implying that the benefit from surgery could be maintained – further work is necessary to confirm or refute these hypotheses.

The controversy surrounding the management of asymptomatic carotid stenosis is such that it has been the subject of a recent heated transatlantic debate which was published in both the Journal of Vascular Surgery (Schneider and Naylor 2010a), and the European Journal for Vascular and Endovascular Surgery (Schneider and Naylor 2010b). There was a similar recent debate presented in the British Medical Journal (Roffi 2010; Spence 2010). In these debates, some experts have called for CEA in all individuals with asymptomatic carotid stenosis, whilst others have recommended that none have revascularisation and be treated with BMT alone.

The need for risk stratification in the appropriate case selection for intervention in asymptomatic carotid stenosis has been called for (Davies et al. 2010a; Rockman and Riles

2010). It is important to consider at all stages in the decision making process that asymptomatic carotid intervention is a prophylactic undertaking.

1.3 STROKE RISK STRATIFICATION

Risk stratification, here, describes efforts to identify those (predominantly) asymptomatic carotid plaques which are more likely to produce emboli and hence cause stroke. Traditionally, stroke risk stratification has centred on the degree of internal carotid artery luminal narrowing and the presence of recent focal neurological symptoms pertaining to the ipsilateral cerebral hemisphere. ACST (Halliday et al. 2004; Halliday et al. 2010) highlighted the need to identify a subgroup of asymptomatic individuals that would benefit from intervention. The identification of high-risk plaques that will cause acute cardiovascular events is an unmet clinical need, and has inspired an intense research effort in the field of imaging and biological markers (Libby et al. 2002; Koenig and Khuseyinova 2007). This has been in the hope that non-invasive preventative screening tools may be developed.

To date, risk stratification has considered age, life expectancy and quality of life, but has otherwise focused on structural plaque features. The main structural predictor is degree of luminal stenosis as reported by the landmark European (ECST 1991) and North American (NASCET 1991) trials, but it is important to remember that these studied symptomatic individuals. Luminal stenosis was assessed in these trials using conventional angiography, however duplex ultrasonography is the main imaging modality used to estimate stenosis by velocity criteria (Oates et al. 2009).

The Asymptomatic Carotid Stenosis and Risk of Stroke (ACSRS) study confirmed, in asymptomatic individuals, a relationship between the degree of stenosis, as assessed by duplex ultrasound, and cerebral hemisphere ischemic events (relative risk 1.6) (Nicolaides et al. 2005). This study also showed that a combination of duplex-assessed stenosis, contralateral hemisphere transient ischemic attack and renal impairment (creatinine >85 μmol/L) defined a high-risk asymptomatic subgroup. Plaque echogenicity on duplex ultrasound, has been linked with histological features of instability (Gray-Weale et al. 1988; Sztajzel et al. 2005). There has been conflicting evidence for the role of plaque echolucency in the context of asymptomatic carotid stenosis (Polak et al. 1998; Gronholdt et al. 2001; Mathiesen et al. 2001), and hazard ratios have not been sufficient to warrant translation into clinical practice (Shalhoub and Davies 2010).

A cost-effective method of identifying those at high risk of stroke would provide substantial benefits to patients, surgeons, neurologists and the taxpayer. Improving the predictive test(s) of those at risk this hopes to offer:

1. A personalised risk estimate to facilitate decision making with regard to surgery, empowering both patients and clinicians;
2. A reduction in unnecessary numbers of CEAs;
3. A surgical cost and bed day reduction;
4. A new surrogate endpoint for studies of plaque stabilising therapies; and
5. Determining intervention criteria for future interventional trials, including those investigating carotid artery stenting.

As per point 5, risk stratification of carotid atherosclerosis will not only facilitate the decision making process with regards whether to intervene on asymptomatic stenoses, but may also help with the choice of intervention, *i.e.* case selection for carotid artery stenting (CAS). The importance of the latter comes with the publication of results of recent randomised controlled trials which have failed to show non-inferiority of CAS as compared with carotid endarterectomy (CEA), for example the Endarterectomy Versus Angioplasty in Patients with Severe Symptomatic Carotid Stenosis (EVA-3S) trial (Mas et al. 2008). Furthermore, having the capacity to risk stratify atherosclerosis *in vivo* may permit the monitoring of response to plaque stabilising therapies.

It is likely that risk stratification will be multifactorial and rely on a combination of the following:

- Clinical parameters
- Imaging
    - Structural
    - Functional
- Biomarkers

A ‘high risk’ asymptomatic group may to be defined by an ‘overlap’ region in the imaging signal, molecular or biomarker levels from plaques or patients with plaques that are symptomatic and those that are asymptomatic.

It is also important to consider what level of risk to benefit a patient is willing to accept and consider patients' perception of risk. Acknowledging this, with regards the management of particularly asymptomatic carotid stenosis, coupled with a recognition of the importance of patient choice and involvement in the decision-making process when it comes to their care, our group has conducted and published work on patient preference in asymptomatic carotid disease (Jayasooriya et al. 2011).

1.3.1 The 'Obsession' with Degree of Luminal Stenosis

Relying solely on the degree of carotid stenosis during the decision-making process for intervention is inadequate as: (1) there is a lack of reliable correlation between the non-invasive imaging currently in widespread use and the invasive catheter angiography employed in the large studies upon which degree of stenosis criteria were established; (2) there are inherent errors in estimating degree of stenosis by invasive catheter angiography; and (3) – and perhaps most importantly – this disregards the fact that stroke risk is also dependent on plaque *stability* and, in the case of symptomatic stenosis, the number of ischaemic events (Ahmed et al. 2010; Archie 2010). This challenge has been recognised for some time in the context of the coronary arterial territory (Topol and Nissen 1995).

Following a study of CEA for symptomatic but 'haemodynamically insignificant' carotid stenosis, relying only – or even largely – on the degree of luminal narrowing when referring patients with even symptomatic carotid stenosis for carotid intervention has been considered by some as inadequate: it overvalues hypoperfusion and undervalues embolisation as the mechanism of ischaemic events (Ahmed et al. 2010). Indeed, we are not treating the lumen, we are treating the plaque.

The ACST (Halliday et al. 2004; Halliday et al. 2010), a recent Cochrane review (Chambers and Donnan 2005) and others (Inzitari et al. 2000) have demonstrated the number needed to treat (NNT) for asymptomatic carotid stenosis as being more than 16 (and even up to 32) to prevent a single stroke. This is considerably higher than in symptomatic patients, where it is 6 to 13 (Rothwell et al. 2003a). One reason for this difference in NNT is that the use of carotid luminal stenosis is a poor risk predictor in asymptomatic patients (Nicolaides et al. 2005). Hence it is estimated that up to 94% of asymptomatic surgery could be avoided (Naylor et al. 2009).

1.4 PLAQUE BIOLOGICAL ATTRIBUTES AND STABILITY

Recently, biological attributes of atherosclerotic plaque have been acknowledged as key determinants of future thrombo-embolic events. These biological attributes are responsible for a number of closely inter-related processes that are felt to be causally linked to plaque vulnerability and include (Figure 2):

- Inflammation (inflammatory cell recruitment and activation) (Discussed in depth in Section 1.5)
- Matrix degradation
- Angiogenesis
- Intra-plaque haemorrhage
- Apoptosis
- Autophagy
- Hypoxia

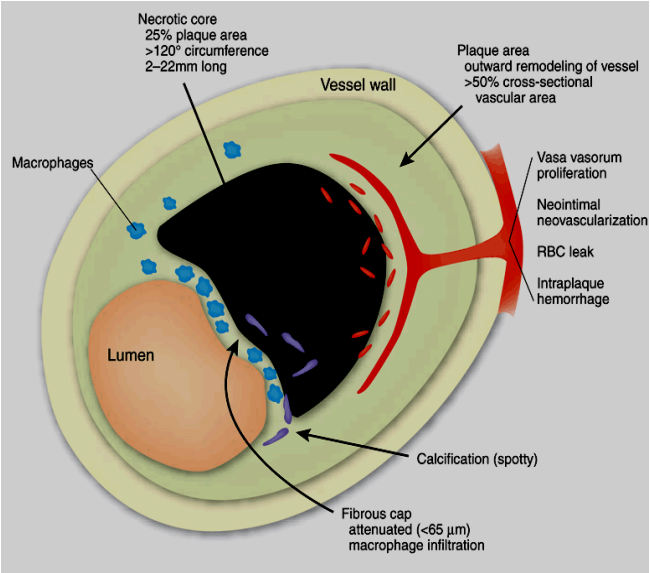


Figure 2 Summary of biological attributes contributing to atheromatous plaque instability

A diagrammatic representation of the numerous important inter-related factors responsible for plaque vulnerability (Narula and Strauss 2007).

1.4.1 Angiogenesis

Associations between human plaque vulnerability and angiogenic activity were originally noted in the late 1980s (Alpern-Elran et al. 1989). Subsequently it was found that plaques bearing hallmarks of vulnerability, including inflammation, haemorrhage, lipid accumulation

and thin fibrous caps, are also associated with increasing neovascularisation (de Boer et al. 1999; McCarthy et al. 1999a; Moreno et al. 2004). Neovascularisation appears to be an early feature of atherosclerosis, predating macrophage infiltration (Fleiner et al. 2004), and as the plaque progresses so too does intimal neovascularisation (Chen et al. 1999).

The majority of studies show carotid plaques retrieved at endarterectomy have many more microvessels and transcripts known to promote neovascularisation when they originate from symptomatic, compared to asymptomatic patients (McCarthy et al. 1999a; Mofidi et al. 2001; Tureyen et al. 2006; Dunmore et al. 2007). Statins have been shown to reduce this intra-plaque angiogenesis (Koutouzis et al. 2007). Symptomatic plaques, in addition, have been shown to contain abnormal, immature or 'incompetent' vessels that may precipitate plaque instability through their acting as sites of vascular leakage and so inflammation (McCarthy et al. 1999a; McCarthy et al. 1999b; Dunmore et al. 2007), or involvement in intra-plaque haemorrhage.

1.4.2 Intra-Plaque Haemorrhage

Intra-plaque haemorrhage, as identified by staining for the red blood cell membrane protein glycophorin A, has been described by Virmani et al as an important feature of unstable atherosclerotic lesions. Furthermore, effective clearance of extracellular haemoglobin is thought to attenuate oxidative haem toxicity, presumed to contribute to plaque instability. In unstable plaques intraplaque haemorrhage (by glycophorin A immunohistochemistry) has been shown to be positively associated with haemoglobin scavenger receptor (CD163) expression and lipid peroxidation in macrophages (by 4-hydroxy-2-noneal) (Crea and Andreotti 2009; Yunoki et al. 2009).

1.4.3 Matrix Degradation

A number of studies have directly implicated MMPs as having an integral role in these processes. For example, studies utilising multianalyte profiling platforms with cell cultures from human carotid endarterectomy plaques have shown that MMPs-1, 2, 3, 9 and 14 are produced by these cells (Monaco et al. 2004). MMPs have also been linked with smooth muscle cell (SMC) migration and accumulation in the intima (Southgate et al. 1996), which is known to be a key step in the formation of atherosclerotic plaques (Bendeck et al. 1994; Zempo et al. 1994). In a rodent model of balloon-injured carotid arteries, viral transfection of baboon TIMP-1 limited SMC migration both *in vivo* and *in vitro*, this effect being reversed by antibodies against TIMP-1 (Forough et al. 1996), further implicating MMP action in atherosclerosis.

1.4.4 The Language of Atherosclerotic Risk and Vulnerability

The term "plaque rupture" in human pathology is not controversial and describes a structural defect in the plaque fibrous cap, with exposure of the thrombogenic necrotic core to blood. This phenomenon is not commonly seen in atheroma-prone mice having not progressed to such a stage (Schwartz et al. 2007), hence adding complexity in relation to the terminology of risk in atherosclerosis. Murine plaques have a superficial xanthoma (including laterally) which penetrates the relatively thin fibrous cap, and plaque 'disruption' may occur due to cell death in the lateral xanthoma (Schwartz et al. 2007).

A need for agreement on nomenclature when referring to high risk, vulnerable and thrombosis-prone (these terms being synonyms) atheromatous plaques has been recognised and an agreement on the use of this terminology has been published (Schaar et al. 2004). This document employs terms as per the definitions in that Special Article.

1.5 INFLAMMATION AND ATHEROSCLEROSIS

Progress has been made in refining our understanding of the process of inflammation which underlies atherosclerosis since the early descriptions by Rudolf Virchow during the 19th century (Mayerl et al. 2006; Methe and Weis 2007) and subsequently Russell Ross in the late 1990s (Ross 1999; Haque et al. 2008; Ridker et al. 2008; Full et al. 2009). Local rheological factors, such as low and oscillatory (with vortices) blood-to-wall shear stress dictate the location of atherosclerotic plaques to characteristic points along the vasculature (Cheng et al. 2006; Caro 2009). The development of an atherosclerotic plaque begins with the recruitment of blood-borne inflammatory cells at sites of lipid deposition (Glass and Witztum 2001) or injury, where they produce pro-inflammatory cytokines and chemokines, growth factors, extracellular matrix degradation enzymes, and pro-angiogenic mediators (Ross 1999; Hansson 2005). It is worth noting that cytokines are signalling molecules involved in communication between cells. Chemokines are a subgroup of cytokines that are chemotactic, *i.e.* **chemo**tactic cyto**kines**. There is considerable interaction between immune cells via cytokines, and the key interactions have been summarised in Figure 3.

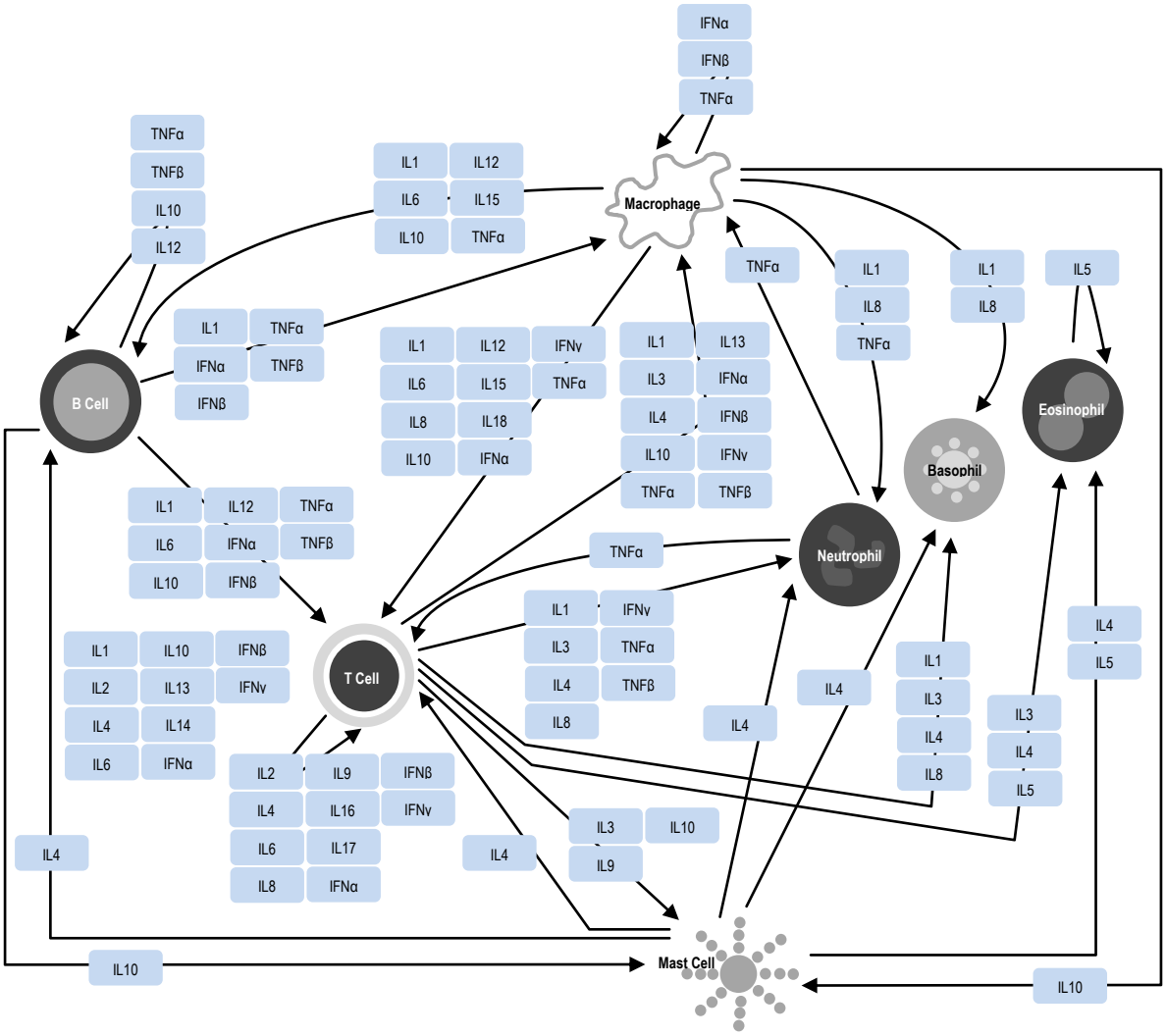


Figure 3 Summary of known interaction between immune cells, through cytokines

A diagrammatic representation of the cells of origin and target cells of key cytokines. This also highlights the cross-communication between innate and adaptive divisions of the immune system.

Atherosclerosis shares features with diseases caused by chronic inflammation (Full et al. 2009). Inflammation is intrinsically linked with disease activity, as the numbers of monocyte-macrophages infiltrating the plaque (Davies et al. 1993) and their location at plaque rupture-sensitive sites (such as the fibrous cap and areas of erosion (van der Wal et al. 1994; Virmani et al. 2003)) is related to plaque vulnerability. Moreover, lymphocyte abundance and their activation markers relate to plaque activity (van der Wal et al. 1994). Macrophage differentiation is acknowledged as critical for the development of atherosclerosis (Gleissner et al. 2010). The intimate relationship between atherosclerosis and inflammation is further exemplified by the involvement of cytokines and chemokines at all stages of the process of atherosclerosis (Tedgui and Mallat 2006). The extent of the inflammatory infiltrates and their strategic location within the protective fibrous cap is associated with plaque rupture and/or

thrombosis (Mauriello et al.). Adventitial inflammation has also been described (Grabner et al. 2009), and is linked with an expansion of the adventitial *vasa vasorum* in unstable atherosclerosis (Dunmore et al. 2007). The inflammatory nature of atherosclerosis is supported by the association between circulating plasma inflammatory markers, particularly C-reactive protein, with cardiovascular outcomes, even in the absence of dyslipidaemia (Ridker et al. 2008). Further evidence for a link between systemic inflammation and cardiovascular disease is the increased incidence of cardiovascular events in chronic inflammatory conditions, such as inflammatory arthritis and systemic lupus erythematosus (Haque et al. 2008; Full et al. 2009). The expanding knowledge base regarding inflammation in atherosclerosis has resulted in a keen interest in targeted therapeutics and functional imaging tools for the high-risk atherosclerotic plaque (Narula and Strauss 2007).

1.5.1 Innate Immunity – A Key Player in Atherosclerosis

How is inflammation established and maintained within an atherosclerotic plaque? Inflammation in physiological conditions is a self-limiting ancient protective mechanism that defends the host from invading pathogens. It relies on two arms: innate immunity and adaptive immunity, with these systems involved in all stages of atherosclerosis, from initiation and progression all the way through to complications (Packard et al. 2009). Innate immunity is activated immediately upon encounter with the pathogen and is executed primarily by myeloid cells with the participation of some "innate" lymphocyte sub-populations. Adaptive immunity is a second line of defence that is based upon the generation of antigen-specific recognition apparatus at cellular (T cell receptor) and humoral (antibody) levels.

In the past decade it has become apparent that the innate arm of the immune inflammatory response is not merely a concoction of non-specific responses and phagocytosis. Rather it is the main orchestrator of the subsequent adaptive responses and is able to sense pathogen associated molecular patterns (PAMPs) with a specificity which was previously unsuspected. In inflammatory conditions, including atherosclerosis, the immune inflammatory apparatus is chronically activated, either due to the persistence of pro-inflammatory stimuli or due to the failure of regulatory mechanisms that should facilitate resolution. Significant progress has been made in the field linking innate immune sensors to the recognition of cholesterol (Duewell et al. 2010) and modified lipoproteins (Miller et al. 2003; Miller et al. 2005; Stewart et al. 2010b). Thus diverse innate immune signalling pathways have been seen to cooperate to induce and maintain inflammation upon exposure to exogenous and, importantly, endogenous molecular patterns (Cole et al. 2010; Duewell et al. 2010).

The most abundant cell types within the atherosclerotic plaque are innate immune cells, such as monocyte-macrophages, dendritic cells (DCs) and mast cells. Monocytes-macrophages came to the forefront of research owing to new awareness that they may represent a more heterogeneous and phenotypically plastic population than previously anticipated.

1.5.2 Macrophage Heterogeneity in Atherosclerosis

More than a century after Élie Metchinkov was awarded the Nobel Prize for discovering the function of the macrophage, there is still considerable interest in the cell type which (in 1908) he credited with influencing development, ensuring homeostasis, and protecting the host from infection through a process he described as 'innate immunity' (Nathan 2008).

Macrophages are a heterogeneous population of cells that adapt in response to a variety of micro-environmental signals; their phenotype is very much a function of environmental cues (Van Ginderachter et al. 2006; Waldo et al. 2008). In a nomenclature mirroring Th1 and Th2 polarisation, macrophages are usually defined as M1 or M2 (Martinez et al. 2006). Characteristic cytokine and chemokine signatures pertaining to human monocyte-to-macrophage differentiation and M1/M2 macrophage polarisation (Table 1) have been described (Martinez et al. 2006; Mantovani et al. 2009).

M1 > M2	**M2 > M1**
CXCL11	Insulin-like growth factor 1
CCL19	CCL23
CXCL10	CCL18
Tumour necrosis factor ligand superfamily, member 2	CCL13
CCL15	Bone morphogenic protein 2
Interleukin 12B	Hepatocyte growth factor
Interleukin 15	Fibroblast growth factor 13
Tumour necrosis factor ligand superfamily, member 10	CXCL1
Interleukin 6	*Transforming growth factor β receptor II*
CCL20	*CXCR4*
Visfatin	*Mannose receptor C type 1 (CD206)*
Endothelial cell growth factor	
CCL1	
CCL17	
CCL22	
CCL13	
Transforming growth factor β2	
CCR7	
Interleukin 2 receptor α chain	
Interleukin 15 receptor α chain	
Interleukin 7 receptor	

Table 1 Cytokines and chemokine gene expression in human macrophage polarisation

Cytokine and chemokine genes, and those of receptors (in italics), known to be differentially transcribed in human M1 and M2 macrophage in vitro polarisation (Adapted from (Martinez

et al. 2006) and (Waldo et al. 2008)). CCL2 was upregulated in M-CSF differentiated macrophages in one study (Waldo et al. 2008), whilst relatively increased by GM-CSF in another (Martinez et al. 2006).

Classically activated (M1) macrophages were the first to be characterised (Gordon 2003; Gordon 2007). M1 macrophages are pro-inflammatory and participate in tissue destruction. Alternatively activated (M2) macrophages contribute to wound healing and regulation of inflammatory processes (Mosser and Edwards 2008).

Macrophage phenotypic polarisation may have a role in the fate of an atherosclerotic plaque. The plaque is an environment with a strong skew towards Th1 lymphocytic responses, resulting in high levels of IFNγ (Hansson 2008; Mallat et al. 2009) which could in theory privilege M1-type macrophage polarisation. However, studies thus far have demonstrated macrophage heterogeneity within atherosclerosis, supporting that both M1 and M2 macrophages are present in human and murine atherosclerotic lesions. In an $ApoE^{-/-}$ murine model of atherosclerosis, early lesions were seen to be infiltrated by M2 (arginase I^{+}) macrophages (Khallou-Laschet et al. 2010). As lesions progressed a phenotypic switch was observed, with an eventual predominance of M1 (arginase II^{+}) macrophages. Upon exposure to the oxidised phospholipid 1-palmitoyl-2-arachidonoyl-sn-3-phosphorylcholine (oxPAPC), murine macrophages adopted a previously undescribed phenotype (Figure 4) (Kadl et al. 2010). A reduction in the expression of genes characteristic of both M1 and M2, coupled with an up-regulation of a unique gene signature that includes haemoxygenase 1, was observed. This population, termed Mox macrophages, are nuclear factor erythroid 2-like 2 (Nrf2)-dependent and have been shown to comprise approximately 30% of all macrophages in advanced atherosclerotic lesions of $LDLR^{-/-}$ mice (Kadl et al. 2010). A variety of subtypes have been described which are considered to fall under the umbrella of alternatively activated M2 macrophages (Mantovani et al. 2004; Mosser and Edwards 2008). An example of this occurs with administration of IL33 (which is functionally atheroprotective (Miller et al. 2008)) to genetically obese diabetic (*ob/ob*) mice, resulting in increased production of Th2 cytokines and polarisation of adipose tissue macrophages to a $CD206^{+}$ M2 phenotype (Miller et al. 2010).

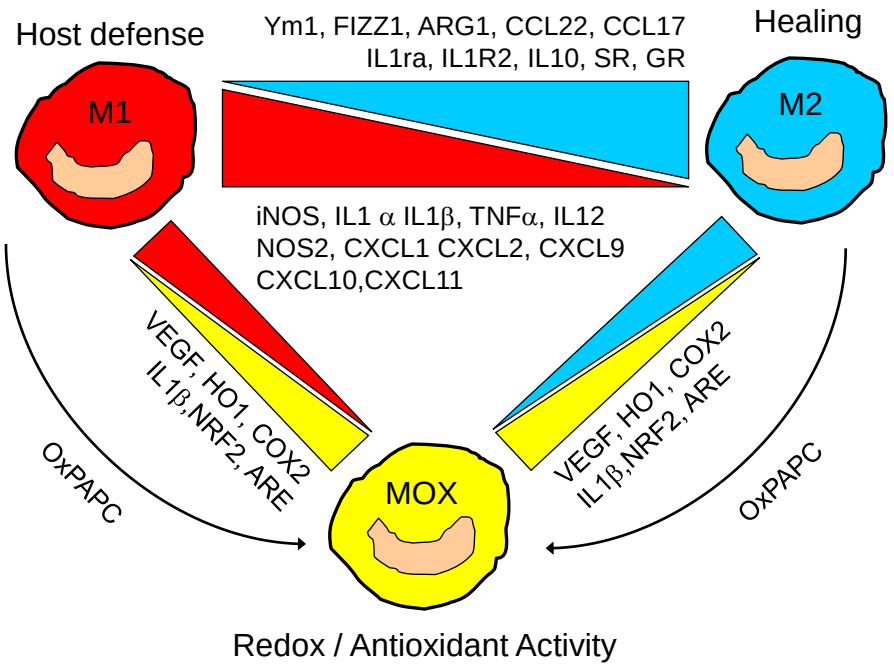


Figure 4 The relationship between M1, M2 and MOX macrophage phenotypes

Macrophages have classically been described as M1 and M2. These two phenotypes differ substantially with respect to the expression of macrophage associated genes. More recently, Kadl et al have described a new subset termed MOX macrophages (Kadl et al. 2010). These are induced by an environment rich in structurally defined oxidation products such as oxidised 1-palmitoyl-2-arachidonoyl-sn-3-phosphorylcholine (oxPAPC) and can be induced from an M1 or M2 phenotype. ARE, antioxidant responsive elements; ARG1, arginase 1; CCL, chemokine ligand; COX2, cyclo-oxygenase 2; CXCL, chemokine CXC motif ligand; FIZZ1, found in inflammatory zone 1; GR, galactose receptor; HO1, heme-oxygenase 1; IL, interleukin; IL1ra; interleukin 1 receptor antagonist; ILR2, interleukin 1 receptor type II, decoy receptor; iNOS, inducible nitric oxide synthase; NRF2, nuclear factor erythroid 2-like 2; SR, scavenger receptor; Ym1, chitinase 3-like 3 lectin.

In human lesions different macrophage phenotypes exist, and do so in different plaque locations. M2 ($CD68^+$ $CD206^+$) macrophages were seen to reside in areas more stable zones of the plaque distant from the lipid core, with their M1 ($CD68^+$ $CCL2^+$) counterparts displaying a distinct tissue localisation pattern (Bouhlel et al. 2007). Subsequent work has confirmed this, finding $CD68^+$ $CD206^+$ cells far from the lipid core (Chinetti-Gbaguidi et al. 2011). $CD68^+$ $CD206^+$ macrophages were also seen to contain smaller lipid droplets compared to $CD68^+$ $CD206^-$ (Chinetti-Gbaguidi et al. 2011). A subset of M2 macrophages has recently been detected in association with intraplaque haemorrhage in coronary atheromata (Boyle et al. 2009). These macrophages express high levels of CD163 (a scavenger receptor

that binds to haemoglobin-haptoglobin (HbHp) complexes). They also express low levels of MHC Class II and display low release of the reactive oxidative species hydrogen peroxide. Expression of CD163 by peripheral blood monocytes was not shown to be different between the $CD14^{+}$ $CD16^{+}$ and $CD14^{++}$ $CD16^{-}$ subsets. However, when monocytes were differentiated into macrophages in the presence of HbHp complexes for 8 days, they matured into a $CD163^{high}$ HLA-DR^{low} phenotype similar to the haemorrhage-associated macrophages within coronary plaques (Boyle et al. 2009). Differentiation into this macrophage subtype was dependent on the expression of CD163 and IL10 during *in vitro* blockade experiments. Interestingly, this polarisation was prevented by the incubation with specific inhibitors of endolysosomal acidification, such as chloroquine which is known to interfere with endosomal TLR signalling (Boyle et al. 2009).

1.5.3 Matrix Metalloproteinases and Tissue Inhibitors of Metalloproteinases in Macrophage Phenotype

Lesion development and stability are not only determined by the influx and differentiation of inflammatory cell subsets, but also their ability to act on vascular extracellular matrix. Importantly, the macrophage subtypes display a differential expression of matrix metalloproteinase (MMP) and tissue inhibitor of metalloproteinase (TIMP) (Chase et al. 2002). In particular, a subset of lesional foam cell macrophages characterised by a high expression of MMP14 (membrane type 1 MMP) and a low expression of TIMP3 were highly invasive and catabolic (Johnson et al. 2008). Moreover, such expression pattern of MMP14 and TIMP 3 was associated with markers of M1 polarisation (Johnson et al. 2008), whilst expression of MMP12 was associated with an M2-typical down-regulation of arginase I (Thomas et al. 2007). Thus MMP expression by macrophage subsets is also heterogeneous, further highlighting the different functionalities of these cells.

The heterogeneity of macrophage phenotypes in the various studies is an important feature of our current view of atherosclerosis. Studies assessing multiple markers in human and murine lesions are needed to map such degree of heterogeneity. How is such heterogeneity generated? It is likely to be the result of recruitment of different monocytes subsets, or stimuli provided by the plaque microenvironment. Gordon and Martinez have proposed a four-stage paradigm of macrophage activation (Figure 5), where differentiation through exposure to growth factors is the first stage (Gordon and Martinez 2010). This stage is followed by priming (through cytokines, particularly IFNγ and IL4), activation (by TLR or similar), and finally resolution and repair (mediated by IL10, transforming growth factor (TGF)-β, nucleotides, glucocorticoids or lipotoxins) (Gordon and Martinez 2010). This review will

explore the potential mechanisms leading to macrophage activation and polarisation in atherosclerosis.

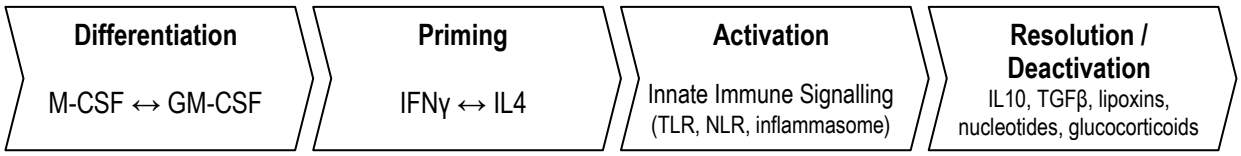


Figure 5 Multi-step paradigm of macrophage activation

Adapted from (Gordon and Martinez 2010). GM-CSF, granulocyte macrophage colony stimulating factor; M-CSF, macrophage colony stimulating factor; IFN, interferon; IL, interleukin; NLR, NOD-like receptor; TGF, transforming growth factor; TLR, toll-like receptor.

1.5.4 Recruitment of Monocyte Subsets to Atherosclerotic Plaques

In both mice and humans, monocytes comprise 5 to 10% of peripheral blood leukocytes (Cole et al. 2010). Two major circulating monocyte subsets have been described in humans and mice alike, the distinction made on the basis of size, granularity, and the differential expression of chemokine receptors and adhesion molecules (Geissmann et al. 2003). The two mouse monocyte sub-populations are represented approximately equally in murine blood; they are distinguished based upon their expression of CCR2, CX_3CR1 and Ly6C (Fleming et al. 1993)) (Strauss-Ayali et al. 2007). $CCR2^+$ CX_3CR1^{low} $Ly6C^+$ monocytes are termed 'inflammatory' monocytes, and $CCR2^-$ CX_3CR1^{high} $Ly6C^-$ are referred to as 'resident' monocytes (Geissmann et al. 2003; Mosser and Edwards 2008; Gautier et al. 2009).

Similarly to mouse monocytes, human monocytes can be separated into two groups based upon cell surface CD14 – a toll-like receptor (TLR) co-receptor sensing exogenous molecular patterns such as lipopolysaccharide (LPS) – and CD16 – a member of the family of Fc (Fragment, crystallisable) receptors FcγRIII. In humans, about 90% of monocytes are $CD14^{++}$ $CD16^-$ and termed 'classical' monocytes (Gautier et al. 2009; Steinman and Idoyaga). $CD14^+$ $CD16^+$ monocytes, which constitute the remaining minority, are referred to as 'non-classical' (Passlick et al. 1989; Ziegler-Heitbrock et al. 1993; Weber et al. 2000; Ancuta et al. 2003) (Table 2).

	Human	Mouse
Classical / Inflammatory	$CD14^{++}$ $CD16^{-}$ (Ziegler-Heitbrock 2007; Yona and Jung) (>90%)	$Ly6C^{+}$ $CCR2^{+}$ $CD62L^{+}$ CX_3CR1^{low} (Geissmann et al. 2003; Ingersoll et al.) (~50%)
Non-Classical / Resident	$CD14^{+}$ $CD16^{+}$ (Ziegler-Heitbrock 2007; Yona and Jung) (<10%)	$Ly6C^{-}$ $CCR2^{-}$ $CD62L^{-}$ CX_3CR1^{high} (Geissmann et al. 2003; Ingersoll et al.) (~50%)

Table 2 A comparison of human and murine monocyte subsets

The differences in surface receptor phenotypes are highlighted. The approximate abundance in peripheral blood is shown in brackets, however this may not reflect the proportions in other sites such as the spleen.

To date, monocyte phenotype data has centred largely on the murine system (Gordon 2003). Similarities between mice and humans may be accounted for, at least in part, by the expression of surface receptors. For instance, chemokine receptors CCR1 and CCR2 are highly expressed on both $CD16^{-}$ human and $Ly6C^{+}$ murine monocytes, and CX_3CR1 is increased on $CD16^{+}$ human and $Ly6C^{-}$ mouse monocytes (Palframan et al. 2001; Geissmann et al. 2003; Gordon and Taylor 2005; Tacke et al. 2007). More than 130 of these gene expression differences were conserved between mouse and human monocyte subsets, with many of these differences also confirmed at the protein level (Ingersoll et al.). A notable difference among these was the high expression of peroxisome proliferator-activated receptor γ (PPARγ, discussed in greater detail below) in $Ly6C^{-}$ mouse monocytes, but not the proposed $CD16^{+}$ counterpart. (Ingersoll et al.).

Two groups independently reported in 2007 that the $Ly6C^{+}$ inflammatory monocyte subset increases its representation dramatically in the peripheral blood of the hypercholesterolemic apolipoprotein E (ApoE) deficient mouse on a high-fat diet (Swirski et al. 2007; Tacke et al. 2007). Conversely, hypercholesterolemia did not affect $Ly6C^{-}$ monocytes and also discouraged the conversion of $Ly6C^{+}$ into $Ly6C^{-}$ monocytes. Other mechanisms proposed for this increase in $Ly6C^{+}$ monocytes during hypercholesterolemia include increased proliferation and reduced apoptosis (Swirski et al. 2009). $Ly6C^{+}$ monocytes are recruited to activated endothelium and are thought to represent the majority of infiltrating macrophages within atherosclerotic plaques (Swirski et al. 2007). Conversely, $Ly6C^{-}$ enter the atherosclerotic plaque in lower numbers and preferentially express CD11c upon entry (Tacke et al. 2007). This differential recruitment based upon Ly6C expression may condition the macrophage phenotype within the plaque, with reports that $Ly6C^{+}$ monocytes differentiate into cells that resemble M1 macrophages and that cells derived from $Ly6C^{-}$ monocytes exhibit M2

characteristics (Nahrendorf et al. 2007; Auffray et al. 2009; Geissmann et al. 2010a; Geissmann et al. 2010b).

Chemokine receptors are necessary for monocytes to traverse the endothelium (Tacke et al. 2007; Saederup et al. 2008) (Tedgui and Mallat 2006). $CX_3CR1^{-/-}$ (fractalkine receptor) (Combadiere et al. 2003; Lesnik et al. 2003), $CX_3CL1^{-/-}$ (fractalkine) (Teupser et al. 2004) and $CCR2^{-/-}$ (Boring et al. 1998; Dawson et al. 1999) mice (in the context of low density lipoprotein receptor (LDLR) or ApoE deficiency) exhibited a reduction in – but not elimination of – atherosclerosis. Furthermore, deficiency of CCR5 (the receptor for CCL5, a chemokine also known as RANTES) in $ApoE^{-/-}$ mice does not appear to be protective in the early stages of atherosclerosis (Kuziel et al. 2003). Subsequently, in a wire injury study also using the $ApoE^{-/-}$ mouse model, the authors found a significant reduction in the area neo-intima formation with concurrent CCR5 deficiency, but not with concurrent absence of the alternative CCL5 receptor CCR1 (Zernecke et al. 2006). More recently, a multiple knockout model has reaffirmed the thinking that CCL2 (MCP1), CCR5 and CX_3CR1 play independent and additive roles in atherogenesis (Combadiere et al. 2008). Combined inhibition of CCL2, CCR5 and CX_3CR1 in $ApoE^{-/-}$ mice results in a 90% reduction in atherosclerosis, which is related to progressive monocytopaenia (Combadiere et al. 2008; Saederup et al. 2008). However, chemokine receptor utilisation during recruitment to atherosclerotic plaques differentiates $Ly6C^+$ and $Ly6C^-$ monocytes. $Ly6C^+$ monocytes are recruited to mouse atherosclerosis via CCR2, CCR5 and CX_3CR1 (Swirski et al. 2009). Conversely, $Ly6C^-$ monocytes are recruited less frequently and through CCR5.

In human atherosclerosis, patients with coronary artery disease have increased numbers of circulating $CD14^+$ $CD16^+$ monocytes compared to controls (Wildgruber et al. 2009). Furthermore, these patients have raised levels of serum TNFα (Schlitt et al. 2004). There is, however, data to the contrary with the finding that inflammatory genes and surface markers were down-regulated in monocytes of patients with coronary atherosclerosis (Schirmer et al. 2009). Of relevance, $CD14^+$ $CD16^+$ monocytes have also been shown to exhibit pro-inflammatory and pro-atherosclerotic activity in a population of elderly human subjects. These activated monocytes exhibited increased interaction with endothelium and had higher expression of chemokine receptors (Merino et al. 2011). Other studies have suggested that the bone marrow is the source of these monocytes (Kuwana et al. 2003; Kamari et al. 2011).

1.5.5 Macrophage Differentiation in Atherosclerosis

Early work relating to the effect of the colony stimulating factors (CSFs) on macrophage phenotype was undertaken by Hamilton and colleagues (Hamilton 1993; Hamilton 2008). A

variety of groups have generated data using monocytes differentiated *in vitro*, via exposure to either M-CSF or GM-CSF (Hashimoto et al. 1999; Hamilton 2008). *In vitro* differentiation with M-CSF results in a macrophage phenotype close to that of M2 (Martinez et al. 2006). GM-CSF plays a role in the induction of a pro-inflammatory macrophage phenotype that resembles M1 polarisation, proficiently producing inflammatory cytokines such as TNFα and IL6, and being involved in tissue destruction (Martinez et al. 2006).

In further murine studies, both M-CSF and GM-CSF have been shown to be important in plaque development. Smith *et al* studied $ApoE^{-/-}$ mice crossbred with the osteopetrotic mutation of the M-CSF gene. These mice were fed a low-fat chow diet with the double mutants exhibiting significantly smaller proximal aortic lesions, at an earlier stage of progression and with fewer macrophages as compared with their control $ApoE^{-/-}$ littermates (Smith et al. 1995). The production of GM-CSF from smooth muscle cells leads to the activation of monocytes during atherogenesis (Stojakovic et al. 2007). In another study using the hypercholesterolaemic $ApoE^{-/-}$ mouse, animals on a high-fat diet were injected with doses of 10 µg/kg GM-CSF or G-CSF daily for 5 days on alternating weeks for a total of 20 doses during an 8 week period, finding that both G-CSF and GM-CSF treatment resulted in increased atherosclerotic lesion extent (Haghighat et al. 2007). LDLR-null mice have been employed in a study which combined 5-bromo-2'-deoxyuridine pulse labelling with *en face* immunoconfocal microscopy to demonstrate that systemic injection of GM-CSF markedly increased intimal cell proliferation, whilst functional GM-CSF blockade inhibited proliferation (Zhu et al. 2009).

In a key study, Waldo and colleagues examined human macrophages differentiated *in vitro* for 7 days with either M-CSF or GM-CSF (Waldo et al. 2008). They characterised gene expression, surface phenotype, cytokine production and lipid handling in these two macrophage groups. With regards to gene expression, they demonstrated differential expression of genes of inflammation (Table 1) and cholesterol homeostasis between the two groups, including that GM-CSF macrophages exhibited a ten-fold increased gene expression of PPARγ. M-CSF differentiated macrophages spontaneously accumulated cholesterol when incubated with unmodified low density lipoprotein (LDL), whilst GM-CSF differentiated macrophages took up similar levels only when exposed to protein kinase C. Macrophages differentiated with M-CSF were shown by immunofluoresence to express CD14 ($CD68^+$ $CD14^+$), whilst GM-CSF differentiated macrophages were $CD68^+$ $CD14^-$. Interestingly, human coronary plaque samples were shown to contain predominantly $CD68^+$ $CD14^+$ (Waldo et al. 2008).

1.5.6 Priming of Macrophages in the Atherosclerotic Plaque

Macrophages are M1-primed by exposure to interferon (IFN)-γ (Mantovani et al. 2004). The key role of IFNγ (McLaren and Ramji 2009) has been confirmed in experimental atherosclerosis whereby ApoE$^{-/-}$ IFNγ receptor$^{-/-}$ mice displayed a substantial reduction in lesion size compared to ApoE$^{-/-}$ (Gupta et al. 1997). This reduction was manifest alongside a reduced level of macrophages and T lymphocytes within the lesions. Furthermore, murine cardiac allografts sited in IFNγ$^{-/-}$ recipients had reduced transplant atherosclerosis (Raisanen-Sokolowski et al. 1998).

Alternative M2 polarisation has originally been described as the result of exposure to interleukin (IL4) (Loke et al. 2002; Gordon and Taylor 2005; Martinez et al. 2006; Bouhlel et al. 2007). M2 macrophages have a notable role in catabasis, the process inflammation resolution which when fails results in progression of atherosclerosis (Tabas 2010).

Wound healing macrophages, concerned primarily with tissue repair, are similar to the alternatively activated (M2) macrophages which have been described above. Wound healing macrophages establish their phenotype upon exposure to IL4 and/or IL13 from Th2 cells and granulocytes. IL4 is an early innate signal released during tissue injury, stimulating macrophage arginase to convert arginine to ornithine which is a step in extra-cellular matrix collagen production (Kreider et al. 2007). This ornithine is a precursor for polyamines which have an effect on cytokine production, affording wound healing macrophages regulatory capabilities (Cordeiro-da-Silva et al. 2004).

Regulatory macrophages, with anti-inflammatory activity, are most reliably defined and identified through IL10 levels or IL10/IL12 ratio (as they also downregulate IL12 (Gerber and Mosser 2001)). These develop in response to a large number of stimuli, including IL10 produced by regulatory T cells, TGFβ (Fadok et al. 1998), and glucocorticoids. The latter attenuate macrophage-mediated inflammation through inhibition of pro-inflammatory cytokine gene transcription (Sternberg 2006), nonetheless capacity for phagocytosis does not appear to be impaired by glucocorticoids (Liu et al. 1999). Unlike wound-healing macrophages, regulatory macrophages do not contribute to the production of extracellular matrix.

1.5.7 Macrophage Activation Pathways in Atherosclerosis

Following the priming stage, activation of macrophages is reliant upon ligation of pattern recognition receptors (PRR) (Mackaness 1964; Gordon 2003), namely nucleotide-binding oligomerisation domain (NOD)-like receptors (NLRs) and TLRs.

1.5.8 Toll-Like Receptor Signalling

TLRs are the most well-characterised PRRs, of which at least ten have been identified in humans (Yan and Hansson 2007). TLRs may be found on the cell surface, as in the case of TLRs 1, 2, 4, 5 and 6, or reside intracellularly (Medzhitov et al. 1997; Medzhitov 2001). TLRs are key activators of monocytes and macrophages.

Upon exposure to ligand, TLRs couple to signalling adaptors to induces two major downstream signalling pathways: the nuclear factor kappa B (NFκB) (Figure 6) and the interferon response factor (IRF) pathways. MyD88 is a universal adapter protein that carries signalling through all TLRs, except TLR3, leading to the activation of NFκB. MyD88-dependent signalling relies on recruitment of Mal (MyD88-adaptor like), which leads to the recruitment of the IL1 receptor-associated kinase (IRAK). Phosphorylation of IRAK signals to tumour-necrosis-factor-receptor-associated factor 6 (TRAF6). The subsequent nuclear translocation of NFκB and translation of inflammatory cytokines is driven by phosphorylation of the IκB kinase (IKK) complex upon activation of TRAF6. MyD88-independent signalling is via TRAM (TRIF-related adaptor molecule) and TRIF (TIR-domain-containing adaptor protein inducing IFNβ), and can activate both NFκB and IRF, inducing interferon synthesis. The importance of IL1/TLR signalling in atherosclerosis has been further highlighted by work implicating IRAK4 kinase in modified LDL-medicated experimental atherosclerosis (Kim et al. 2011).

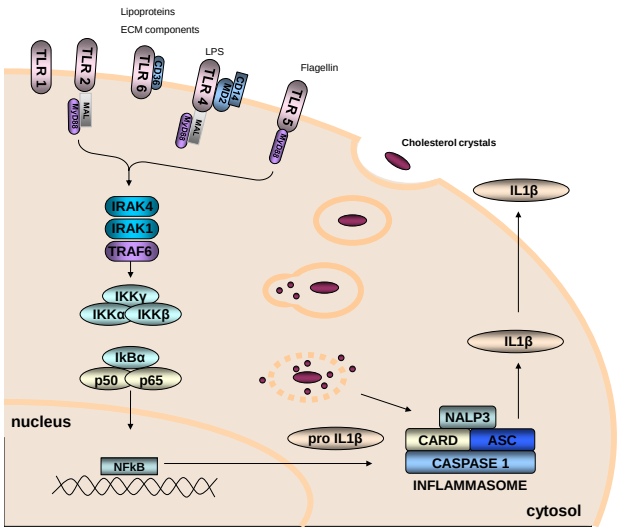


Figure 6 The interaction between TLR and inflammasome signalling

The interaction between innate signalling, through TLRs, and inflammasome signalling in the transcription and translation of the pro-inflammatory cytokine IL1. Oxidised LDL is a ligand for TLR, resulting in IL1 RNA transcription. Inflammasomes (which may be activated by cholesterol crystals (Duewell et al. 2010)) initiate intracellular pathways which result in the post-translational modification and, ultimately the secretion of IL1 protein. Therefore, a connection between TLR and inflammasome pathways in the innate inflammatory process in atherosclerosis is alluded to.

The most characterised recognition system is the one sensing LPS. Serum LPS-binding protein (LBP) transfers LPS to CD14, which delivers it to the co-receptor MD2 (Wright et al. 1990; Tobias et al. 1993). The availability of all members of the complex dictates the sensitivity of recognition of endotoxin at extremely low concentrations. Cells that do not express CD14, such as endothelial cells, are relatively unresponsive compared to $CD14^{+}$ monocytes (Wright et al. 1990; Tobias et al. 1993). CD14 acts as a co-receptor (along with TLR4 and MD2) for the detection of bacterial LPS. CD14, however, can only bind LPS in the presence of LBP. TLR2 may also be activated via scavenger co-receptors, including CD36 (Hoebe et al. 2005).

1.5.9 Toll-Like Receptor Agonists

Initially, ligands binding to PRRs such as TLRs on/in innate immune cells were believed to be of a pathogenic aetiology; molecules or small molecular motifs derived from, conserved within or associated with groups of microorganisms (such as bacterial LPS). These have been nominated pathogen associated molecular patterns (PAMPs). More recently, such ligands have been classified as danger associated molecular patterns (DAMPs) encompassing a wider definition which embodies the existence of endogenous danger signals. The concept that

oxidation reactions involving lipids, proteins and DNA produce non-microbial 'oxidation-specific epitopes' has emerged (Miller et al. 2011). Of particular interest is that host-derived oxidation-specific epitopes represent endogenous DAMPs, are recognised by PRRs and are capable of driving the inflammation seen in atherosclerosis (Miller et al. 2011).

DAMPs that may bind TLRs are numerous, some of which have been proposed as endogenous culprits in atherosclerosis. Examples of endogenous ligands to TLR2 include necrotic cell products (Li et al. 2001), apolipoprotein CIII (Kawakami et al. 2008), serum amyloid A (Cheng et al. 2008), versican (Kim et al. 2009). Hyaluronan fragment (Scheibner et al. 2006), biglycan (Schaefer et al. 2005), oxLDL (Xu et al. 2001; Holvoet et al. 2006) and heat shock proteins (Asea et al. 2002) have been shown to act through both TLR2 and TLR4. Long surfactant protein A (Guillot et al. 2002), tenascin C (Midwood et al. 2009), fibrinogen (Smiley et al. 2001), fibronectin EDA (Okamura et al. 2001), heparan sulphate (Kodaira et al. 2000), β-defensin 2 (Biragyn et al. 2002), amyloid β peptide (Stewart et al. 2010b) and minimally modified LDL (mmLDL) (Miller et al. 2005) act via TLR4 alone. TLR3 detects mRNA (Kariko et al. 2004; Cole et al. 2011), whilst TLR7 and TLR9 detect nucleic acid-containing immune complexes (Leadbetter et al. 2002; Boule et al. 2004). TLRs 5, 6 and 8 are yet to have endogenous ligands allocated to them (Cole et al. 2010).

Although both mmLDL and oxLDL are seen as ligands to TLR4, the pathways by which recognition occurs differ. The recognition of mmLDL is similar to that of LPS and involves CD14 and MD2 (Miller et al. 2003), whilst oxLDL initiates inflammatory responses through a TLR4/TLR6 heterodimer in association with CD36 but independently of CD14 (Stewart et al. 2010a). A lipidic component of LDL, namely oxPAPC, has been shown as capable of inducing IL8 transcription via TLR4 in a manner which is independent of both CD14 and CD36 (Walton et al. 2003b). Further work, however, has seen oxPAPC inhibiting TLR4-dependent IL8 induction, along with inhibition of E-selectin and CCL2, whilst IL1β and TNFα signalling remained unhindered (Walton et al. 2003a).

1.5.10 Toll-Like Receptor Expression in Atherosclerosis

TLRs are differentially expressed by the various cell types in atherosclerosis, with TLR2 and TLR4 found on monocytes, macrophages, foam cells and myeloid DCs, as well as smooth muscle cells and B lymphocytes (Cole et al. 2010). Human and mouse atherosclerosis is characterised by an increased expression of TLR1, TLR2 and TLR4 (and to some extent TLR5), mainly by macrophages and endothelial cells (Xu et al. 2001; Edfeldt et al. 2002). In mouse atherosclerosis, TLR4 expression is exclusively by macrophages (Xu et al. 2001). There has been shown to be co-localisation of p65 (an NFκB family member) with both TLR2

and TLR4 in macrophages in atherosclerosis (Edfeldt et al. 2002). This supports the role of TLRs not only in atherosclerotic lesion size, but also lesion stability. The differential expression of the various TLRs by monocyte subsets and macrophage subtypes remains largely unknown at present, however there is some data to support the relative transcription of TLR5 being higher in M2 polarised human macrophages as compared with M1 (Martinez et al. 2006).

The circulating monocytes of ApoE$^{-/-}$ mice with advanced atherosclerosis have increased TLR2 and TLR4 expression (Schoneveld et al. 2008). This is also the case for monocytes from patients with arterial disease when comparison is made with controls subjects (Methe et al. 2005; Geng et al. 2006; Shiraki et al. 2006; Kuwahata et al. 2009). Interestingly, enhanced TLR signalling is restricted to patients with acute coronary syndromes (Liuzzo et al. 2001a; Ashida et al. 2005; Versteeg et al. 2008).

1.5.11 Role of Toll-Like Receptors in Atherosclerosis

When recognising ligands, the majority of TLRs associate the signalling adaptor MyD88 to initiate an intracellular signalling cascade. MyD88 becomes engaged through the sensing of mmLDL in a TLR-dependent and TLR-independent manner (Miller et al. 2003; Bae et al. 2009). Studies involving the MyD88 knockout mouse have shown that serum cholesterol levels are related to the activation of innate immune signalling pathways. More specifically, removing the MyD88 pathway led to a reduction in aortic atherosclerosis (by approximately 60%) and a decrease in macrophage recruitment to the artery wall (by approximately 75%), associated with reduced chemokine levels (Bjorkbacka et al. 2004; Michelsen et al. 2004). In a functional human atherosclerosis study, a significant reduction of pro-inflammatory cytokines and MMPs was found after MyD88 inhibition (Monaco et al. 2009).

The role of TLR2 and TLR4 has been extensively studied in models of atherosclerosis. The first indication of a role for TLR4 in atherosclerosis came from the finding that C3H/HeJ mice – that hold a missense mutation of TLR4's cytoplasmic component – are resistant to atherosclerosis (Ishida et al. 1991; Nishina et al. 1993). In accordance, specific deletion of TLR4 in ApoE$^{-/-}$ mice resulted in a 24% reduction in whole aortic atherosclerotic lesion area and significantly attenuated macrophage infiltration within these lesions (Michelsen et al. 2004). TLR2 deletion in LDLR$^{-/-}$ mice limits lesion area by between a third and two-thirds (Michelsen et al. 2004; Mullick et al. 2005; Liu et al. 2008; Madan and Amar 2008), reducing intra-lesion inflammation as evidenced by a reduction in total infiltrating macrophage numbers (Liu et al. 2008; Madan and Amar 2008), and attenuates macrophage to smooth muscle cell ratio and extent of apoptosis (Madan and Amar 2008).

Both TLR2 and TLR4 are known to be important in post-vascular injury neo-intimal lesion formation (Vink et al. 2002; Schoneveld et al. 2005). In a hypercholesterolaemic rabbit model of atherosclerosis, carotid artery liposomal transfection of TLR2 and TLR4 cDNA revealed that upregulation of either TLR *alone* did not significantly affect carotid atherosclerosis. Interestingly, transfection of both TLR2 and TLR4 together resulted in a synergistic acceleration of atherosclerosis (Shinohara et al. 2007).

A different picture came from bone marrow chimera studies. Bone marrow transplantation from $TLR2^{-/-}$ to $LDLR^{-/-}$ mice was unable to prevent diet-induced atherosclerotic lesions (Mullick et al. 2005). Bone marrow transfer from C3H/HeJ to ApoE knockouts did not alter atherosclerosis susceptibility (Shi et al. 2000). Synthetic TLR2 ligand administered dramatically increases atherosclerosis in $LDLR^{-/-}$ mice, with TLR2 deficient bone marrow transfer into this model preventing TLR2 ligand-induced atheroma (Mullick et al. 2005). Such studies raise the question of whether TLR2 signalling in myeloid cells is relevant in atherosclerosis, as compared with TLR2 expression by cells resident in the arterial wall. Importantly, it supports the role of endogenous TLR2 ligand action on myeloid cells in atherosclerosis, with exogenous agonists activating TLR2 on cells of a non-myeloid lineage.

Oxidised phospholipids, oxLDL, saturated fatty acids, and lipoprotein A triggered *in vitro* apoptosis in macrophages, under conditions of endoplasmic reticulum stress, via a mechanism requiring both CD36 and TLR2 (Seimon et al. 2010). Subsequent *in vivo* work with $LDLR^{-/-}$ mice transplanted with $TLR2^{-/-}$ $TLR4^{-/-}$ bone marrow revealed a reduction in both macrophage apoptosis and atherosclerotic plaque necrosis as compared with $LDLR^{-/-}$ mice transplanted with wild-type bone marrow, offering insight into the contribution of TLR signalling in advanced atherosclerosis (Seimon et al. 2010).

Functional studies on human carotid endarterectomy specimens have shown sustained TLR2 activation in cells isolated from human atheromata (Monaco et al. 2009). TLR2 and MyD88 play a key role in NFκB activation, and in the production of inflammatory mediators CCL2, IL6, IL8, MMPs 1, 2, 3 and 9 (Monaco et al. 2009). Conversely TLR4, and its downstream signalling adaptor TRAM, were shown not to be rate-limiting for cytokine production in this context. This adds weight to the role of some (but not all) TLRs in plaque vulnerability.

Recent work has elucidated a protective role for TLR3 in the vessel wall (Cole et al. 2011). In a perivascular collar induced injury mouse model, the double stranded RNA analogue

poly(I:C) reduced neointima formation in a TLR3-dependent manner, with an increase in atherosclerosis with TLR3 deficiency in the context of ApoE knockout (Cole et al. 2011).

Importantly, TLR2, TLR4 and TLR9 ligands promote lipid uptake by macrophages and, hence, foam cell formation (Oiknine and Aviram 1992; Funk et al. 1993; Lee et al. 2008; Kim et al. 2009). Differentiated macrophages exhibit macropinocytosis (fluid phase uptake of lipids) which is dependent upon TLR4 (Choi et al. 2009).

Furthermore, and as alluded to above, TLR ligation may influence atherosclerosis through alterations in MMP and TIMP expression. The effect of LPS on human blood monocytes has been investigated and MMP3 is upregulated (Bar-Or et al. 2003), whilst MMPs 1, 2, 7, 10 and 14 and TIMPs 1, 2 and 3 are not upregulated by LPS (Welgus et al. 1990; Bar-Or et al. 2003). Controversially, two separate studies have found upregulation (Ardans et al. 2002) and no upregulation (Bar-Or et al. 2003) of MMP9 in human blood monocytes stimulated with LPS. In human macrophages (from various sites) meanwhile, MMPs 2, 3, 8, 9 and 14, and TIMP1 have all been upregulated by LPS (Shapiro et al. 1990; Welgus et al. 1990; Saren et al. 1996; Fabunmi et al. 1998; Herman et al. 2001).

1.5.12 NOD-Like Receptors and Inflammasomes and Atherogenesis

NLRs are PRRs that sense intra-cellular microbial and non-microbial signals, in a similar fashion to the extra-cellular detection of these entities by most TLRs. NLRs have the capacity to form large cytoplasmic complexes known as "inflammasomes" (Martinon et al. 2009) through the assembly of NLRs, caspase and apoptosis-associated speck-like protein containing a caspase recruitment domain (ASC). ASC acts to link the NLR and caspase, the latter of which are usually caspase 1 and 11 (Wang et al. 1998). The inflammasome acts as a scaffold for the activation of caspase 1 as its central effector molecule (Mariathasan and Monack 2007). Upon activation, inflammasome caspase 1 proteolytically activates pro-inflammatory cytokines, notably the conversion of pro-IL1β and pro-IL18 to IL1β and IL18, respectively.

It is largely agreed that inflammasome activation resulting in active IL1β release requires two separate signals (Burns et al. 2003). A priming signal may be triggered by TLR activation, with resultant NFκB production leading to pro-IL1β synthesis, as well as inflammasome components such as caspase 11 (Mariathasan and Monack 2007). Recognition of peptidoglycan by NOD1 and NOD2 can also trigger activation of NFκB signal transduction through Rip2 kinase (Yan and Hansson 2007). The second signal, which activates the caspase 1 of a complete inflammasome, allowing the conversion of available pro-IL1β to IL1β

includes activation by ATP of the $P2X_7$ purinergic receptor with potassium efflux. The second signal may also be achieved by PAMPs such as bacterial toxins and viral DNA, or other DAMPs including oxidative stress, large particles and ultraviolet light (Martinon et al. 2009).

Inflammasomes have been described in a number of inflammatory conditions (Martinon et al. 2009) and evidence for their role in atherosclerosis is emerging. The NLRP3 inflammasome is currently the most characterised inflammasome (Figure 6). Recent work has shown that cholesterol crystals activate the NLRP3 inflammasome, which in turn results in cleavage and secretion of IL1 family cytokines (Duewell et al. 2010). Furthermore, LDLR-deficient mice transplanted with NLRP3-deficient bone marrow and fed a high-cholesterol diet had markedly decreased early atherosclerosis and inflammasome-dependent IL18 levels (Duewell et al. 2010). $LDLR^{-/-}$ mice bone-marrow transplanted with ASC-deficient or IL-1α/β-deficient bone marrow and fed on a high-cholesterol diet had consistent and marked reductions in both atherosclerosis and IL18 production (Duewell et al. 2010). Furthermore, ASC deficiency also attenuates neointimal formation after vascular injury via reduced expression of IL1β and IL18, with $ASC^{-/-}$ bone marrow chimeras also exhibiting significantly reduced neointimal formation (Yajima et al. 2008). These findings taken together suggest that crystalline cholesterol acts as an endogenous danger signal, its deposition in arteries being an early cause rather than a late consequence of inflammation.

Both IL1 and IL18 signal through MyD88, and their absence in experimental mouse atherosclerosis also has the effect of limiting atherosclerosis development (Elhage et al. 2003; Kirii et al. 2003). Devlin *et al* showed that IL1ra knockout mice on a cholesterol/chocolate diet, exhibited a 3-fold decrease in non-high-density lipoprotein (HDL) cholesterol and a trend toward increased foam cell lesion area compared to controls (Devlin et al. 2002). Complementing this experiment they showed, conversely, that increased IL1ra expression (using an IL1ra transgenic/$LDLR^{-/-}$ mouse on a cholesterol-saturated fat diet) resulted in a 40% increase in non-HDL cholesterol levels. Thus concluding that under certain conditions, chronic IL1ra depletion or over-expression could have an important effect on lipid metabolism.

This was also verified in human atherosclerotic arteries (Dewberry et al. 2000), although more recently, IL1ra administration has been shown to have lesser effect on inflammatory molecule production when compared to TLR inhibition in the context of human atherosclerosis (Monaco et al. 2009).

1.5.13 Macrophage Deactivation Pathways in Atherosclerosis

PPARγ has recently been highlighted as an important determinant of macrophage phenotype and function (Figure 7), which may explain the favourable effect of PPARγ modulation in experimental atherosclerosis (Nakaya et al. 2009; Ishii et al.). PPARγ is a ligand-activated nuclear receptor involved in reverse cholesterol transport and other metabolic cellular activities (Gordon and Martinez 2010). Its anti-inflammatory properties occur through negative interference with nuclear factor κB (NFκB), signal transducer and activator of transcription (STAT), and activating protein 1 (AP1) pathways (Chinetti et al. 2000). PPARγ is strongly induced by IL4 (Bouhlel et al. 2007; Odegaard et al. 2007). PPARγ upregulation may also be stimulated by oxidised LDL, with PPARγ being highly expressed in the foam cells of atherosclerotic lesions, and ligand activation of PPARγ promoting oxidised LDL uptake and foam cell formation (Tontonoz et al. 1998).

The functional relationship between PPARγ and the wound healing M2-type macrophage phenotype (Straus and Glass 2007; Heilbronn and Campbell 2008) has been proposed through the positive correlation between PPARγ expression levels and the M2 markers CD206 (Coste et al. 2003), CD36 scavenger receptor (Tontonoz et al. 1998), IL10 (Kim et al. 2005) and alternative activated macrophage associated CC-chemokine 1 (AMAC1; CCL18) (Bouhlel et al. 2007). Primary human monocytes differentiated *in vitro* with IL4 in the presence of PPARγ agonist (termed M2γ macrophages) resulted in increased CD206 and reduced CD163 expression, above and beyond that which was seen with IL4 alone (Bouhlel et al. 2007) (Figure 7). M2γ culture supernatant exerted a greater anti-inflammatory effect on M1 macrophages as compared with M2 culture supernatant (Bouhlel et al. 2007). Subsequent work has shown that M2γ macrophages have down-regulation of the nuclear liver x receptor α with resultant enhanced phagocytosis but reduced cholesterol handling (Chinetti-Gbaguidi et al. 2011). PPARγ also limits MMP9 through inhibition of NFκB activation (Hetzel et al. 2003).

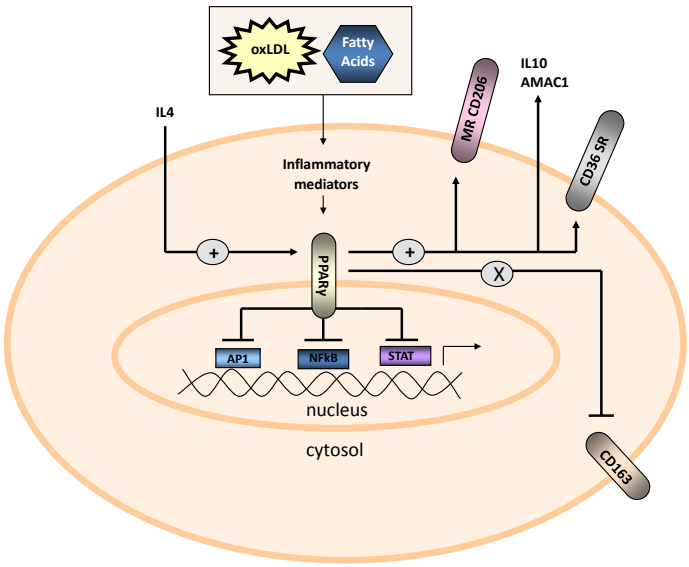


Figure 7 The influence of PPARγ on macrophage phenotype

Peroxisome proliferator-activated receptor γ (PPARγ) is a ligand-activated nuclear receptor with potent anti-inflammatory properties that modulates the immune inflammatory response. It has been observed in human atherosclerotic lesions and is involved in macrophage cholesterol homeostasis, cellular differentiation, lipid storage, insulin modulation, macrophage lipid homeostasis and anti-inflammatory activities. Molecules such as oxidised low density lipoprotein (oxLDL) or fatty acids may stimulate inflammatory mediators such as 9- and 13- hydroxyoctadecadienoic acid (HODE) generated via the 12,15 lipoxygenase pathway. These are ligands for PPARγ. IL4 is a cytokine that can stimulate PPARγ. PPARγ activation is also associated with the expression of M2 macrophage markers such as the mannose receptor (MR) also known as CD206 (Bouhlel et al. 2007). AMAC1, alternative activated macrophage associated CC-chemokine 1; AP1, activator protein 1; CD, cluster of differentiation; IL, interleukin; NFκB, nuclear factor kappa B; SR, scavenger receptor; STAT, signal transducer and activator of transcription.

However, in the clinical arena, PPARγ agnonists have been shown to have complex and opposing effects on circulating levels of pro- and anti-inflammatory molecules (Marx et al. 2003; Moulin et al. 2005; Glatz et al. 2010; Halvorsen et al. 2010). Furthermore, macrophages have been observed adhering to areas of intimal thickening in PPARγ-dependent manner (Fernandez 2008).

Therefore, monocyte-macrophage dichotomy is affected by the macro- and micro-environment, resulting in significant impact on the development and outcome of atherosclerotic disease. Rapid advances are occurring in the fields of atherosclerosis

inflammation and innate immunity, particularly the sensing of endogenous danger signals, foam cell generation, failure of egression, and the classical polarisation of leukocytes able to produce inflammatory mediators and matrix degrading enzymes. This work would benefit from being complemented by further research in the field of immunoregulation and adaptive immunity, with a clinical focus on dampening such host-detrimental responses.

Inflammatory monocyte levels are elevated during hypercholesterolemia and are preferentially recruited to atherosclerotic plaques. During disease progression, alternative activation of macrophages induced by M2 stimuli may have a resolving effect on disease. Activation of the immune system by endogenous lipid components of a lesion are now considered to be mediated by stimulation of the TLR and inflammasome pathways. Lipids and inflammation have been highlighted as cooperating in macrophage behaviour in atherosclerosis. Oxidised LDL is seen to signal through TLR (Miller et al. 2003; Miller et al. 2005; Stewart et al. 2010b), cholesterol crystals signalling through NLR (Duewell et al. 2010), and oxPAPC signalling via NRF2 (Kadl et al. 2010). The convergence of these pathways gives rise to the activation of resident monocyte-macrophages leading to cytokine and chemokine production. Moreover, TLR activation might have a role in biasing macrophage polarisation towards an M1 phenotype, together with Th1 lymphocytes present in the plaque. These exciting new findings highlight a wealth of novel potential therapeutic and diagnostic targets that may be exploited in the future treatment of cardiovascular disease.

1.6 IMAGING IN ATHEROSCLEROSIS

Imaging of atherosclerotic cardiovascular disease has certainly evolved from the time when only advanced plaques could be observed. Prospects in current imaging of atherosclerosis include: early detection of disease; stratifying individuals in accordance with their risk of developing signs, symptoms or complications of atherosclerotic lesions; assessing outcomes of novel treatment; and furthering our understanding of atherosclerosis biology (Sanz and Fayad 2008). Of particular interest is cellular and molecular imaging. It is important to consider the distinction between actively and passively targeted imaging.

It is noteworthy that with regards common imaging modalities, there is an inverse relationship between spatial resolution and sensitivity for contrast agent detection (Table 3) (Rudd et al. 2009).

Imaging Modality	Spatial Resolution	Sensitivity for Contrast Agent Detection
Contrast Enhanced Ultrasound (CEUS)	< 1 mm	single microbubble (1 – 10 µm)
Computed Tomography (CT)	< 1 mm	> millimolar
Magnetic Resonance Imaging (MRI)	~ 1 mm	> micromolar
Positron Emission Tomography (PET)	~ 3 mm	< nanomolar
Single Positron Emission Computed Tomography (SPECT)	> 4 mm	< nanomolar

Table 3 The inverse relationship between the relative spatial resolution and sensitivity for contrast agent detection of common imaging techniques

Modified from Inflammation Imaging in Atherosclerosis (Rudd et al. 2009). Ultrasound spatial resolution approximately 0.2 mm based upon a 7.3 MHz transducer for normal B-mode.

As can be seen from Table 3, none of the imaging techniques tend not to offer both high spatial resolution and contrast sensitivity. To overcome these limitations, there is the concept of integrated, hybrid or multimodal imaging, which combines multiple imaging modalities in a single platform and uses one machine for more than one type of imaging (Sanz and Fayad 2008). A typical example of this is positron emission tomography / computed tomography (PET/CT), which harnesses the contrast sensitivity of PET for functional assessment and the spatial resolution of CT for structural and anatomical aspects. The acquired images are then overlaid, employing fixed points as landmarks for accurate positioning. An exception to this generalisation, however, is CEUS, which has both high spatial resolution and good contrast sensitivity, coupled with excellent temporal resolution so allowing for the undertaking of dynamic investigations.

The features of an ideal imaging test, therefore, are:

- Accuracy;
- Reproducibility; and
- Generalisability (also termed applicability or external validity)

Molecular imaging has facilitated the development of platforms that can transport contrast agents to specific biological targets in atherosclerosis. “Theranostics” is the concept that, in the future, molecular diagnostics may be coupled with therapeutic agents, such that therapeutic delivery and diagnosis is simultaneous, targeted and limited in systemic toxicity (Rudd et al. 2009).

1.7 SYSTEMS BIOLOGY – THE '-OMIC' DISCIPLINES

1.7.1 The Complex Biology of Atherosclerosis

As described above in Section 1.4, atherosclerosis is a multi-stage entity characterised by the interaction between multiple biological processes. These centre upon inflammation, but also include: matrix degradation; angiogenesis; intra-plaque haemorrhage; oxidative stress; lipid metabolism; apoptosis; and autophagy (Narula and Strauss 2007). This being by no means an exhaustive list offers insight into the complexity (both within each process and between processes) of the biology of atherosclerosis development, its progression and the complications which can result from destabilisation of an atherosclerotic plaque.

1.7.2 The Utility of Effective Atherosclerosis Research

Effective atherosclerosis research has the facility to: elucidate the detail of the mechanisms responsible for atherosclerosis destabilisation; uncover targets for functional imaging to risk stratify atherosclerosis in terms of its likelihood to cause complications in a particular individual at a particular time (including the response to therapies initiated to lower risk); discover biomarkers or biomarker 'patterns' for high risk atherosclerosis; and contribute to the development of targeted plaque stabilising therapies. Furthermore, as atherosclerosis is a systemic condition, affecting the arterial tree throughout the body, an understanding of the focal atherosclerosis in the one arterial territory is important as it may be relevant to our understanding of atherosclerosis in other arterial territories.

Reflecting its share of the global burden of morbidity and mortality, the research of atherosclerosis has been increasing steadily over the past two decades (Figure 8). This was particularly the case since the late 1990s with the formal acknowledgement that atherosclerosis is an active process driven by inflammation (Ross 1999) – as opposed to the passive accumulation of lipid in an arterial wall.

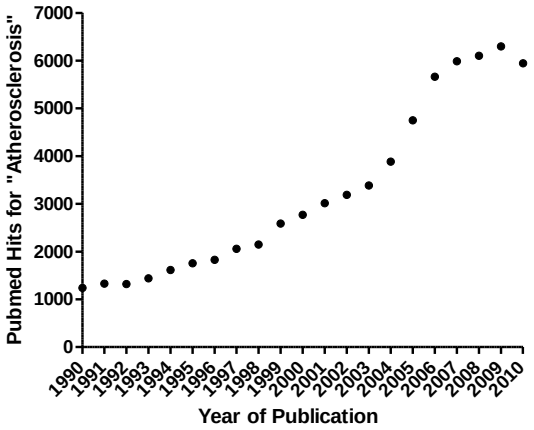


Figure 8 The rise of atherosclerosis research

A graph charting the year-on-year (non-cumulative) number of Pubmed indexed publications for the search term "atherosclerosis" in the two decades from 1990 to 2010. In 1990 there was just over 1,000 publications in a 12 month period, with approximately three times as many (2,771) in a twelve-year period in 2000, with a peak of 6,299 in 2010. Cumulatively, that represents 68,300 publications.

With various campaigns relating to atherosclerosis and the rise in research has come heightened awareness and knowledge, but also an increase in expectation among both the public and the scientific community. Critically, assertions have been made as regards the challenge presented in the assimilation and interpretation of such data, particularly by practicing clinicians (Fraser and Dunstan 2010). One of the numerous reasons for the quantity of publications is the use of low throughput laboratory techniques by focal research groups working in isolation. This results in the duplication of process and, often, data and publications based upon small numbers of samples. Such an approach, however, is essential particularly for (but not exclusively in) the validation of findings and is often driven by a very narrow experimental hypothesis. In this sense, traditional laboratory methodologies are reductionist in philosophy, understanding the complex processes underlying atherosclerosis by deconstructing them into constituent components or pathways.

1.7.3 A Systems Biology Approach

Systems biology is a term which describes a holistic and integrative approach to the understanding of physiology and pathology. By adopting a stance which is opposing (yet complimentary) to conventional research techniques, it offers an overview and – in many cases – looks at the 'net' biological effect imposed by a disease or non-disease state. To expand on this requires a reminder of the synthetic 'workflow' of a cell (Figure 9). What is

shown is a simplification of a single pathway in a single cell of a particular cell type. In reality, there are multiple interacting pathways in multiple cells of different types, with microenvironmental conditions asserting alterations at multiple levels on multiple pathways.

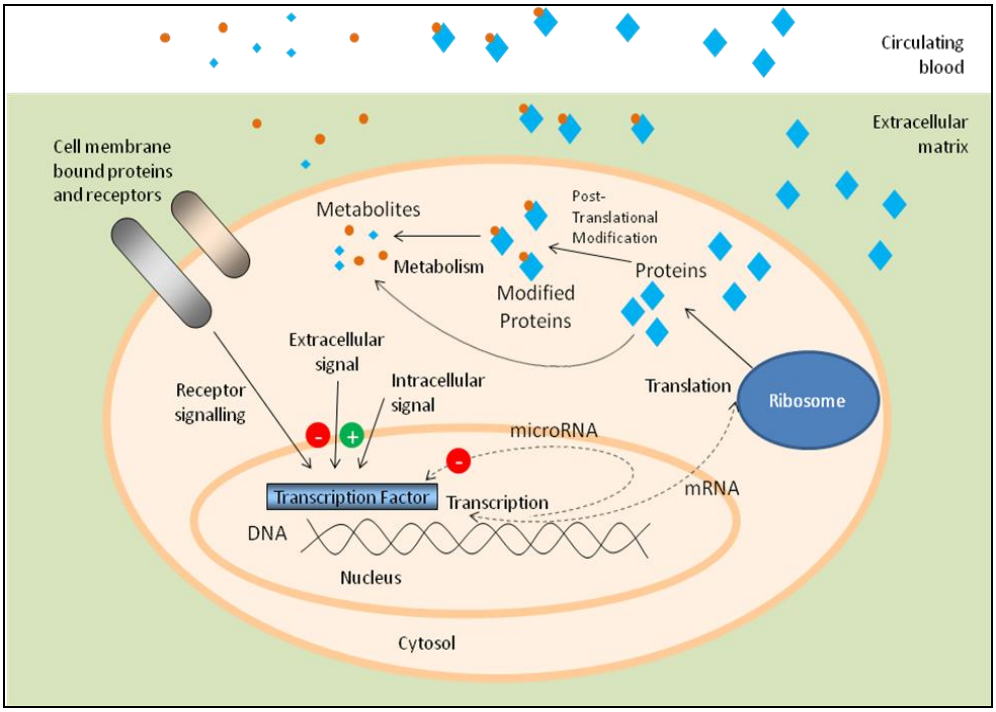


Figure 9 The synthetic 'workflow' of a cell

A combination of extrinsic and intrinsic signals act to activate or inhibit transcription factors within a cell. These transcription factors modulate the generation of ribonucleic acid (RNA) from deoxyribonucleic acid (DNA). Messenger RNA (mRNA) locates to a ribosome where amino acids are assembled in accordance with the mRNA's code to produce proteins. During transcription, in addition to mRNA, mircoRNAs are generated (an average of 22 nucleotides in length) which can alter gene transcription. Once a protein is synthesised, it may be subject to post-translational modifications (such as phosphorylation, methylation or cleavage). Both modified and unmodified proteins are subject to metabolism, resulting in metabolites (a term usually reserved for molecules less than 1 kiloDalton in size). These biological entities may be found within different 'compartments' of atherosclerotic environment: the cell nucleus; cytoplasm; extracellular matrix; and some components are released (passively or actively) into the bloodstream.

1.7.4 The Variety of Disciplines which Constitute Systems Biology

The 'Omics' is the collective term for the disciplines which employ high-throughput techniques to provide an overview of a state or process ongoing in an organism by way of a 'top-down' approach (Figure 10). This includes (most commonly) the status of DNA,

transcription, translation, metabolism (Figure 11), although other disciplines are interested specifically in lipids (lipidomics) and carbohydrates (glycomics) to name but a couple.

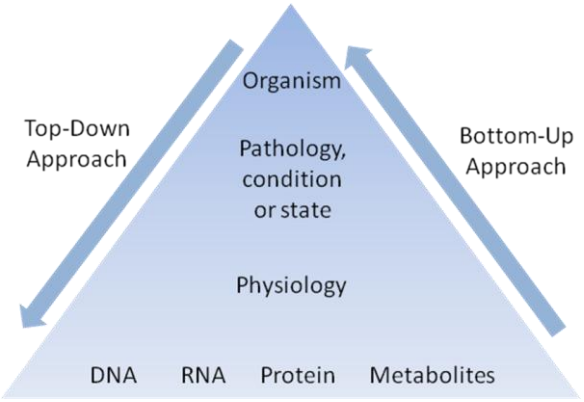


Figure 10 A 'top-down' approach to biology

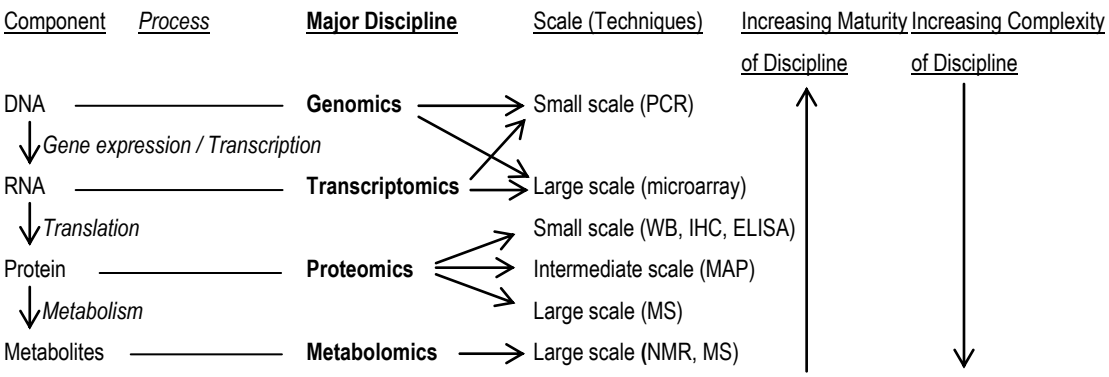


Figure 11 Summary of the key disciplines in systems biology

It is noteworthy that the increasing complexity results from the incremental rise in the number of biological analytes when moving from DNA to metabolites. ELISA, enzyme-linked immunosorbent assay; IHC, immunohistochemistry; MAP, multi-analyte profiling; MS, mass spectrometry; NMR, nuclear magnetic resonance; PCR, polymerase chain reaction; WB, Western blotting.

The investigation in the 'omic' disciplines may be hypothesis-driven or non-hypothesis-driven, the former being studies on small to intermediate scale and the later being a large scale examination of the genome, transcriptome, proteome or metabolome requiring complex (often multivariate) statistical analysis. The proteome also includes the secreted proteome, or 'secretome'. The use of these techniques in surgical research is growing.

1.8 BIOMARKERS IN CAROTID ATHEROSCLEROSIS

Biomarkers relate to different stages of disease development: screening biomarkers assess patients with no apparent disease; diagnostic biomarkers for those suspected of having disease; and prognostic biomarkers for individuals with overt disease (Gerszten and Wang 2008). There are a number of diagnostic and prognostic biomarkers available, with the latter holding the possibility of use as surrogate endpoints in trials.

Prevention of cardiovascular events will impact on public-health burden, but there are no widely accepted screening biomarkers as the value and appropriate use of proposed screening biomarkers remains a source of debate (Wilson 2004). Putative screening biomarkers may be classified according to the known roles of the molecules: inflammation (C-reactive protein, interleukin-6, lipoprotein-associated phospholipase A2); thombosis and haemostasis (fibrinogen, plasminogen-activator inhibitor 1); neurohormonal activation (renin, brain natriuretic peptide); insulin resistance (insulin, haemoglobin A1C); and endothelial dysfunction (homocysteine; urinary albumin) (Gerszten and Wang 2008).

Looking at data from the well known Framingham Study, when ten biomarkers were combined into a 'multimarker score', those with high scores had a twofold higher risk of major cardiovascular events and a fourfold higher risk of death than individuals with low scores (Wang et al. 2006). Despite this, compared to a risk score based upon conventional risk factors alone, the multimarker score was associated with a moderate increase in the receiver operating characteristic (ROC) area under the curve (AUC) (an objective assessment of a screening test's sensitivity and specificity) (Ware 2006).

1.8.1 Lysozyme

Carotid atheroma can be detected by duplex ultrasound but more sophisticated techniques, still under investigation, are required to assess plaque vulnerability. A simple blood test using a soluble biomarker of vascular atheroma would have considerable clinical utility and some possible advantages over other technically demanding and costly approaches. A proteomic study originally identified arterial plasma lysozyme as being a putative biomarker in coronary atherosclerosis and pilot study has detected elevated levels of plasma lysozyme in the arterial blood of patients with coronary artery disease (Abdul-Salam et al. 2010). As a constituent of macrophages (Unanue et al. 1976) it has biological plausibility as a marker of atheroma and a chapter in this thesis (Chapter 7) explores plasma lysozyme in patients with carotid atherosclerosis.

1.9 AIMS

Stroke is a condition which is related to significant morbidity and mortality, and stroke prevention is a global priority. Ischaemic stroke related to the extracranial circulation comprises approximately 20% of all strokes. Of these, only 15% experience prior symptoms, with the remaining 85% considered asymptomatic before their stroke. It is the selection for preventative intervention of these asymptomatic individuals, with atherosclerotic stenosis at their carotid bifurcation that I would like to place as the focus of this research. I would like to explore in whom, how and why carotid atherosclerosis develops and changes from being a chronic pathology to an acute pathology.

This work aims to:

- Investigate the effectiveness of functional imaging techniques (PET / CT and microbubble contrast enhanced ultrasound) to probe carotid plaques for features, such as inflammation and intra-plaque neovascularisation, which have been implicated in plaque vulnerability;
- Explore the differences in the molecular and cellular microenvironment between symptomatic and asymptomatic carotid atherosclerosis using histology and multi-analyte profiling;
- Determine the relationship between imaging signal and plaque biological features;
- Understand the utility of systems biology research (transcriptomics, proteomics, lipidomics and metabolomics) in revealing differences between unstable and stable atherosclerosis; and
- Look at putative biomarkers of atherosclerosis – lysozyme – in the context of carotid atherosclerosis and plaque vulnerability.

2 ASSESSMENT OF CAROTID ATHEROSCLEROSIS BY ^{11}C-PK11195 POSITRON EMISSION TOMOGRAPHY / COMPUTED TOMOGRAPHY

2.1 INTRODUCTION

Different imaging techniques are currently under evaluation for detecting inflammatory cells in atherosclerotic plaques amongst which positron emission tomography (PET) has emerged as a promising modality due to its high sensitivity (Rudd et al. 2009). The ^{11}C-labeled PET tracer PK11195 is a specific ligand of the translocator protein (18 kDa) (TSPO; Figure 12), formerly known as peripheral benzodiazepine receptor (PBR), a protein that is highly expressed in activated cells of the mononuclear phagocyte lineage (Veenman and Gavish 2006). TSPO is expressed in large numbers on macrophages, in the range of 250,000 binding sites per cell (Zavala et al. 1984; Canat et al. 1993a). PK11195 is a PET ligand which binds with high affinity to the PBR (Jones et al. 2002), and has been used to detect neuroinflammation (Banati et al. 1999; Banati et al. 2000; James et al. 2006).

Recently, specific *in vitro* binding of ^{3}H-PK11195 to macrophages has been shown in human carotid endarterectomy samples (Fujimura et al. 2008b; Bird et al. 2010), with tritiated ^{3}H-PK11195 binding shown to parallel that of the pan-macrophage marker CD68 in intensity and distribution (Fujimura et al. 2008a). In an atherosclerosis mouse model, uptake of PK11195 to inflamed plaque is greater than uptake to non inflamed plaque (Laitinen et al. 2009). A pilot study in patients with large vessel vasculitis has demonstrated that ^{11}C-PK11195 PET/computed tomography angiography (PET/CTA) can be used to assess vascular inflammation *in vivo* in humans (Lamare et al. 2010; Pugliese et al. 2010).

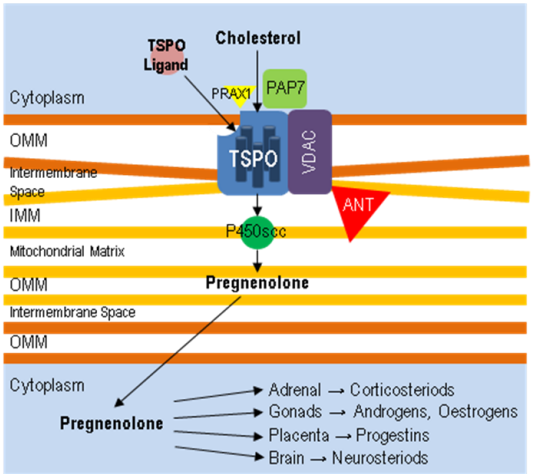


Figure 12 **Schematic showing the TSPO location on the outer mitochondrial membrane of activated cells of the mononuclear lineage and downstream signalling**

ANT, adenine nucleotide translocator; IMM, inner mitochondrial membrane; OMM, outer mitochondrial membrane; PAP7, peripheral benzodiazepine receptor associated protein 7;

PRAX1, peripheral benzodiazepine receptor associated protein 1; scc, side chain cleavage; TSPO, translocator protein 18kDa; VDAC, voltage-dependent ion channel.

By detecting TSPO, PK11195 PET/CT may represent a means to quantify intraplaque inflammation and assess the vulnerable atherosclerotic plaque *in vivo*.

2.2 METHODS

2.2.1 Study Approvals

The study protocol received research ethics committee approval (09/H0707/2) and all patients gave written informed consent. Radiation exposure was licensed by the UK Administration of Radioactive Substances Advisory Committee (ARSAC; RPC 262-425 (24111)).

2.2.2 Patients

Twenty-three asymptomatic and 9 symptomatic patients with a carotid stenosis >50% (confirmed by duplex ultrasonography using velocity criteria) (Oates et al. 2009) were recruited from a vascular tertiary referral centre serving a hyper-acute stroke unit. Asymptomatic subjects were identified through screening carotid ultrasonography of patients with cardiovascular risk factors and/or arterial disease in other territories such as coronary or lower limb. Exclusion criteria were age less than 40 years or more than 85 years, contraindications to iodinated contrast agents (including known intolerance to contrast agents or a glomerular filtration rate <60 mL/min/1.73 m^2) or a positive pregnancy test in women of child-bearing potential. Patients were defined as symptomatic if they had unilateral amaurosis fugax, clinical features consistent with a cortical TIA, or a completed hemispheric stroke in the carotid territory of interest in the preceding three months.

2.2.3 ^{11}C-PK11195 Radiotracer Synthesis

^{11}C-PK11195 was prepared according to a previously published protocol (Tomasi et al. 2008). ^{11}C-methyl iodide was incubated with 1.0 mg of desmethyl-PK11195 (ABX, Radeberg, Germany) and 1.0 mg of powdered potassium hydroxide in 200 µl of dimethyl sulfoxide for 1.5 min at 90°C. The crude product was purified on a semi-preparative Phenomenex Ultracarb 7µ octadecylsilane (ODS) 250 x 10 mm column using 70% ethanol, 30% water as the high-performance liquid chromatography (HPLC) solvent. After evaporation of the HPLC solvent, the purified product was formulated in 0.9% saline with 5% ethanol and filtered through a 0.22 µm sterile filter. Measurement of concentration and radiochemical purity of ^{11}C-PK11195 batches was performed by HPLC using an analytical Luna C8 150 x 4.6 mm

column (Phenomenex), a UV detector set at 277 nm, and a radioactivity detector in series. Radiochemical purity was .99.5%.

2.2.4 PET/CT Scanning Protocol

Imaging was performed using a 16-slice PET/CT scanner (Discovery RX, GE Healthcare, Milwaukee, Wisconsin) with a 15 cm field of view. After acquisition of the localiser, a low-dose CT scan was acquired in helical mode for attenuation correction with the following parameters:

- 120 kV
- 20 mAs
- 8 x 2.5 mm slice thickness
- pitch of 1.675
- 0.5 s rotation time

A line passing 2 cm below the carina was used as lower limit of the PET field of view, which thus encompassed the aortic arch, common carotid arteries, and carotid bifurcations. After injection of 6.85 MBq/kg of ^{11}C-PK11195, PET emission data were acquired over 60 min in list mode format and rebinned into 18 temporal frames:

- 30 s background
- 1 x 15 s
- 1 x 5 s
- 1 x 10 s
- 1 x 30 s,
- 4 x 60 s
- 7 x 300 s
- 2 x 600 s

After the PET scan, CT angiography was performed with the same field of view as the PET scan. A bolus of 70 ml of contrast (Ultravist 370, Schering, Berlin, Germany) was injected at a rate of 3.5 ml/s into an antecubital vein. A bolus tracking technique was used to synchronise the arrival of contrast in the ascending aorta with the CT angiography scan. The CT angiography acquisition parameters were:

- 120 kV

- 180 mAs
- 16 x 0.625 mm slice thickness
- pitch of 1.0
- 0.5 s rotation time

Using these parameters, scan times for CT angiography were in the range of 12 to 16 s. The effective dose of CT (including localiser, attenuation correction, and CT angiography) was estimated from the product of the dose-length product and an organ-weighting factor for the chest (0.014 mSv x mGy^{-1} x cm^{-1}) as proposed by the European Working Group for Guidelines on Quality Criteria in CT (Bongartz et al. 2004; Hausleiter et al. 2009).

2.2.5 Image Reconstruction

All PET emission scans were normalised and corrected for randoms, dead time, scatter and attenuation. Correction for radiotracer decay was deferred to the post-processing of the images. The 18 frames of the dynamic emission scans were reconstructed using the 3D re-projection algorithm (3DRP) (Kinahan and Rogers 1989) (with the ramp and Colsher filters set to Nyquist frequency) and using an ordered subset expectation maximisation (OSEM) algorithm with 2 iterations and 21 subsets. The matrix size was 256 x 256 x 47 for both reconstructions.

Reconstruction parameters for CT angiography were 0.625 mm slice thickness, 0.625 mm increment, 30 cm wide reconstruction field-of-view, window width of 300 Hounsfield units (HU) and window level of 30 HU.

Images were transferred to a dedicated workstation (Advantage Workstation 4.2, GE Healthcare) for visual assessment. In case of misalignment between the CT and the PET datasets, images were manually re-aligned using the vertebrae and the sternum as anatomical landmarks. A 25 min static frame was created by addition of OSEM PET dynamic frames 5 min after tracer injection. CT images were reduced to a matrix size of 256 x 256 x 47 to match the size of the reconstructed PET images, and superimposed to the PET images to help defining the regions of interest (ROI).

2.2.6 Measurement of ^{11}C-PK11195 Uptake

Quantitative measurement of ^{11}C-PK11195 uptake was performed using dedicated software (MATLAB, The MathWorks Inc.). After PET and CT images were resliced to obtain magnified cross-sections of the carotid artery, ROIs were placed on the CT images

encompassing the carotid plaque and superimposed on the PET images. To quantify plaque tracer uptake, standardised uptake values (SUV) were calculated as the average radioactivity concentration in each volume of interest (in Bq/mL) divided by total injected activity per body weight (in Bq/g). A background SUV was obtained in a venous structure (superior vena cava, subclavian or internal jugular vein) and plaque target-to-background ratios (TBR) were calculated as the ratio of plaque SUV over venous blood SUV (Kropholler et al. 2009).

2.2.7 CT Assessment of Carotid Stenosis and Plaque Composition

CT analysis was performed from axial source images and multiplanar reformations. The amount of plaque calcification (PC) was semi-quantitatively determined from carotid cross-sections according to a previously reported scale:(Rominger et al. 2009) A score of 0 was assigned when PC was absent, 1 was assigned for small PCs covering <10% of the vessel circumference, 2 was assigned if the PC involved 10-25% of the vessel circumference, 3 if 26-50%, and 4 if >50% of the vessel circumference were involved (Figure 13).

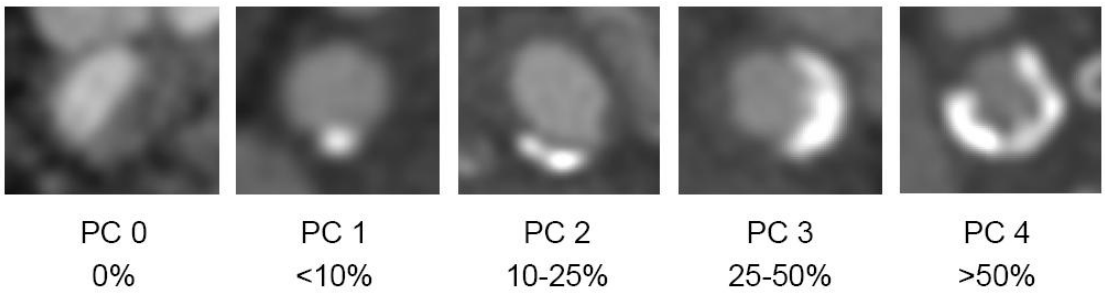


Figure 13 Semiquantitative plaque calcification scoring system.
A score of 0 was assigned when plaque calcification (PC) was absent, 1 for small PCs covering <10% of the vessel circumference, 2 if the PC involved 10-25% of the vessel circumference, 3 if 26-50%, and 4 if >50% of the vessel circumference were involved.

Additionally, all plaque cross-sections were analyzed to identify areas of low attenuation at fixed window settings (width 700 HU, level 200 HU). In at least 5 planes, a circular or elliptical ROI ($\geq 2mm^2$) was placed within the plaque, at sufficient distance from calcifications or areas contaminated with contrast material to avoid beam-hardening artefacts. CT attenuation was measured as the mean CT density (in HU) in the region of interest with the lowest attenuation.

The severity of stenosis was determined according to the NASCET criteria (NASCET 1991). In brief, on cross-sections strictly perpendicular to the axis of the vessel, the minimal luminal diameter (MLD) was measured using an electronic calliper and compared to the reference

diameter (RD) in a more distally located nondiseased segment. The degree of stenosis was calculated as (RD-MLD)/RD.

2.2.8 Ex Vivo Plaque Processing

Eight patients (5 asymptomatic, 3 symptomatic) underwent carotid endarterectomy within 9±11 days of the PET/CT study. The diseased intimal arterial segments were immediately snap frozen in liquid nitrogen and stored at -80 °C for batch analysis. Frozen samples were embedded in optimum cutting temperature compound (TissueTek, Qiagen) and adjacent 12 µm cryosections were used for autoradiography, immunohistochemistry and immunofluorescence.

2.2.9 Autoradiography

TSPOs were labelled with ^{3}H-PK11195 (specific activity 86.4 Ci/mmol; 1 mCi/mL, PerkinElmer Inc) for autoradiography. Nonspecific binding was determined in the presence of excess nonradioactive PK11195 (1 µmol). Slides were apposed to 3H-sensitive film for 5 months. Calibration standards were included in the cassette (^{3}H-microscales 0 – 16 nCi/mg and 3 – 110 nCi/mg; GE Lifesciences, UK). Films were developed using an automatic film processor (Amersham Hyperprocessor, GE Lifesciences, UK) under safelight conditions. Quantitative analysis was performed using a computerised image-analysis system (MCID, Interfocus, Cambridge, UK). Optical density readings, corrected for background, were made and values standardised against the linear portion of a curve generated using ^{3}H-microscale standards and expressed as nCi/mg. Specific binding values were determined by subtracting non-specific binding values from total binding values.

2.2.10 Immunohistochemistry

Tissue sections processed for immunohistochemistry were fixed in ice-cold 70% ethanol for 10 min, followed by 10 min incubation in 0.3% H_2O_2 and 30 min incubation in 10% normal goat serum to block non-specific labelling. Adjacent tissue sections were thereafter incubated with primary antibodies raised against either TSPO (rabbit anti-TSPO, RnD Systems, 1:100) or CD68 (mouse anti-CD68, Dako, 1:100) overnight at 4°C. Secondary labelling was performed using species-specific kits with horseradish peroxidase (HRP)-conjugated secondary antibodies (Envision) and incubation for 30 min at room temperature. The substrate of 3,3'-diaminobenzidine (DAB; 0.7 mg/mL, Sigma) was used as a chromogen. Plaque sections were counterstained in hematoxylin, dehydrated and mounted in DPX mounting media (Merck). The slides were rinsed with phosphate buffered saline between each step

during the process. Images of TSPO and CD68 labelled tissue sections were captured using a Motic camera and software connected to a Nikon microscope.

2.2.11 Confocal Fluorescence Microscopy

Selected sections were double-labelled for TSPO and CD68 to evaluate co-expression. Following incubation with primary antibodies overnight at 4°C, the sections were incubated with fluorescence secondary antibodies (ALEXA546 anti-rabbit and ALEXA488 anti-mouse, Invitrogen, 1:1000) for 1 h at room temperature. Finally, the tissue sections were mounted in Vectashield mounting media with DAPI (Vector Labs). The fluorescent slides were imaged using a Nikon/Perkin-Elmer spinning disc confocal microscopy system.

2.2.12 Statistical Analysis

Statistical analysis was performed with SPSS 16.0.1 (SPSS, Inc, Chicago, Illinois). Continuous variables are expressed as mean ± standard deviation (SD) or median (with range) where appropriate. Categorical variables are expressed as frequencies (percentages). The Mann Whitney test was used for comparison of continuous values and the χ square or Fisher's exact test for comparison of categorical data. Agreement between CTA and Duplex ultrasound for the measurement of stenosis severity was determined with linear correlation and Bland-Altman limits of agreement (Bland and Altman 1986). Receiver operating characteristics (ROC) analysis was used to determine optimal cut-offs for CTA and PET derived parameters to predict ischemic events and their respective diagnostic accuracies. Pearson's method was used to assess the correlation between ^{11}C-PK11195 PET TBR and ^{3}H-PK11195 plaque autoradiography. Binary logistic regression was employed to determine the association of CTA and PET derived parameters with the occurrence of ischemic events. A p value < 0.05 was considered statistically significant.

2.3 RESULTS

2.3.1 Patients

Thirty-four patients were enrolled in the study and 32 successfully underwent the PET/CTA scan (9 symptomatic and 23 asymptomatic patients). In 2 patients the scans were unsuccessful due to failed tracer production (n=1) or technical problems (n=1). The patient baseline characteristics are shown in Table 4. In the symptomatic group the index cerebrovascular events were amaurosis fugax (n=4), hemispheric TIA (n=4), and hemispheric stroke (n=1). The interval between index event and PET/CTA scan was 20 ± 21 days (range 5 to 75 days). Effective radiation dose was 3.2 ± 1.2 mSv and 2.1 ± 0.5 mSv for CTA and PET respectively, and 5.3 ± 1.7 mSv for the combined PET/CTA study.

	All patients (n=32)	**Symptomatic (n=9)**	**Asymptomatic (n=23)**	***P* Value**
Age, years	70±9	68±6	70±10	0.57
Female gender (%)	11 (34%)	4 (44%)	7 (30%)	0.68
Body mass index (kg/m^2)	26.1±4.5	24.1±3.7	26.8±4.6	0.22
Previous history of stroke or transient ischaemic attack (%)	17 (53%)	9 (100%)	8 (35%)	0.001
Carotid endarterectomy (%)	8 (25%)	3 (33%)	5 (22%)	0.65
Cardiovascular risk factors (%)				
Smoking	21 (66%)	6 (67%)	15 (65%)	>0.99
Arterial hypertension	22 (69%)	5 (56%)	17 (74%)	0.41
Dyslipidemia	23 (72%)	7 (78%)	16 (70%)	>0.99
Diabetes mellitus	7 (22%)	2 (22%)	5 (22%)	>0.99
Positive family history	11 (34%)	2 (22%)	9 (39%)	0.44
Pharmacotherapy (%)				
Aspirin	25 (78%)	7 (78%)	18 (78%)	>0.99
Statin	31 (97%)	8 (89%)	23 (100%)	0.28
Angiotensin converting enzyme inhibitors / angiotensin II receptor blocker	14 (44%)	4 (44%)	10 (43%)	>0.99
Beta-receptor antagonists	8 (25%)	2 (22%)	6 (26%)	>0.99
Calcium channel blocker	11 (34%)	1 (11%)	10 (43%)	0.11

Table 4 Characteristics of the symptomatic and asymptomatic patient groups

There were no statistically significant differences in the demographic cardiovascular risk factors or pharmacotherapeutic parameters when comparing patients with symptomatic to those with asymptomatic carotid stenosis. Data are given as mean ± standard deviations unless otherwise indicated.

2.3.2 PET/CTA Imaging

A total of 36 carotid stenoses were available for image analysis (4 asymptomatic subjects had bilateral stenoses). There was no significant difference in the severity of carotid stenoses on CT angiography between symptomatic and asymptomatic patients (77±16% versus 68±16%, p=ns) (Table 5). An excellent agreement was found between CTA- and ultrasound-derived stenosis severity (r=0.93, P<0.001; limits of agreement -15% to 10%) with only a slight underestimation with CTA by 3% compared to ultrasound.

	All stenoses (n=36)	**Symptomatic stenoses (n=9)**	**Asymptomatic stenoses (n=27)**	***P* Value**
Carotid stenosis by duplex ultrasonography (%)	70±17	77±16	68±16	ns
Plaque standardised uptake value for ^{11}C-PK11195	0.62±0.10	0.69±0.08	0.60±0.10	0.02
Plaque target-to-background for ^{11}C-PK11195	0.91±0.16	1.06±0.20	0.86±0.11	0.008
CT plaque attenuation	76±44	46±31	86±44	0.008
Plaque calcification score	2.4±1.3	2.6±1.7	2.4±1.2	0.61

Table 5 ^{11}C-PK11195 PET / CT imaging results

^{11}C-PK11195 SUV and TBR were higher in the carotid plaques of symptomatic compared to asymptomatic patients (Table 5) (Figure 14, Figure 15, Figure 16, Figure 17). No differences were noted for SUV values in venous blood (0.66±0.10 versus 0.70±0.09, p=ns). On CTA the mean PC score was comparable in both patient groups (Table 5). However, carotid plaques of symptomatic patients had areas of lower attenuation compared to asymptomatic plaques (46±31 versus 86±44 HU, p=0.008). There was no significant correlation between ^{11}C-PK11195 TBR and either CT plaque attenuation (r=-0.11, p=0.54) or PC score (r=0.23, p=0.89). Figure 17 shows the distribution of ^{11}C-PK11195 TBR and CT plaque attenuation amongst symptomatic and asymptomatic patients.

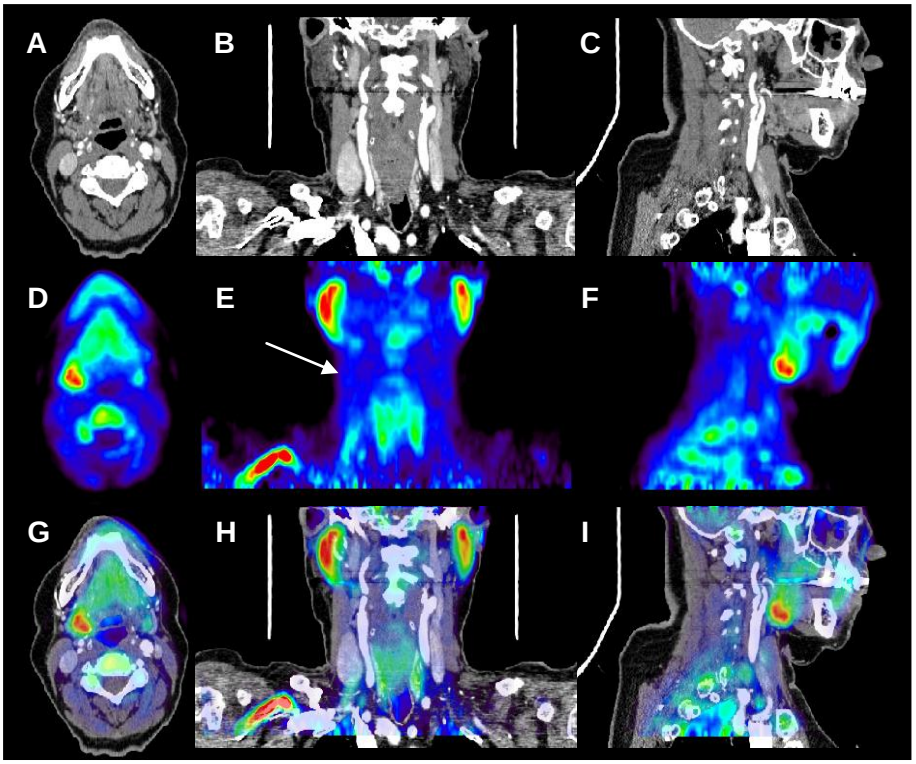


Figure 14 ^{11}C-PK11195 PET / CT imaging of an asymptomatic carotid atheroma

^{11}C-PK11195 PET/CT axial (A, D and G), coronal (B, E and H) and saggital (C, F and I) images, respectively, of an 81 year old female patient with a 50% right-sided internal carotid artery stenosis. Anatomy is demonstrated by CT angiography (A, B and C), ligand uptake by PET (D, E and F), with these merged (G, H and I). No uptake is seen in at the right carotid bifurcation (white arrow).

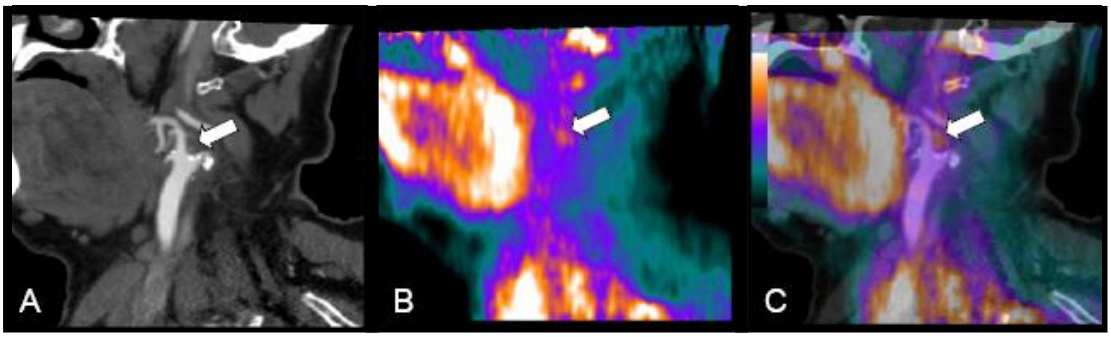


Figure 15 ^{11}C-PK11195 PET / CT imaging of symptomatic carotid atherosclerosis

CT angiography (A), ^{11}C-PK11195 PET (B) and PET/CT fusion (C) in a 52 year old patient with right amaurosis fugax 2 weeks prior to the PET/CT scan. The white arrows denote a focal area of ^{11}C-PK11195 uptake at the carotid bifurcation.

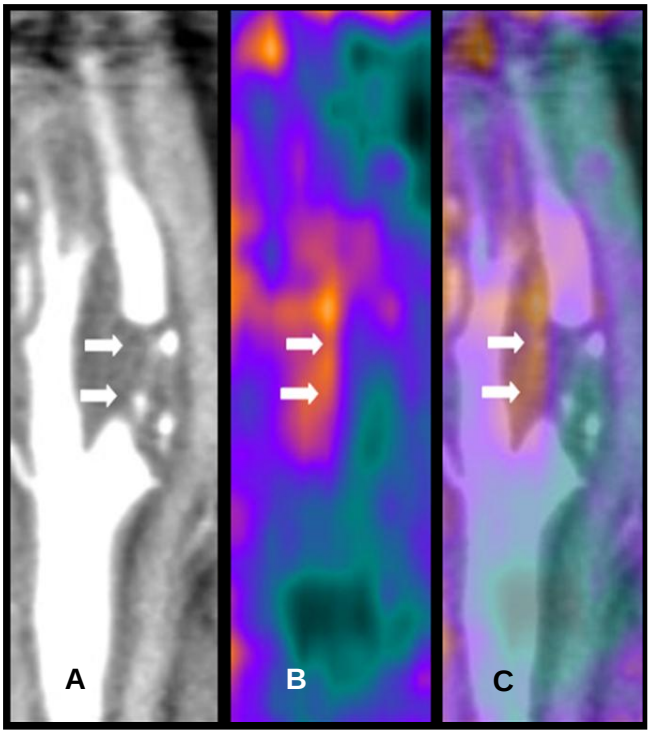


Figure 16 **^{11}C-PK11195 PET / CT imaging of a symptomatic carotid atheroma – close-up**

Magnified saggital images of the left carotid bifurcation of a 66 year old male with a 90% stenosis. A. Computed tomography angiography revealing the stenosis (white arrows). B. PET image showing increased uptake (white arrows). C. Merged images locating the increased uptake to the area of stenosing plaque (white arrows).

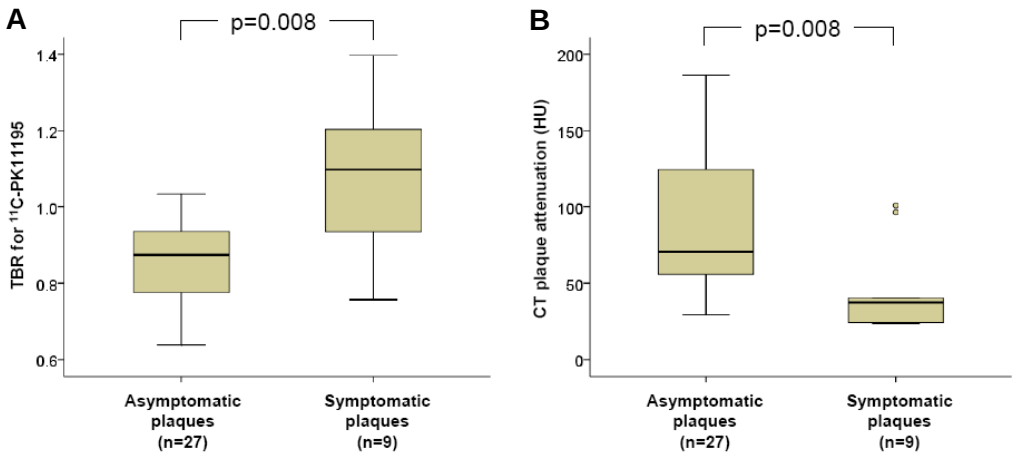


Figure 17 **Quantification ^{11}C-PK11195 PET / CT imaging parameters**

Distribution of ^{11}C-PK11195 TBR (A) and CT plaque attenuation (B) values in symptomatic and asymptomatic plaques. Each box plot shows median (thick lines), quartiles (upper and lower box boundaries), and extreme values (whiskers) within a category.

Features associated with the presence of cerebrovascular events on logistic regression analysis were: ^{11}C-PK11195 TBR (p=0.01) and CT plaque attenuation (p=0.04) (Figure 18). ROC analysis revealed an optimal cut-off to discriminate between symptomatic and asymptomatic patients at 0.92 for ^{11}C-PK11195 TBR and at 40 HU for CT plaque attenuation. Sensitivity, specificity, negative and positive predictive values for TBR, CT plaque attenuation, one feature positive, and two features positive plaques are shown in Figure 19.

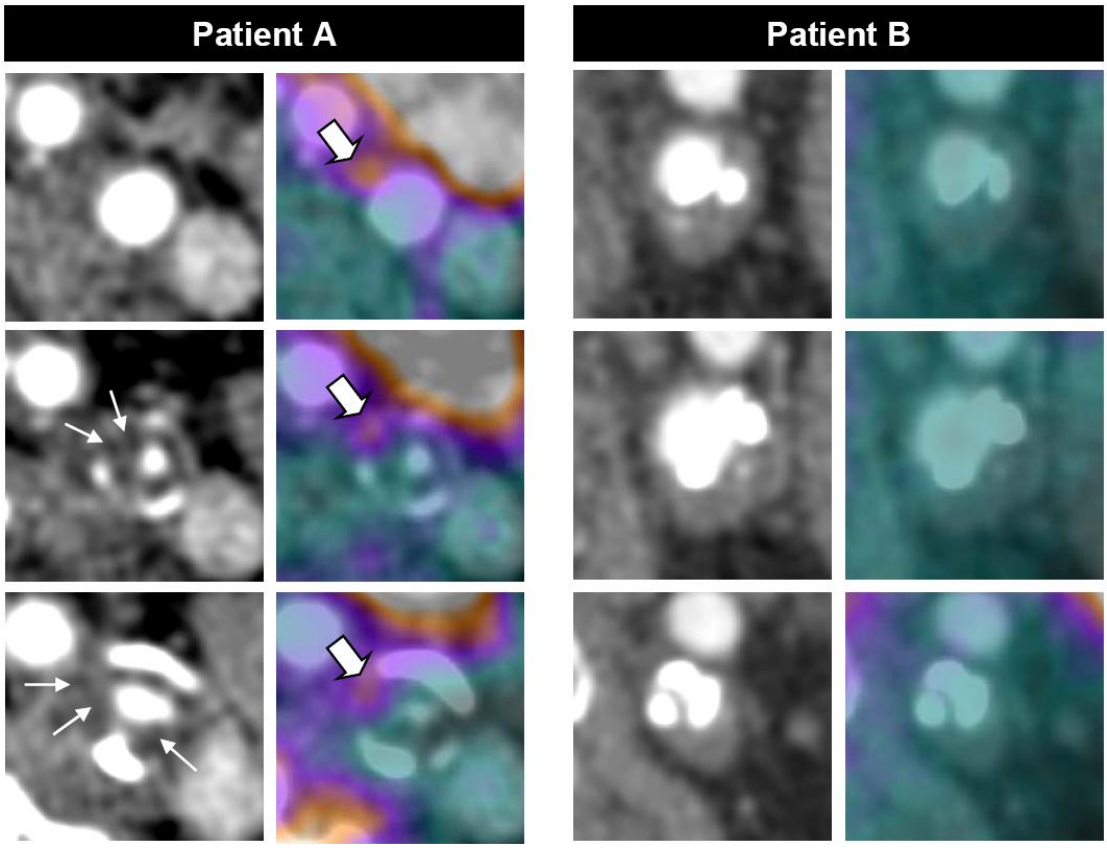


Figure 18 Axial co-registration of ^{11}C-PK11195 PET and CT images

CT angiography and co-registered PET/CT cross-sections at 3 mm intervals illustrate differences in plaque composition and ^{11}C-PK11195 uptake on PET/CT among symptomatic (Patient A) and asymptomatic (Patient B) patients. In patient A, areas of low attenuation (23.5 HU) can be seen (white arrows, first column) in close vicinity with foci of increased ^{11}C-PK11195 uptake (block arrows, second column). In contrast, in patient B, plaque CT attenuation was higher (76.2) indicating a predominance of fibrotic tissue (column 3), and no ^{11}C-PK11195 uptake was noted (column 4).

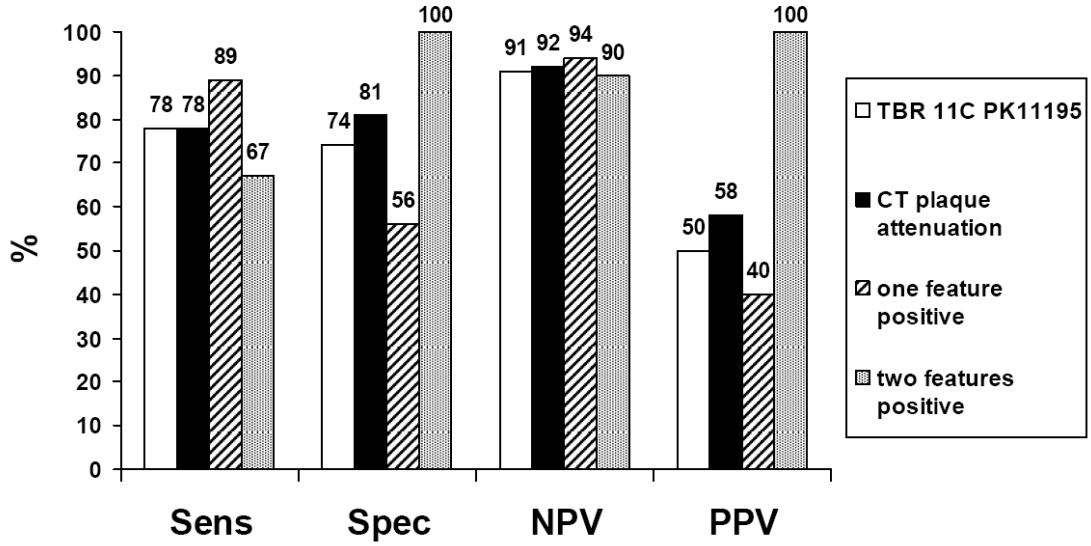


Figure 19 Discriminatory value of carotid plaque ^{11}C-PK11195 PET / CT

Sensitivity (Sens), specificity (Spec), negative (NPV) and positive predictive value (PPV) to identify patients with cerebrovascular events.

2.3.3 Ex Vivo Analysis

Autoradiography, immunohistochemistry and immunofluorescence. Mean ^{3}H-PK11195 specific binding on autoradiography was 60.6±16.0%, with no significant difference between plaque sections from symptomatic (n=3) or asymptomatic (n=5) patients.

TSPO^{+} and CD68^{+} cells were observed in all tissue specimens, and both markers were seen in corresponding areas on adjacent plaque sections (Figure 20 C-F). TSPO expression by macrophages was confirmed by double immunofluorescence and confocal microscopy (Figure 20 G-J). There was no significant difference in the presence of TSPO^{+} CD68^{+} cells between the symptomatic or asymptomatic group. TSPO^{+} and CD68^{+} cells were located in areas of high ^{3}H-PK11195 specific binding on autoradiography (Figure 20 A-F).

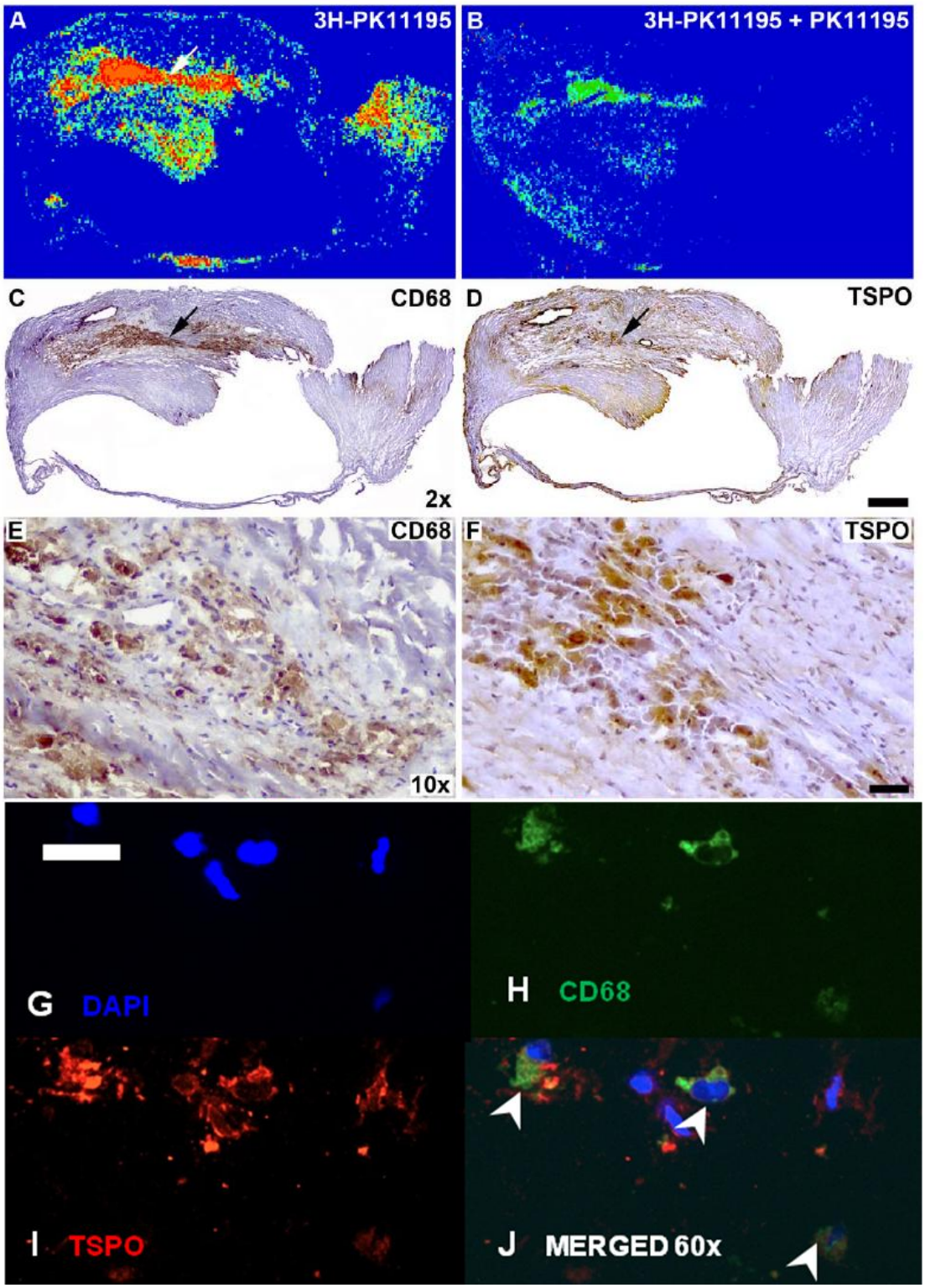


Figure 20 **^{3}H-PK11195 autoradiography, CD68 and TSPO immunohistochemistry and double immunofluorescence confocal microscopy**

Representative autoradiography, immunohistochemistry and immunofluorescence microscopy results in endarterectomy samples. ^{3}H-PK11195 total binding to atherosclerotic plaques in vitro (A). The non-specific binding of ^{3}H-PK11195 was assessed by blockage with excess unlabelled PK11195 (B). Tissue sections were immunohistochemically labelled for

macrophages (CD68; C) and TSPO (D). The arrows in C and D show the location of the area captured at higher magnification in E and F, respectively. Areas with high specific binding of ^{3}H-PK11195 had a high density of TSPO+ and CD68+ cells (arrows in A, C and D). Double immunofluorescence labelling and spinning disc confocal microscopy for DAPI (G, blue); CD68 (H, green) and TSPO (I, red) confirms expression of TSPO by macrophages in carotid atherosclerosis (J, merged, white arrowheads). Scale bars: C and D 800 μm; E and F 40 μm; G, H, I and J 20 μm.

TBR on ^{11}C-PK11195 PET significantly correlated with specific binding by ^{3}H-PK11195 autoradiography (r=0.77, p=0.025) (Figure 21).

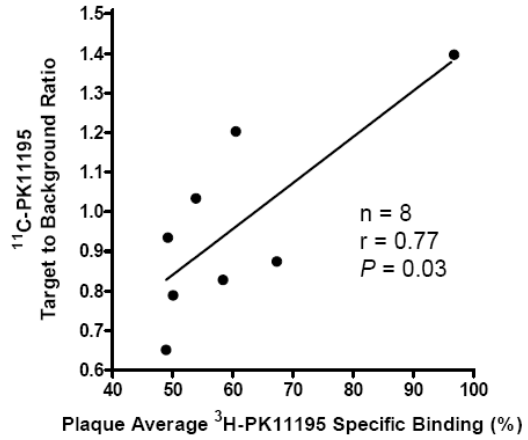


Figure 21 *In vivo* and *in vitro* PK11195

Correlation of in vivo ^{11}C-PK11195 target-to-background ratio with average ex vivo plaque PBR density (measured as average ^{3}H-PK11195 specific binding).

2.4 DISCUSSION

It has been demonstrated that ^{11}C-PK11195 PET allows the noninvasive detection and quantification of intraplaque inflammation in patients with carotid stenoses. Moreover, the combination of ^{11}C-PK11195 PET with contrast-enhanced CTA provides an integrated assessment of plaque structure, composition and biological activity and allows the distinction between recently symptomatic vulnerable plaques and asymptomatic plaques with a high positive predictive value. Focal ^{11}C-PK11195 uptake did not correlate with either the presence of low attenuation plaques or the PC score. This is in line with prior reports obtained with ^{18}F-fluorodeoxyglucose (FDG) PET/CT (Ben-Haim et al. 2004) and indicates that information obtained with these two modalities is complementary and enhances the diagnostic performance of the hybrid technique to detect potentially vulnerable plaques. The absence of either increased ^{11}C-PK11195 TBR >0.92 or low CT attenuation areas <40 HU was associated

with asymptomatic plaques, whereas all plaques positive for both features were found in patients with an ipsilateral event.

TSPOs were discovered in the 1970's as benzodiazepine binding sites outside the central nervous system (Braestrup and Squires 1977). Subsequent studies have shown a high TSPO density in circulating human phagocyte populations, particularly in monocytes and polymorphonuclear neutrophils, with up to 750,000 binding sites per cell (Canat et al. 1993a). TSPO expression is higher in mature monocytic cell lines compared to promonocytic or promyelocytic lines and its density increases by a factor of 2 to 3 after *in vitro* monocyte activation with IFNγ or phorbol 12-myristate 13-acetate. Stimulated human monocytes can express more than 2,000,000 binding sites for PK11195 and this increase is paralleled by an enhanced expression in CD11a and CD11b surface antigens and augmented production of IL1, IL8, and TNF, indicating that TSPO over-expression is a marker of activated phagocytes (Canat et al. 1993b). PK11195 is a selective TSPO ligand which binds specifically to macrophages in specimens of human carotid atherosclerotic plaque (Fujimura et al. 2008b; Bird et al. 2010). ^{11}C-PK11195 PET/CTA has been shown to allow *in vivo* detection and quantification of vascular inflammation in patients with large vessel vasculitides and can distinguish symptomatic from asymptomatic patients in the context of vasculitis (Pugliese et al. 2010).

The present study builds on these existing data and further extends the use of ^{11}C-PK11195 PET/CTA imaging onto patients with atherosclerotic disease. These results, if confirmed by larger prospective studies, would suggest that ^{11}C-PK11195 PET/CTA may be used in asymptomatic patients with carotid stenoses to improve their risk stratification and allow clinicians to identify patients at risk for ischemic cerebrovascular events.

The PET tracer FDG, a biological glucose analogue, has been extensively evaluated for measuring intraplaque inflammation in atherosclerotic lesions (Rudd et al. 2002; Tawakol et al. 2006). However, since FDG is taken up by any metabolically active tissue, concerns have been raised about the specificity of this tracer for imaging inflammatory cells. Indeed, micro-autoradiography studies in aortic sections of ApoE$^{-/-}$ mice have shown that ^{14}C-FDG uptake correlates poorly with fat content and selective macrophage staining with anti-CD68 (Matter et al. 2006). Davies and colleagues reported that *in vivo* FDG microPET SUV in atherosclerotic lesions of rabbit aorta were not correlated with macrophage density ($r=0.16$, $p=0.57$) and there was no significant difference in FDG uptake seen between rabbits with highly inflamed aortic walls, those with low levels of inflammation or controls (Davies et al. 2010b). Conversely, a high degree of specific binding to macrophages of atherosclerotic

plaques has been observed with ^{3}H-PK11195 in autoradiographic studies which is confirmed by the ex vivo results of the present study (Fujimura et al. 2008b). However, no definite conclusion on the relative specificity of the aforementioned tracers can be drawn until a direct head-to-head comparison is performed.

One of the strengths of this work compared to prior PET/CT studies (Rudd et al. 2007; Rudd et al. 2008) was the use of contrast-enhanced CTA with a high-end CT device. This facilitated delineation of the atherosclerotic plaque thereby improving co-registration with the PET signal, and allowed concurrent evaluation of plaque composition. Measurement of CT attenuation within carotid plaques has been shown to identify lipid-rich cores, fibrous tissue and areas of calcifications on histology (de Weert et al. 2006). The presence of low attenuation plaques has previously been identified as an important predictor for plaque rupture and thrombotic events in the coronary vasculature (Motoyama et al. 2009). In this work, a cut-off at 40 HU was identified to provide the best statistical discrimination between symptomatic and asymptomatic plaques, indicating that the presence of lipid-rich areas was a significant determinant of plaque vulnerability. A similar cut-off (30 HU) has been found to be a good discriminator between rupture-prone and stable plaques in the coronary circulation (Motoyama et al. 2009). PCs were not associated with ischemic events in this study, which is contrary to prior reports where calcified plaques were up to 21 times less likely to be symptomatic (Nandalur et al. 2005).

2.4.1 Clinical Implications

The management of carotid atherosclerotic disease includes risk factor modification, medical treatment, carotid endarterectomy, and recently also percutaneous transluminal angioplasty and stenting. The choice of intervention is tailored based upon the individual's risk of suffering an ischemic cerebrovascular event. Whereas carotid endarterectomy has been demonstrated to improve prognosis in symptomatic patients, its role is less clearly established in asymptomatic patients where the potential benefit has to be weighed against the risk of perioperative mortality and morbidity (Biller et al. 1998). To date, the decision to perform CEA in asymptomatic patients has been largely based upon the severity of the stenosis. Nonetheless, significant proportion of plaque ruptures occur in stenoses of low and intermediate severity (Falk et al. 1995; Topol and Nissen 1995; Nicolaides et al. 2005). Recently, other plaque features such as plaque composition, morphology and biological activity have been proposed as important determinants of the risk of rupture, calling for effective imaging techniques with the potential to identify vulnerable plaque characteristics (Naghavi et al. 2003).

^{11}C-PK11195 PET/CT may facilitate the monitoring of response to plaque stabilising therapeutic agents, identifying those individuals whose plaques may not be safely managed by pharmacotherapeutics alone. It is noteworthy; however, that macrophage activation was evident, detectable and significantly different between symptomatic and asymptomatic groups despite the patients studied being on best medical therapy, including a statin in 97% of individuals.

2.4.2 Limitations

This work is a proof of principle study. The relatively small number of patients is therefore acknowledged. This precluded the use of multivariate models to test for independent characteristics associated with ischemic events and warrants larger prospective trials to confirm these findings. The fact that more asymptomatic than symptomatic individuals were scanned was related to the logistic challenge posed by the imaging facility being located at a site different to the hyperacute stroke and vascular units – Hammersmith Hospital and Charing Cross Hospital, respectively. It was difficult to transport patients who had suffered disabling strokes, particularly in the narrow time window between symptoms and carotid endarterectomy practiced by our unit, and that notice was necessary to book the PET/CT scanner and produce the radiopharmaceutical.

The proximity of the blood pool and limited thickness of the arterial wall can result in spillover and partial volume effects. However, this should affect asymptomatic and symptomatic patients to the same extent, and is unlikely to account for any of the differences observed between the two groups. Additionally, care was taken to restrict the ROIs to the plaque and avoid the residual vessel lumen. Correction for spillover and the quantification of receptor kinetics should overcome these potentially confounding factors and further quantitative studies are indicated.

The short physical half-life of ^{11}C-labeled compounds mandates an onsite cyclotron facility, thus limiting its clinical applicability. However, the introduction of new ^{18}F-labeled TSPO ligands, which are currently under pre-clinical investigation and have shown high affinity across species in the brain, may overcome some of these limitations (Briard et al. 2009).

Finally, the added radiation exposure from PET and CT remains an important concern, particularly if repeated studies are performed to assess inflammatory activity before and after treatment. The total effective radiation dose in the patients in this study was well below 10 mSv, which is comparable to a standard cardiac FDG scan (Einstein et al. 2007).

2.4.3 Conclusions

Imaging intraplaque inflammation *in vivo* with ^{11}C-PK11195 and PET combined with contrast-enhanced CT angiography is feasible and can distinguish between recently symptomatic and asymptomatic plaques. The information obtained from both modalities is complementary and allows a comprehensive assessment of plaque composition and inflammatory activity. Plaques with low CT attenuation and increased ^{11}C-PK11195 uptake seem to be those at highest risk of thromboembolic events.

3 ASSESSMENT OF CAROTID ATHEROSCLEROSIS BY DYNAMIC AND LATE PHASE MICROBUBBLE CONTRAST ENHANCED ULTRASOUND

3.1 INTRODUCTION TO CONTRAST ENHANCED ULTRASOUND IN CAROTID ARTERIAL DISEASE

3.1.1 Microbubbles, Non-Linear Behaviour and Mechanical Index

Microbubble-based contrast agents are injected intravenously to enhance ultrasound scans, and are comprised of 1 to 10 μm diameter albumin or lipid shells filled with air or high molecular weight gas. Their small size allows them to recirculate, whereas larger bubbles are retained in the pulmonary circulation.

The discovery that gas filled bubbles can act as ultrasound contrast agents was initially made because the density change from blood to intrabubble gas causes reflection of sound waves, just as the density change from air to cliff-face creates an audible "echo". However, modern ultrasonic methods of distinguishing microbubble from native tissue rely on the fact that ultrasound waves cause microbubbles to compress and expand, whereas tissue is virtually incompressible (Cosgrove 2006). By fortunate coincidence, the resonance frequency for microbubbles (the frequency at which compression and expansion occurs most readily) is within the range of frequencies used for clinical ultrasound. Sound waves of very low energy, therefore, will return detectable signal from microbubbles, provided the transmitted wave is around the microbubble resonance frequency. Native tissue, however, will not respond to such low energy waves.

When exposed to ultrasound, microbubbles behave in a highly non-linear fashion, *i.e.* they respond differently to different portions of the incident acoustic wave. A typical acoustic wave generated by a diagnostic ultrasound scanner is made of a few cycles of a sinusoidal wave at a centre frequency of 1 to 10 MHz. Positive pressure compresses a microbubble, while negative pressure dilates it. When a microbubble expands while exposed to negative pressures, its radius can increase by as much as several hundred percent. On the other hand, as a microbubble contracts in response to positive pressures, the decrease in its radius is limited due to the gas inside the microbubble rapidly stiffening, making it less compressible. As a result, when a microbubble is exposed to ultrasound, its radius oscillates in a non-symmetric fashion: the microbubble behaves non-linearly.

The mechanical index (MI) is defined as the peak rarefactional pressure (negative pressure) divided by the square root of the ultrasound frequency. It can also be defined as the peak rarefactional pressure multiplied by the square root of the ultrasound period. Typical MI used for conventional B-mode imaging is high enough to destroy most microbubbles (Villarraga et al. 1997; Walker et al. 1997). Triggered imaging techniques have been used in radiology to

image flow in the parenchyma of abdominal organs (Heckemann et al. 2000; Kim et al. 2000; Wilson et al. 2000). With the more recent development of non-linear imaging techniques which take advantage of the highly non-linear behavior of the microbubbles, it is now possible to image ultrasound contrast agents non-destructively in real time. Real-time low mechanical index (MI < 0.1) harmonic imaging is currently the preferred imaging mode in radiological applications of contrast-enhanced ultrasound. Another benefit of imaging ultrasound contrast agent at a low MI is that it prevents non-linear propagation in tissue from occurring, thereby increasing the contrast-to-tissue ratio when a harmonic imaging technique is used.

Unlike most contrast agents used for computed tomography (CT) and magnetic resonance imaging (MRI), microbubbles remain within the vascular space and are hence well suited to study the vasculature. By improving visualisation of the lumen, contrast enhanced ultrasound (CEUS) can improve current carotid structural scans. Furthermore, CEUS may be able to add extra information on plaque characteristics, such as neovascularisation, deemed to elucidate plaque instability. In addition, manufacturing microbubbles targeted to specific vascular endothelial ligands, CEUS may have the ability to probe plaque biology.

Unlike most contrast agents used for computed tomography (CT) and magnetic resonance imaging (MRI), microbubbles remain within the vascular space and can hence be used to study the vasculature. By improving visualisation of the lumen, contrast enhanced ultrasound (CEUS) can improve current carotid structural scans. Furthermore, CEUS may be able to add extra information on plaque characteristics, such as neovascularisation, deemed to elucidate plaque instability. In addition, manufacturing microbubbles targeted to specific vascular endothelial ligands, CEUS may have the ability to probe plaque biology.

3.1.2 The Current Carotid Ultrasound Examination

With the publication of the results of the European Carotid Surgery Trial (ECST) (ECST 1991) and the North American Symptomatic Carotid Endarterectomy Trial (NASCET) (NASCET 1991), the importance of accurate assessment of the degree of internal carotid artery diameter reduction has been highlighted. There has been extensive work undertaken in the generation of reliable and reproducible criteria for the calculation of internal carotid artery stenosis using unenhanced duplex ultrasonography. This is based on largely velocity criteria, is standardised and been used in the creation of national and international society consensus documents (Nicolaides et al. 1996; Sidhu and Allan 1997; Filis et al. 2002; Grant et al. 2003; Oates et al. 2009). Duplex ultrasonography is likely to remain the first line imaging modality

in this context (Sidhu and Allan 1997); as such, much work has been undertaken in its refinement.

3.1.3 The Need to Improve the Current Ultrasound Assessment

Traditionally, stroke risk stratification has revolved around the degree of internal carotid artery luminal narrowing, and the presence of recent focal neurological symptoms pertaining to the ipsilateral cerebral hemisphere. However, it has become apparent that the degree of stenosis alone is a relatively poor predictor of future stroke in asymptomatic patients. Indeed, the Asymptomatic Carotid Surgery Trial (ACST) (Halliday et al. 2004; Halliday et al. 2010), Asymptomatic Catrotid Atherosclerosis Study (ACAS) (ACAS 1995), and the results of a recent Cochrane Review on the subject (Chambers and Donnan 2005) highlighted the need to identify a subgroup of asymptomatics that would benefit from intervention.

The attempt to define this subgroup has inspired research into imaging modalities which can identify, *in vivo*, plaques at high risk of causing acute cardiovascular events. Histological and functional techniques have determined the features of such plaques, including: inflammation; extra-cellular matrix degradation; neovascularisation; intra-plaque haemorrhage; and apoptosis (Libby et al. 2002; Virmani et al. 2006; Koenig and Khuseyinova 2007).

3.1.4 Imaging Neovascularisation: The Rationale

Imaging intraplaque neovascularisation may be a means by which ultrasound can identify the high-risk plaque. In healthy large vessels, the vasa vasorum runs through adventitia and outer media (Geiringer 1951), penetrating intima only in pathology (Doyle and Caplice 2007). Recent work has afforded a central role to intraplaque neovascularisation in initiation, progression and rupture of atherosclerotic plaques (Chen et al. 1999; de Boer et al. 1999; Fleiner et al. 2004; Moreno et al. 2004; Moreno et al. 2006a; Moreno et al. 2006b; Moulton 2006; Virmani et al. 2006; Langheinrich et al. 2007). In animal models, progression of disease can be reduced if neovascularisation is inhibited with angiostatin (Moulton et al. 2003), and growth enhanced by administration of Vascular Endothelial Growth Factor (VEGF) (Celletti et al. 2001).

3.1.5 Contrast Enhanced Ultrasound to Image Neovascularisation

Limiting the success of MRI in imaging plaque neovascularisation is the ceiling on imaging timepoints and the fact that the contrast agent leaks from the vascular space. CEUS does not suffer from these limitations and allows quantification of vessels measuring less than 100 μm in diameter (Leen et al. 2004). Unlike CT or MRI contrast agents, microbubbles remain

within the vasculature and act as 'surrogate red blood cells'; hence they are true intravascular tracers which can be imaged in real time (Granada and Feinstein 2008). Combined with high temporal and spatial resolution of ultrasound, CEUS is well placed to study neovascularisation.

Hitherto, three groups have correlated CEUS imaging results with histological plaque neovascularisation. Feinstein reported a moderate correlation value of 0.64 (Shah et al. 2007); Coli reported an increase in neovascularisation in patients demonstrating extensive enhancement (Coli et al. 2008); Giannoni et al. reported diffuse contrast uptake in plaques from symptomatic patients (Giannoni et al. 2009), all of whom had increased number of microvessels confirmed on histology. The latter group described the common presence of small vessels within plaque underlying ulcerations (Vicenzini et al. 2007). Up until this point, these three groups used subjective visual assessment made by human readers to ascribe binary or discreet scores to the imaging findings – quantification can be improved by generating time-signal intensity curves and using automated image analysis to produce a continuous variable. This approach has been demonstrated by Xiong and colleagues who studied 104 carotid stenoses, revealing that plaque enhanced intensity and the intensity normalised against carotid luminal intensity were both significantly greater in symptomatic versus asymptomatic atheromata (Xiong et al. 2009).

An alternative approach is to investigate periadventitial, rather than intra-plaque, vasa vasorum. A recent study compared quantified B-flow imaging (BFI) CEUS of periadventitial vasa vasorum in patients with atherosclerotic carotid stenosis compared with control carotids, showing a significant difference as well as a correlation of BFI with intima-media thickness (IMT) (Magnoni et al. 2009).

Future work will have to address current unanswered questions about how best to quantify microbubble signal, particularly how normalisation can account for administered contrast dose and pharmacokinetic factors. Acquisition techniques and methods of image analysis need to be standardised, including in motion correction. Work with flow phantoms may help with these issues. Validation of the technique against a standardised clinical score, such as the modified Rankin (Bonita and Beaglehole 1988; van Swieten et al. 1988), Barthel (Wade and Collin 1988) or Frenchay (Holbrook and Skilbeck 1983), is required. Alternatively, comparison with a standardised plaque histological score can be undertaken, such as that produced by the American Heart Association in 1995 (Stary et al. 1995a; Stary et al. 1995b), or a modification (Virmani et al. 2000).

3.1.6 Microbubbles to Improve Structural Imaging of Plaque

Further to potentially providing information on neovascularisation as a biological feature of the atherosclerotic plaque, CEUS has been shown to increase accuracy, sensitivity and specificity of the structural disease assessment (Sidhu et al. 2006). The concept of "Doppler-rescue" has emerged, whereby contrast is introduced during an US examination at the point of failure to obtain diagnostic images with unenhanced scanning. It should be stated that in experienced hands, "Doppler-rescue" is rarely required and this, generally, would indicate the need for alternative imaging. This should also be considered against the recent advances in imaging technology. Furthermore, CEUS has been shown to be of use in the depiction of unsuspected wall irregularities, ulceration, and dissection (Kono et al. 2004), as well as improve the resolution of IMT (Vicenzini et al. 2009).

3.1.7 Potential Problems with Contrast Enhanced Ultrasound

A small number of microbubbles will be destroyed by the incoming ultrasound wave, and when this occurs capillary damage may ensue. This in turn recruits vascular endothelial growth factor (VEGF)-producing inflammatory cells, stimulating neovascularisation (Yoshida et al. 2005). This phenomenon may be a deterrent in the use of CEUS in diagnostics due to the theoretical risk of potentiating plaque instability by promoting angiogenesis. However, at the low mechanical index employed for CEUS, very few microbubbles will be affected and this is therefore a theoretical risk.

The undesirable effects that have been associated with SonoVue®, the most commonly used microbubble in the UK, were in general, non-serious, transient and resolved spontaneously without residual effects. In clinical trials, the most frequently reported adverse reactions were headache (2.3%), injection site pain (1.4%), and injection site bruising, burning and paraesthesia (1.7%) (Bracco 2005). Fatal adverse events (AEs) have occurred following the administration of microbubbles. In the case of SonoVue®, approximately 160,000 doses have been administered and 3 deaths have been temporally related, although causal relationship was uncertain. This fatal AE rate is an order of magnitude higher than for MRI and CT contrast agents, probably reflecting the comorbidities of the recipients (microbubbles are commonly used in high-risk patients for echocardiography) (Dijkmans et al. 2005).

It is important to consider the cost related to the use of ultrasound contrast agents. Although not formal health economic assessment has been undertaken for the use of microbubbles in carotid arterial disease, the technique has been described as being cost-effective in the context of gastrointestinal imaging (Wilson et al. 2009).

3.2 METHODS

3.2.1 Study Approvals

The study protocol received research ethics committee approval (08/H0706/106) and all patients gave written informed consent. The study was further registered as a clinical trial (EudraCT 2008-005900-25) and with the Medicines and Healthcare products Regulatory Agency (MHRA; 19174/0268/001-0001).

3.2.2 Equipment and Settings

Equipment details and settings are detailed in Table 6.

Ultrasound machine	Phillips iU22
Probe	Linear 12-5 MHz
B-mode gain	85%
Contrast gain	85%
Time gain curve	Vertical central / unadjusted
B-mode mechanical index	0.06
Contrast mechanical index	0.06
Dynamic contrast mode	Non-linear / pulse inversion
Late phase contrast mode	Non-linear / power modulation
Intermediate power 'flash' frame mechanical index	0.34
Depth	4.0 cm
Frame rate	12 Hz
Persistence	Medium
Contrast agent	SonoVue
Contrast injection volume	2.0 mL x 2
Dynamic contrast ultrasound recording time	2 minutes
Late phase time post contrast injection	6 minutes
Frame acquisition rate	6 per second

Table 6 Contrast enhanced ultrasound imaging and acquisition parameters

3.2.3 Study Subjects

Between December 2008 and May 2009, subjects aged 18 years or over who presented to the vascular clinic for a carotid duplex ultrasound scan and whose scan showed an atherosclerotic plaque of > 30% stenosis by velocity criteria were recruited. We excluded subjects who experienced myocardial infarction or unstable angina (as defined by the European Society of Cardiology (Bassand et al. 2007; Thygesen et al. 2007)) in the 14 days prior to the study, those with New York Heart Association III or IV heart failure, or prosthetic heart valves, these being contraindications to contrast administration.

Plaques were defined as symptomatic if symptoms consistent with stroke, transient ischaemic attack (TIA) or amaurosis fugax had occurred within 12 months of entry into the study, in the

neurovascular territory of the plaque studied. Plaques were defined as asymptomatic if no such events had ever occurred within their neurovascular territory.

3.2.4 Unenhanced Duplex Ultrasonography and Gray-Scale Median Score

The ultrasound examination was performed with the subject in the supine position. Luminal stenosis was measured in the sagittal plane using the velocity criteria which approximates the NASCET criteria (NASCET 1991; Sidhu and Allan 1997; Oates et al. 2009). This measurement was made by a clinical vascular scientist (with a minimum of 5 years experience in carotid ultrasound) as part of the subjects' routine care. The Gray-scale median score was calculated using the QLAB (Philips; Bothel, WA) quantification software as previously described, with the luminal blood and carotid wall adventia as reference points for normalisation (Sabetai et al. 2000).

3.2.5 Contrast Agent, Preparation and Administration

The contrast agent used was SonoVue™ (Bracco spa, Milan, Italy) which consists of a phospholipid shell containing the inert gas sulphur hexafluoride. The agent is prepared immediately prior to the examination by mixing 25 mg of the lyophilisate powder with 5 mL of saline. 2 mL of this preparation was injected as an intravenous bolus into an antecubital vein. Subjects were observed for 30 minutes following administration of the contrast agent and verbally asked about the occurrence of adverse events.

3.2.6 Dynamic Contrast Enhanced Ultrasound

The carotid bifurcation was imaged in longitudinal projection. The transducer was kept parallel to the vessel so that the near and far wall adventitia were imaged at right angles. CEUS was performed after a bolus injection of SonoVue. With contrast non-linear imaging mode, a mechanical index (MI) of 0.06 was used to achieve optimum visualisation of the plaque vascularity with minimal artefact. Continuous real-time (6 Hz) recording was employed.

Digital Imaging and Communications in Medicine (DICOM) cineloops during the early wash-in, the peak of the injection, and the wash-out phase over 30 to 120 seconds were collected and saved for quantitative analysis. Preliminary data showed that two minutes of acquisition provides a more complete curve than one minute. Using the fundamental B mode image, a single region of interest (ROI) was drawn on the outline of the plaque. The ROI is automatically mapped to the same position on the contrast image and QLAB calculates the signal intensity of each pixel within the ROI. The mean signal intensity is then automatically

calculated. The transfer function of the injection dose and delivery (wash-in and wash-out) will be deconvolved to avoid user biased results by using a ROI (of the same volume as that of the plaque) placed centrally in the carotid lumen away from the plaque region. "Native" raw image data was collected for precise quantification of the intensity corresponding to blood volume (peak enhancement, I_p, Figure 22) in both plaque and lumen. Curves are constructed of the contrast intensity data for the plaque and lumen ROIs as a function of time using the QLAB quantification software (Figure 23). The specific haemodynamics of the plaque neovascularisation will be calculated as normalised peak enhancement of the wash-in curve.

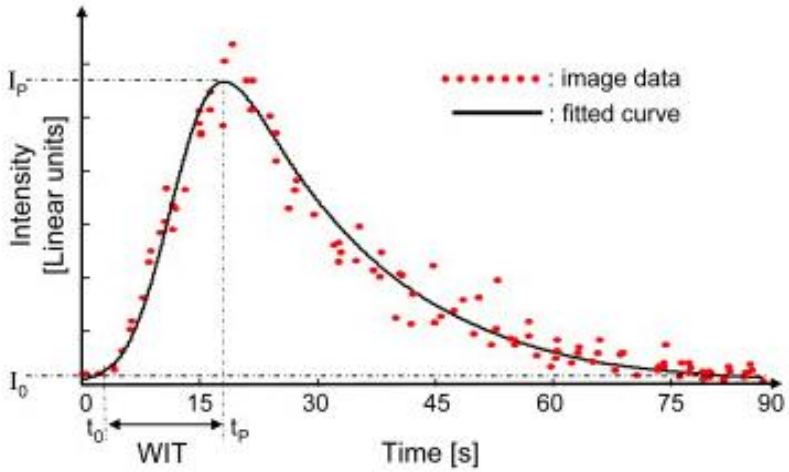


Figure 22 Dynamic contrast enhanced ultrasound time-intensity curve and parameters

The intensities at the 'wash in' and peak phases lie more closely on the curve than at the 'wash out' phase. I_p, peak intensity; t_p, time to peak; WIT, wash in time. From (Averkiou et al. 2010).

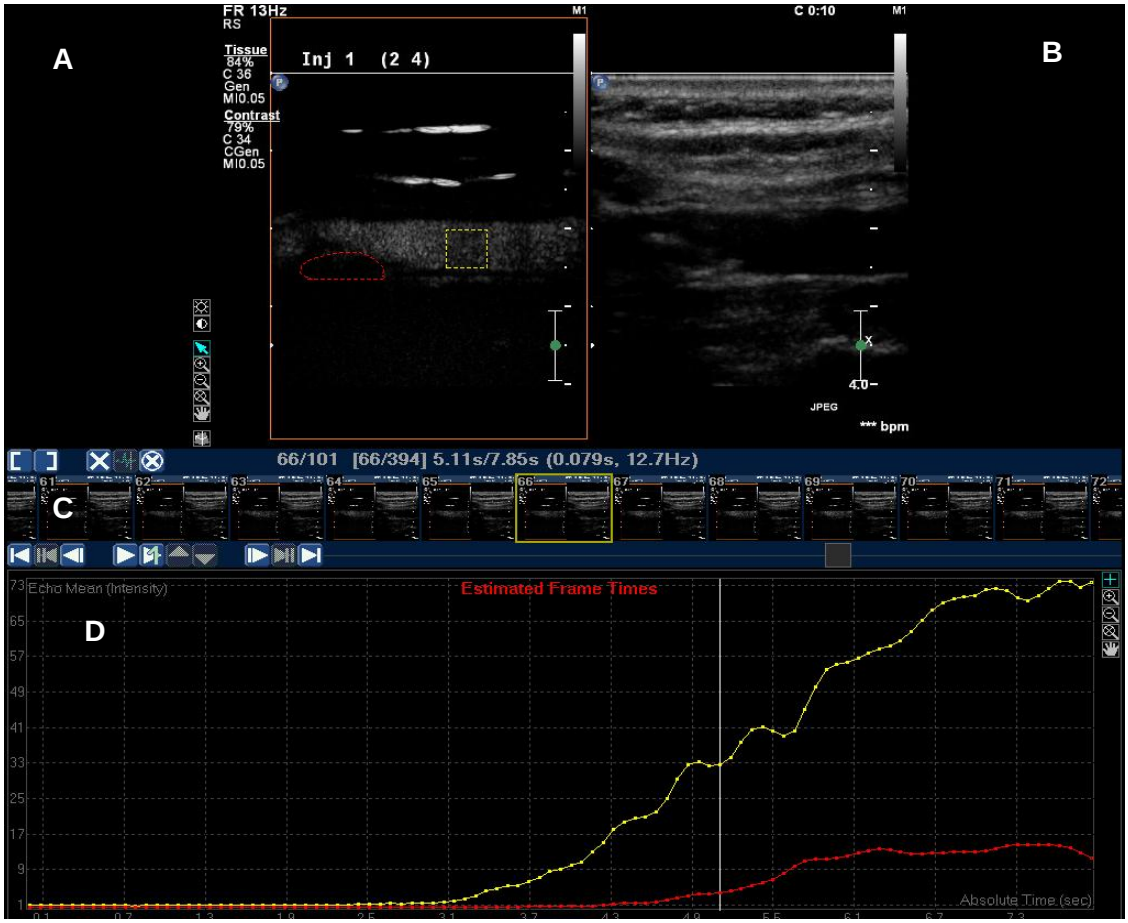


Figure 23 Dynamic contrast enhanced ultrasound image analysis and quantification

In longitudinal section. A. Contrast mode, with regions of interest drawn over the plaque (red) and the lumen (yellow, for normalisation). The regions of interest are similar in size. B. Fundamental B-mode image for the same time-point. This allows the anatomy to be seen. C. The process is repeated over all the acquired frames from the point of contrast injection to two minutes post-injection. D. Time-intensity curves. These plot the intensity of contrast within the plaque (red) and lumen (yellow) for each acquired frame for the time from contrast injection to peak intensity. The vertical white line identifies the point plotted for the images shown in A and B.

3.2.7 Late Phase Contrast Enhanced Ultrasound

Late-phase contrast enhanced ultrasound (LP-CEUS) utilises flash-imaging at intermediate mechanical index (MI: 0.34) of the carotid bifurcation and internal carotid artery, using a non-linear imaging (power modulation) contrast mode, 6 minutes following bolus intravenous contrast injection. Six flash frames were acquired in less than 1 second in the axial orientation at the level of greatest stenosis. Plaque and lumen ROIs are drawn on QLAB to generate to

mean signal intensities from which a normalised peak plaque signal intensity at 6 minutes can be calculated (Figure 24).

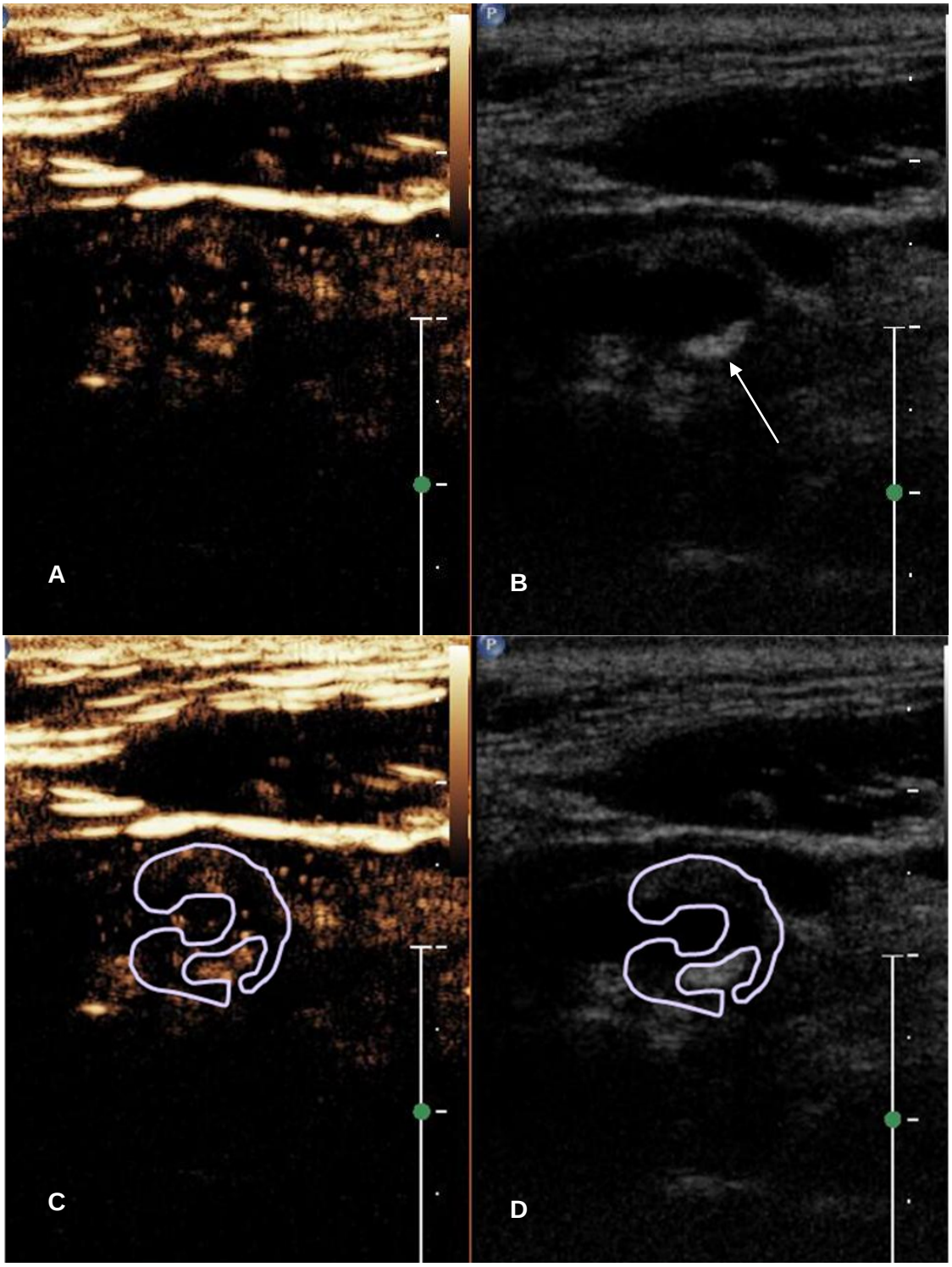


Figure 24 Late phase contrast enhanced ultrasound image analysis

In transverse section. A. Contrast mode at six minutes from the point of contrast injection, flash-imaging at intermediate mechanical index (MI: 0.34). B. Fundamental B-mode image for the same time-point. This allows the anatomy to be seen and, in this case the identification of an area of plaque calcification. C. Image as seen in A, with region of interest (ROI) drawn around the plaque. The area of calcification, as identified in B, is excluded from the ROI so as to prevent a false high contrast value. D. Image as seen in B, with plaque ROI drawn.

3.2.8 Blinding and Standardisation of Contrast Enhanced Ultrasound Image Acquisition and Data Processing

Both scanning and image analysis were performed blinded to the patients' clinical information (including symptomatic status).

Steps were taken in order to standardise the CEUS image acquisition. These included the use of a 3-way tap in the administration of contrast into the end of the cannula (not though the filter/valve at the top of the cannula, as this may interfere with the microbubble integrity), using a large intra-venous cannula of at least 20 gauge, and asking patients to avoid foods and drinks containing caffeine for 12 hours prior to imaging. Tea, coffee, chocolate and colas may theoretically cause vasoconstriction, although this is unlikely owing to the described immaturity of the microvessels under investigation (Dunmore et al. 2007).

QLAB software (Philips, Bothel, WA) was used to quantify echo intensity of the plaque from the acquired cine-loop. For LP-CEUS, a single ROI was drawn on the outline of the plaque on the contrast enhanced image, with the B mode image displayed alongside as reference. Areas of calcium causing signal artefact (formally defined as areas confirmed through quantification as being of aberrant signal >1 order of magnitude above the signal quantified from the remainder of the plaque) were not included in the plaque ROI analysed. The mean signal intensity was automatically calculated. A second ROI was drawn around the residual lumen to calculate mean signal intensity in the lumen. The raw linear data was log transformed, and the signal intensity of the plaque was normalised against the lumen signal intensity to account for patient factors such as volume of distribution and cardiac output. Intra-observer variability by Cohen's kappa for this analysis was 0.88, representing substantial agreement.

3.2.9 Statistical Analysis

The number of subjects enrolled in the study provided 90% power to detect effect sizes (difference/standard deviation) of 1.1 with a 5% type-I error rate. Sample size calculations were performed using PASS (NCSS, Kaysville, Utah).

The raw linear data generated from QLAB was found to be log-normally distributed, and therefore was log transformed for statistical analysis. The signal intensity of the plaque was normalised by dividing the plaque signal intensity by the lumen signal intensity (because the data was log transformed, normalisation required subtracting the lumen signal intensity from the plaque signal intensity). The normalised signal was compared between the two groups

(symptomatic and asymptomatic) using the t-test, assuming unequal variances (GraphPad Prism 5.01, GraphPad Software, San Diego, CA). Within the symptomatic group, plaques in the territory of a stroke were compared to those in the territory of a TIA. Within the asymptomatic group, plaques from subjects who had never had a cerebrovascular event were compared to those who had a history of such an event affecting the contralateral hemisphere. These comparisons were made using the t-test. Pearson correlation was used to investigate both the relationship between gray scale median and LP-CEUS signal, and the relationship between LP-CEUS signal and luminal stenosis. Baseline frequencies between the two groups were compared using Fisher's exact test or t-tests where appropriate. The possible relationship between subject characteristics and LP-CEUS was assessed using analysis of variance (ANOVA) with the characteristic as a covariate (SAS 9.1.3, SAS Institute Inc., Cary, NC). Sensitivity and Specificity of LP-CEUS for correctly identifying plaques as symptomatic or asymptomatic were derived by using receiver operating characteristic (ROC) curve analysis. Cut-off values were chosen which minimised the difference between sensitivity and specificity. A p value of 0.05 was used to determine significance for all statistical tests. Multivariate logistic regression analysis was performed using Stata 11 (Statacorp LP, TX).

3.3 RESULTS

3.3.1 Patient Numbers and Characteristics

Thirty-seven patients were enrolled, with a mean age of 69.9 years (+/- 8.5 years standard deviation). 27 (73%) were male, with a mean age of 69.7 years (range 58-86) and 10 (27%) were female, with a mean age of 70.3 years (range 49-86) with no significant difference in the ages of men and women. In total, 16 patients were recruited into the symptomatic group and 21 into the asymptomatic group. Of the symptomatic group, the time from cardiovascular event to LP-CEUS assessment was less than 30 days for 10 patients (63%), and less than 50 days for 14 patients (88%). With regard to the cerebrovascular events, 6 patients (37.5%) had had a stroke, 8 (50%) had had a TIA, and 2 (12.5%) had had amaurosis fugax. Of the asymptomatic group, 7 (33%) had previously been diagnosed with TIA or stroke which affected the hemisphere contralateral to the plaque which was studied. The remaining 14 (67%) of the asymptomatic group had never been diagnosed with TIA, stroke or amaurosis fugax. There was no significant difference between the symptomatic and asymptomatic groups in age, gender, or history of diabetes mellitus, hypertension, statin use and smoking (Table 7).

Characteristic	Symptomatic (n=16; 43%)	Asymptomatic (n=21; 57%)	*p* Value
Age (years)	71 +/- 9.9	69 +/- 7.5	0.65
Male Sex	11 (69%)	16 (76%)	0.72
Diabetes Mellitus	3 (19%)	3 (14%)	1.00
Statin Use	15 (94%)	16 (71%)	0.24
Hypertension	12 (75%)	17 (81%)	0.70
Smoking History	11 (69%)	13 (62%)	0.74

Table 7 Characteristics of the symptomatic and asymptomatic patient groups

This table shows that there were no statistically significant differences in the demographic or clinical parameters when comparing patients with symptomatic to those with asymptomatic carotid stenosis. Data are numbers of patients, with percentages in parentheses, with the exception of age, were data are means +/- standard deviations.

3.4 DYNAMIC CONTRAST ENHANCED ULTRASOUND

Thirty-five of the 37 patients (95%) who underwent carotid plaque assessment by D-CEUS had images acquired which were of sufficient quality to allow for accurate intensity quantification. Of the two patients whose images were not analysed, one was from the symptomatic group and the other from the asymptomatic. The peak plaque echo intensity, normalised for the carotid artery luminal intensity, was higher in symptomatic than asymptomatic plaques (Figure 25)

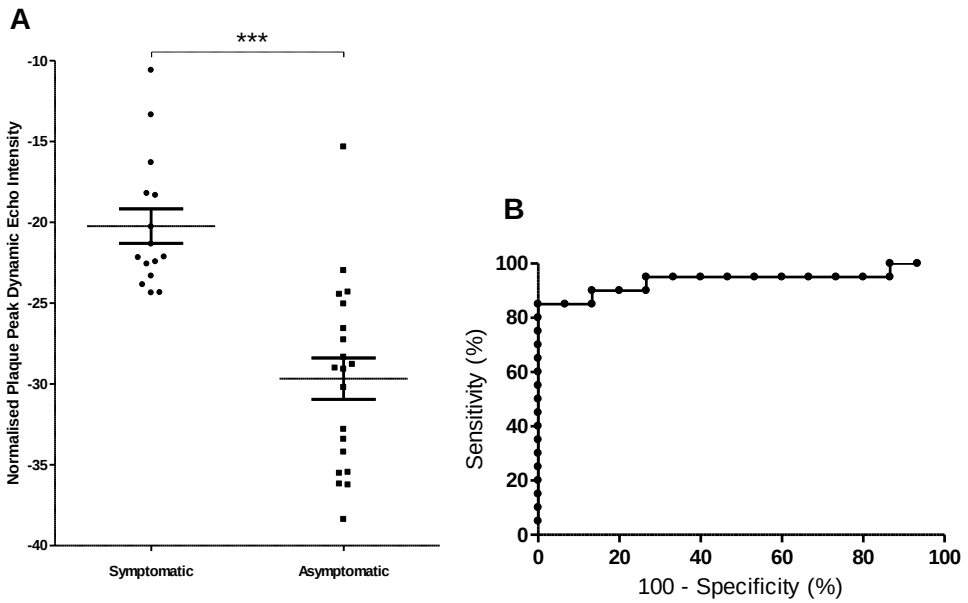


Figure 25 Normalised plaque peak dynamic echo intensity

A. The peak carotid plaque intensity during D-CEUS, when normalised for luminal intensity, was higher in symptomatic than asymptomatic patients. Mean and standard error of mean

*shown. n=35, ***p<0.0001. B. Receiver operator characteristic curve analysis area under the curve for D-CEUS is 0.94.*

3.5 LATE PHASE CONTRAST ENHANCED ULTRASOUND

3.5.1 Relationship between Late Phase Signal and Symptomatology

The LP-CEUS examination was well tolerated by all patients and of the 37 patients enrolled, all produced evaluable LP-CEUS data. Percentage luminal stenosis ranged from 30-99% and whilst the mean stenosis in the symptomatic group was greater than in the asymptomatic group, the difference between the two groups did not achieve statistical significance (p=0.06) (Table 8). Given the standard deviation observed in this study and the sample size, a difference of 20.5% in stenosis would have been required to provide 90% power to detect a difference between the two groups.

Variable	Symptomatic (n=16)	Asymptomatic (n=21)	Difference (Symptomatic – Asymptomatic)	*p* Value
Luminal Stenosis	79% (69%-89%)	67% (58%-75%)	12% (–0.4% to 25%)	0.06
LP-CEUS	0.39 (-0.11 to 0.89)	-0.69 (-1.04 to -0.34)	1.08 (0.49 to 1.66)	0.0008
GSM	17 (13 to 20)	29 (21 to 37)	–12 (–3 to –21)	0.009

Table 8 Ultrasound features of carotid plaque in patients with and without symptoms

This table summarises the unenhanced carotid duplex and LP-CEUS results from 37 patients. Data is expressed as mean (95% confidence interval). GSM, Gray-scale median.

At 6 minutes, when late phase flash imaging is performed, there are very few microbubbles within the circulation in the lumen of the carotid artery. A logarithmic scale is used. When there is signal maintained within the plaque at 6 minutes, this tends to exceed the signal from the lumen, as such a positive value for normalised late phase signal is obtained. Where there is little signal within the plaque at 6 minutes, the signal from the lumen tends to exceed that from the plaque, such that a negative value for normalised late phase signal is recorded.

The LP-CEUS normalised plaque intensity was significantly greater in the symptomatic group 0.3899 (95% CI: -0.1056 to 0.8854) than the asymptomatic group -0.6869 (95% CI: -1.036 to -0.3380), (p=0.0005) (Figure 26A). However, there was overlap in signal intensity between the two groups. Of note, the lowest signal intensity from the symptomatic group was derived

from the patient who had the longest event to scan time (of nearly 1 year). For this patient, the signal fell below the mean of the asymptomatic group.

Receiver operator characteristic analysis revealed a sensitivity and specificity of 75% and 86%, respectively, for a LP-CEUS normalised peak intensity cut off > 0.00 (Figure 26B).

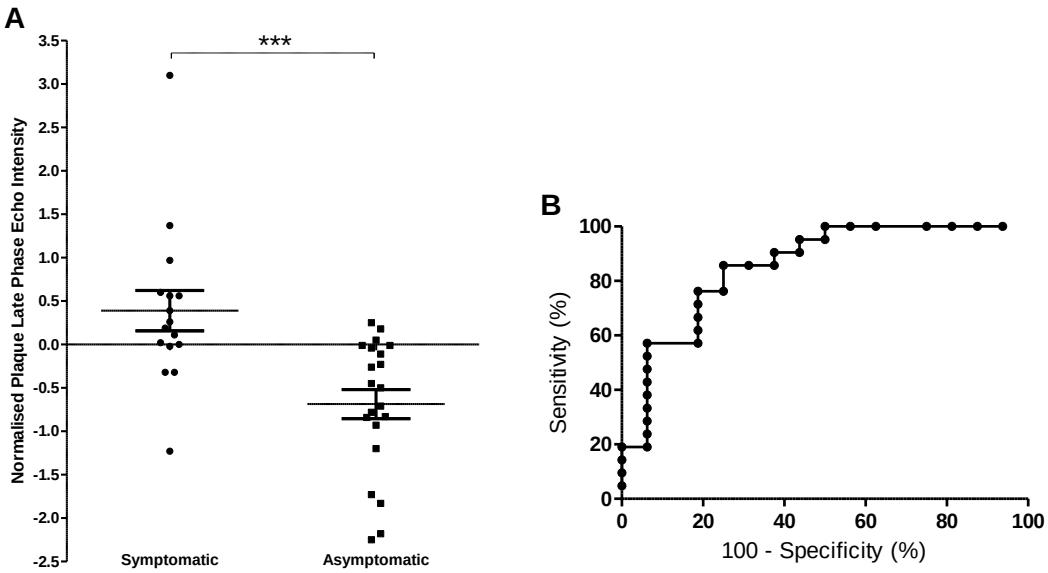


Figure 26 Normalised plaque late phase intensity

*A. The carotid plaque intensity during LP-CEUS, when normalised for luminal intensity, was higher in symptomatic than asymptomatic patients. Mean and standard error of mean shown. n=37, ***p=0.0005. B. Receiver operator characteristic curve analysis area under the curve for LP-CEUS is 0.88.*

3.5.2 Relationship between Late Phase Signal and Time Since Symptoms

Of the symptomatic group, the time from cardiovascular event to LP-CEUS assessment was less than 30 days for 10 subjects (63%), and less than 50 days for 14 subjects (88%). With regard to the cerebrovascular events, 6 subjects (37.5%) had had a stroke, 8 (50%) had had a TIA, and 2 (12.5%) had had amaurosis fugax. Of the asymptomatic group, 7 (33%) had previously been diagnosed with TIA or stroke which affected the hemisphere contralateral to the plaque which was studied. The remaining 14 (67%) of the asymptomatic group had never been diagnosed with TIA, stroke or amaurosis fugax.

Figure 27 demonstrates the relationship between normalised LP-CEUS signal and the time since symptoms. There is a weak but significant correlation, however this is likely to be driven by a single outlying point representing a patient who experienced symptoms approaching 1 year prior to scanning.

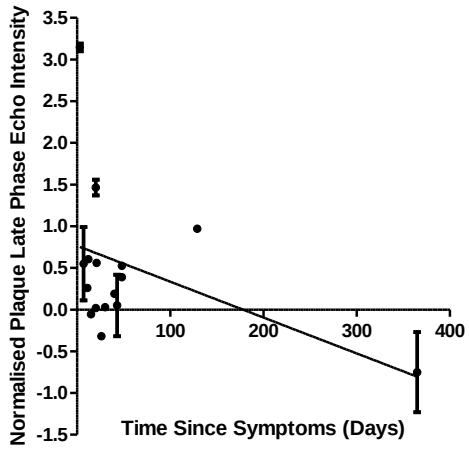


Figure 27 Normalised plaque late phase and declines with time since symptoms

For symptomatic plaques, the carotid plaque intensity during L-CEUS, when normalised for luminal intensity, was seen to be inversely related to time since symptoms. n=16, r=0.1811, p=0.0339.

3.5.3 Relationship between Late Phase Signal and Gray-Scale Median Score

There was a significant difference between the two groups with regard to GSM (Figure 28). The asymptomatic group had a higher GSM score than the symptomatic group (asymptomatic mean 29.01 (95% CI: 32.844 to 25.176), symptomatic mean 16.95 (95% CI: 18.544 to 15.356) (p=0.0124)). There was a moderate (rho=–0.44, p=0.016) inverse correlation between normalised plaque intensity and GSM score, demonstrating the tendency for plaques with greater normalised plaque intensity to have a lower GSM score.

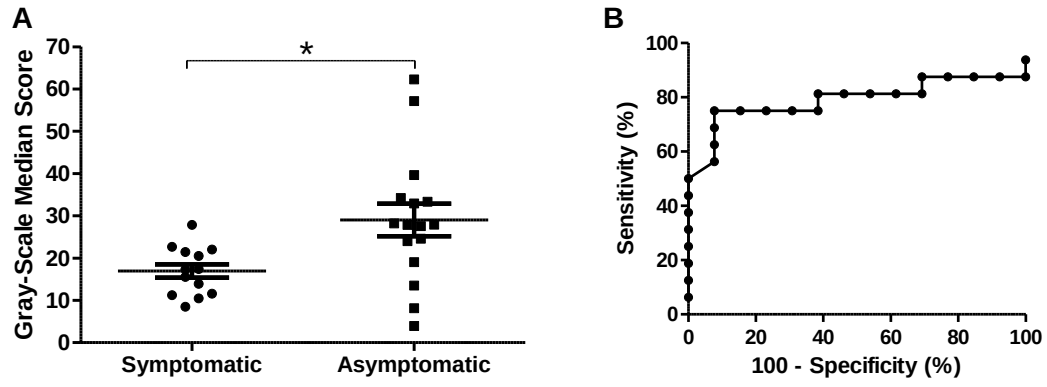


Figure 28 Gray-scale median score

*A. The carotid plaque gray-scale median (GSM) score, was lower in symptomatic than asymptomatic patients. Mean and standard error of mean shown. *p=0.0124. B. Receiver operator characteristic curve analysis area under the curve for GSM is 0.79.*

3.5.4 Relationship between Late Phase Signal and Stenosis

There was no correlation between normalised LP-CEUS plaque intensity and percentage luminal stenosis (p=0.27).

3.5.5 Relationship between Late Phase Signal and Patient Characteristics

There was no evidence of a relationship between diabetes, smoking history, or statin dose with LP-CEUS signal, nor of differential LP-CEUS signal between those patients in the symptomatic group with TIA versus CVA. Within the asymptomatic group, there was no significant difference in LP-CEUS signal between those patients who had never had a cerebrovascular event and those who had a history of such an event affecting the contralateral hemisphere.

3.5.6 Relationship between Late Phase Signal and Dynamic Signal

Figure 29 demonstrates the relationship between normalised LP-CEUS signal and the normalised peak intensity on dynamic CEUS. As only a trend towards moderate correlation is seen between the two, combining the parameters was initially undertaken to observe whether this improved the capacity of CEUS to discriminate on the basis of symptomatic status. To account for the differences in magnitude between the LP-CEUS and D-CEUS signals, LP-CEUS signal was multiplied by a factor of 50 before summing with D-CEUS signal. The resultant CEUS 'score' discriminated symptomatic from asymptomatic carotid stenosis, at a cut off of -25, with improved sensitivity (90%) and specificity (88%) (Figure 30).

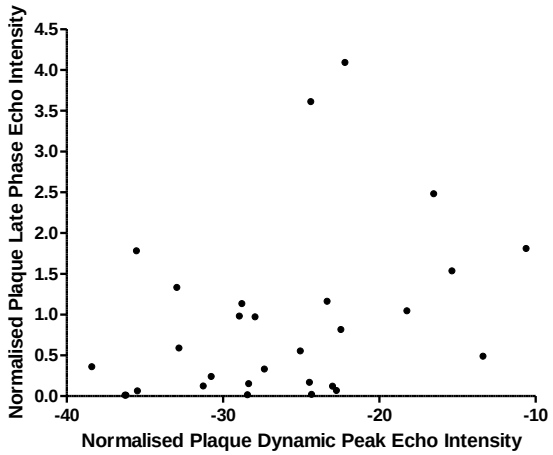


Figure 29 There is a trend towards positive correlation between normalised plaque late phase and dynamic peak signals

There is a trend towards moderate correlation between normalised D-CEUS and LP-CEUS plaque signals. n=29, Pearson r=0.3753, p=0.0571.

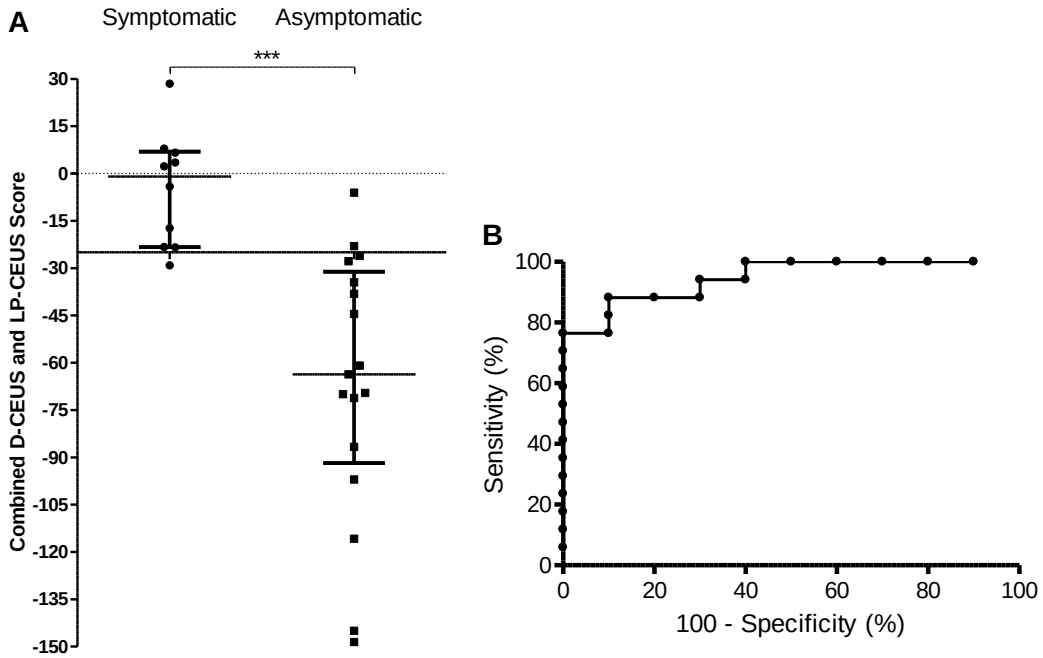


Figure 30 Combined LP-CEUS and D-CEUS score

*A. As only a trend towards moderate correlation is seen between LP-CEUS and D-CEUS, combining these to determine a CEUS 'score' was undertaken. At a cut off of -25, there was a sensitivity of 90% and a specificity of 88% to separate symptomatic from asymptomatic carotid plaque. Mean and standard error of mean shown. n=27, ***p=0.0002. B. Receiver operator characteristic curve analysis area under the curve for the CEUS 'score' is 0.95.*

3.5.7 Multivariate Logistic Regression Analysis

To determine whether any covariates were significantly related, a coefficient correlation matrix was generated, based on 27 patients (Table 9). This identified that both LP-CEUS and D-CEUS as significant co-variates in the context of symptomatic status. LP-CEUS and D-CEUS were entered into a multi-variate logistic regression model (Table 10).

	Age	Gender	Statin use	Creatinine	Degree of stenosis	Symptomatic status	D-CEUS
Age	1.0000						
p							
Gender	-0.1220	1.0000					
p	0.5443						
Statin use	0.1665	-0.0088	1.0000				
p	0.4065	0.9652					
Creatinine	0.4436	0.2737	-0.0142	1.0000			
p	0.0205	0.1672	0.9441				
Degree of stenosis	0.1033	0.0805	0.3658	0.0325	1.0000		
p	0.6082	0.6898	0.0606	0.8723			
Symptomatic status	0.2006	0.1037	0.1040	0.1118	0.2338	1.0000	
p	0.3157	0.6067	0.6059	0.5788	0.2406		
D-CEUS	-0.1686	0.1858	0.0550	0.0789	0.2644	0.6372	1.0000
p	0.4005	0.3534	0.7852	0.6958	0.1825	**0.0004**	
LP-CEUS	-0.0262	0.1186	-0.1645	0.0912	-0.0074	0.6147	0.4935
p	0.8967	0.5557	0.4122	0.6510	0.9710	**0.0006**	**0.0089**

Table 9 Correlation coefficient matrix

This matrix shows D-CEUS and LP-CEUS as significant (and correlated) covariates – highlighted in bold – in the context of symptomatic status that would warrant their inclusion in a multivariate model.

	Coefficient	Standard Error	z	P>|z|	95% Confidence Interval
D-CEUS	**0.2860495**	0.1438309	1.99	0.047	0.0041461 – 0.5679528
LP-CEUS	**4.598986**	2.625238	1.75	0.080	-0.5463852 – 9.744357
Constant	**6.597783**	3.448486	1.91	0.056	-0.161125 – 13.35669

Table 10 Multivariate logistic regression model for symptomatic status

After adjustment for both D-CEUS and LP-CEUS, there is still borderline significant evidence to suggest that both measurements are independently associated with symptomatic status. Given the correlation between the D-CEUS and LP-CEUS in this dataset, the p-values are likely to be overestimated and the association be stronger than presented in this model. Based on this data:

Odds of being symptomatic =

6.6 + 0.3 (Log normalised D-CEUS signal) + 4.6 (Log normalised LP-CEUS signal)

3.6 DISCUSSION

3.6.1 Contrast Enhanced Ultrasound as Compared to Functional and Structural Imaging Modalities

Imaging techniques to identify biological features of the plaque *in vivo* could improve risk stratification, facilitating clinicians' treatment decisions and monitoring response to plaque-

stabilising therapies. To this end, imaging intraplaque inflammation, neovascularisation, haemorrhage and apoptosis have been attempted with some success using MRI and/or nuclear medicine. However, high prevalence of carotid disease and expense associated with these techniques preclude them from replacing ultrasound as first line investigation (Rudd et al. 2002; Kerwin et al. 2003; Trivedi et al. 2003; Cappendijk et al. 2004; Kietselaer et al. 2004).

Using (non-contrast enhanced) ultrasound to identify plaque constituents has been attempted with "Gray-Scale Median" (GSM) evaluation. Studies in which patients were imaged prior to surgical endarterectomy have consistently demonstrated that plaques which are echolucent on ultrasound, with a low GSM, have high lipid, haemorrhage and macrophage on histology. Conversely, echogenic plaques, with a high GSM, have a higher fibrous content (El-Barghouty et al. 1996b; Gronholdt et al. 1997; Gronholdt et al. 1998; Gronholdt et al. 2002). GSM is also associated with clinical findings: evidence of cerebral infarction on CT is more common in the presence of echolucent plaques rather than echogenic, regardless of symptomatic status (el-Barghouty et al. 1995; el-Barghouty et al. 1996a). Echogenicity on ultrasound has also been shown to predict ipsilateral ischaemic stroke; patients with echolucent plaques are at increased risk compared to those with echorich plaques (Hayward et al. 1995; Polak et al. 1998; Gronholdt et al. 2001; Mathiesen et al. 2001). However, hazard ratios for development of stroke that are associated with differing echogenicity scores are not sufficiently great to warrant translation into clinical practice. Furthermore, studies investigating the use of GSM in selection for carotid artery stenting (CAS) have had conflicting results. The Imaging in Carotid Angioplasty and Risk of Stroke (ICAROS) study revealed that high echolucency increases risk of stroke as a complication of CAS (Biasi et al. 2004). Subsequently, Reiter and colleagues showed no such relationship between plaque echolucency and stroke risk with CAS (Reiter et al. 2006).

3.6.2 Dynamic Contrast Enhanced Ultrasound

Dynamic contrast enhanced ultrasound (D-CEUS) peak plaque intensity, normalised against the peak luminal intensity, is significantly higher in symptomatic plaques as compared with asymptomatic plaques. This approach, employing time-intensity curves, has been used by Xiong and colleagues who studied 104 carotid stenoses, revealing that plaque enhanced intensity and the intensity normalised against carotid luminal intensity were both significantly greater in symptomatic versus asymptomatic atheromata (Xiong et al. 2009).

Moreover, we have shown that in symptomatic individuals D-CEUS signal declines with time since symptoms. This is in keeping with evidence that remodelling of the plaque occurs following stroke (Peeters et al. 2009).

3.6.3 Late Phase Contrast Enhanced Ultrasound

This study has demonstrated that the late phase CEUS (LP-CEUS) signal intensity of the carotid plaque is greater in plaques deemed responsible for cerebrovascular events compared to asymptomatic plaques. These results imply that once the majority of microbubbles have been cleared from the circulation, they are still present within the carotid plaque in sufficient numbers to be detected and quantified by this novel ultrasound technique. The results also imply that more microbubbles are retained within those plaques deemed responsible for a cerebrovascular event, compared to asymptomatic plaques.

This finding may merely represent the fact that symptomatic plaques have more intraplaque blood volume than asymptomatic plaques, and thus contain more circulating microbubbles in the late phase, just as they do with dynamic contrast enhanced ultrasound (D-CEUS) (Xiong et al. 2009). But this is unlikely because, during the dynamic phase, the signal from the lumen is approximately two orders of magnitude greater than the signal from the plaque. Were the late phase plaque signal purely a result of circulating microbubbles, it should only represent a small fraction of the late phase lumen signal. The fact that the late phase signals of plaque and lumen are of similar magnitude, implies that microbubbles have accumulated within the plaque.

It is hypothesised that the microbubbles may be retained on the endothelium or may leave the microvessel and enter the plaque parenchyma; and retained in isolation or within phagocytosing macrophages. It is likely that a number of interrelated endothelial processes are responsible for this microbubble accumulation: endothelial activation; endothelial permeability and leakage (of the microbubbles themselves or of inflammatory cells containing them); and endothelial charge changes.

Biological plausibility of this theory is provided by preclinical work demonstrating that microbubbles are passively targeted to tissue with activated endothelium and/or inflammation (Lindner et al. 2000a; Lindner et al. 2000b; Tsutsui et al. 2004b). Lipid microbubbles, such as SonoVue, adhere through opsonisation by serum compliment. In contrast, albumin-shelled microbubbles adhere through leukocyte β_2-integrin Mac-1 (CD11b/CD18) (Lindner et al. 2000a).

A potential explanation for the retention of microbubbles by the endothelium is that there are charge changes when the endothelium is activated. Furthermore, a role for the negatively charged endothelial glycocalyx has been postulated. Glycocalyx has emerged as a potential

orchestrator of vascular homeostasis (Broekhuizen et al. 2009) with cytokine 'scavenging' (Lortat-Jacob et al. 2002) and mechanosensing (Florian et al. 2003) functions. With regards the latter, the 'state' of the endothelial gycocalyx, *i.e.* the presence of hyaluronan and sialic acid which cover cytokine binding sites on selectins, actively determines whether and to what extent cytokines will be able to induce localised vessel wall inflammation (Mulivor and Lipowsky 2002; Varki 2008). It is thought that when endothelium becomes activated or inflamed, it sheds its overlying matrix, including the negative glycocalyx, resulting in a charge change to more positive. It has been observed that endotoxin administration in rats induced microvascular dysfunction in conjunction with immediate glycocalyx degradation, suggesting a role for Toll-like receptors (TLRs) in glycocalyx perturbation (Marechal et al. 2008; Broekhuizen et al. 2009). Furthermore, in a human study, it was shown that a controlled inflammatory challenge leads to instantaneous shedding of glycocalyx constituents and leucocyte activation, pointing towards glycocalyx as a protective shield against inflammatory stimuli (Nieuwdorp et al. 2009). As SonoVue is negatively charged, this may be one mechanism through which microbubbles are retained in LP-CEUS. It can be stained for using anti-heparan sulphate antibodies, and may be enzymatically removed from endothelial cells using heparinise III.

It is thought that by detecting retained untargeted microbubbles, LP-CEUS has the potential to detect inflammation and/or endothelial activation within human carotid plaque *in vivo*. This is the first study demonstrating microbubbles passively targeting atherosclerotic carotid plaque in humans. This finding may have important clinical consequences for patients at high risk of plaque rupture and consequent stroke, because *ex vivo* analysis of atherosclerotic plaques has demonstrated that plaques causing rupture are characterised by an abundance of macrophages and an inflammatory infiltrate (Moreno et al. 1994; van der Wal et al. 1994; Boyle 1997; Schaar et al. 2004; Virmani et al. 2006). The fact that the signal intensity derived from the symptomatic group overlaps with the asymptomatic group implies LP-CEUS may have the potential to identify asymptomatic patients who are at high risk of cerebrovascular events who might benefit from intensive medical treatment or surgical intervention. Histological validation studies will be required to determine whether features of the plaque which pertain to inflammation or endothelial dysfunction correlate with the LP-CEUS signal. Such studies may also shed light on the mechanism by which non-targeted microbubbles adhere to the plaque, which is currently unclear. Prospective studies will subsequently be required to investigate the natural history of the LP-CEUS signal, whether it predicts the clinical outcome, and if so over how long a time frame.

As expected from previous studies, GSM score was greater in asymptomatic compared to symptomatic plaques (Grogan et al. 2005). Although the strength of the correlation was only moderate, the LP-CEUS signal was inversely associated with GSM score. Such a correlation is expected as plaques with a low GSM score have high lipid, haemorrhage and macrophage content (El-Barghouty et al. 1996b; Gronholdt et al. 1997; Gronholdt et al. 1998; Gronholdt et al. 2002), and would therefore be expected to retain more microbubbles.

Several studies hitherto have used CEUS to assess the carotid plaque, but these have used the contrast as a blood pool agent and acquired data during the dynamic phase (D-CEUS) in order to detect intraplaque angiogenesis (Shah et al. 2007; Coli et al. 2008; Giannoni et al. 2009; Xiong et al. 2009). In the majority of these studies, visual assessment of the post processed data was used (Shah et al. 2007; Coli et al. 2008; Giannoni et al. 2009). In only one study was the signal quantified with image analysis software, and the results used to perform a ROC analysis (Xiong et al. 2009). The ROC analysis of the present study compares favourably to that generated from the aforementioned D-CEUS study (Sensitivity and specificity 75% and 86% respectively for the present study, compared to 74% and 75% respectively for the D-CEUS study). Such comparisons between the two techniques are premature at this stage, as both techniques are in their infancy. However, LP-CEUS offers distinct advantages over D-CEUS: the examination is technically much easier to perform, and because image acquisition lasts less than 1 second, motion artefacts do not cause a problem.

3.6.4 Limitations of Late Phase Contrast Enhanced Ultrasound

The symptomatic and asymptomatic groups were both heterogeneous. The symptomatic group was comprised of patients with TIA, stroke or amaurosis fugax. Recent evidence suggests that plaques deemed responsible for stroke heal differently than those deemed responsible for TIA in the post event period (Peeters et al. 2009). The asymptomatic group was comprised of patients who had never had a cerebrovascular event, and those who had had an event affecting the contralateral hemisphere. MRI studies with iron oxide particles show that plaques which are contraleral to symptomatic plaques have greater inflammation than plaques from patients who have never had cerebrovascular event (Tang et al. 2007), reflecting the systemic nature of atherosclerosis. Although no evidence of a difference in LP-CEUS signal was detected between these subgroups, the study was not powered for this purpose and such differences cannot be excluded. A larger study would be required to definitively address the relationship between LP-CEUS and these characteristics. Furthermore, numbers were too small to allow for a comprehensive multivariate logistic regression analysis.

The symptomatic group was also heterogeneous with regards to the time from cerebrovascular event to LP-CEUS assessment. Because the plaque heals following stroke (Peeters et al. 2009), had the inclusion criteria for the symptomatic group been more stringent, and stipulated an event to scan time of less than 2 weeks, the ROC analysis may have yielded improved sensitivity and specificity.

The non-linear pulse sequence used was not designed for this indication and represents a crude means of detecting the very low concentration of microbubbles expected to be present in the plaque in the late phase. To accurately quantify the degree of microbubble retention and correlate the signal with histological features of the plaque, improved non-linear pulse sequences developed specifically for this purpose are required.

Contrast modes for three-dimensional ultrasound are not currently available. Because the late phase technique destroys retained bubbles, this study was limited to assessing one single slice of the plaque. The assumption that the single slice is representative of the entire plaque is no doubt incorrect.

As with the majority of modalities which measure signal intensity, the late phase signal in the plaque requires normalisation to avoid variation from factors which affect the overall intensity of the image. To mitigate these sources of variation, the plaque signal was divided by the lumen signal. However, this quantification method will be sensitive to factors which affect luminal signal. Furthermore, the kinetics of those microbubbles flowing within the vascular space probably differ from those of microbubbles retained in the plaque, and so this method will also be sensitive to the time point at which LP-CEUS is performed. Further studies are required to investigate the most appropriate method to normalise the signal.

3.6.5 Conclusion

By quantifying microbubble retention within the carotid plaque, LP-CEUS is able to show differences between groups of plaques within the neurovascular territory of recent cerebrovascular events and asymptomatic plaques; it thus has promise as a tissue specific marker of inflammation. This technique may be useful in helping to identify those asymptomatic patients who might benefit from intensive medical or surgical therapy, or as a biomarker to investigate pharmacodynamic effects of experimental molecules.

4 MULTI-ANALYTE PROFILING IN CAROTID ATHEROSCLEROSIS

4.1 INTRODUCTION

As described in Section 1.5, atherosclerosis shares features with diseases caused by chronic inflammation (Full et al. 2009). Inflammation is intrinsically linked with disease activity, as the numbers of monocyte-macrophages infiltrating the plaque (Davies et al. 1993) and their location at plaque rupture-sensitive sites (such as the fibrous cap and erosion sites (van der Wal et al. 1994; Virmani et al. 2003)) is related to plaque vulnerability. Moreover, lymphocyte numbers and their activation markers relate to plaque activity (van der Wal et al. 1994). Macrophage differentiation is acknowledged as being critical for the development of atherosclerosis (Gleissner et al. 2010).

Genetic ablation or intervention studies in mouse models of atherosclerosis have mapped the cellular components of the inflammatory infiltrates in the plaques and the soluble mediators necessary for their recruitment and activation (Weber et al. 2008). There is less knowledge on human atherosclerotic disease, and even less on the mechanisms that make the human plaque prone to complications. Our group has previously demonstrated the effectiveness of isolation of viable cells from CEA specimens. This system reflects the complex cellular interactions occurring *in vivo*. The mixed cell population contains macrophages, lymphocytes and smooth muscle cells, and displays spontaneous cytokine, chemokine and matrix metalloproteinase (MMP) production (Monaco et al. 2004; Monaco et al. 2009; Cole et al. 2011). Inflammatory molecule production has been shown to be dependent upon toll-like receptor (TLR) 2 signalling (Monaco et al. 2009), and the nuclear factor κB (NFκB) pathway via myeloid primary differentiation response gene 88 (MyD88) (Monaco et al. 2004).

The number, phenotype and fate of infiltrating cells within the plaque is highly dependent on soluble mediators such as cytokines and chemokines contained within the milieu of the plaque. As instability in atherosclerosis is determined by the balance of cytokines, chemokines and other relevant mediators, this micro-environment is determined by the complex interaction between cell types within tissue (Hamilton 2008). The characterisation of soluble mediators may yield quantitative and functional information on the plaque inflammatory milieu. Such characterisation may identify targets for plaque stabilising therapies, as well as risk stratification through both functional imaging and biomarkers. Moreover, the investigation of soluble mediators has the potential to identify blood-borne biomarkers, whether individual or as part of a bio-molecular signature. This study aimed to map the components of this milieu for the first time and to study the clustering and relationships between such mediators with the aim to understand the specific “cocktail” of mediators associated with the high-risk plaque.

4.2 METHODS

4.2.1 Ethical Approval and Regulation, Sample and Data Collection, and Definition of Symptomatic Status

This investigation into factors influencing carotid artheromatous plaque instability received research ethics committee approval (08/H0706/129 and Riverside Research Ethics Committee RREC 2989). Informed consent was obtained from all patients enrolled. Diseased intimal arterial segments were collected from consenting patients undergoing carotid endarterectomy surgery at Charing Cross Hospital, London, for both asymptomatic and symptomatic carotid stenosis, and anonymised according to the rules set out in the Human Tissue Act (2004). A patient was considered symptomatic if the patient had experienced, within the last 6 months, focal neurological symptoms pertaining to the ipsilateral carotid territory (stroke, transient ischemic attack or amaurosis fugax). The symptomatic status was confirmed by the neuro-vascular multi-disciplinary team. Demographic, clinical and pharmacotherapeutic data was compiled for all patients.

4.2.2 Carotid Atheromatous Plaque Processing Protocol

In order that a number of laboratory techniques may be employed upon the carotid plaques obtained at carotid endarterectomy, a protocol was devised to permit the plaque to be process in a manner that would allow for this. Primarily, the plaque is divided symmetrically, longitudinally through the point of greatest stenosis. Half of the plaque is then committed to the plaque digestion and atheroma cell culture pathway. The other half is axially cut into between 3 and 5 parts (depending upon the size of the plaque), equal in size. The top, middle and bottom parts are used for histological assessment of the upstream, middle and downstream areas of the plaque (Figure 31).

The protocol described also prescribed that the plaque be placed in red cell lysis buffer prior to being divided. This is to allow for the removal of any red blood cells. However, if the plaque is cut and the sections placed in lysis buffer, this may inadvertently lyse any inflammatory cells within the plaque.

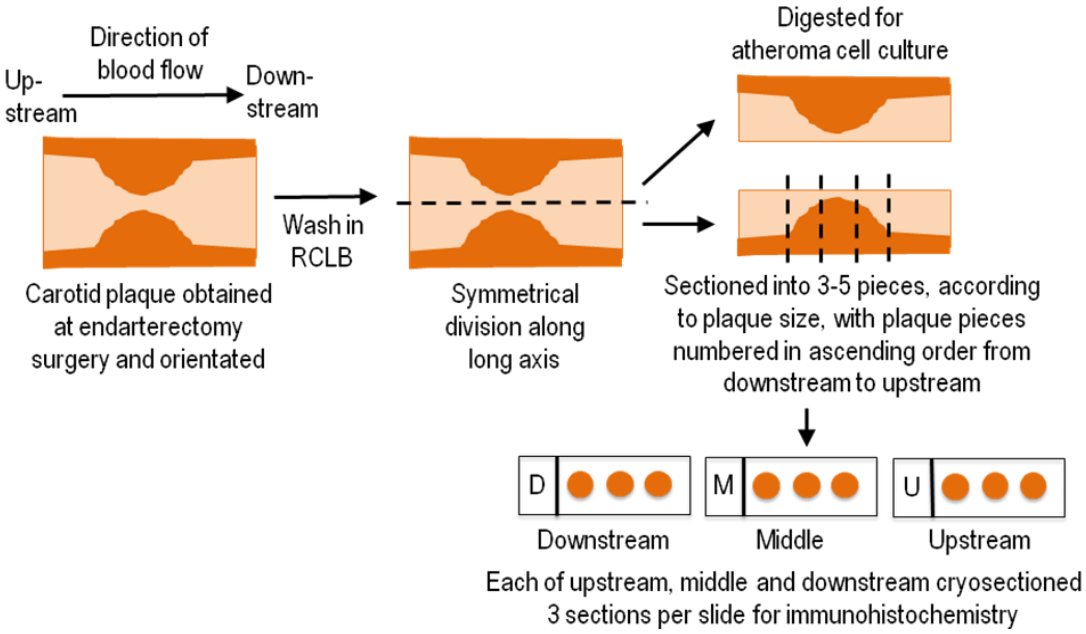


Figure 31 Carotid plaque processing protocol

This protocol allows the representative undertaking of atheroma cell culture and immunohistochemistry. D, downstream; M, middle; RCLB, red cell lysis buffer; U, upstream.

4.3 Carotid Plaque Histology

Histological analysis of carotid plaque sections was required to explore the biological features of the plaque related to patient symptomatic status, production of soluble analytes and findings on functional imaging (Chapter 5). The histology comprised, generally, immunohistochemistry and picrosirius red staining.

Immunofluorescent staining was not undertaken when semi-automated quantification was required as atherosclerotic plaques contain a considerable amount of lipid, which is autofluorescent and therefore may interfere with accurate quantification and interpretation following this technique.

4.3.1 Tissue Embedding

The plaque regions are placed within optimised cutting temperature (OCT) embedding matrix (Lamb) upon 3mm thick cork discs (Lamb). This is rapidly frozen using Frostbite (Surgipath) before inverting into a bath of 100% isopropanol surrounded by dry ice to snap freeze.

4.3.2 Cryosectioning

Cryosectioning was undertaken using a Leica CM1900 UV cryostat (Leica Microsystems) at -25 ± 1 °C. 5µm sections were transferred three to a slide.

4.3.3 Carotid Plaque Immunohistochemistry

Cryosections from each of the three regions (top, middle and bottom) were immunohistochemically stained for the macrophage marker CD68 (PG-M1, Dako, 1:500) and the endothelial cell marker CD31 (for intraplaque neovascularisation; JC70A, Dako, 1:1000) by the avidin-biotin complex technique with 3,3'-diaminobenzidine visualisation.

In general, immunohistochemical staining involved the following steps:

- Blocking of endogenous peroxidase activity
- Primary antibody application
- Secondary antibody application
- Substrate preparation and development
- Counterstaining

The immunohistochemistry (IHC) method used is based on the Standard Operating Procedures implemented within Charing Cross Hospital Department of Histopathology, and recommendations made by Vector Laboratories Limited, Novocastra Laboratories Limited and Dako Limited for use of their products in immunohistochemical investigations.

Frozen tissue sections were initially 'fixed' in acetone at room temperature for 10 minutes.

4.3.4 Blocking

Background staining (specific or non-specific) could cause false positivity. Endogenous peroxidase activity in erythrocytes, leucocytes and other cells may result in heavy non-specific background staining when using a horseradish peroxidase (HRP) conjugated antibody. This could lead to false positives or masking of the actual staining (false negative). Such activity was blocked by immersing the sections in a 2% solution of Sigma 30% hydrogen peroxide (EC label 23-1-765-0) in 300mL of BDH methanol for 10 minutes. The sections were then rinsed in running tap water for approximately 2 minutes.

A further cause of non-specific background staining is non-immunological binding of the specific immune sera by hydrophobic and electrostatic forces to certain sites within the tissue sections. This was reduced by blocking these sites with normal serum.

4.3.5 Avidin-Biotin Complex Immunohistochemistry Technique

The general IHC protocol employed used the avidin-biotin complex (ABC) peroxidase technique. This technique involved three layers. The first layer was the primary antibody (study marker). The second layer was the biotinylated secondary antibody. Biotin is a low molecular weight vitamin which can be conjugated to a variety of biological molecules including antibodies. The third layer was a complex of avidin-biotin peroxidase. Avidin is a large glycoprotein which can be labelled with peroxidase or fluorescein (chromogen), and has a very high affinity to biotin. Due to the very high affinity of avidin-biotin interaction, the binding of the primary antibody to the target antigen (first layer) will be amplified at the second and third layers, hence increasing the sensitivity of the method (and reducing the amount of primary antibody needed).

4.3.6 Diaminobenzidine Visualisation

In order to visualise the antibody/antigen complex, a chromogen, peroxidase substrate diaminobenzidine (DAB) SK-4100 (Vector Laboratories) was added. DAB produced a brown precipitate which is insoluble in alcohol in the presence of hydrogen peroxide. Since peroxidise is found in the avidin-biotin complex, addition of DAB to sections results in production of this precipitate.

Five millilitres of distilled water, 2 drops of buffer stock solution, 4 drops DAB stock solution and 2 drops hydrogen peroxidase were mixed and added to each slide for 5 minutes. The reaction was stopped by immersion of the slide in running water. Surgipath Harris's haematoxylin, followed by 0.3% acid was then applied and this differentiates the haematoxylin counterstain. The antigenic sites were thus stained dark brown due to the DAB precipitate and the cell nuclei blue from the haematoxylin.

4.3.7 Picro-sirius Red Staining

Picrosirius red staining was employed to visualise collagen, particularly in the context of the fibrous cap. This would facilitate accurate measurement of fibrous cap thickness. Picro-sirius red stain was made by combining sirius red F3B (0.5g) with saturated aqueous picric acid (500mL). Slides were placed in picro-sirius red solution for 1 hour, prior to washing in two changes of acidified (acetic acid) water (Puchtler et al. 1973; Junqueira et al. 1979).

4.3.8 Dehydration, Mounting and Coverslip Application

The slides were then subjected to serial 70% and 90% alcohol baths and finally completely dehydrated with 99% IMS. The alcohol was removed using xylene and the sections were mounted in Pertex mountant with 50 x 35mm glass coverslips on a Leica Auto-coverslipper.

4.3.9 Histology Quality Control

All histology was supervised and checked for quality by Dr Ann Sandison, Consultant Histopathologist and Honorary Clinical Senior Lecturer and Dr Federico Roncaroli, Reader in Neuropathology and Honorary Consultant Histopathologist.

4.3.10 Image Acquisition and Analysis

Cap thickness was measured from sections stained with picro-sirius red using an Olympus BH2 microscope (Olympus Corporation), with Jenoptik digital camera and linked ProgRes® CapturePro (version 2.5) image acquisition software (Jenoptik Laser, Optik, Systeme GmbH).

To reduce selection bias when quantifying immunohistochemical staining, whole plaque sections were imaged at x4 magnification using a motorised stage microscope (Eclipse 50i, Nikon) – camera (QImaging) system (Figure 32). Semi-automated image analysis was undertaken using Vision software (version 5.0, Clemex Technologies Incorporated, Longueuil, Quebec, Canada) (Figure 33). This is a ‘routine’ and ‘bitplane’ based system for automated image analysis in accordance with user-defined parameters. The percentage area of immunopositivity by colour thresholding was determined, with the average across the 9 slides calculated, for each of CD68 and CD31.

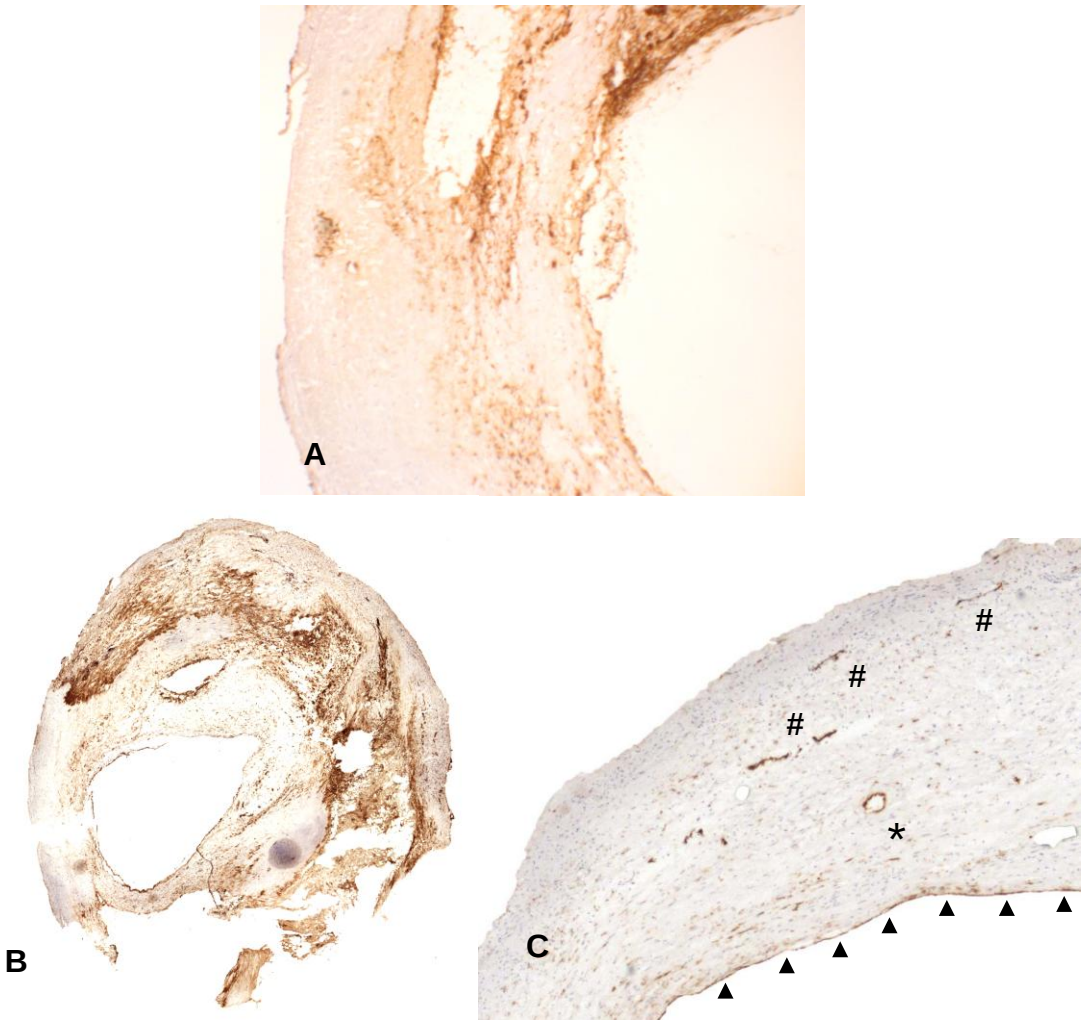


Figure 32 Image acquisition of stained histological sections comparing conventional and motorised stage microscope - camera setups

Cryosectioned tissue immunohistochemically stained for the endothelial marker CD31 as a marker of neovascularisation. Immunopositivity is indicated by dark brown. A. Conventional image acquisition of 'representative' or 'randomly selected' images. A magnification of x2.5 would be required to obtain as large a field of view as possible. B. This image is made up of 35 individual images, each representing a single field of view through a x4 microscope objective. A shading correction has been applied to ensure the staining intensity is uniform on the image regardless of whether we are looking at the centre or the edge of the field of view. C. Magnification of the high resolution images obtained on the motorised stage microscope acquisition system allows visualisation of microvessels in axial (*) and longitudinal section (#), as well as the luminal endothelium (arrowheads).

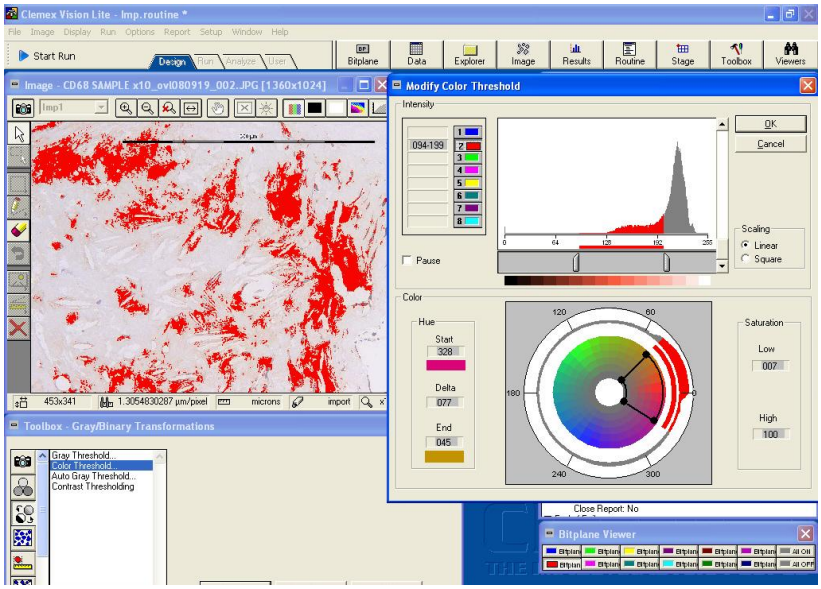


Figure 33 Image analysis for quantification of histological staining

Clemex Vision is a system for automated image analysis. This is a 'routine'-based system whereby the user produces a protocol for analysis which is saved, and may be opened and reproduced for subsequent analyses, to reduce variability between runs of analysis. It works by producing a 'bitplane' (shown as a red overlay on the image being analysed) in accordance with the user-defined parameters. Quantification is based upon calculations related to bitplane-highlighted regions of the image. In this image, a colour threshold has been set using the tools on the right, and this produced the red bitplane overlay on the image on the left. This is then used for calculation for calculation of percentage area immunopositivity.

4.4 Carotid Plaque Enzymatic Digestion and Culture

Carotid atherosclerotic plaque specimens were dissociated via an enzymatic mixture in order to obtain a single cell suspension for culture as previously described, characterised and validated (Monaco et al. 2004) (Figure 34).

Supernatants were removed after 24 hours and stored at -80°C for single-batch analysis. Multi-analyte profiling using a Luminex 100 platform was used to quantify supernatant protein levels of cytokine and chemokine (Milliplex, Millipore Corporation, Mo), matrix metalloproteinase (MMP) and tissue inhibitor or metalloproteinase (TIMP) (Fluorokine, R&D Systems, Abingdon, UK). Each supernatant sample was analysed in duplicate. Viability was monitored with the use of 3-(4,5-dimethyl-2-yl)-2,5-diphenyltetrazolium (MTT) (Sigma, UK) (Mosmann 1983).

4.4.1 Plaque Enzymatic Digestion

Atheromatous plaque enzymatic digestion was undertaken entirely within a class II laminar flow cabinet. Diseased intimal arterial segments were isolated under a Wild-Heerbrugg M8 dissecting microscope (Heerbrugg, Switzerland). Adherent thrombi were removed, and tissue fragments were incubated in collagenase type I (400 U/mL), elastase type III (5 U/mL) and DNAse (300 U/mL), with 1 mg/mL soybean trypsin inhibitor (SBTI; Sigma, UK), polymixin B (2.5 mg/mL; Sigma, UK) and 2 mM $CaCl_2$, in RPMI 1640 (BioWhittaker, UK) with 10% foetal bovine serum (Biosera, UK) in a shaker at 37°C. Cells were recovered every 20 minutes by filtering through an 80 mm Nylon mesh (Falcon, UK), and fresh enzymatic mixture was added, in order to avoid activation by collagen fragments, according to previous studies (Figure 34).

Every step of the digestion and culture protocol has been carried out in lipopolysaccharide (LPS)-free conditions: polymixin has been added to the enzymatic mixture (a potential source of LPS contamination); LPS content in all media, reagents, and supernatants from experiments was assessed via the Limulus Amebocyte assay (Sigma, UK) and has consistently been demonstrated as below detection limits.

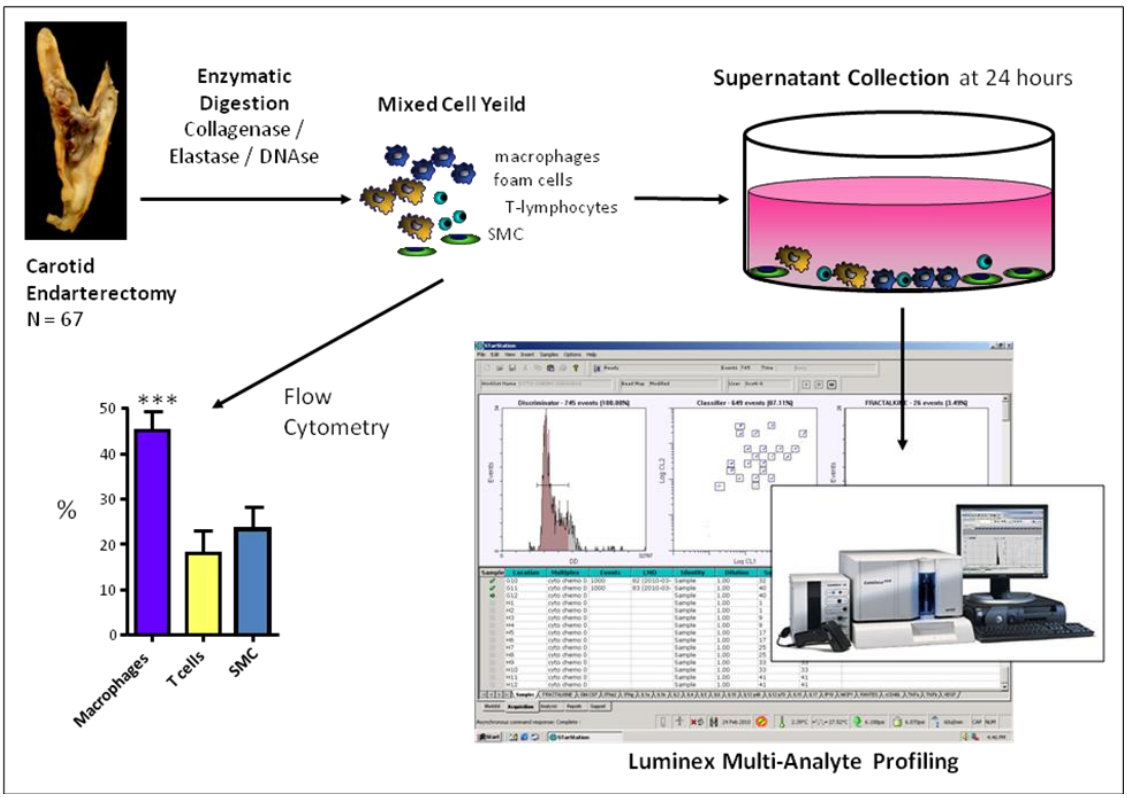


Figure 34 Carotid atheroma cell culture work-flow

Carotid plaque specimens were enzymatically digested using a collagenase / elastase / DNAse mixture as previously described and validated (Monaco et al. 2004). Previous work

has demonstrated by flow cytometry that the macrophage is the predominant cell type in this mixed cell culture system. The cells obtained were cultured at a uniform concentration of 1x10^6 cells/mL for 24 hours prior to supernatant collection. The supernatant from 67 atheroma cell cultures was batch analysed for the quantification of a total of 45 protein analytes across four panels on a Luminex 100 platform.

4.4.2 Plaque Cell Culture

Cell fractions were pooled, and cultured at 1x10^6 cells/mL in RPMI 1640 containing 10% FCS and 10% human serum (BioWhittaker, UK). Viability was monitored using MTT (3-(4,5-dimethyl-2-yl)-2,5-diphenyltetrazolium; Sigma, UK). The cells were cultured in the wells of a 96 well plate. This increased the cell density and allowed the culture to reach near-confluence. This is known to facilitate the production and release of cytokines and chemokines into the culture supernatant.

4.4.3 Storage of Culture Supernatant

At the 24 hours, the culture supernatant was aspirated and stored in multiple aliquots in a -80ºC freezer.

4.5 MULTI-ANALYTE PROFILING

4.5.1 Principles of Multi-Analyte Profiling

Multi-analyte profiling (MAP) requires systems such as Luminex that are capable of performing a variety of bioassays, including immunoassays, on the surface of fluorescent-coded beads known as microspheres. Luminex employs proprietary techniques to internally colour-code microspheres with two fluorescent dyes. Through precise concentrations of these dyes, up to 100 distinctly coloured bead sets can be created, each of which is coated with a specific capture antibody.

After an analyte from a test sample is captured by the bead, a biotinylated detection antibody is introduced. The reaction mixture is then incubated with streptavidin-phycoerythrin (PE) conjugate, the reporter molecule, to complete the reaction on the surface of each microsphere. The microspheres are allowed to pass rapidly through a laser which excites the internal dyes marking the microsphere set. A second laser excites PE, the fluorescent dye on the reporter molecule.

Finally, high-speed digital-signal processors identify each individual microsphere and quantify the result of its bioassay based on fluorescent reporter signals, termed the mean

fluorescent intensity (MFI). The capability of adding multiple conjugated beads to each sample results in the ability to obtain multiple results from each sample.

Multi-analyte profiling was undertaken using human multiplex panels: Milliplex (Millipore Corporation, Missouri, USA); and Fluorokine (R&D Systems, Abindgon, UK). The choice of panel was determined by the availability of analytes on the panels produced by each manufacturer.

Prior to use in the assay, all reagents were allowed to warm to room temperature (20-25°C). Samples which were frozen were initially defrosted on ice before being allowed to equilibrate to room temperature. The assay is run in duplicate.

4.5.2 Milliplex Multi-Analyte Profiling

Initially, the 96-well filter plate is wet by pipetting 200 µL of assay buffer into each well. The plate is then sealed and allowed to mix on a plate shaker for 10 minutes at room temperature. The assay buffer is removed by vacuum manifold. Twenty-five microlitres of each standard, quality control solution and background (assay buffer) were placed in the appropriate wells. Twenty-five microlitres of assay buffer is further added to each of the sample wells. Twenty-five microlitres of the relevant culture medium is added to the standard, quality control and background wells. Twenty-five microlitres of the samples are added to the appropriate wells. Twenty-five microlitres of the bead mixture is then added to each well. The plate is sealed, covered with a light opaque lid and incubated with agitation on a plate shaker for 1 hour at room temperature.

At this point the fluid is gently removed by vacuum manifold. The plate is washed twice with 200 µL per well of wash buffer, removing the wash buffer by vacuum filtration between each wash. Twenty-five microlitres of detection antibodies are then added into each well. The plate is sealed, covered with a light opaque lid and incubated with agitation on a plate shaker for 30 minutes at room temperature.

Twenty-five microlitres of streptavidin-phycoerythrin is added to each well. The plate is sealed, covered with a light opaque lid and incubated with agitation on a plate shaker for 30 minutes at room temperature, before the contents are gently removed by vacuum. The plate is washed twice with 200 µL per well of wash buffer, removing the wash buffer by vacuum filtration between each wash. One hundred and fifty microlitres of sheath fluid is then added to all wells and the beads resuspended on a plate shaker for 5 minutes.

4.5.3 Fluorokine Multi-Analyte Profiling

Initially, the 96-well filter plate is wet by pipetting 100 µL of wash buffer into each well, which is then removed by vacuum manifold. Fifty microlitres of resuspended bead mixture is then added to each well. Fifty microlitres of each sample, standard and background (diluted calibrator diluent) were placed in the appropriate wells. The plate is securely covered with a foil plate sealer, and incubated with agitation on a plate shaker for 2 hours at room temperature.

At this point the fluid is gently removed by vacuum manifold. The plate is washed three times with 100 µL per well of wash buffer, removing the wash buffer by vacuum filtration between each wash. Fifty microlitres of the diluted biotin detection antibody cocktail is then added into each well. The plate is securely covered with a foil plate sealer, and incubated with agitation on a plate shaker for 1 hour at room temperature.

The fluid is gently removed by vacuum manifold and the plate is washed three times with 100 µL per well of wash buffer. Fifty microlitres of diluted streptavidin-phycoerythrin is added to each well. The plate is securely covered with a foil plate sealer, and incubated with agitation on a plate shaker for 30 minutes at room temperature.

The fluid is gently removed by vacuum manifold and the plate is washed three times with 100 µL per well of wash buffer. One hundred microlitres of wash buffer is then added to all wells and the beads resuspended on a plate shaker for 2 minutes.

4.5.4 Multi-Analyte Profiling Plate Analysis

The plate is run on a Luminex 100 analyser. STarStation version 2.0 (Applied Cytometry, Sheffield, UK) was used for data acquisition (Figure 34).

4.5.5 Cytokines and Chemokines

The candidate molecules explored in the Milliplex cytokine and chemokine panels used, are outlined in Table 11. Plaque culture supernatants were used undiluted for this assay.

Cytokine	Role
IL1α	Pleotropic cytokine, polymorphism of its gene known to be associated with rheumatoid arthritis
IL1β	Produced as a pro-protein by activated macrophages and activated by caspase 1
IL2	Leukocytotrophic cytokine involved in T cell proliferation
IL4	Promotes T cell differentiation to TH2 lymphocytes
IL5	Produced by TH2 and mast cells, and stimulates B cell growth and immunoglobulin secretion. IL5 is often co-secreted with IL3, IL4 and GM-CSF owing to the proximity of the genes on chromosome 5 in humans
IL6	Secreted by T calls, macrophages and vascular smooth muscle cells, and is upstream of C-reactive protein production through liver stimulation of the acute phase response
IL10	Anti-inflammatory molecule produced primarily by monocytes and downregulates expression of TH1 cytokines and macrophage co-stimulatory molecules, can block NFκB activity and induce TNFβ
IL11 (AGIF)	Involved in haemato- and lymphopoeisis
IL12 (p40)	Produced by dendritic cells and macrophages, and stimulate T cell growth and production of IFNγ and TNFα. IL12 is also known to be anti-angiogenic, through IFNγ and IP10
IL12 (p70)	
IL15	Pro-inflammatory cytokine sectreted by monocytes which shares structural similarities to IL2
IL17	Pro-inflammatory cytokine family, which induces the synthesis of a number of pro-inflammatory cytokines and chemokines by T cells, and has been linked to rheumatoid arthritis
IL29	Type III interferon involved in the innate immune response to viral infection
GM-CSF	Macrophage differentiation
TNFα	Pro-inflammatory
TNFβ	Lymphotoxin produced by T cells induced by IL10
IFNα2	Involved in the innate immune response to viral infection and acts upon dendritic cells
IFNγ	Involved in innate and adaptive immunity with a number of functions including: increased antigen presentation of macrophages; activation and increase of lysosome activity in macrophages; suppression of TH2 activity; increased expression of MHC I; promotes adhesion and binding for leukocyte migration; promotes natural killer cell activity; activates antigen presenting cells; and promotes TH1 differentiation
VEGF	Pro-angiogenic
sCD40L	Is a member of the TNF molecule superfamily and expressed primarily by T cells
M-CSF	Influences haematopoietic stem cells to differentiate into macrophages

Chemokine	Role
CCL2 (MCP1)	Monocyte, dendritic and T cell recruitment
CCL5 (RANTES)	Chemotactic for T cells, eosinophils and basophils, and leukocyte recruitment to areas of inflammation
CCL14a (HCC1)	Antibodies used in the assay were raised against the mature propeptide 1-74 which is a low-affinity agonist of CCR1 and which is converted to a high-affinity agonist of CCR1 and CCR5 on proteolytic processing by serine proteases
CCL19 (MCP3)	Binds to CCR7 and chemotracts dendritic cells, as well as T and B cells
CCL20 (MIP3α)	Strongly chemoattractant for lymphocytes, is induced by IFNγ and TNF, and down-regulated by IL10. Linked to IL17 and TH17
CXCL6	Chemoattractant for neutrophilic granulocytes through interaction with CXCR1 and CXCR2
CXCL7	Released in large amounts from platelets upon their activation, stimulating mitogenesis, extracellular matrix synthesis, glucose metabolism and production of plasminogen activator. Antibodies used in the assay were raised against the mature 76-AA chemokine
CXCL9 (MIG)	T cell chemoattractant, which is induced by IFNγ and closely related to CXCL10 and CXCL11
CXCL10 (IP10)	Secreted in response to IFNγ and chemotracts monocytes, macrophages, T, dendritic and natural killer cells
CXCL11 (I-TAC)	Inducible by interferons
CX3CL1 (Fractalkine)	Soluble fractalkine chemotracts T cells and monocytes whilst cell-bound fractalkine promotes leukocyte adhesion to activated endothelial cells.
XCL1 (Lymphotaxin)	Small cytokine which attracts T cells

Table 11 Candidate cytokines and chemokines for exploration using multi-analyte profiling and their roles

4.5.6 Matrix Metalloproteinases and Tissue Inhibitors of Metalloproteinases

The candidate molecules explored in the MMP and TIMP Fluorokine panels, are outlined in Table 12. These MMPs and TIMPs were quantified on two different panels owing to interference between the two molecular groups if run together. MMP concentrations of greater than 66 ng/mL will interfere with the correct running of the TIMP assays. Plaque culture supernatants are diluted 1:4 for the MMP panel and 1:10 for the TIMP panel.

MMP	Role
MMP1	Interstitial collagenase and has been implicated in arthritis
MMP2	Gelatinase A degrading type IV collagen which is a major structural component of the basement membrane, and has involved in vascularisation and the inflammatory response
MMP3	Stromelysin which is thought to be involved in the progression of atherosclerosis
MMP7	Matrilysin
MMP8	Neutophil collagenase, stored in secondary granules within neutrophils and is involved in the degradation of type I, II and III collagen
MMP9	Gelatinase B degrades type IV and V collagen
MMP12	Macrophage elastase degrades both soluble and insoluble elastin
MMP13	Collagenase 3 which cleaves collagen type II more efficiently than it does collagen type I and III

TIMP	Role
TIMP1	Inhibitory against most MMPs, is pro-proliferative and anti-apoptotic, and is inducible in response to cytokines
TIMP2	Interacts with MMP 2 and MMP14, and is able to directly suppress the proliferation of endothelial cells hence may suppress a tissue response to angiogenic factors
TIMP3	
TIMP4	Interacts with MMP2

Table 12 Candidate matrix metalloproteinases and tissue inhibitors of metalloproteinases for exploration using multi-analyte profiling and their roles

4.5.7 Multi-Analyte Profiling Assay Sensitivity

The working MAP assay sensitivity was considered to be the lowest concentration on the standard curve. For the cytokine and chemokine panel this was 3.2 pg/mL. For the MMP and TIMP panels, these vary according to the analyte and are described in Table 13.

MMP	Sensitivity (pg/mL)
MMP1	10.70
MMP2	95.34
MMP3	16.05
MMP7	102.19
MMP8	91.91
MMP9	60.36
MMP12	15.09
MMP13	86.42

TIMP	Sensitivity (pg/mL)
TIMP1	15.50
TIMP2	57.61
TIMP3	155.01
TIMP4	6.17

Table 13 Multi-analyte profiling assay sensitivity for MMP and TIMP analysis

The working MAP assay sensitivity was considered to be the lowest concentration on the standard curve.

4.5.8 Statistical Analysis

Data was analyzed with Prism (version 5.02, GraphPad Software, Calif). Data was not normally distributed, therefore non-parametric methods were employed. A p-value of 0.05 was considered statistically significant. All tests used were 2-tailed.

4.5.9 Pathway Analysis

Analyte differences between symptomatic and asymptomatic groups were converted to ratios. The resulting data sets were analyzed using Ingenuity Pathway Analysis (Ingenuity Systems, version 7.6). A 1.5-fold cut-off value was set to identify proteins whose expression was significantly increased or decreased, creating a highly interconnected protein network. Biological functions and processes were attributed to predefined canonical pathways by mapping the proteins in the network to functions in the Ingenuity ontology. A right-tailed Fisher's exact test was performed to determine the significance (p-value) of any over-representation of proteins to a function compared to the result expected by a random set of proteins.

4.6 RESULTS

Sixty-seven patients (32 asymptomatic, 35 symptomatic) underwent carotid endarterectomy and consented to the use of their plaque tissue. There was a higher proportion of patients with a formal diagnosis of hypertension in the asymptomatic group compared with the symptomatic group (84% versus 66%; p=0.0329). The groups were otherwise well matched for demographic, clinical and pharmacotherapeutic parameters, as well as degree of carotid luminal stenosis (Table 14). There were no statistically significant relationships between these parameters and analyte levels, including no significant correlation between analyte levels and time from symptoms in the symptomatic group.

	Asymptomatic n = 32	Symptomatic n = 35
Age (years)	70 (60 – 78)	70 (67 – 74)
Male gender	26 (81%)	23 (72%)
Family history of arterial disease	9 (28%)	6 (19%)
Smoking	18 (56%)	17 (53%)
Hypertension	27 (84%) *	21 (66%)
Diabetes mellitus	4 (13%)	11 (34%)
Dyslipidaemia	20 (63%)	24 (75%)
Serum Cholesterol	3.6 (3.4 – 4.5)	3.7 (3.3 – 4.4)
Aspirin	24 (75%)	27 (77%)
Statin	28 (88%)	33 (94%)
ACEi or A2RA	20 (63%)	20 (57%)
Plaque carotid luminal stenosis	81 (75 – 90)	88 (80 – 93)
Time from symptoms to carotid endarterectomy (days)	N.A.	20 (12 – 41)

Table 14 Subject characteristics

*Demographic and clinical information relating to the patients from which the 67 studied arterial intimal segments were obtained. Data are presented as median (inter-quartile range), or number (%). There were significantly more patients with hypertension in the asymptomatic group compared to the symptomatic group (*p=0.0329; Fisher's exact test). ACEi, angiotensin converting enzyme inhibitor; A2RA, angiotensin 2 receptor antagonist; N.A., not applicable.*

4.6.1 Histological Analysis

The minimum thickness of the fibrous cap was significantly less when analysing carotid plaque sections where collagen was stained with picro-sirius red (Figure 35). Immunohistochemistry confirmed that macrophage abundance (CD68, Figure 36A) and neovascularisation (CD31, Figure 36B) were significantly higher in sections from symptomatic compared with asymptomatic plaques. Furthermore, there was a significant positive correlation between CD68 and CD31 immunopositivity amongst matched pairs of sections (Figure 36C).

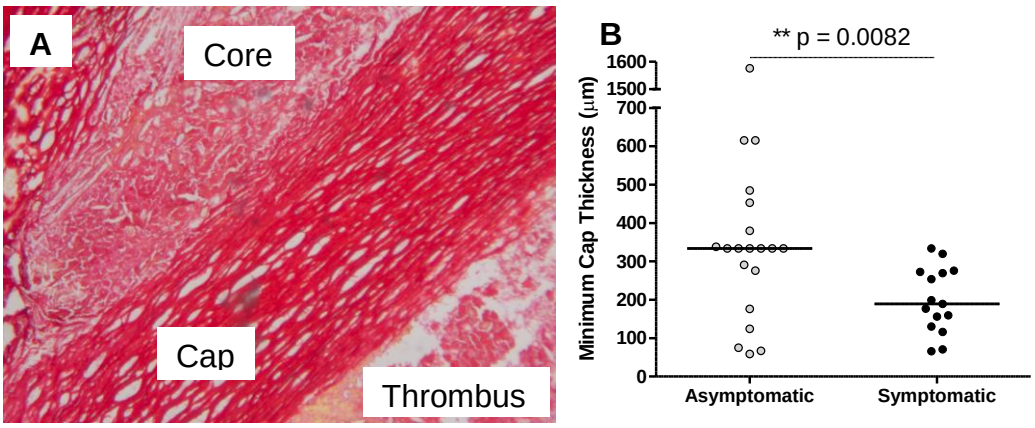


Figure 35 Plaque cap thickness on picro-sirius red staining

A. A representative section of carotid plaque stained with picro-sirius red, showing clear distinction between necrotic core and fibrous cap, thus facilitating measurement of the cap at its thinnest point. This example section also illustrates thrombus on the plaque surface in the context of this symptomatic plaque. B. Minimum cap thickness was measured, showing significantly thinner fibrous caps in symptomatic plaques (n=35 plaques; Mann Whitney test, bar denotes median).

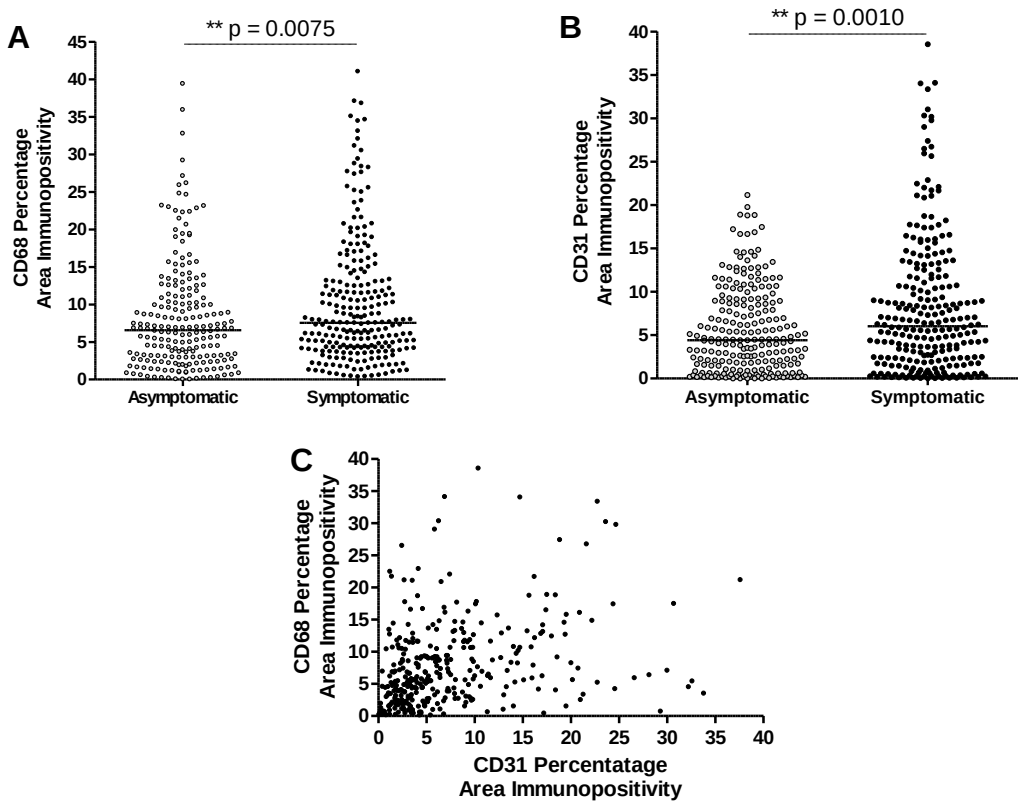


Figure 36 CD68 and CD31 percentage area immunopositivity

A. CD68 percentage area immunopositivity measured carotid plaque sections revealed macrophage abundance as being significantly higher in symptomatic compared with

asymptomatic (n=452 sections, Mann Whitney test, bar denotes median). B. CD31 immunopositivity was also significantly higher amongst symptomatic plaques (n=476 sections, Mann Whitney test, bar denotes median). C. There was a significant positive correlation between CD68 and CD31 immunopositivity (n=339 paired sections; Spearman r=0.3683; p<0.0001).

4.6.2 Analyte Detection by Multi-Analyte Profiling

The viable cell number obtained from carotid plaque enzymatic digestion was 11 ± 8.5 $x10^6$ (mean ± standard deviation). We were able to detect 41 of the 45 analytes (Table 15 and Table 16). There was a predominance of myeloid-derived over lymphoid-derived cytokines in keeping with the predominance of macrophages in the culture system, as previously published (Monaco et al. 2004; Monaco et al. 2009). The results are summarised in Table 15 and Table 16 and illustrated in Figure 37, Figure 38 and Figure 39.

Cytokine	Detected (n = 67)	Asymptomatic (n = 32)		Symptomatic (n = 35)		Symptomatic versus Asymptomatic (p value, Mann Whitney Test)
		Median (pg/mL)	Inter-Quartile Range (pg/mL)	Median (pg/mL)	Inter-Quartile Range (pg/mL)	
GM-CSF	64	69.25	21.93 - 241.4	246.7	95.15 - 433.1	**p = 0.0061**
IFNα2	26	3.200	3.200 - 7.749	3.200	3.200 - 9.488	p = NS
IFNγ	8	3.200	3.200 - 3.200	3.200	3.200 - 3.200	p = NS
IL1α	45	3.395	3.200 - 36.46	16.62	6.132 - 45.03	**p = 0.0225**
IL1β	58	16.58	4.031 - 67.61	72.89	20.36 - 263.0	**p = 0.0037**
IL2	2	3.200	3.200 - 3.200	3.200	3.200 - 3.200	p = NS
IL4	38	3.447	3.200 - 10.17	7.343	3.200 - 9.010	p = NS
IL5	1	-	-	3.200	3.200 - 3.200	-
IL6	67	1790	579.2 – 4180	8398	1463 - 9892	**p = 0.0118**
IL10	63	62.21	13.70 - 274.0	225.9	47.99 - 572.3	**p = 0.0263**
IL11	0	-	-	-	-	**-**
IL12 (p40)	38	6.939	3.200 - 29.76	9.607	3.200 - 18.66	p = NS
IL12 (p70)	3	3.200	3.200 - 3.200	3.200	3.200 - 3.200	p = NS
IL15	2	3.200	3.200 - 3.200	3.200	3.200 - 3.200	p = NS
IL17	1	-	-	3.200	3.200 - 3.200	-
IL29	0	-	-	-	-	**-**
M-CSF	63	330.9	180.1 - 586.7	552.1	329.4 - 846.4	**P = 0.0082**
sCD40L	26	13.92	4.766 - 25.00	31.57	14.54 - 71.29	**p = 0.0162**
TNFα	65	148.1	61.67 - 319.5	436.3	147.7 - 1032	**p = 0.0063**
TNFβ	0	-	-	-	-	-
VEGF	51	35.68	3.200 - 62.74	38.29	16.00 - 67.23	p = NS

Chemokine	Detected (n = 67)	Asymptomatic (n = 32)		Symptomatic (n = 35)		Symptomatic versus Asymptomatic (p value, Mann Whitney Test)
		Median (pg/mL)	Inter-Quartile Range (pg/mL)	Median (pg/mL)	Inter-Quartile Range (pg/mL)	
CCL2	67	318.3	121.3 - 1050	1180	369.4 - 3757	**p = 0.0162**
CCL5	65	43.81	26.85 - 83.11	120.5	56.44 - 203.4	**p = 0.0002**
CCL14a	67	34.53	25.44 - 66.13	62.36	29.64 - 86.34	p = NS
CCL19	0	-	-	-	-	**-**
CCL20	45	9.770	9.770 - 25.27	53.10	14.62 - 100.7	**p = 0.0003**
CXCL6	9	9.770	9.770 - 9.770	9.770	9.770 - 9.770	p = NS
CXCL7	67	118.9	64.24 - 271.9	178.7	97.31 - 386.5	p = NS
CXCL9	51	80.60	48.83 - 224.9	252.7	112.2 - 400.0	**p = 0.0011**
CXCL10	60	13.92	4.766 - 25.00	31.57	14.54 - 71.29	**p = 0.0162**
CXCL11	6	1.950	1.950 - 1.950	1.950	1.950 - 1.950	p = NS
CX3CL1	59	16.00	9.607 - 20.74	16.00	9.607 - 18.37	p = NS
XCL1	38	19.53	19.53 - 19.53	19.53	19.53 - 19.53	p = NS

Table 15 Analyte detection – cytokines and chemokines

Cells were isolated from carotid atherosclerotic plaques as a mixed cell suspension and cultured at 1x10^6 cells/mL for 24 hours, at which point the supernatant was aspirated. In this unstimulated system, the cells displayed a spontaneous cytokine and chemokine production. All samples were analysed in duplicate and data are given to 4 significant figures. IL, interleukin; GM-CSF, granulocyte macrophage colony-stimulating factor; TNF, tumor necrosis factor; IFN, interferon; VEGF, vascular endothelial growth factor; sCD40L, soluble cluster of differentiation 40 ligand; M-CSF, macrophage colony-stimulating factor; CX3CL1, fractalkine; CCL2, monocyte chemotactic protein 1 (MCP1); CCL5, regulated upon activation, normal T cell expressed and secreted (RANTES); CXCL6, granulocyte chemotactic protein 2 (GCP2); CXCL7, neutrophil activating protein 2 (NAP2); CXCL9, monokine induced by interferon gamma (MIG); CXCL10, interferon-inducible protein 10

(IP10); CXCL11, interferon-inducible T cell alpha chemoattractant (I-TAC); CCL14a, hemofiltrate CC chemokine 1 (HCC1); CCL19, inflammatory protein 3β (MIP3β); CCL20, macrophage inflammatory protein 3α (MIP3α); XCL1, lymphotactin; NS, non-significant.

Matrix Metallo-proteinase	Detected (n =67)	Asymptomatic (n = 32)		Symptomatic (n = 35)		Symptomatic versus Asymptomatic (p value, Mann Whitney Test)
		Median (pg/mL)	Inter-Quartile Range (pg/mL)	Median (pg/mL)	Inter-Quartile Range (pg/mL)	
MMP1	64	625.0	182.3 - 2007	1753	433.4 - 8569	**p = 0.0366**
MMP2	58	679.3	511.2 – 1284	892.7	496.8 - 1291	p = NS
MMP3	36	16.05	16.05 - 131.2	118.2	16.05 - 341.9	**p = 0.0076**
MMP7	37	255.5	102.2 - 1016	686.8	102.2 - 2129	p = NS
MMP8	47	404.0	91.91 - 1067	616.6	378.0 - 1903	**p = 0.0464**
MMP9	66	3456	1309 - 8011	8391	3799 - 22050	**p = 0.0039**
MMP12	67	480.3	257.4 - 1322	666.7	272.3 - 1278	p = NS
MMP13	3	86.42	86.42 - 86.42	86.42	86.42 - 86.42	p = NS

Tissue Inhibitor of Metallo-proteinase	Detected (n =67)	Asymptomatic (n = 32)		Symptomatic (n = 35)		Symptomatic versus Asymptomatic (p value, Mann Whitney Test)
		Median (pg/mL)	Inter-Quartile Range (pg/mL)	Median (pg/mL)	Inter-Quartile Range (pg/mL)	
TIMP1	67	4451	2936 - 9697	4014	2201 - 9970	p = NS
TIMP2	67	5829	3829 - 131400	42560	3870 - 119500	p = NS
TIMP3	9	155.0	155.0 - 155.0	155.0	155.0 - 155.0	p = NS
TIMP4	3	-	-	6.170	6.170 - 6.170	-

Table 16 Analyte detection – MMPs and TIMPs

Cells were isolated from carotid atherosclerotic plaques as a mixed cell suspension and cultured at $1x10^6$ cells/mL for 24 hours, at which point the supernatant was aspirated. In this unstimulated system, the cells displayed a spontaneous matrix metalloproteinase (MMP) and tissue inhibitor of metalloproteinases (TIMP) production. All samples were analysed in duplicate and data are given to 4 significant figures. NS, non-significant.

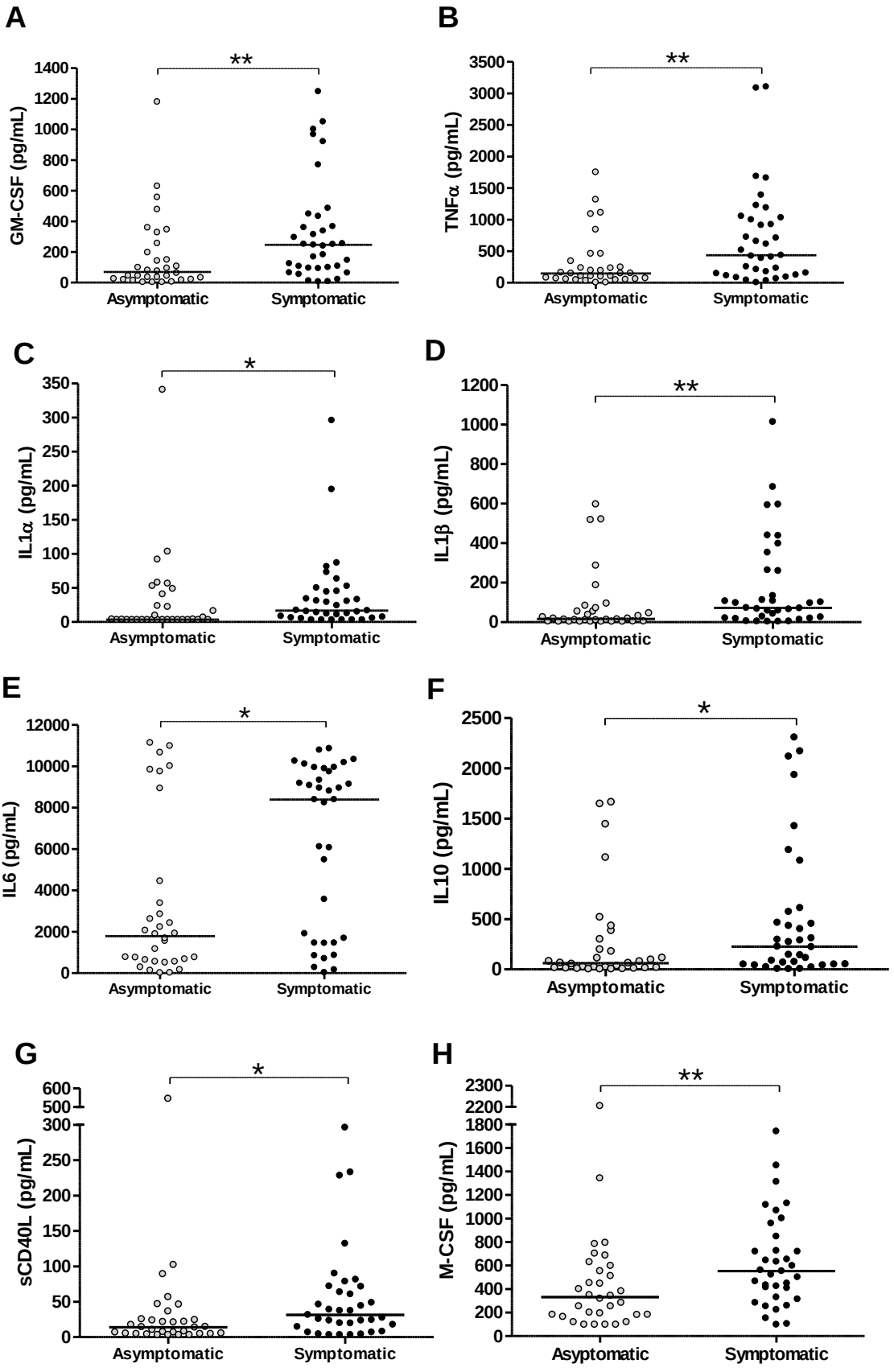

A
GM-CSF (pg/mL)
1400
1200
1000
800
600
400
200
0
**
Asymptomatic
Symptomatic
B
TNFα (pg/mL)
3500
3000
2500
2000
1500
1000
500
0
**
Asymptomatic
Symptomatic
C
IL1α (pg/mL)
350
300
250
200
150
100
50
0
*
Asymptomatic
Symptomatic
D
IL1β (pg/mL)
1200
1000
800
600
400
200
0
**
Asymptomatic
Symptomatic
E
IL6 (pg/mL)
12000
10000
8000
6000
4000
2000
0
*
Asymptomatic
Symptomatic
F
IL10 (pg/mL)
2500
2000
1500
1000
500
0
*
Asymptomatic
Symptomatic
G
sCD40L (pg/mL)
600
500
300
250
200
150
100
50
0
*
Asymptomatic
Symptomatic
H
M-CSF (pg/mL)
2300
2200
1800
1600
1400
1200
1000
800
600
400
200
0
**
Asyptomatic
Symptomatic

Figure 37 Plaque culture supernatant levels of cytokines in distinguishing symptomatic from asymptomatic plaques

*Cells were isolated from carotid atherosclerotic plaques as a mixed cell suspension and cultured at $1x10^6$ cells/mL for 24 hours in the absence of any stimulus. Supernatants were collected, aliquoted and frozen at -80°C for single batch analysis. Multi-analyte profiling was accomplished on a Luminex 100 platform. Levels of cytokine production in vitro were significantly higher in atheroma cells from symptomatic versus asymptomatic plaques for the following mediators: A. Granulocyte macrophage colony-stimulating factor (GM-CSF); B. Tumor necrosis factor α (TNFα); C. Interleukin (IL) 1α; D. IL1β; E. IL6; F. IL10; G. Soluble CD40 ligand (sCD40L); H. Macrophage colony-stimulating factor (M-CSF). Each dot represents a single donor; medians are shown as dark horizontal lines; ** $p < 0.005$; * $p < 0.05$ (Mann Whitney test; n = 67).*

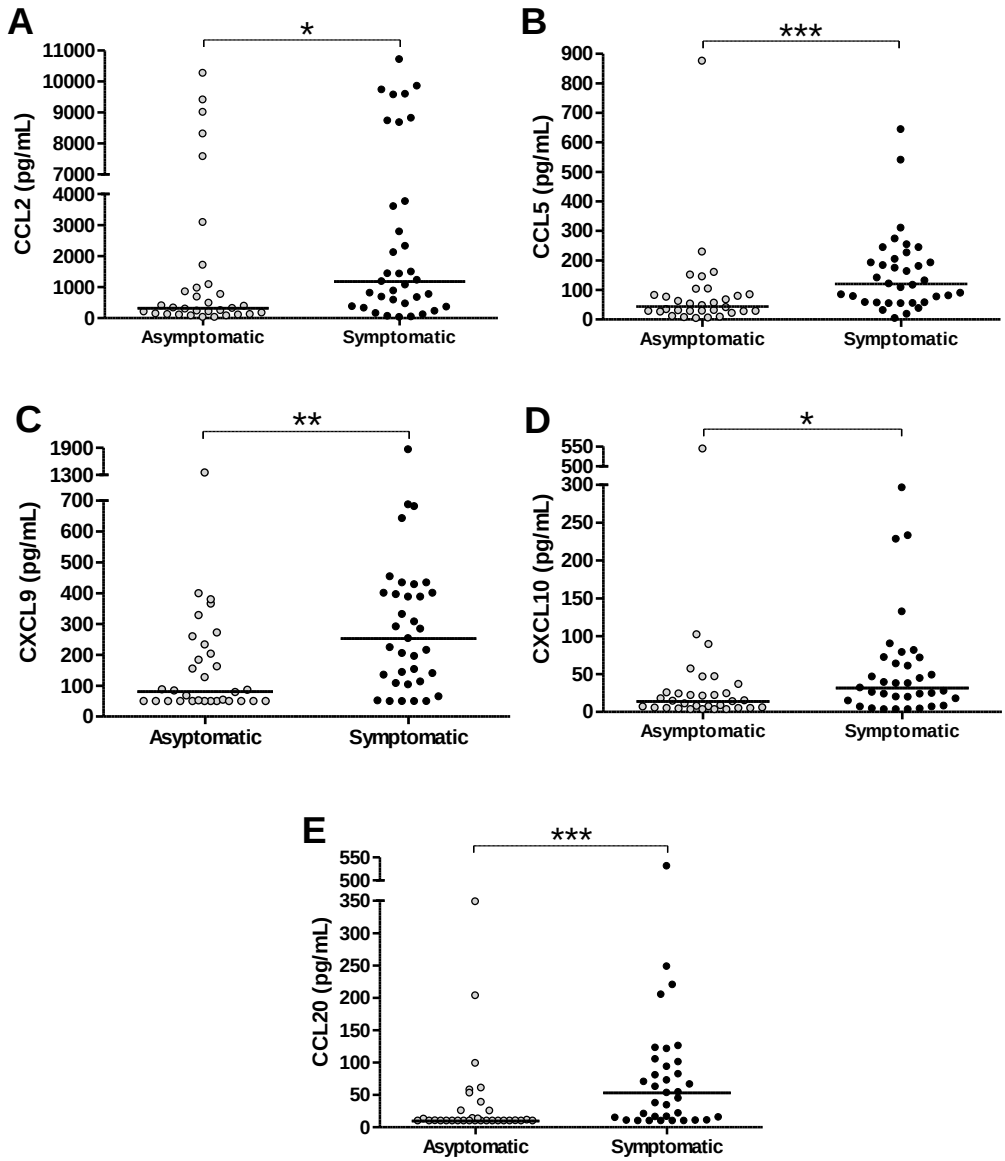


Figure 38 Plaque culture supernatant levels of chemokines in distinguishing symptomatic from asymptomatic plaques

*Cells were isolated from carotid atherosclerotic plaques as a mixed cell suspension and cultured at 1x10^6 cells/mL for 24 hours in the absence of any stimulus. Supernatants were collected, aliquoted and frozen at -80°C for single batch analysis. Multi-analyte profiling was accomplished on a Luminex 100 platform. Levels of chemokine production in vitro were significantly higher in atheroma cells from symptomatic versus asymptomatic plaques for the following mediators: A. CCL2 (monocyte chemotactic protein 1; MCP1); B. CCL5 (regulated upon activation, normal T cell expressed and secreted; RANTES); C. CXCL9 (monokine induced by interferon gamma; MIG); D. CXCL10 (interferon-inducible protein 10; IP10); E. CCL20 (macrophage inflammatory protein 3α; MIP3α). Each dot represents a single donor; medians are shown as dark horizontal lines; *** p < 0.0005; ** p < 0.005; * p < 0.05 (Mann Whitney test; n = 67).*

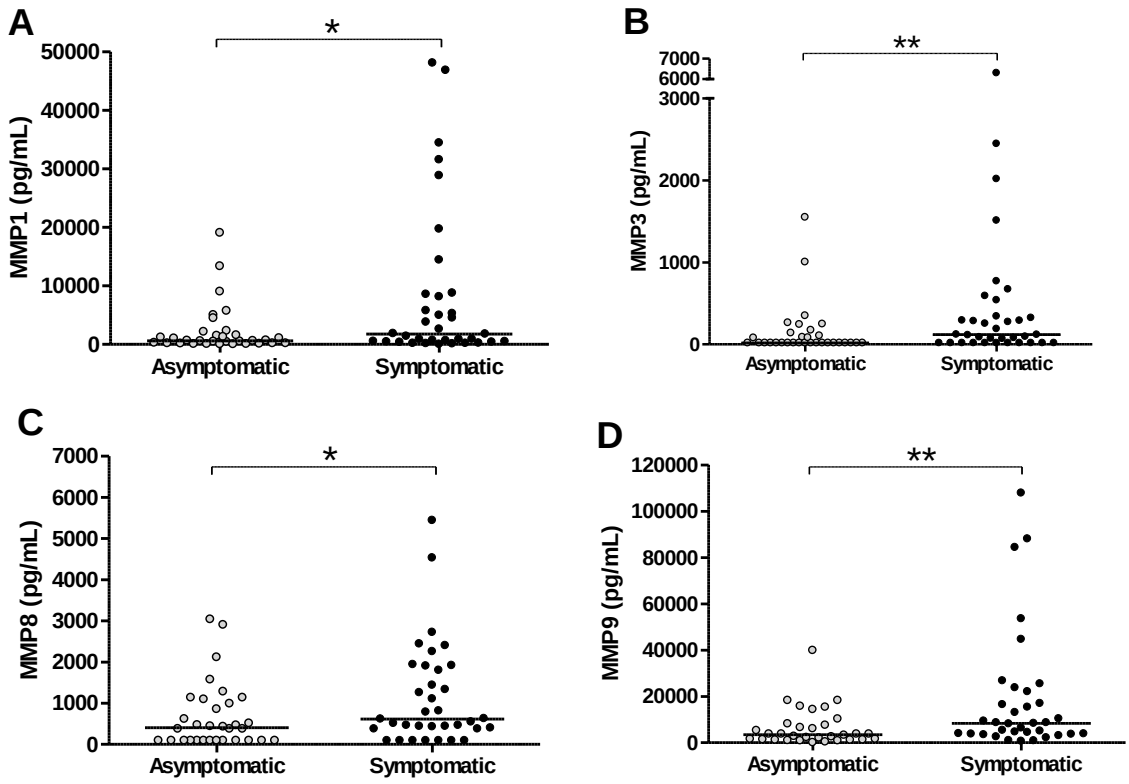


Figure 39 Plaque culture supernatant levels of matrix metalloproteinases in distinguishing symptomatic from asymptomatic plaques

*Cells were isolated from carotid atherosclerotic plaques as a mixed cell suspension and cultured at 1x10^6 cells/mL for 24 hours in the absence of any stimulus. Supernatants were collected, aliquoted and frozen at -80°C for single batch analysis. Multi-analyte profiling was accomplished on a Luminex 100 platform. Levels of matrix metalloproteinase (MMP) production in vitro were significantly higher in atheroma cells from symptomatic versus asymptomatic plaques for the following mediators: A. MMP1; B. MMP3; C. MMP8; D. MMP9. Each dot represents a single donor; medians are shown as dark horizontal lines; ** p < 0.005; * p < 0.05 (Mann Whitney test; n = 67).*

4.6.3 Cytokines

In the atheroma cell culture system, there was a significantly higher production of classical pro-inflammatory cytokines from symptomatic compared with asymptomatic atherosclerosis. Levels of tumor necrosis factor (TNF)-α (median 436.6 pg/mL versus 148.1 pg/mL; p=0.0063), interleukin (IL)-1α (16.62 pg/mL versus 3.395 pg/mL; p=0.0225), IL1β (72.89 pg/mL versus 16.58 pg/mL; p=0.0037), IL6 (8398 pg/mL versus 1790 pg/mL; p=0.0118) and soluble CD40 ligand (31.57 pg/mL versus 13.92 pg/mL; p=0.0162) were significantly higher in the symptomatic than asymptomatic supernatant. Interestingly, IL10 production was also higher in symptomatic atheroma cell culture (225.9 pg/mL versus 62.21 pg/mL; p=0.0263).

4.6.4 Chemokines

CCL2 (monocyte chemotactic protein, MCP1; 1180 pg/mL versus 318.3 pg/mL; p=0.0162) and CCL5 (regulated on activation normal T cell expression and secreted, RANTES; 120.5 pg/mL versus 43.81 pg/mL; p=0.0002) production was higher in symptomatic atheroma culture.

CXCL9 (monokine induced by interferon gamma, MIG; 252.7 pg/mL versus 80.60 pg/mL; p=0.0011) and CXCL10 (interferon-inducible protein 10, IP10; 31.57 pg/mL versus 13.92 pg/mL; p=0.0162) were higher from symptomatic plaques. Both these chemokines are known to be induced by interferon γ (IFNγ). Of note, IFNγ was detected in 8 of the 67 cultures (Table 15) and no difference was demonstrated on the basis of symptomatic status.

CCL20, also known as liver and activation-regulated chemokine (LARC) or macrophage inflammatory protein-3α (MIP-3α), was significantly higher in the symptomatic group than asymptomatic (53.10 pg/mL versus 9.770 pg/mL; p=0.0003).

4.6.5 Colony Stimulating Factors

Levels of production of both granulocyte-macrophage colony-stimulating factor (GM-CSF; 246.7 pg/mL versus 69.25 pg/mL; p=0.0061) and macrophage colony-stimulating factor (M-CSF; 552.1 pg/mL versus 330.9 pg/mL; p=0.0082) were significantly higher in cultures obtained from symptomatic patients.

4.6.6 Matrix Metalloproteinases

MMP1 (1753 pg/mL versus 625.0 pg/mL; p=0.0366), MMP3 (118.2 pg/mL versus 16.05 pg/mL; p=0.0076), MMP8 (616.6 pg/mL versus 404.0 pg/mL; p=0.0464) and MMP9 (8391 pg/mL versus 3456 pg/mL; p=0.0039) levels were significantly higher in symptomatic than asymptomatic plaques.

4.6.7 Tissue Inhibitors of Metalloproteinases

There was no significant difference in the production of TIMP1 (4014 pg/mL versus 4451 pg/mL; p=NS), TIMP2 (42560 pg/mL vs 5829 pg/mL; p=NS), TIMP3 (155.0 pg/mL versus 155.0 pg/mL; p=NS) and TIMP4 (6.170 pg/mL versus 6.170 pg/mL; p=NS) between symptomatic and asymptomatic atherosclerosis.

4.6.8 Analyte Inter-Relationships and Pathway Analysis

The inter-relationship between analytes were computed statistically and via the use of Ingenuity pathways. The statistical analysis revealed significant relationship between analytes (Figure 40), for example the concentrations of classical pro-inflammatory cytokines TNFα, IL1α and IL1β were positively correlated to the IFNγ–dependent chemokine CXCL10 ($p<0.001$), colony stimulating factors GM-CSF ($p>0.001$) and M-CSF ($p<0.001$) and also, of note, to IL10 production ($p>0.001$). Moreover, the pro-inflammatory cytokines displayed positive correlation with levels of the catabolic enzymes MMP1 ($p<0.001$), MMP3 ($p<0.001$) and MMP9 ($p\leq0.005$).

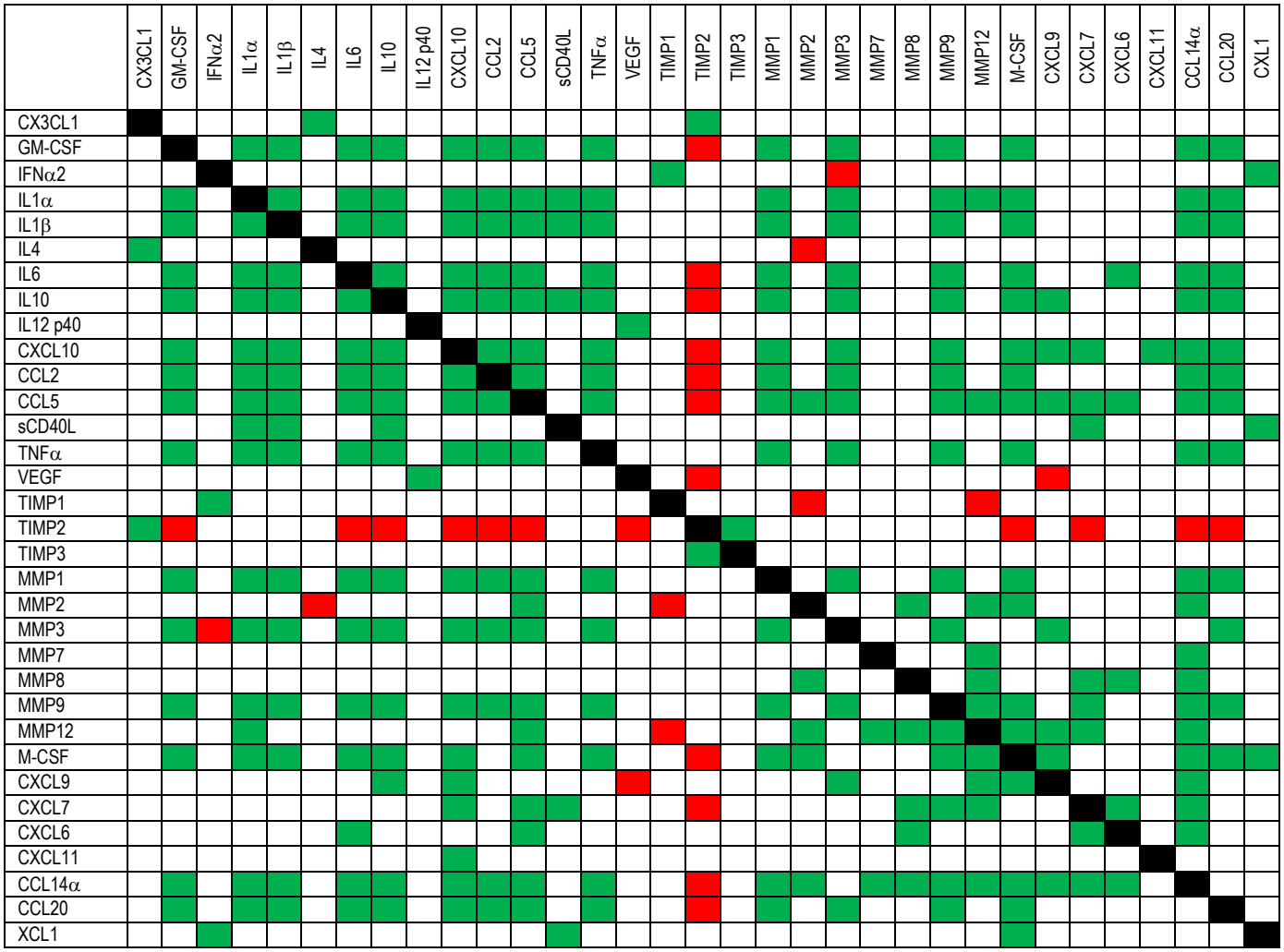


Figure 40 Analyte inter-relationships

Cells were isolated from carotid atherosclerotic plaques as a mixed cell suspension and cultured at 1x10^6 cells/mL for 24 hours, at which point the supernatant was aspirated. In this unstimulated system, the cells displayed a spontaneous protein production. All samples were analysed in duplicate. The inter-relationship of cytokines, chemokine, matrix metalloproteinase (MMP) and tissue inhibitor of metalloproteinases (TIMP) was assessed with Spearman correlations. Statistically significant ($p<0.05$) positive correlations are displayed in green and negative correlations highlighted in red. IL, interleukin; GM-CSF, granulocyte macrophage colony-stimulating factor; TNF, tumor necrosis factor; IFN, interferon; VEGF, vascular endothelial growth factor; sCD40L, soluble cluster of differentiation 40 ligand; M-CSF, macrophage colony-stimulating factor; CX3CL1, fractalkine; CCL2, monocyte chemotactic protein 1 (MCP1); CCL5, regulated upon activation, normal T cell expressed and secreted (RANTES); CXCL6, granulocyte chemotactic protein 2 (GCP2); CXCL7, neutrophil activating protein 2 (NAP2); CXCL9, monokine induced by interferon gamma (MIG); CXCL10, interferon-inducible protein 10

(IP10); CXCL11, interferon-inducible T cell alpha chemoattractant (I-TAC); CCL14a, hemofiltrate CC chemokine 1 (HCC1); CCL19, inflammatory protein 3β (MIP3β); CCL20, macrophage inflammatory protein 3α (MIP3α); XCL1, lymphotactin; NS, non-significant.

Bioinformatic analysis identified detected soluble analytes within seven networks (Table 17). A merge of networks 2 and 3 is shown in Figure 41. The canonical pathways associated with differences between data sets obtained from symptomatic and asymptomatic patients are shown in Figure 42. The most statistically significant of the canonical pathways raised in Ingenuity were: role of cytokines in mediating communication between immune cells ($p=9.64x10^{-26}$); altered T and B cell signalling in rheumatoid arthritis ($p=5.46x10^{-23}$); communication between innate and adaptive immune cells ($p=1.27x10^{-22}$); role of hypercytokinemia / hyperchemokinaemia in the pathogenesis of influenza ($p=1.88x10^{-22}$); role of macrophages, fibroblasts and endothelial cells in rheumatoid arthritis ($p=2.37x10^{-17}$); atherosclerosis signalling ($p=4.58x10^{-16}$); and T helper cell differentiation ($p=5.37x10^{-14}$).

No.	Molecules in Network	Key Functions
1	C1q, Casein, collagen, Collagen type I, Collagen type III, Collagen type IV, Collagen(s), Cyclooxygenase, Eotaxin, ERK1/2, Fcer1, Fibrin, Fibrinogen, Gelatinase, Igfbp, Integrin, Laminin, **MMP2**, **MMP3**, **MMP7**, **MMP8**, **MMP9**, **MMP12**, **MMP13**, **MMP1** (includes EG:4312), **PPBP**, Secretase gamma, STAT1/3/5 dimer, Tenascin, Tgf beta, Timp, **TIMP2**, **TIMP3**, **TIMP4**, Trypsin	Post-Translational Modification, Connective Tissue Disorders, Genetic Disorder
2	Angiotensin II receptor type 1, C/ebp, **CCL20**, Cebp, **CX3CL1**, **CXCL6**, **CXCL9**, **CXCL10**, **CXCL11**, Elastase, ETS, Ferritin, Ggt, HLA-DR, Ifn, IFN alpha/beta, Ifn gamma, IFN TYPE 1, IL23, IL-1R, IL1/IL6/TNF, **IL12B**, JUN/JUNB/JUND, **LTA**, MHC CLASS I (family), NFkB (complex), NfkB-RelA, Pro-inflammatory Cytokine, REL/RELA/RELB, SAA, sphingomyelinase, TH1 Cytokine, Tlr, Tnf, Tnf receptor	Cell-To-Cell Signaling and Interaction, Infection Mechanism, Infectious Disease
3	Akt, Ap1, **CCL2**, **CCL5**, CD3, CD80/CD86, Collagen Alpha1, **CSF1**, **CSF2**, Cytochrome p450, Ikb, Ikk (family), IL1, **IL2**, **IL17A** (includes EG:3605), **IL1A**, JINK1/2, Lfa-1, MAP2K1/2, Mek, N-cor, NFAT (complex), Nfat (family), NFkB (family), NfkB1-RelA, p70 S6k, Pak, Pde4, Pdgf, Rap1, Rxr, Sphk, TCR, VitaminD3-VDR-RXR, **XCL1**	Antigen Presentation, Cell-To-Cell Signaling and Interaction, Hematological System Development and Function
4	Angiotensin II receptor type 1, C1R, CCL1, CCL8, CCL9, **CCL20**, CCL21, CCL22, CCR2, CHEMOKINE, Ck2, **CX3CL1**, CXCL1, CXCL5, **CXCL6**, **CXCL9**, **CXCL11**, CXCL16, IKK (complex), IL-1R, KLF1, LTBR, MAP4K4, Neurotrophin, NFkB (complex), NFKBIE, PELI1, PELI3, PTPN2, RNASE2, S100B, spermine, TFPI, TLR8 (includes EG:51311), TNFRSF6B	Cellular Movement, Hematological System Development and Function, Immune Cell Trafficking
5	Adaptor protein 1, Alp, Arginase, Calpain, Caspase, Caspase 3/7, Cpla2, Creb, Cyclin A, Cyclin E, Cytochrome c, Growth hormone, Histone h3, Histone h4, HLA Class I, Hsp27, Hsp70, Hsp90, **IFNA2**, **IFNG**, **IL1B**, IRG, LDL, Mlc, Nos, PLA2, Ptger, Rb, RNA polymerase II, Rsk, Smad, Sod, **TNF**, Tni, **VEGFA**	Lipid Metabolism, Small Molecule Biochemistry, Cardiovascular System Development and Function
6	ALT, Fc gamma receptor, Fcgr3, Gm-csf, GOT, HISTONE, HLA-DQ, IFN Beta, Ifnar, Iga, Ige, IgG, IgG1, IgG2a, Igm, **IL5**, **IL10**, **IL15**, IL-2R, IL12 (complex), Il12 receptor, Il8r, Immunoglobulin, Interferon alpha, JAK, Laminin1, Ldh, MHC Class I (complex), MHC Class II (complex), PI3K (complex), PLC gamma, STAT5a/b, TH2 Cytokine, TLR2/TLR4, VAV	Cellular Development, Hematological System Development and Function, Hematopoiesis
7	ADCY, Alpha tubulin, **CCL14**, ERK, Estrogen Receptor, F Actin, Focal adhesion kinase, FSH, G protein, G protein alphai, Gsk3, hCG, Hemoglobin, **IL4**, **IL6**, IL12 (family), Insulin, Jnk, Lh, Mapk, Mmp, NGF, P110, P38 MAPK, p85 (pik3r), PDGF BB, Pka, Pkc(s), Pld, Rac, Ras, Ras homolog, Shc, STAT, Vegf	Cardiovascular System Development and Function, Tissue Morphology, Cell-To-Cell Signaling and Interaction

Table 17 Biological networks in human carotid atherosclerosis

The seven networks into which bioinformatic analysis placed detected soluble analytes. The molecules and key functions of the networks are shown. Detected analytes are highlighted in bold. CSF1, colony stimulating factor 1 (M-CSF); CSF2, colony stimulating factor 2 (GM-CSF); LTA, lymphotaxin α (tumor necrosis factor β); PPBP, pro-platelet basic protein (CXCL7).

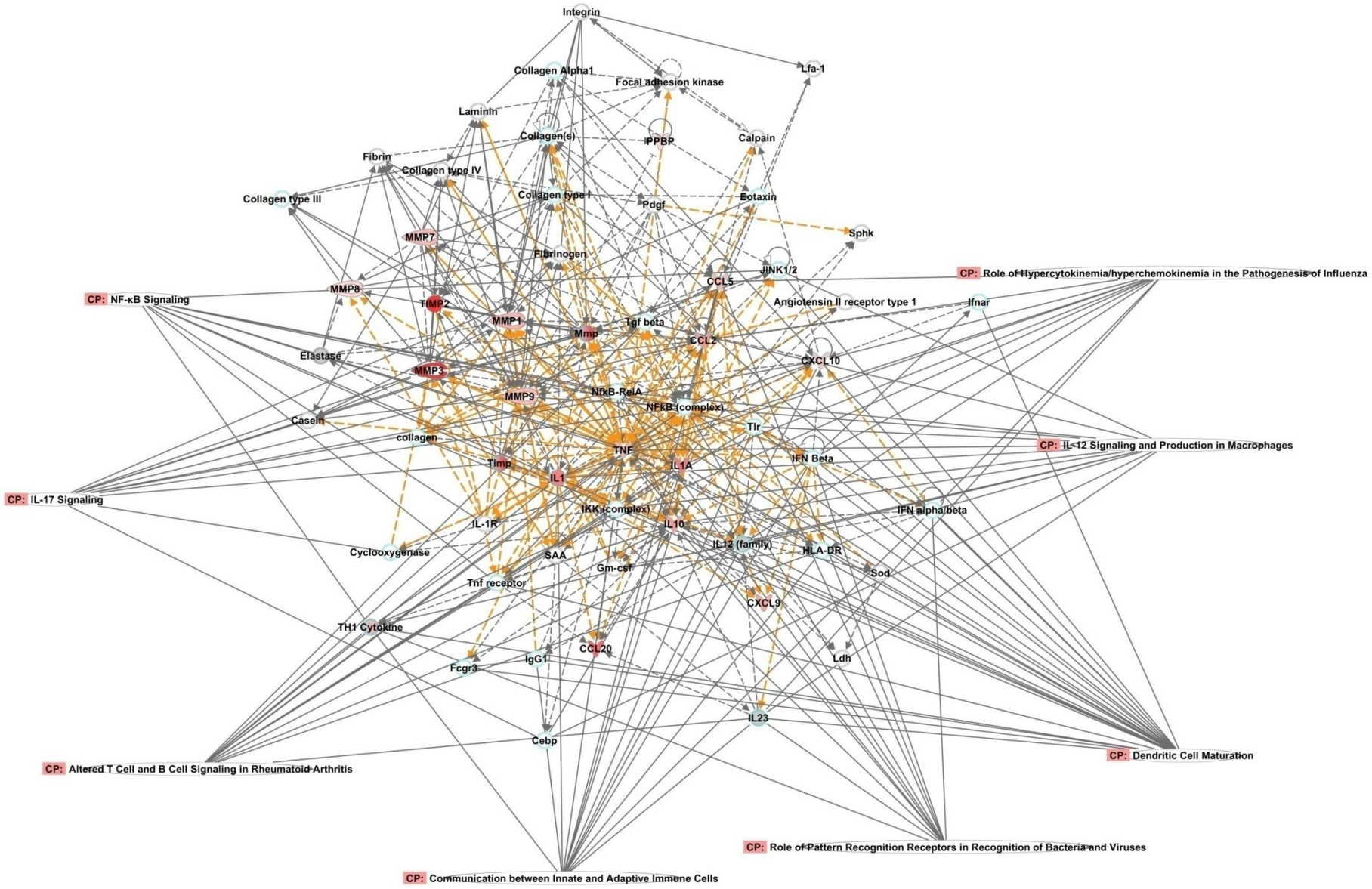


Figure 41 Network analysis

The inter-relationship between cytokines, chemokines and matrix metalloproteinases as constructed through application of a bioinformatic approach with Ingenuity Pathway Analysis. Key canonical pathways (CP) are highlighted at the periphery of the network.

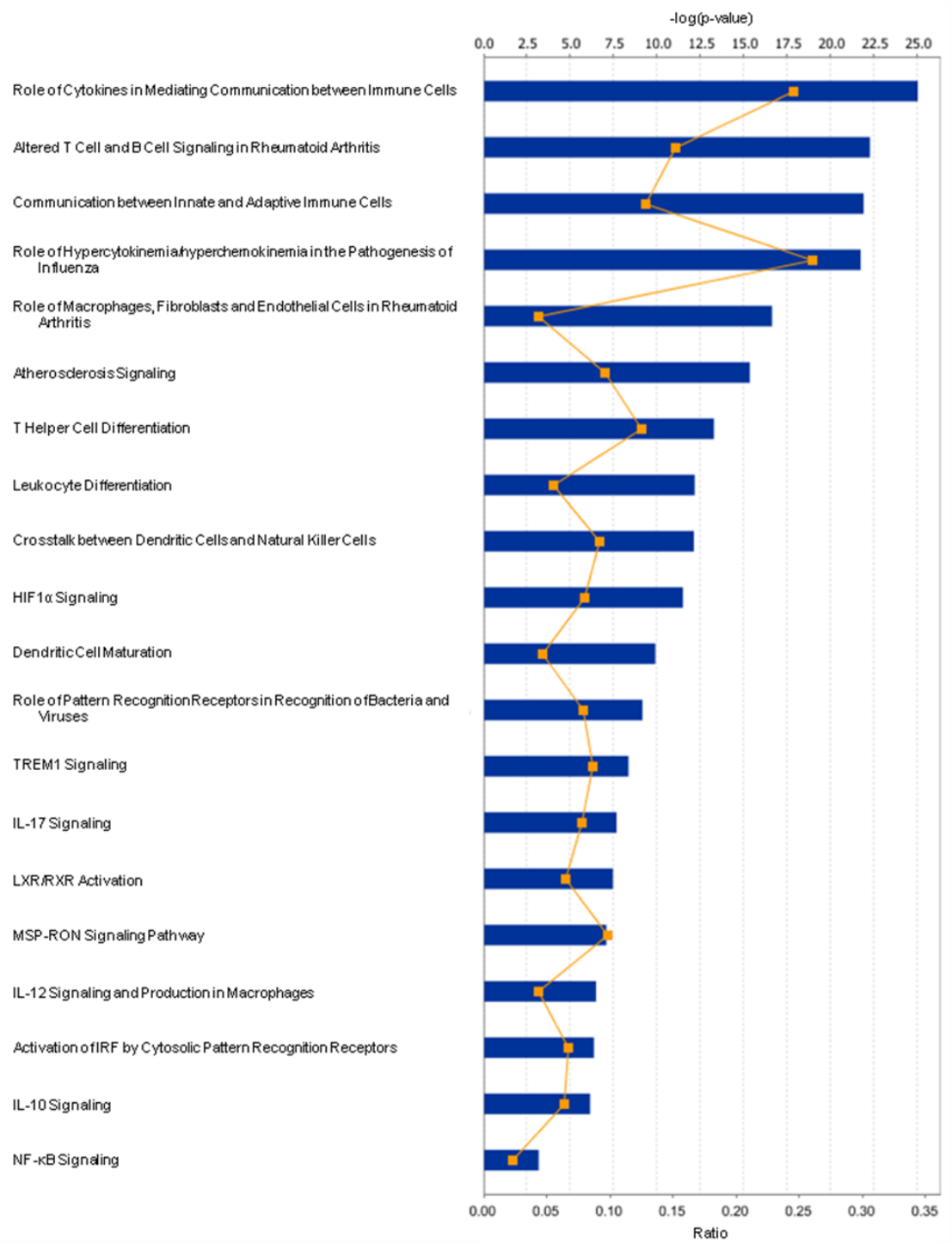


Figure 42 Key canonical pathways in human carotid atherosclerosis

The bars relate to the top Y axis show the –log(p-value), reflecting the likelihood that a specific canonical pathway and the data are related by chance. The points related to the lower Y axis show the ratio of analytes we have detected by multi-analyte profiling divided by the total number of molecules known to make up that pathway. HIF1α, hypoxia inducible factor 1α; IL, interleukin; IRF, interferon regulatory factor; LXR/RXR, liver X receptor / retinoid X receptor; MSP, macrophage-stimulating protein; NFκB, nuclear factor κB; RON, receptor d'origine nantais; TREM1, triggering receptor expressed on myeloid cells 1.

4.7 DISCUSSION

The aim of this study was to characterise the inflammatory microenvironment of the high-risk plaque with a combination of multianalyte profiling and pathway analysis. It was identified that the recently unstable human carotid plaque contains a pro-inflammatory microenvironment that may favour the recruitment of Th1 lymphocytes and monocytes and the generation of M1-polarised macrophages (Figure 43).

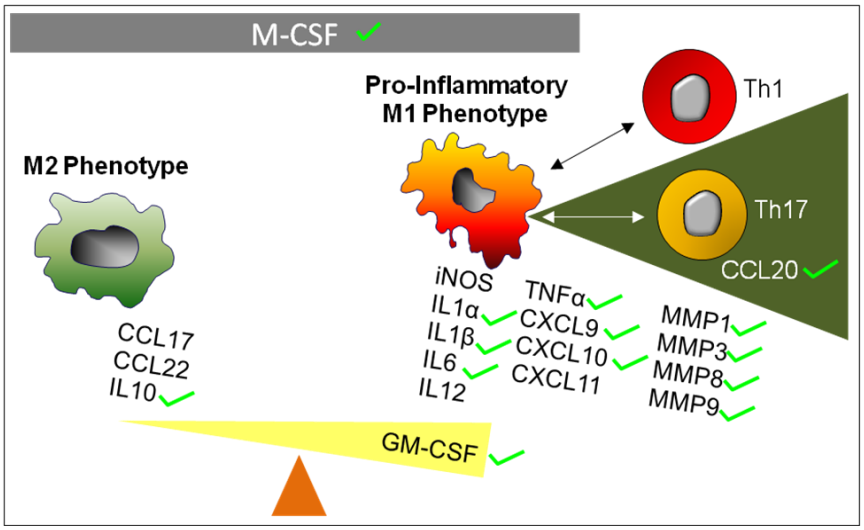


Figure 43 **A schematic summarising the soluble analytes with differential protein production between symptomatic and asymptomatic carotid atherosclerosis, reflecting a predominance of pro-inflammatory M1-macrophage polarisation**

In this study, bioinformatic analysis showed inflammatory cell recruitment featured as one of the hallmarks of human atherosclerosis instability, with cell-to-cell signalling and interaction, and immune cell trafficking, with leukocyte extravasation signalling emerging as a top canonical pathways. In particular, unstable atherosclerosis was associated with an increased production of CCL2/MCP1 and CCL5/RANTES. CCR2-/- in the context of apolipoprotein E (apoE)-/- (Boring et al. 1998) and low density lipoprotein receptor (LDLR)-/- (Gu et al. 1998) mice independently resulted in markedly decreased lesion formation. In human atherosclerosis, CCL2 is elevated in patients with proven coronary artery disease compared with individuals with normal angiograms (Martinovic et al. 2005). No association has previously been found between CCL2 production and unstable atherosclerosis. CCL5 expression in atherosclerotic plaques is associated with macrophages, monocytes, smooth muscle cells and T lymphocytes (Ahn et al. 2007). CCL5 recognition is promiscuous and involves CCR1, CCR3 and CCR5, with the functions of CCR1 and CCR5 now shown to be

distinct (Potteaux et al. 2005; Potteaux et al. 2006; Braunersreuther et al. 2007; Quinones et al. 2007; Zernecke and Weber 2010). The complexity of the biological role of CCL5/RANTES in atherosclerosis is reflected by contradictory results in clinical studies (Rothenbacher et al. 2006; Cavusoglu et al. 2007; Kraaijeveld et al. 2007).

Ingenuity pathway analysis also implicated the MSP/RON signalling pathway as important in the difference between symptomatic and asymptomatic atherosclerosis (Figure 44).

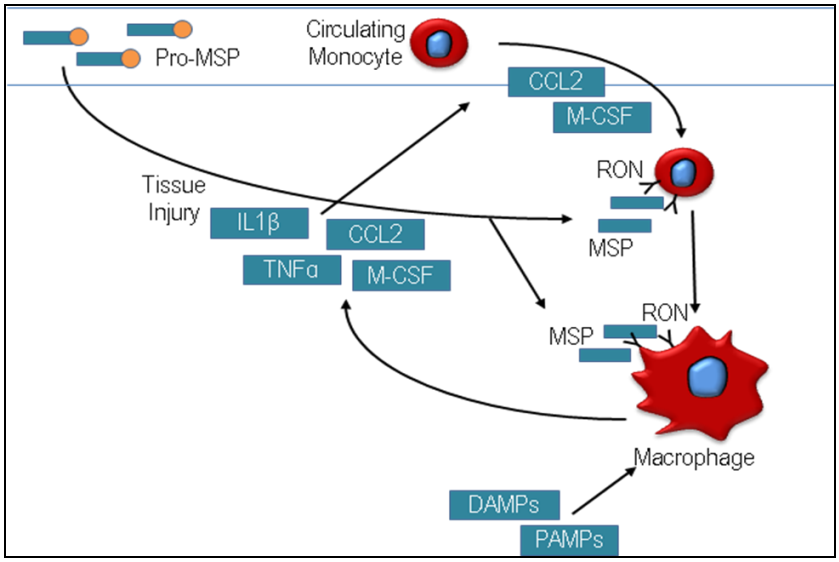


Figure 44 The MSP/RON Pathway

Ingenuity pathway analysis highlighted the MSP/RON pathway (known to play a role in inflammation and the response to tissue injury) as being important in the difference between symptomatic and asymptomatic atherosclerosis. MSP's inactive precursor Pro-MSP is produced in the liver and is activated by proteolytic cleavage in the context of tissue injury. RON is expressed by monocytes and macrophages. When MSP binds RON, RON kinase and second messenger pathways are activated (Correll et al. 1997; Nanney et al. 1998; Danilkovitch and Leonard 1999). DAMP, danger-associated molecular pattern; IL, interleukin; M-CSF, macrophage colony stimulating factor; MSP, macrophage-stimulating protein; PAMP, pathogen-associated molecular pattern; RON, receptor d'origine nantais; TNF, tumour necrosis factor.

T lymphocytes are also recruited to atherosclerotic lesions, with IFNγ-producing Th1 lymphocytes particularly implicated in their pathogenesis. Deletion of IFNγ and its receptors have a profound effect on atherosclerotic plaque development (Koga et al. 2007a; Koga et al. 2007b). Activation of the chemokine receptor CXCR3 by IFNγ-inducible proteins CXCL9 and CXCL10 is required for the recruitment of CXCR3-positive Th1 in atherosclerosis (Mach

et al. 1999). A murine CXCL10-/- apoE-/- double knockout exhibited reduced aortic atherosclerosis, with reduced CD4+ and CXCR3+ T cells, and increased IL10 and transforming growth factor (TGF)-β1 expression (Heller et al. 2006), highlighting the importance of CXCL10/CXCR3 signalling in regulating T cell responses in atherosclerosis. Human carotid atheroma-associated endothelial cells, smooth muscle cells and macrophages all express CXCL10, with CXCL9 expressed by endothelial cells and macrophages (Mach et al. 1999). CXCL10 levels are higher in individuals with coronary artery disease than in controls (Rothenbacher et al. 2006). It has been shown for the first time that production of the IFNγ–inducible CXCR3 ligands CXCL9 and CXCL10 is significantly higher in symptomatic than asymptomatic atherosclerosis, underlining the importance of the recruitment of Th1 lymphocytes in carotid instability. Interestingly, CD40L – also increased in unstable atherosclerosis in this study – has previously been found to have an additive effect together with IFNγ in inducing CXCL10 production (Mach et al. 1999). Communication between innate and adaptive immune cells, highlighted as a significant canonical pathway in symptomatic plaques, also concurs with the positive correlation of CXCL10 with each of IL1α, IL1β and TNFα. Pattern recognition receptors as inducers of the innate immune signalling supports the findings from previous work in this context (Monaco et al. 2004; Monaco et al. 2009).

It was not possible to consistently detect IFNγ production by plaques cells, however expression of IFNγ-inducible chemokines could represent an IFNγ 'signature' that marks the high-risk carotid plaque. It is likely that IFNγ production is strictly confined to the early instability phase and only its late effectors are detectable at the time of carotid endarterectomy. In support of these observations, circulating monocytes isolated from patients with unstable angina exhibit signatures of IFNγ activation, when compared to chronic stable angina (Liuzzo et al. 2001b).

CCL20 interacts with CCR6 and is responsible for the chemotraction of immature dendritic cells, and effector/memory T- and B-cells (Schutyser et al. 2003). CCL20 production is known to be augmented in a number of human inflammatory conditions (Mosser and Edwards 2008) including rheumatoid arthritis (Chabaud et al. 2001; Matsui et al. 2001; Chevrel et al. 2002; Page et al. 2002) similarities to which have been drawn by the pathway analysis performed in this work. This study is the first to show CCL20 production in atherosclerosis and also that CCL20 production is significantly higher in plaques responsible for recent cerebrovascular events. In a murine model of rheumatoid arthritis, CCR6 expression was shown on IL17-producing Th17 lymphocytes, as well as CCL20 production by Th17 cells (Hirota et al. 2007). Th17 cells, which are distinct from Th1 and Th2 (Harrington et al. 2005),

have been demonstrated in mouse (Smith et al. 2010; Xie et al. 2010) and human atherosclerosis (Eid et al. 2009; Taleb et al. 2009). The expression of CCL20 may therefore relate to Th17 recruitment to the lesions, as supported by the identification of IL17 signalling as a key canonical pathway by bioinformatic analysis. It is yet unclear, however, whether IL17 has a detrimental or protective role in atherosclerosis (Eid et al. 2009; Taleb et al. 2009; Taleb et al. 2010). Importantly, CCL20 is also up-regulated by IFNγ (Martinez et al. 2006; Mosser and Edwards 2008). In support of this, the production of CXCL10 and CCL20 was confirmed to be positively correlated.

A recent review by Gordon and Martinez, proposed a sequential four-stage paradigm of macrophage activation: differentiation; priming (also termed polarisation); activation; and resolution (Gordon and Martinez 2010). Macrophages are plastic and capable of modifying their behaviour upon microenvironmental cues, undergoing so-called classic (or M1) 'activation' in response to bacterial motifs (*e.g.* LPS) and IFNγ, a type of priming that mirrors Th1 lymphocyte polarisation. They produce pro-inflammatory cytokines such as IL1, IL12 and TNFα (Mantovani et al. 2004). Alternative (or M2) macrophage polarisation was first identified upon exposure to IL4 (Gordon and Martinez 2010). M2 macrophages are heterogenous and can be generated by different inflammatory and opsonic signals: IL4/IL13, immune complexes, TGFβ and IL10. Lipids are also known to affect macrophage activation patterns (Gordon and Martinez 2010; Kadl et al. 2010). Interestingly, M2 macrophages accumulate first in murine atherosclerosis, while lesion progression correlates with predominance of M1 over M2 macrophages (Khallou-Laschet et al. 2010). Both IFNγ and TLR4 – the LPS receptor – are implicated in M1 polarisation (Martinez et al. 2008) and their genetic deletion reduces atherosclerosis development (Michelsen et al. 2004).

The chemokine data presented here pointing toward an IFNγ signature is also supported by a significant elevation of cytokines typically produced by classically primed macrophages, namely TNFα, IL6, IL1α and IL1β, in unstable plaques. Elevated plasma TNFα levels have been found to be predictive of recurrent coronary events following myocardial infarction (Ridker et al. 2000). Similarly, IL6 plasma levels are higher in patients with unstable than stable angina (Biasucci et al. 1996). The analytes seen to be more abundant in atherosclerosis responsible for recent symptoms comply largely with the cytokine and chemokine signature for M1 polarisation described by Martinez et al in study of transcriptional profiling in human monocyte-to-macrophage polarisation (Martinez et al. 2006). LPS- and IFNγ-differentiated M1 macrophages had increased gene expression of TNF (21 fold), IL6 (7 fold), CXCL10 (59 fold), CXCL9 (58 fold), CCL5 (19 fold) and CCL20 (7 fold), than IL4-differentiated M2 macrophages (Martinez et al. 2006). A similar pattern has been observed when comparing

murine macrophages, with increased TNFα, IL1α, IL1β, IL6, M-CSF, CCL2, CCL5, CXCL9 and CXCL10 gene expression in M1 over M2 macrophages (Kadl et al. 2010). M1 predominance is supported by identification of IL12 signalling and production in macrophages as a key canonical pathway in symptomatic human atherosclerosis. The increased production of IL12 by symptomatics in the atheroma culture system employed did not reach statistical significance, in part due to IL12 protein detection in under half of supernatants.

The differentiation of monocytes to macrophages is essential in atherosclerotic lesion development; M-CSF-deficient mice are atherosclerosis resistant (Smith et al. 1995). Growth factors have a role in conditioning preferential paths of macrophage activation and M-CSF alone may drive the acquisition of M2 properties (Martinez et al. 2006). GM-CSF-differentiated macrophages recapitulate many features of classically activated macrophages, including production of inflammatory cytokines such as TNFα and IL6, and their involvement in tissue destruction (Martinez et al. 2006). In this study, both M-CSF and GM-CSF are increased in unstable plaque pointing to an important role for macrophage differentiation in plaque instability, implicating a toll of GM-CSF for the first time in this process. In the context of rheumatoid arthritis, a mechanism of interaction between macrophages and neighbouring cells has been proposed, whereby macrophages release IL1 and TNFα which stimulate M-CSF and GM-CSF from these neighbouring cells (Hamilton 1993). Indeed, levels of production of GM-CSF in this study significantly correlated with those of IL1α, IL1β and TNFα, supporting the possibility that similar mechanisms might be at play in atherosclerosis.

IL10 is anti-atherogenic (Mallat et al. 1999a), and is associated with regulatory T cells(Taleb et al. 2008) and a specific subset of M2c or regulatory macrophages (Mosser and Edwards 2008). In apoE-/- mice, IL10 was more abundant in plaques with a vulnerable phenotype (Cheng et al. 2007). Intra-plaque haemorrhage is a promoter of lesion progression (Virmani et al. 2005) and carotid plaque-responsible symptomatology (Takaya et al. 2006). In human coronary atheroma, CD163+ macrophages have been detected at sites of haemorrhage (Boyle et al. 2009) and linked to an IL10 positive feedback loop. Hence the increased IL10 observed in the symptomatic group may reflect the presence of such CD163+ macrophages in regions of haemorrhage or plaque remodelling.

There is an inextricable link between inflammation and matrix degradation in atherosclerosis (Galis et al. 1994a). Production of MMPs 1, 3, 8 and 9 is significantly higher within symptomatic compared with asymptomatic plaques. Moreover, the top network identified by pathway analysis is pertinent to matrix degradation. Previous studies have observed that

MMPs 1, 3, 8 and 9 co-localise with macrophages (Galis et al. 1994b; Pasterkamp et al. 2000) and are related to unstable atherosclerosis (Loftus et al. 2000; Molloy et al. 2004). In keeping with this data, recent work has confirmed the association of MMPs 8 and 9 with an inflammatory human carotid atherosclerosis phenotype (Sluijter et al. 2006; Newby et al. 2009). Interestingly, MMP1, 3 and 9 concentrations were found to positively correlate with GM-CSF, TNFα, IL1α, IL1β, IL6, IL10, CCL2, CCL5, CCL20 and CXCL10 protein production.

To date, macrophage polarisation data is concentrated largely on the murine system (Gordon 2003), with studies showing both conservation (Gordon and Taylor 2005) and discrepancy (Raes et al. 2005; Scotton et al. 2005; Martinez et al. 2006; Mantovani et al. 2009) in macrophage heterogeneity between mice and humans. It has been proposed that macrophage polarisation and activation have a role in atherosclerosis (Mantovani et al. 2009). However, previous studies on macrophage polarisation have focused on experimental animal atherosclerosis or gene expression of monocytes differentiated *in vitro*, including using M-CSF and GM-CSF (Hashimoto et al. 1999). Cell phenotypes generated *in vitro* might not reflect cells that have matured within atherosclerotic plaques *in vivo*, with exposure to a complex cytokine and growth factor microenvironment (Johnson and Newby 2009). This underlines the utility of employing an unstimulated mixed atheroma-derived cell culture representative of *in vivo* conditions. Of note, differences in cytokine, chemokine and MMP expression were evident despite 61 of the 67 patients in this study being subject to long-term statin therapy (Tang et al. 2009). This suggests that tailored therapies targeting inflammation may deliver an advantage as compared to standard treatment in terms of modulating inflammation.

4.7.1 Limitations of the Study

It would have been of considerable interest to demonstrate the $TIMP3^{low}$ $MMP14^{high}$ phenotype of the highly invasive foam-cell macrophages as previously described (Johnson et al. 2008). With regards to TIMP3, only 9 out of the 67 samples had detectable levels. Furthermore MMP14 (membrane type-1 MMP), being membrane bound, is not amenable to analysis. This highlights the limitations of the atheroma cell culture and supernatant analysis system employed in this study.

The utilisation of mixed cell type culture has the intrinsic limitation of not allowing the precise identification of which cell type is ultimately responsible for the production of which cytokine(s). Tissue size and hence number of cells extracted are important limiting factors. Moreover, a high amount of cell loss and death are observed with further isolation attempts.

Additional technological development is necessary prior to enabling cell isolation and single cell type analyses.

4.7.2 Conclusions

This data demonstrate that symptomatic human atherosclerotic carotid disease is associated with a cytokine and chemokine pattern consistent with the predominance of pro-inflammatory M1-type macrophage polarisation. Furthermore, IFNγ signatures are observed, including the novel finding of CCL20 with its significant elevation in symptomatic atherosclerosis. The role of anti-inflammatory and anti-atherogenic cytokines such as IL10 are highlighted in attempting to offer regulation in the plaque microenvironment. This study has implications for future therapeutic and diagnostic applications for high-risk atherosclerosis.

5 THE RELATIONSHIP BETWEEN LATE-PHASE CONTRAST ENHANCED ULTRASOUND AND ATHEROSCLEROTIC PLAQUE BIOLOGICAL FEATURES

5.1 INTRODUCTION

Inflammation, angiogenesis and matrix degradation – determined by the balance between matrix metalloproteinases (MMPs) and tissue inhibitors of metalloproteinases (TIMPs) – are among the key features which contribute to plaque vulnerability (Ross 1999; Narula and Strauss 2007).

Therefore, functional imaging modalities are being developed to visualise these biological features *in vivo* as a means of stroke prediction. Methods of assessing plaque inflammation based on magnetic resonance imaging (MRI) are expensive and not appropriate for a screening test given the prevalence of asymptomatic carotid atherosclerosis. Likewise computed tomography, positron emission tomography (PET) and single photon emission computed tomography (as well as being expensive) also rely on ionising radiation (Rudd et al. 2009).

Contrast enhanced ultrasound (CEUS), in its dynamic phase (the period immediately following contrast administration), has been studied as a translational modality for assessing carotid atherosclerosis. Dynamic CEUS can assess the carotid vasa vasorum and plaque neovascularisation, relating findings to histological evaluation of angiogenesis (Giannoni et al. 2009), and cardiovascular disease and past cardiovascular events (Staub et al. 2010).

Previously, animal studies have linked microbubble persistence in the microcirculation at 12 to 30 minutes with adhesion to and phagocytosis by leukocytes (Lindner et al. 2000a; Lindner et al. 2000b). Late-phase- (LP-) CEUS at 6 minutes post-contrast injection has been used to quantify retention of microbubble contrast within human carotid plaques *in vivo*, this being able to distinguish asymptomatic from atherosclerosis responsible for recent focal neurological symptoms pertaining to the ipsilateral anterior cerebral circulation (Chapter 3). It is hypothesised that, at this 6 minute timepoint, microbubbles are adhering to activated intra-plaque microvascular endothelium, hence it is proposed that LP-CEUS is identifying inflammation within atherosclerosis.

The biological characteristics of human atherosclerosis which are represented by changes in LP-CEUS signal have not previously been examined. The aim of this study is to investigate whether LP-CEUS reflects key plaque biological features.

5.2 METHODS

5.2.1 Study Subjects

Consecutive patients who were due to undergo carotid endarterectomy for primary atherosclerotic stenosis of the carotid bifurcation from the vascular surgery clinics of a tertiary referral centre were recruited. Exclusion criteria were as outlined in Section 3.2.3.

Between December 2008 and May 2009, a total of 31 subjects were enrolled (mean age 70.5 years ± 9.0 [standard deviation]), of these 24 (77%) were male. The carotid plaques from sixteen (52%) patients were symptomatic; a plaque was considered symptomatic if symptoms consistent with stroke, transient ischemic attack or amaurosis fugax had occurred in the neurovascular territory of the plaque studied in the 12 months prior to the study. The symptomatic status was decided by a neurovascular multi-disciplinary team. For the symptomatic group, the median time from symptoms to LP-CEUS scan was 21.0 days (inter-quartile range 11.3 – 40.8). The median time from LP-CEUS scan to carotid endarterectomy surgery was 1 day (inter-quartile range 1 – 1).

5.2.2 Conventional Ultrasound, Late-Phase Contrast Enhanced Ultrasound and Analysis

Measurement of carotid stenosis by unenhanced duplex ultrasonography was undertaken as described in Section 3.2.4. LP-CEUS was subsequently performed as per Section 3.2.7 and analysed using QLAB software (Philips, Bothel, WA) as detained in Section 3.2.8. On the logarithmic scale, a plaque contrast signal greater than luminal signal resulted in a normalised signal >0 and where the plaque signal was less than the luminal signal, normalised LP-CEUS was <0. According to receiver operating characteristic curve analysis, a normalised plaque LP echo intensity of 0 was the optimum cut-off point to distinguish symptomatic from asymptomatic plaques. The subjects were grouped according to a normalised plaque LP-CEUS intensity cut-off of 0.

5.2.3 Carotid Endarterectomy Specimen Processing

Where possible, fresh specimens were divided symmetrically along their long axis, allowing for representative undertaking of both immunohistochemistry and atheroma cell culture (Section 4.2.2) (n=19). Where there was insufficient material to undertake both techniques (n=12), specimens were assigned to either histology alone (n=10) or atheroma cell culture alone (n=2).

5.2.4 Histology

Atheroma specimens (n=29) were axially divided into three regions representing the proximal, middle and distal plaque regions. Three 7 µm cryosections from each of the three regions were immunohistochemically stained for the macrophage marker CD68 (PG-M1, Dako, 1:500) and the endothelial cell marker CD31 (JC70A, Dako, 1:1000) by the ABC technique with DAB visualisation. Whole plaque sections were imaged at x4 magnification using a motorised stage microscope (Eclipse 50i, Nikon) – camera (QImaging) system. Semi-automated image analysis was undertaken using Vision software (version 5.0, Clemex). The percentage area of immunopositivity by colour thresholding was determined, with the average across the 9 slides calculated, for each of CD68 and CD31. Plaque minimum cap thickness was calculated for 17 plaques (Section 4.3).

This study adheres to the recommendations made for the performance, reporting and interpretation of imaging-pathological correlation studies (Lovett et al. 2005).

5.2.5 Atheroma Cell Culture and Multi-Analyte Profiling

Fresh diseased intimal arterial segments (n=21) were enzymatically digested and cultured (Section 4.4) and supernatant subject to multi-analyte profiling (Section 4.5).

5.2.6 Statistical Analysis

Data was analysed with Prism (version 5.02, GraphPad Software, California). Where data was not normally distributed, groups were compared by Mann-Whitney test. Normally distributed data was compared using unpaired t test and relationships assessed by Pearson's correlation. All tests used were 2-tailed and a p-value less than 0.05 was considered statistically significant. No post-test was used.

5.3 RESULTS

Fifteen (48%) subjects had a LP-CEUS signal <0, and 16 (52%) had ≥0. The characteristics of the groups are shown in Table 18. The groups were well matched in terms of degree of carotid luminal stenosis under investigation, demographic and clinical parameters, and statin use. Both groups had a median 1 day interval between LP-CEUS evaluation and carotid endarterectomy surgery. There were significantly more symptomatic stenoses in the LP-CEUS ≥0 group (p=0.001). There was no significant difference in venous plasma C-reactive protein between the two groups.

	LP-CEUS signal <0 (*n* = 15)	**LP-CEUS signal ≥0** (*n* = 16)	***P* value**
Symptomatic	3 (1 CVA, 1 TIA, 1 Am Fu)	13 (4 CVA, 7 TIA, 2 Am Fu)	**0.001**
Time from symptoms to LP-CEUS scan (days)	19 (15.0 – 44.0)	21 (9.0 – 40.5)	0.893
Luminal stenosis (%)	75.0 (65.0 – 90.0)	84.5 (80.0 – 91.5)	0.233
Age (years)	70 ± 9.2	71 ± 9.1	0.794
Male sex	12	12	1.000
Diabetes mellitus	2	2	1.000
Statin use	13	15	0.600
Antiplatelet use	13	14	1.000
Hypertension	11	13	0.685
Smoking history	9	11	0.716
Venous plasma C-reactive protein (mg/L)	4.3 (1.3 – 9.0)	1.6 (1.3 – 3.7)	0.237
Time from LP-CEUS scan to carotid endarterectomy surgery (days)	1 (1 – 1)	1 (1 – 1)	0.977

Table 18 Characteristics of the high and low LP-CEUS signal groups

Demographic and clinical information relating to the 31 patients included in the study. Parametric data are presented as mean ± standard deviation, and non-normally distributed data shown as median (inter-quartile range). Am Fu, amaurosis fugax; CVA, cerebrovascular accident; TIA, transient ischemic attack.

5.3.1 Histological Analysis

CD68 and CD31 average percentage area immunopositivity, as well as plaque minimum cap thickness data were normally distributed. CD68 average percentage area immunopositivity was significantly higher in subjects where normalised plaque late-phase intensity was ≥0 versus <0 (n=29, mean 11.80 versus 6.684, p=0.004, Table 19, Figure 45A, Figure 46). There was a significant positive correlation between normalised LP-CEUS signal and CD68 percentage area immunopositivity (n=29, r=0.4661, p=0.011, Figure 45B). CD31 average percentage area immunopositivity was significantly higher in subjects where normalised plaque late-phase intensity was ≥0 versus <0 (n=29, mean 9.445 versus 4.819, p=0.025, Table 19, Figure 45C). There was no significant correlation between normalised LP-CEUS signal and CD31 percentage area immunopositivity (n=29, r=0.1800, p=0.3501, Figure 45D). Regarding minimum cap thickness, there was a trend towards there being thinner caps where normalised plaque late-phase intensity was ≥0 (n=17, mean 187.1µm versus 341.8µm, p=0.0771, Figure 45E), however there was a significant negative correlation between these parameters (n=17, r=-0.51475, p=0.0345, Figure 45F).

	Average % Area Immunopositivity ± Standard Deviation		***P* value (unpaired t test)**
	LP-CEUS signal <0 (*n* = 14)	**LP-CEUS signal ≥0** (*n* = 15)	
CD68	6.684 ± 3.558	11.80 ± 4.947	**0.004**
CD31	4.819 ± 3.300	9.445 ± 6.520	**0.025**

Table 19 Analysis of immunohistochemistry

29 specimen were immunohistochemically stained for the macrophage marker CD68 (inflammation) and the endothelial marker CD31 (angiogenesis). Whole sections were imaged using a motorised stage microscope-camera system, with semi-automated image analysis to quantify percentage area immunopositivity of staining. The average percentage area immunopositivity from 9 sections for each stain was determined. Data are given to 4 significant figures and P values to 3 decimal places. CD, cluster of differentiation.

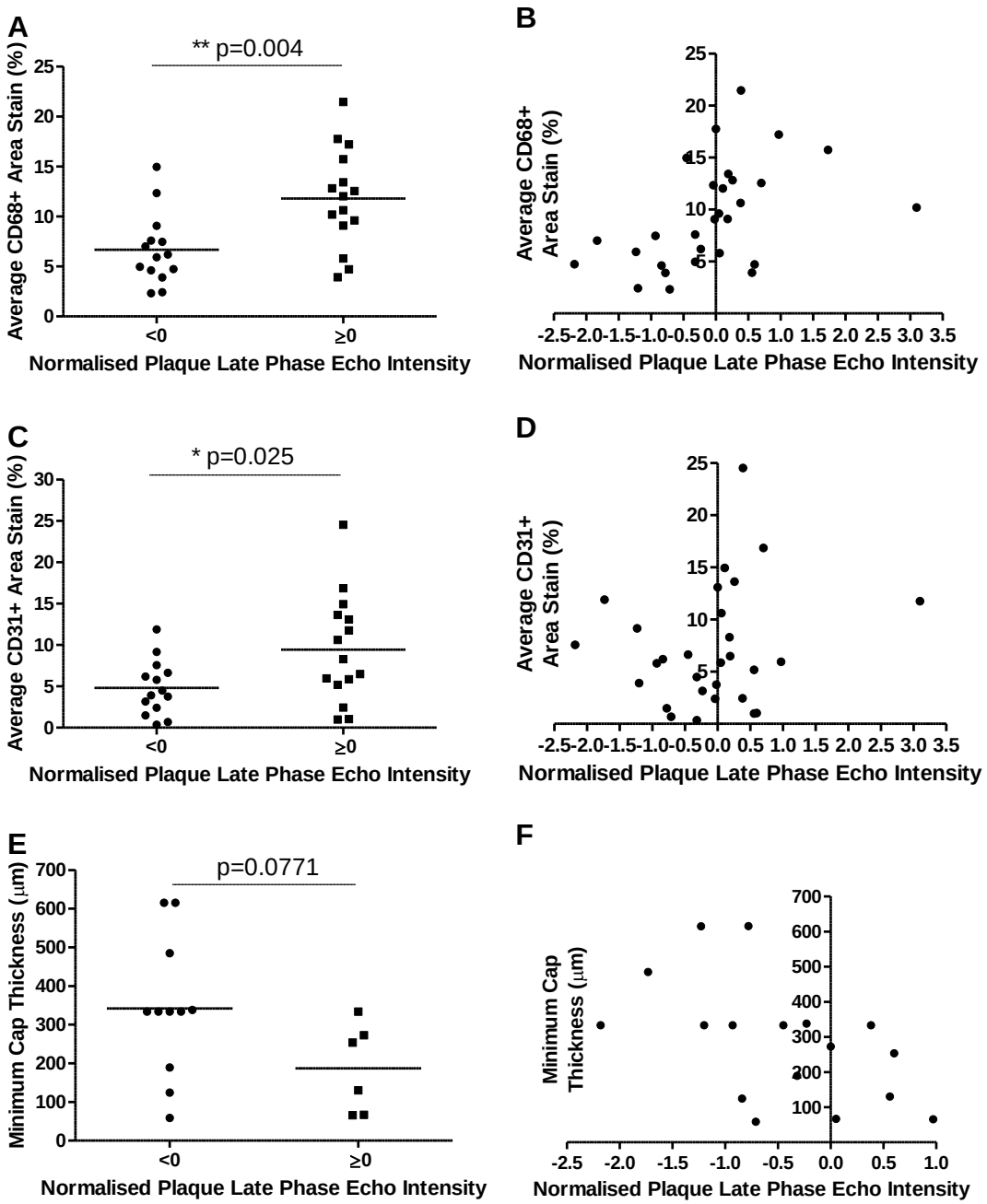


Figure 45 The relationship between normalised plaque late phase echo intensity and CD68, CD31 and minimum plaque cap thickness

CD68 (A) and CD31 (C) average percentage area immunopositivity were significantly higher in subjects (n=29) where normalised plaque late-phase intensity was ≥0 versus <0. There was a trend towards a reduced minimum plaque cap thickness where normalised plaque late-phase intensity was ≥0, although this did not reach statistical significance (E, n=17, p=0.0771). Normalised signal was not significantly correlated to CD31 percentage area staining (D, n=29, r=0.1800, p=0.3501), but was positively correlated with CD68 immunopositivity (B, n=29, r=0.4661, p=0.011) and negatively correlated with minimum cap thickness (F, n=17, r=-0.51475, p=0.0345). Bar denotes mean; CD, cluster of differentiation.

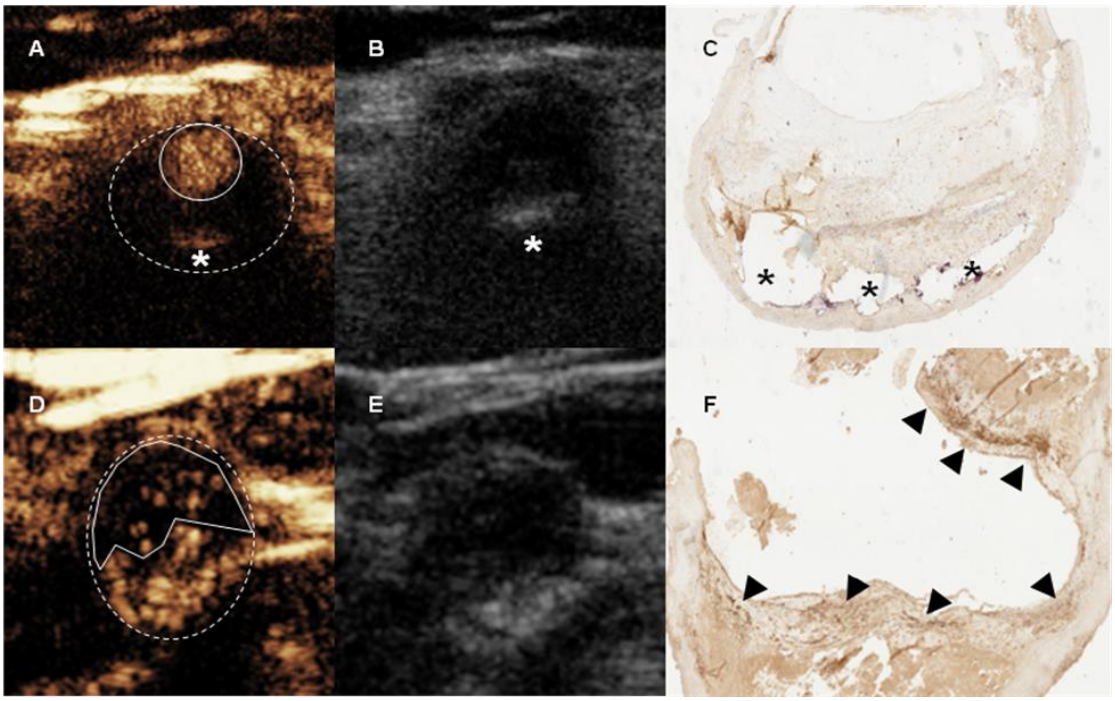


Figure 46 LP-CEUS and B-mode ultrasound comparison with plaque CD68 imunohistochemistry

Image panel of representative axial late-phase contrast enhanced ultrasound (LP-CEUS) images (A and D) with corresponding B-mode ultrasound images (B and E) and CD68 immunohistochemistry (C and F) for plaques with LP-CEUS signal <0 (A-C) and >0 (D-F). The lumen is delineated by a solid line and the plaque by a dashed line. In A and B, plaque calcification is evident and reflected in the histology by calcium clefts (asterisks). In A, there is more luminal than plaque late-phase enhancement, and there is scant staining of macrophages in C. In D, there is more plaque than luminal late-phase enhancement, with areas of focal intense staining for CD68 (arrowheads).

5.3.2 Multi-Analyte Profiling

There was detection of 11/18 cytokines, 4/4 chemokines, 7/8 MMPs and 4/4 TIMPs. Data for detected analytes is summarised in Table 20 and Table 21). IL6, MMP1 and MMP3 were significantly higher in the LP-CEUS ≥0 versus the <0 group (IL6 median 5797 versus 764.0, p=0.030; MMP1 median 2173 versus 480.7, p=0.043; MMP3 median 184.7 versus 16.05, p=0.024, Figure 47). There was a trend towards increased production of IL1β (p=0.101), CCL2 (p=0.082) and CCL5 (p=0.102), with a trend towards reduced TIMP1 production (p=0.070), from plaques above the 0 cut-off.

Cytokine or Chemokine	LP-CEUS signal <0 (*n* = 9)		LP-CEUS signal ≥0 (*n* = 12)		*P* value (Mann-Whitney Test)
	Median (pg/mL)	Inter-Quartile Range (pg/mL)	Median (pg/mL)	Inter-Quartile Range (pg/mL)	
IL1α	3.200	3.200 – 5.626	12.28	3.200 – 23.40	0.205
IL1β	4.778	3.200 – 24.96	69.46	12.70 – 292.6	0.101
IL4	3.200	3.200 – 7.764	3.200	3.200 – 3.572	0.563
IL6	764.0	360.8 – 2736	5797	1613 – 9765	**0.030**
IL10	54.03	9.567 – 87.01	148.0	30.61 – 545.0	0.337
IL12 (p40)	3.200	3.200 – 12.87	3.200	3.200 – 3.200	0.476
GM-CSF	49.96	22.37 – 114.7	175.3	42.76 – 428.0	0.127
TNFα	191.2	77.45 – 239.2	540.3	112.2 – 930.2	0.127
IFNα2	3.200	3.200 – 4.143	3.200	3.200 – 3.200	0.351
VEGF	16.00	3.200 – 35.68	16.00	3.200 – 28.85	0.942
sCD40L	3.200	3.200 – 8.323	3.200	3.200 – 6.405	0.924
CX3CL1	16.00	12.80 – 20.16	16.00	13.60 – 16.00	0.557
CCL2	162.5	107.9 – 536.9	783.4	244.2 – 1427	0.082
CCL5	33.34	18.75 – 61.75	107.8	35.90 – 187.4	0.102
CXCL10	6.698	3.913 – 22.87	16.00	4.075 – 24.85	0.519

Table 20 Analysis of cytokine and chemokine multi-analyte profiling

Cells were isolated from carotid atherosclerotic plaques as a mixed cell suspension and cultured at $1x10^6$ cells/mL for 24 hours, at which point the supernatant was aspirated. In this unstimulated system, the cells displayed a spontaneous cytokine and chemokine production. All samples were analysed in duplicate, data are given to 4 significant figures and P values to 3 decimal places. IL, interleukin; GM-CSF, granulocyte macrophage colony-stimulating factor; TNF, tumour necrosis factor; IFN, interferon; VEGF, vascular endothelial growth factor; sCD40L, soluble cluster of differentiation 40 ligand; CX3CL1, fractalkine; CCL2, monocyte chemotactic protein 1 (MCP1); CCL5, regulated upon activation, normal T cell expressed and secreted (RANTES); CXCL10, interferon-inducible protein 10 (IP10).

Matrix Metalloproteinase or Tissue Inhibitor of Metalloproteinase	LP-CEUS signal <0 (*n* = 9)		LP-CEUS signal ≥0 (*n* = 12)		***P* value (Mann-Whitney Test)**
	Median (pg/mL)	**Inter-Quartile Range (pg/mL)**	**Median (pg/mL)**	**Inter-Quartile Range (pg/mL)**	
MMP1	480.7	134.8 – 1901	2173	669.1 – 7865	**0.043**
MMP2	671.6	480.8 – 899.8	702.8	478.8 – 1026	0.749
MMP3	16.05	16.05 – 51.71	184.7	29.70 – 477.3	**0.024**
MMP7	102.2	102.2 – 877.3	652.9	102.2 – 3008	0.205
MMP8	461.1	91.91 – 1986	419.6	91.91 – 1885	0.942
MMP9	3799	2801 – 7861	8527	3971 – 16840	0.155
MMP12	468.5	279.3 – 806.5	1174	502.9 – 1569	0.127
TIMP1	7901	3645 – 16680	3694	1273 – 4128	0.070
TIMP2	110200	104200 – 253300	124500	42800 – 180400	0.749
TIMP3	155.0	155.0 – 155.0	155.0	155.0 – 155.0	0.115
TIMP4	6.170	6.170 – 6.170	6.170	6.170 – 6.170	0.185

Table 21 Analysis of matrix metalloproteinase and tissue inhibitor of metalloproteinase multi-analyte profiling

Cells were isolated from carotid atherosclerotic plaques as a mixed cell suspension and cultured at $1x10^6$ cells/mL for 24 hours, at which point the supernatant was aspirated. In this unstimulated system, the cells displayed a spontaneous matrix metalloproteinase (MMP) and tissue inhibitor of metalloproteinases (TIMP) production. All samples were analysed in duplicate, data are given to 4 significant figures and P values to 3 decimal places.

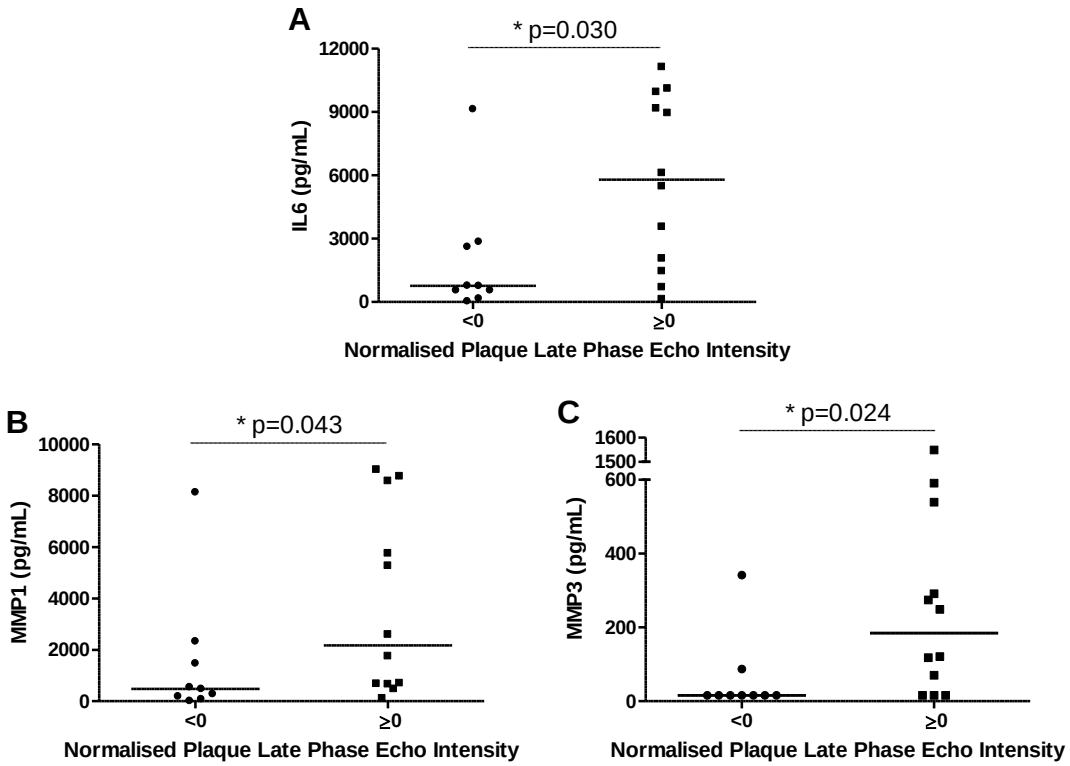


Figure 47 IL6, MMP1 and MMP3 production is significantly higher from plaques with a LP-CEUS signal ≥0

IL6 (A), MMP1 (B) and MMP3 (C) production in atheroma cell culture, as determined by multi-analyte profiling, were significantly higher in subjects (n=21) where normalised plaque late-phase intensity was ≥0 versus <0. Bar denotes median; CD, cluster of differentiation.

5.4 DISCUSSION

These results show that human atherosclerotic plaques with a normalised LP-CEUS signal ≥0 have significantly more inflammation (CD68, IL6), angiogenesis (CD31) and matrix degradation (MMP1, MMP3) than plaques with a normalised LP-CEUS signal <0. Inflammation, angiogenesis and matrix degradation are key biological features involved in the initiation, progression and complications of atherosclerosis (Narula and Strauss 2007).

IL6 plasma levels are significantly higher in patients with unstable as compared with stable angina (Biasucci et al. 1996). Previous studies have observed that MMPs 1 and 3 co-localise with macrophages (Galis et al. 1994b; Pasterkamp et al. 2000) and are related to unstable atherosclerosis (Loftus et al. 2000; Molloy et al. 2004). Furthermore, it is possible that this pattern of inflammation and matrix degradation in the context of vulnerable atherosclerosis is

attributable to pro-inflammatory M1 macrophage polarisation (Martinez et al. 2006; Waldo et al. 2008; Mantovani et al. 2009).

Studies have shown that carotid plaques retrieved at endarterectomy have many more microvessels and transcripts known to promote neovascularisation when they originate from symptomatic, compared to asymptomatic patients (McCarthy et al. 1999a; Mofidi et al. 2001; Tureyen et al. 2006; Dunmore et al. 2007). High-risk plaques, in addition, have been shown to contain abnormal, immature or 'incompetent' vessels that may precipitate plaque instability through their acting as sites of vascular leakage and so inflammation (McCarthy et al. 1999a; McCarthy et al. 1999b; Dunmore et al. 2007). With regards to dynamic CEUS, the peak intensity achieved following the administration of contrast relates to microvascular volume (Averkiou et al. 2010).

This clinical study supports previous pre-clinical investigation showing that non-targeted microbubbles are passively retained within tissue where there is inflammation, endothelial activation, or both (Lindner et al. 2000a; Lindner et al. 2000b; Tsutsui et al. 2004b). It is hypothesised that the microbubbles adhere to endothelium or may leave the microvessel and enter the plaque parenchyma, are retained in isolation or within phagocytosing macrophages. It is likely that a number of interrelated endothelial processes are responsible for this microbubble accumulation: endothelial activation; endothelial permeability and leakage (of the microbubbles themselves or of inflammatory cells containing them); and endothelial charge changes, although this is an area of ongoing study.

A number of other methods have been proposed for the risk stratification in carotid atherosclerosis. These include transcranial Doppler (Markus et al. 2010) and the presence of sub-clinical cerebral ischemia using computed tomography (Kakkos et al. 2009) or magnetic resonance imaging (Romero et al. 2009). However, these modalities are not carotid-specific, and may be reflecting silent embolisation from another source, for example of cardiac origin. Fluorodeoxyglucose (FDG) PET studies have shown that *in vivo* FDG signal corresponded to *in vitro* active plaque inflammation (Graebe et al. 2009). This approach, however, is limited by non-specificity and the use of tracers targeted to specific ligands has been proposed and is currently being examined in the clinical setting. Ultrasmall super-paramagnetic iron oxide (USPIO) MRI relies on USPIO being internalised by circulating monocytes, some of which enter the inflamed carotid as macrophages. The USPIO is detected by MRI in carotid plaques where there exists inflammation. Studies have shown that there is a larger signal drop (suggesting more USPIO uptake) in symptomatic as compared with asymptomatic carotid plaques (Howarth et al. 2009).

These findings were made in the context of a study group where more than 90% were taking statins. This shows that despite statin use, there is ongoing production of inflammatory mediators and that the presence of inflammation is still detectable through imaging.

5.4.1 Study Limitations

The limitations of this work include the numbers of subjects enrolled and the potential for sampling error. Ultrasound is a planar imaging technique and LP-CEUS at a single level in the plaque (at the point of greatest stenosis) was compared with nine immunohistochemically stained sections taken at points throughout the plaque and atheroma cell culture data representative of at least half the plaque. Such may be overcome through the use of 3- or 4-dimensional volumetric ultrasound acquisition technology. These probes are under investigation by our group, however, the spatial resolution is, at present, not adequate for their use in the context of LP-CEUS.

5.4.2 Conclusion

This chapter demonstrates that LP-CEUS reflects the biological features of inflammation, angiogenesis and matrix degradation, which are key to plaque rupture. These findings support the further study of LP-CEUS as a tissue-specific marker of inflammation with potential utility in risk stratification of carotid atherosclerosis.

6 THE UTILITY OF A SYSTEMS BIOLOGY APPROACH IN EXAMINING CAROTID ATHEROSCLEROSIS BIOLOGY

6.1 INTRODUCTION

In order to look at the utility of the 'omic' disciplines in exploring the biology of atherosclerosis, carotid atherosclerotic plaques were examined using four systems biology approaches:

- Transcriptomics
- Proteomics
- Lipidomics
- Metabonomics

6.2 TRANSCRIPTOMICS

Transcriptomics (epigenomics, gene expression or transcription profiling are synonyms) looks at RNA and is therefore a means of identifying which genes are 'activated' or transcribed. As a patient's genotype is the same regardless of which somatic cell is looked at, genomics is patient-specific. On the other hand, gene transcription varies within individuals from tissue to tissue and under different circumstances, such that they will have a unique genotype but a number of transcriptomic profiles.

A further challenge with transcriptomics is that, whilst the genome is relatively stable and DNA is relatively robust, RNA is less so and subject to degradation. RNA quality is looked at prior to a transcriptomic study and this is achieved by calculation of the RNA integrity number (RIN) from a number of parameters obtained by electrophoresis of the RNA (Figure 49).

Following RNA extraction from samples, double stranded complementary DNA (cDNA) is synthesised. This is a stable copy of the RNA which can be used for gene profiling. The cDNA is labelled, hybridised and quantified producing a gene expression pattern (Archacki and Wang 2006). Microarrays allow the comparison of global expression changes in thousands of genes. Results can be validated using real time PCR (Hiltunen et al. 2002; Archacki et al. 2003; Randi et al. 2003; Archacki and Wang 2004; Fu et al. 2008). These techniques have led to the identification of unique subsets of genes associated with specific diseases and disease processes (Archacki and Wang 2004).

There have been several studies validating the technique of gene expression profiling in normal and atherosclerotic tissue (Hiltunen et al. 2002; Archacki et al. 2003; Randi et al.

2003; Tabibiazar et al. 2005; Bijnens et al. 2006; Fu et al. 2008). Seo and colleagues generated gene expression data from human aortas with varying degrees of atherosclerosis to create genomic phenotypes which may allow prediction of disease states from any given sample of aorta (Seo et al. 2004). Microarray analysis has also demonstrated that 97% genes are unaffected when atherosclerotic samples were taken during surgery compared to post mortem samples. Differentially expressed genes were shown to be involved in basal cell metabolism and hypoxia at mRNA level, but these changes were not reflected in protein expression (Sluimer et al. 2007).

Further to the assessment of presence or absence of atherosclerosis (*i.e.* atherosclerotic 'burden') is examination of the transcriptional profile of plaque instability. Papaspyridonos and colleagues examined total RNA from stable and unstable areas from 3 human carotid plaques, identifying the differential expression of 170 genes between these areas of which four varied by greater than fivefold: retinoic acid receptor responder; junctional adhesion molecule; haemoglobin scavenger receptor CD163; and ganglioside activator protein GM2A (Papaspyridonos et al. 2006) (Table 22).

RIN may be artificially lowered in circumstances were degraded RNA exists, for example in the mural thrombus of an aneurysm or – in the context of atherosclerosis – the necrotic core of a plaque. This is one reason for why transcriptome-wide analysis of human atherosclerotic tissue has not been readily performed (Table 22).

One way round the challenges inherent to transcriptomics of human atherosclerosis tissue is by profiling peripheral blood in the context of atherosclerotic disease. This has the further inherent utility for direct discovery of biomarkers. An example of this was a study which used arrays to expression profile peripheral blood from 10 patients with carotid stenosis and 10 matched controls. Of the 14,000 transcripts represented on the arrays, 82 genes were found to be differentially expressed between these two groups (Rossi et al. 2010). Fourteen of the 82 differentially expressed genes were selected as candidate genes and subsequently confirmed by PCR on separate validation groups of 40 patients with carotid stenosis and 40 controls. These genes were largely involved in immune activities and oxygen transport (Rossi et al. 2010) A summary of this and other studies pertaining to transcriptomic studies in human atherosclerosis to date can be seen in Table 22.

Study Reference	Methodology	Sample Source	Results	Genes of Interest
(Rossi et al. 2010)	Carotid stenosis versus healthy individuals	Plasma from 40 patients with carotid stenosis and 40 healthy controls	82 genes differentially expressed	Immune activities and oxygen transport
(Fu et al. 2008)	Peripheral arterial disease as classified by the American Heart Association	30 whole femoral arteries from live subjects: 14 advanced; 11 intermediate; 5 normal	366 genes differentially regulated in intermediate and 447 in advanced	Immune and inflammatory genes enriched especially Toll-like receptor signalling and natural killer cell-mediated cytotoxicity
(Papaspyridonos et al. 2006)	Plaque instability	3 human carotid plaques	170 genes differentially expressed	Retinoic acid receptor responder, junctional adhesion molecule, haemoglobin scavenger receptor CD163, ganglioside activator protein GM2A
(Sluimer et al. 2007)	Advanced atherosclerotic plaques. Surgery versus autopsy samples	26 carotid segments taken at autopsy from 11 donors. 11 samples from live donors	97.2% genes have similar expression levels in advanced lesions	Differentially expressed genes involved in basal cell metabolism and hypoxia driven pathways
(Tabibiazar et al. 2005)	3 cohorts of 5 mice with varying disease susceptibility and diet compared to human data sets to identify shared genes	Entire aortas from euthanized mice. Once data sets were identified, they were compared with those of 40 coronary artery samples from 17 transplant patients	Established 'classifier gene set' which can distinguish specimens with atherosclerotic disease state	Gene subset was found to be equivalent in human subjects when grading human coronary disease
(Seo et al. 2004)	Human aorta samples with varying degrees of atherosclerosis	Cadaveric whole aortas. Severity assessed as mild proximally with increasing severity distally	Identified gene expression 'signatures'. A set of 208 genes relating to disease severity	Multiple, including apoE, osteopontin, OLR1. Cell cycle regulation and inflammatory response
(Randi et al. 2003)	Comparison of coronary plaques in stable and unstable angina	8 coronary plaques from live subjects	Examination of genes using data sets for inflammation, adhesion and haemostasis	Lymphocyte adhesion molecule (MadCAM) in all plaques. Anticoagulant protein S and TF increased. COX1, IL7, MCP1 and MCP2 decreased in unstable plaques
(Archacki et al. 2003)	Differential gene expression in human coronary artery disease. Atherosclerosis versus normal	9 severe and 6 non-atherosclerotic human coronary arteries from explanted hearts	Established gene profiling as reliable tool for analysis of atherosclerosis. 56 genes differentially expressed	Altered gene expression of inflammation, cell necrosis/apoptosis, altered cell migration, matrix degradation genes
(Hiltunen et al. 2002)	Human arterial samples from varying locations from aorta to lower limb	12 arterial samples obtained after amputation of limb or from organ donors	75 differentially expressed genes previously unknown to be associated with atherosclerosis	Sub-group for cell signalling and proliferation selected for further analysis; receptors for signalling in activated macrophages, angiogenic and vasculoprotective
(Faber et al. 2001)	Comparison of human stable and ruptured plaques. American Heart Association classification	20 human arterial plaques from varying locations (10 stable, 10 ruptured)	3,000 clones upregulated and 2000 downregulated in ruptured plaques	SSH6 and Perilipin (SSH1 SSH11) expressed in ruptured plaques in the cytoplasm of cells surrounding cholesterol clefts and in foam cells

Table 22 Summary of transcriptomic studies in human atherosclerosis

ApoE, apolipoprotein E; COX, cyclooxygenase, IL, interleukin; MCP, monocyte chemotactic protein; ORL, oxidised low density lipoprotein receptor; SSH, suppression subtractive hybridisation; TF, tissue factor.

Contemporary microarrays, including the Affymetrix Human Exon 1.0 ST array used in this study, have multiple probes per exon. In the case of the Affymetrix Human Exon 1.0 ST, there are approximately four probes per exon, equating to roughly 40 probes per gene. This allows for two complementary levels of analysis: gene expression and alternative splicing. Multiple probes per exon enable 'exon-level' analysis, allowing the distinction between different isoforms of a gene, with detection of specific alterations in exon usage that may contribute to disease aetiology. 'Gene-level' expression analysis, in which multiple probes on different exons are summarised into an expression value of all transcripts from the same gene, is also possible.

6.2.1 Transcriptomic Aims

The primary aim of the transcriptomic section of this chapter was to assess the utility of transcriptomics to distinguish between stenosing plaque and intimal thickening, highlighting differentially expressed and differentially spliced genes. A secondary aim was to determine whether transcriptomics was able to separate stable from unstable atherosclerosis.

6.3 TRANSCRIPTOMIC METHODOLOGY

6.3.1 Sample Selection, RNA Extraction and Processing

Eighteen carotid endarterectomy specimens were initially identified for this experiment. These were each 'chipped' into two areas where possible to give samples relating to stenosing atheroma and areas of intimal thickening (Figure 48). Regions of stenosing atherosclerosis from symptomatic plaques were considered to be unstable, whilst all areas of intimal thickening and the stenosing atherosclerosis from asymptomatic plaques were considered stable (Figure 48).

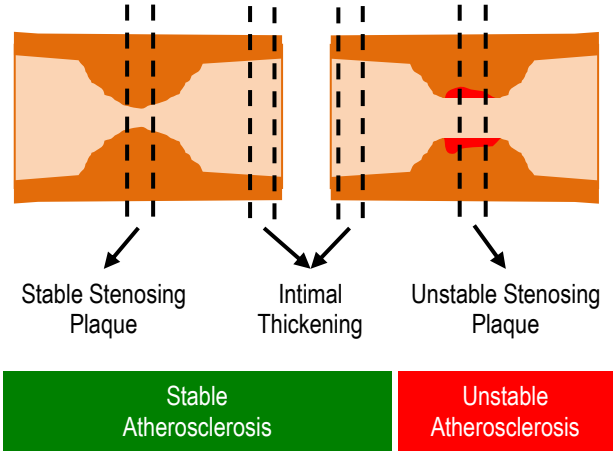


Figure 48 Carotid endarterectomy specimen processing for transcriptomic profiling

Where possible each of the eighteen carotid endarterectomy specimens were processed to yield samples of stenosing atheroma and intimal thickening for further analysis. Regions of stenosing atherosclerosis from symptomatic plaques were considered to be unstable, whilst all areas of intimal thickening and the stenosing atherosclerosis from asymptomatic plaques were considered stable.

In total from the initial 18 endarterectomy specimens, RNA was extracted from 44 samples (27 samples of stenosing atheroma and 17 samples from intimal thickening). Total RNA was extracted using a commercially available kit in accordance with the manufacturer's instructions (miRNAeasy, Qiagen). Extracted RNA was assessed by both Nanodrop and Agilent 2100 bioanalyser (Figure 50, Table 23). There was a weak but significant correlation between the results of Nanodrop assessment and the RNA integrity number (RIN) as seen in Figure 50.

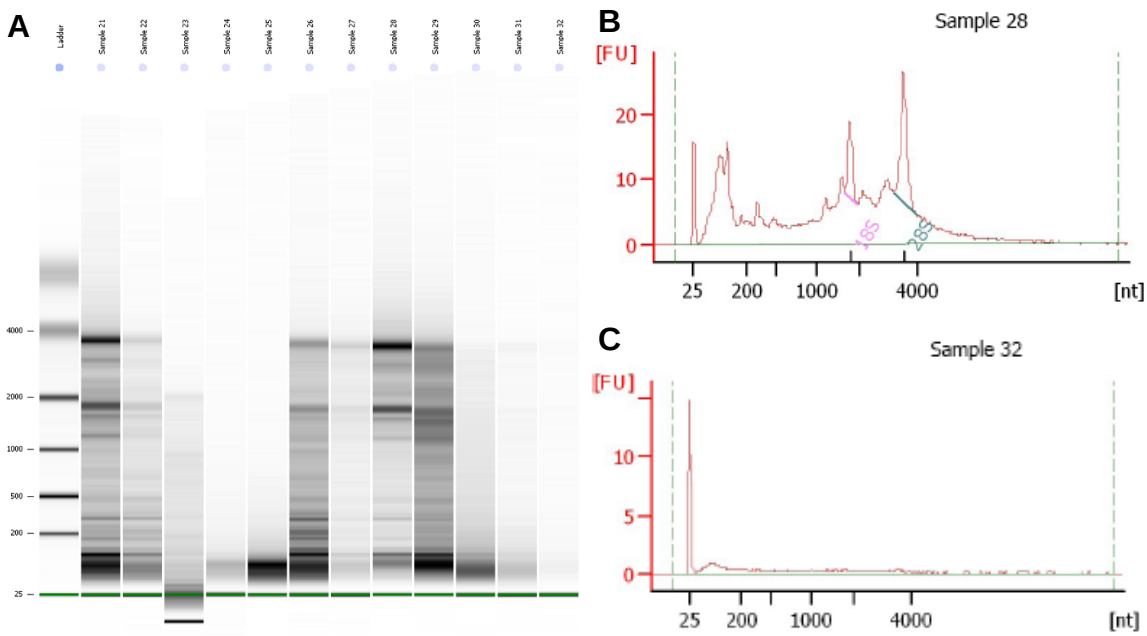


Figure 49 Agilent bioanalyser output for assessment of RNA quality

The Agilent 2100 bioanalyser offers an indirect assessment of mRNA quality by informing about ribosomal RNA. Up to 12 samples undergo electrophoresis per 'chip' (A) before lane is represented individually in graph form (B and C). B demonstrates a sample with an RNA integrity number (RIN) of 5.2, where 18S and 28S ribosomal RNA peaks are clearly seen and labelled. C shows the graph for a sample with a RIN of 1.0, and 18S and 28S ribosomal RNA peaks are not visible.

Sample Number	Nanodrop 260nm / 280nm Ratio	Agilent Bioanalyser RNA Integrity Number
V0012 SP	**2.05**	**3.9**
V0012 SP	1.85	2.9
V0012 IT	**1.77**	**3.3**
V0162 SP	1.56	3.0
V0162 SP	1.34	2.8
V0162 SP	1.23	3.7
V0162 IT	1.45	2.9
V0162 SP	1.29	3.4
V1299 IT	**2.06**	**2.5**
V1299 SP	1.80	2.4
V1299 SP	**1.94**	**3.8**
V1355 IT	1.44	2.4
V1355 SP	1.65	2.4
V1376 IT	**1.86**	**3.2**
V1376 SP	**1.79**	**2.3**
V1377 SP	1.96	2.4
V1377 SP	**2.03**	**3.1**
V1420 IT	**2.01**	**2.6**
V1420 SP	**2.00**	**3.9**
V1236 IT	**2.03**	**3.4**
V1236 SP	**2.06**	**5.0**
V1388 IT	**2.04**	**2.9**
V1388 SP	**2.20**	**2.4**
V1241 IT	1.76	2.3
V1241 SP	1.41	2.5
V1465 IT	**2.11**	**3.0**
V1465 SP	**1.95**	**2.7**
V1468 IT	**2.01**	**5.2**
V1468 SP	**1.86**	**3.0**
V1139 IT	1.29	2.4
V1139 SP	1.35	2.2
V1139 SP	1.64	1.0
V1470 IT	1.28	1.5
V1470 SP	1.14	1.2
V1471 IT	1.51	2.3
V1471 SP	1.66	2.4
V1477 IT	**1.99**	**4.5**
V1477 SP	1.32	2.4
V1477 SP	**1.97**	**4.5**
V1476 IT	1.55	2.4
V1476 SP	1.31	2.4
V1486 IT	1.49	2.5
V1486 SP	1.37	2.5
V1486 SP	1.43	2.4

Table 23 Extracted RNA assessed by Nanodrop and Agilent bioanalyser

Eighteen carotid endarterectomy specimens yielded 44 samples – 27 stenosing plaque (SP) and 17 intimal thickening (IT). 260nm / 280nm ratio was determined by Nanodrop and RNA integrity number by Agilent bioanalyser. The samples highlighted in bold are those which were selected to proceed to transcriptomic analysis.

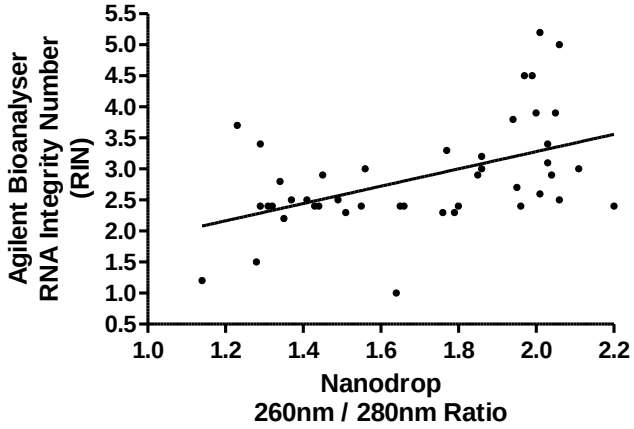


Figure 50 Relationship between Nanodrop and Agilent bioanalyser data

Linear regression, $r^2 = 0.2373$, $p = 0.0008$, $n = 44$ samples from 18 carotid endarterectomy specimens.

Of the 44 available samples, 19 (highlighted in Table 23) were selected for Affymetrix Exon Array 1.0ST based on RNA quality, of which 2 did not pass the preliminary quality control process. Results were obtained from 17 samples: 7 paired samples (5 from symptomatic and 2 asymptomatic patients) and 3 unpaired samples (1 stenosing atheroma and 1 intimal thickening from a symptomatic patients, and 1 intimal thickening from an asymptomatic individual) (Table 24).

Sample	IT / SP	Symptoms	Age (years)	Gender	Ischaemic heart disease	Peripheral arterial disease	Hypertension	Diabetes mellitus	Smoking history	Plasma creatinine (µmol/L)	Plasma C-reactive protein (mg/L)	Carotid Stenosis (%)	Statin use	Antiplatelet use	Time from symptoms to surgery (days)
V0012	IT & SP	1	76	F	0	0	1	0	1	-	-	90-95	1	1	22
V1236	IT & SP	0	85	M	0	1	1	0	1	169	-	85	1	1	-
V1299	IT & SP	1	79	M	0	0	1	0	0	103	82	90-95	1	0	2
V1376	IT & SP	1	60	M	1	0	0	1	1	72	0.6	90	1	1	29
V1377	IT	1	73	M	0	0	1	1	1	95	0.8	-	1	1	3
V1388	IT	0	66	F	0	0	1	0	0	63	1.9	80	1	0	-
V1420	SP	1	51	M	0	0	1	0	1	74	0.9	55-65	0	0	3
V1465	IT & SP	0	67	M	0	0	1	1	0	101	1	75-80	0	1	-
V1468	IT & SP	1	55	M	0	0	0	0	0	79	1.1	80-90	0	1	2
V1477	IT & SP	1	54	M	0	0	1	0	0	73	5.8	60-75	1	1	63

Table 24 Characteristics of the individuals included in the transcriptomic study

Demographic, clinical and pharmacotherapeutic information relating to the subjects included in the study. F, female; IT, intimal thickening; M, male; SP, stenosing plaque.

6.3.2 Transcriptomic Data Analysis

Initial quality control analysis was undertaken using Expression Console (Version 1.1, Affymetrix) to examine the spread of signal intensities across samples following normalisation. Subsequent analysis was performed using Genomics Suite (Version 6.5, Partek, St Louis, Missouri, USA). Only 'core' probe sets were used for the analysis, thus employing only the highest quality annotation data from RefSeq and GenBank. Clustering and separation of sample groups was examined using unsupervised statistical methods: hierarchical clustering and principal components analysis (PCA). The primary aim was investigated by paired samples T-test to compare levels of gene expression and differential splicing between the seven stenosing plaque / intimal thickening sample pairs.

6.4 TRANSCRIPTOMIC RESULTS

6.4.1 Initial Analysis

Quality control analysis confirmed that the normalised expression signal was comparable across the 17 analysed samples (Figure 51).

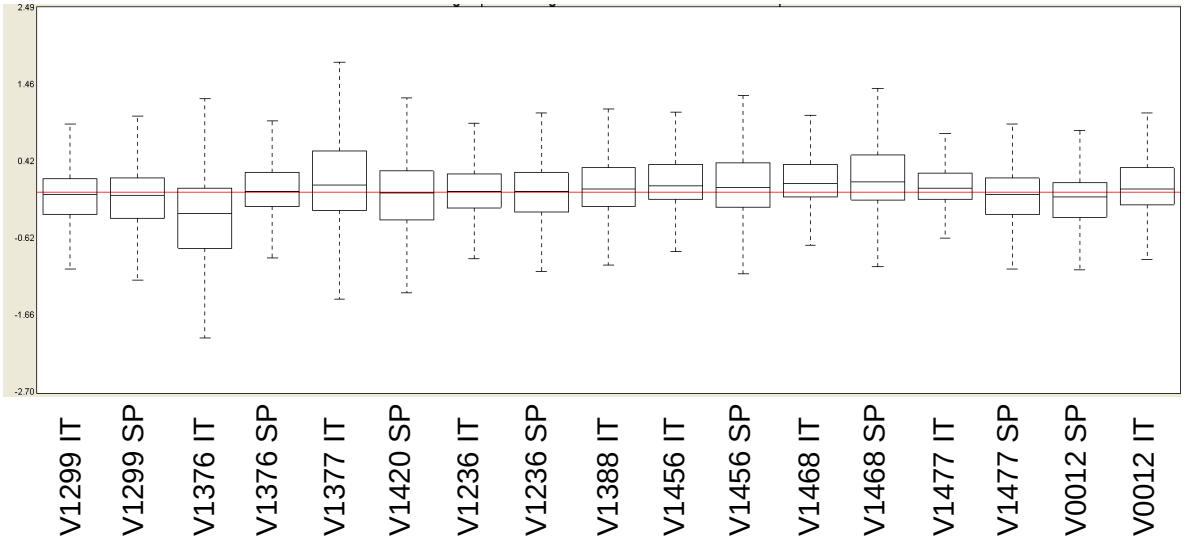


Figure 51 Relative Log expression signal

The spread of the 17 sample intensities are plotted following normalisation.

Initial analysis showed that there was no clustering of samples based upon which carotid endarterectomy specimen the samples were from (Figure 52).

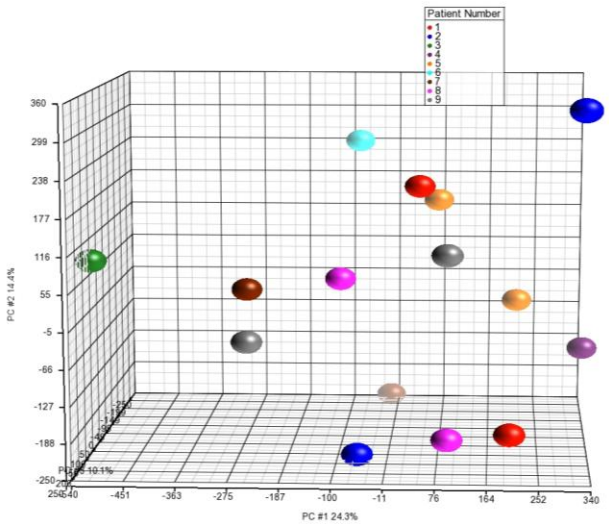


Figure 52 Sample pairs derived from the same carotid endarterectomy specimen were not seen to cluster

Paired samples from the same carotid endarterectomy specimen are shown in the same colour (7 pairs). There are three unpaired samples (Patient Number 3, 4 and 6).

6.4.2 Stenosing Plaque and Intimal Thickening

Analysing the seven stenosing plaque / intimal thickening sample pairs, hierarchical clustering analysis (unsupervised) was able to separate all but a single sample into two groups (Figure 53).

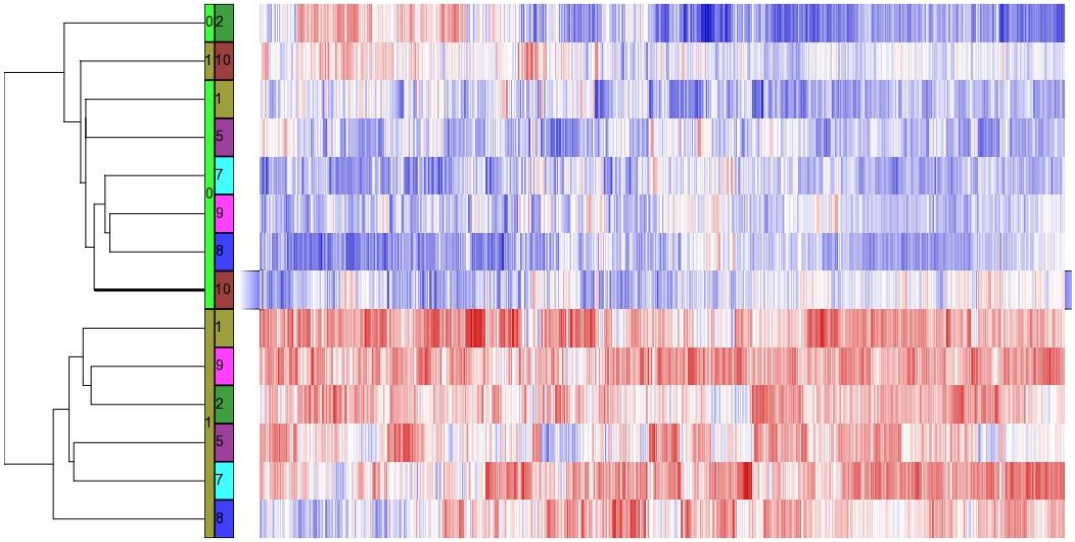


Figure 53 Hierarchical clustering analysis of stenosing plaque and intimal thickening paired samples

Hierarchical clustering (unsupervised) analysis was able to separate all but a single sample into two groups. The first separation is made upon stenosing plaque (1) or intimal thickening (0). The subsequent breakdown is according to sample pairs labelled 1, 2, 5, 7, 8, 9 and 10. Upregulated genes are shown in blue and downregulated genes in red.

Principal components analysis (PCA) represented 39.3% of the data variation on 2 principal components (PCs) (Figure 54) and 48.8% of the data variation on 3 PCs (Figure 55). A clear separation between the stenosing plaque and intimal thickening samples was observed.

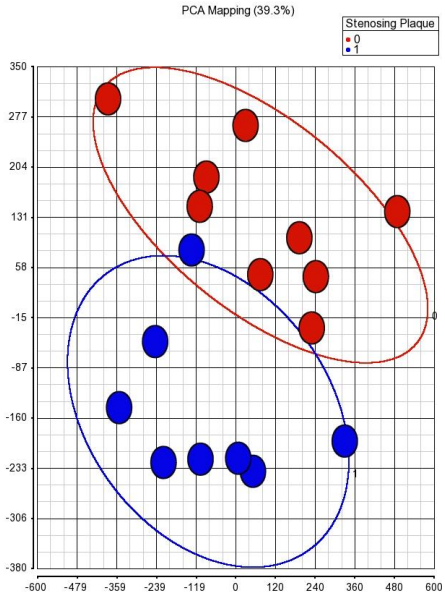


Figure 54 Separation of stenosing plaque and intimal thickening on 2-dimensional principal components analysis

39.3% of the data variation was represented by two principal components. Clustering of intimal thickening (red, 0) and stenosing plaque (blue, 1) tissue transcriptomic data was seen, with a good separation observed between the two groups. Ellipses represent 2 standard deviations.

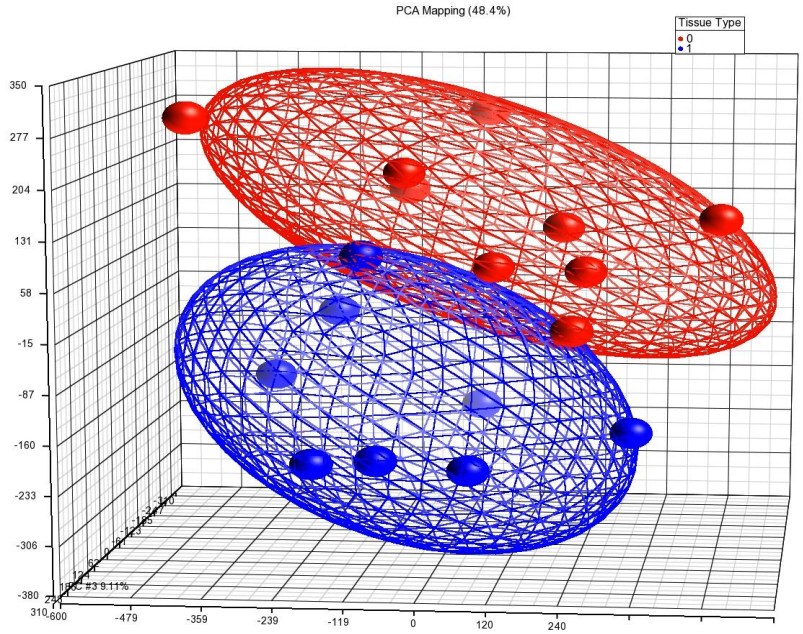


Figure 55 Separation of stenosing plaque and intimal thickening on 3-dimensional principal components analysis

48.4% of the data variation was represented by three principal components. Clustering of intimal thickening (red, 0) and stenosing plaque (blue, 1) tissue transcriptomic data was seen,

with a good separation observed between the two groups. Ellipsoids represent 2 standard deviations.

Differential expression analysis was performed based on the Genbank RNA transcript 'core' geneset of 22,011 genes. 2,988 (14%) genes were seen to display significant ($p<0.05$) differential expression between the intimal thickening and stenosing plaque paired samples. Differential splicing analyses was also performed based on the Genbank RNA transcript 'core' 232,487 probe sets. 1,912 (11%) genes were seen to display significant ($p<0.05$) differential splicing between the two paired sample groups. Common amongst both the differentially expressed and differentially spliced gene lists was the interferon regulatory factor 5 (IRF5) (Figure 56).

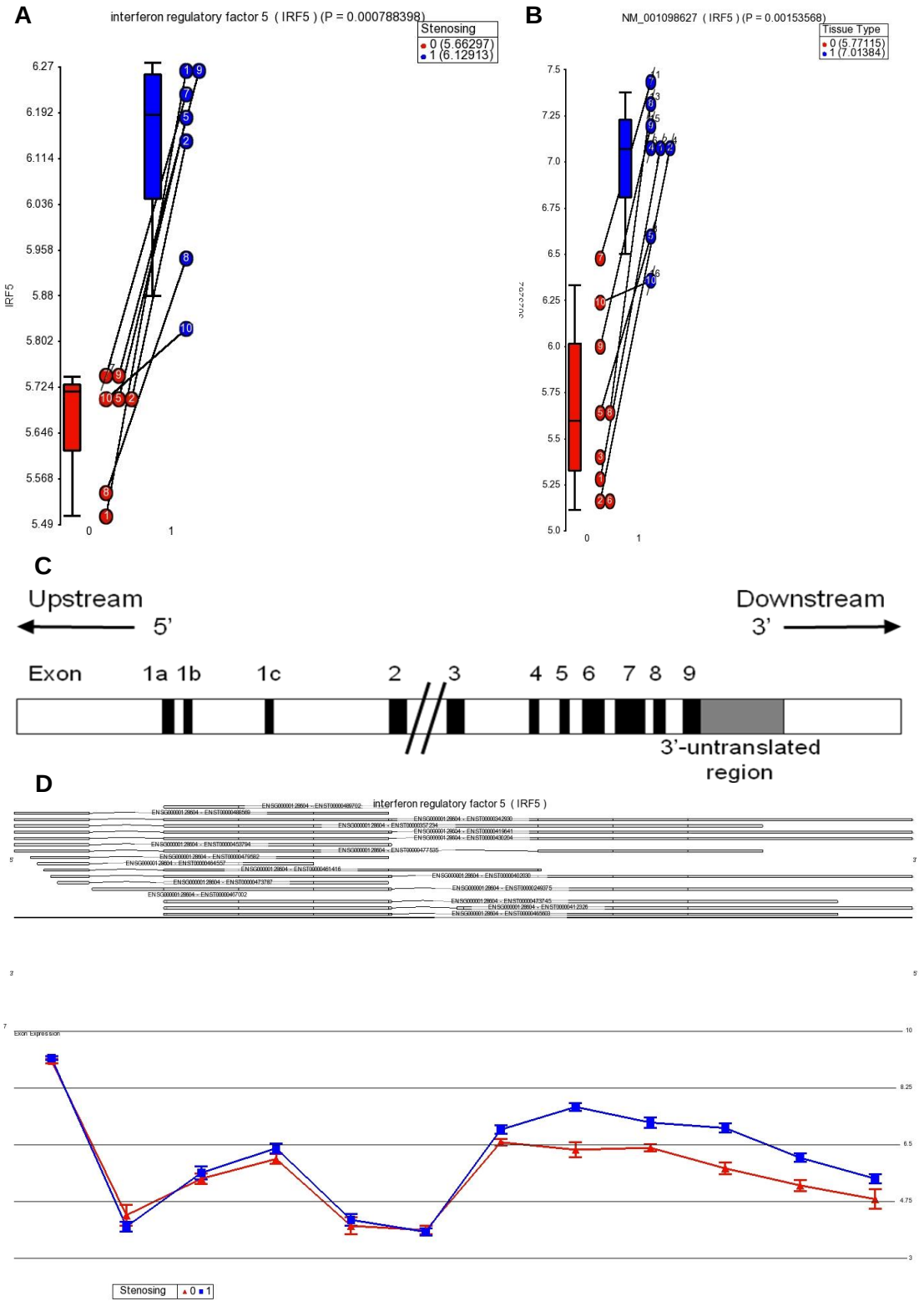


Figure 56 Differential expression and splicing of interferon regulatory factor 5 (IRF5) comparing stenosing atherosclerosis and intimal thickening

A. Interferon regulatory factor 5 (IRF5) expression is significantly higher in stenosing plaque (SP, blue) compared with intimal thickening (IT, red) (paired T-test, p = 0.0008). B. IRF5 was seen to be differentially spliced in SP (blue) compared with IT (red) (paired T-test, p =

0.0015). C. The IRF5 gene organisation. Its location is on chromosome 7q32. Modified from (Cunninghame Graham et al. 2007; Malarstig et al. 2008). D. In the core probe set, 12 probes are allocated to IRF5. Comparing SP (blue) with IT (red), there appears to be no difference as regards exon splicing of the 5' end of the IRF5 gene, whilst difference in splicing is seen to be located on the 3' end, with a consistent difference in all five of the 3' end probes.

6.4.3 Stable and Unstable Atherosclerosis

A clear separation on PCA was also observed between the stable and unstable atherosclerosis (Figure 57).

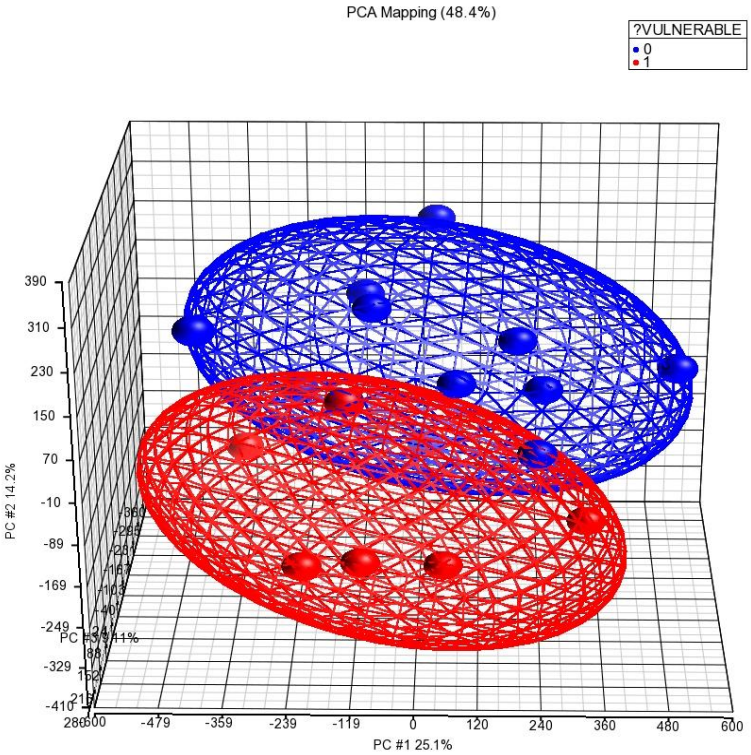


Figure 57 Separation of stable and unstable atherosclerosis on 3-dimensional principal components analysis

Clustering of unstable atherosclerosis (defined as stenosing plaque from symptomatic patients; red, 0) and stable atherosclerosis (defined as all areas of intimal thickening, or stenosing plaque from asymptomatic patients; blue, 1) tissue transcriptomic data was seen, with a good separation observed between the two groups. Ellipsoids represent 2 standard deviations.

6.5 TRANSCRIPTOMICS DISCUSSION

Based upon the 'core' probe set analysis, transcriptional profiling analysis hierarchical clustering, and two- and three-dimensional PCA were able to demonstrate good clustering of intimal thickening and stenosing plaque samples, with a clear separation between these two tissue types. Furthermore, when samples were separated based on stable and unstable atherosclerosis, clustering and separation was again observed. This highlights the utility of transcriptomics coupled to unsupervised statistical analysis to separate samples in accordance with biologically and clinically relevant parameters.

A difference in both expression and splicing of IRF5 in the context of advanced atherosclerosis may contribute to the explanation for why there is an increase in inflammatory cytokines in advanced atherosclerosis (Sections 1.5 and 4). This finding remains to be validated using probes specific for the different gene isoforms. It is further worth investigating whether the 3' end of the IRF5 gene has known (or yet to be discovered) functional domains. This finding may be a step towards completing the picture which sees pattern recognition receptor activation resulting in pro-inflammatory cytokine production (Watters et al. 2007; Kawai and Akira 2010) (Figure 58). This systems biology approach, generally regarded as non-hypothesis driven, has been powerful in the generation of hypotheses to be further addressed experimentally.

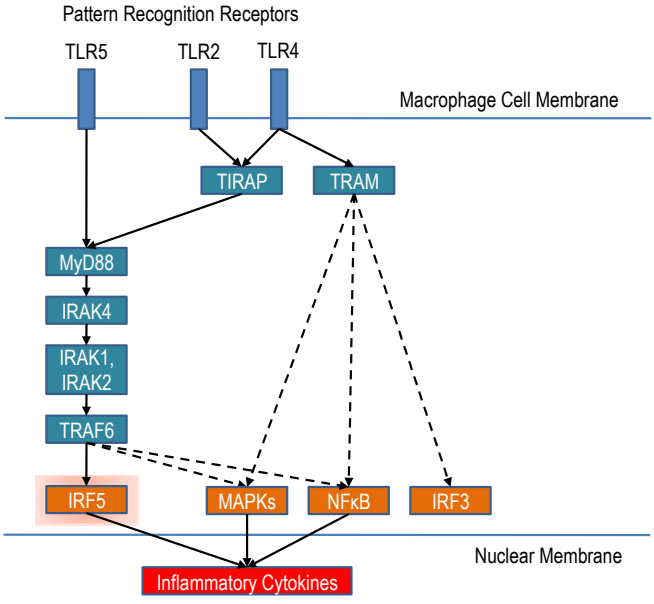


Figure 58 Interferon regulatory factor 5 in the pattern recognition receptor pathway

Interferon regulatory factor 5 (IRF5) in the pattern recognition receptor pathway (PRR). IRF5 is a nuclear transcription factor signalling downstream of PRRs, including Toll-like

receptors (TLRs) 2, 4 and 5 (Modified from (Watters et al. 2007; Kawai and Akira 2010)). IRF5 promotes the transcription of inflammatory cytokines and has recently been implicated in the M1 polarisation of human macrophages in vitro *(Krausgruber et al. 2011). IRAK, interleukin 1 receptor-associated kinase; MAPK, mitogen-activated protein kinase; MyD88, myeloid differentiation primary response gene 88; NFκB, nuclear factor κB; TIRAP, Toll-interleukin 1 receptor domain containing adaptor protein; TRAF, tumour necrosis factor receptor associated factor; TRAM, TRIF related adaptor molecule.*

Furthermore, this finding concurs with the recent publication from the Kennedy Institute at Imperial College London that IRF5 promotes the transcription of inflammatory cytokines and has recently been implicated in Th1 and Th17 responses, and M1 polarisation of human macrophages *in vitro* (Krausgruber et al. 2011).

IRF5 has been intimately implicated in TLR signalling, with a target gene profile including the cytokines and chemokines IL6, CCL2 and CCL5 (Kozyrev and Alarcon-Riquelme 2007) which were seen to be upregulated in advanced atherosclerosis in Chapter 4. Several single nucleotide polymorphisms (SNPs) of IRF5 have been found to be associated with systemic lupus erythematosus (SLE) (Sigurdsson et al. 2005; Graham et al. 2006; Cunninghame Graham et al. 2007; Malarstig et al. 2008). In the context of SLE, SNPs have been shown to be responsible for IRF5 transcript variants with differences at both the 5'(Graham et al. 2006; Graham et al. 2007) and 3' (Cunninghame Graham et al. 2007) ends.

A study has compared IRF5 gene expression in 99 carotid endarterectomy specimens obtained from the Biobank of Karolinska Endarterectomies (BIKE) – with or without macroscopic signs of plaque rupture and superimposed thrombus – with eight control iliac artery samples from organ donors without macroscopic or microscopic signs of atherosclerosis (Malarstig et al. 2008). IRF5 mRNA expression was significantly increased in atherosclerotic compared with control tissue, however it is noted that in this study intimal disease was compared with control artery comprising intima, media and adventitia. Furthermore, the location within the plaque where the tissue was sampled for mRNA extraction is not declared. In this study, modification of IRF5 expression is explained by gene SNPs (Malarstig et al. 2008), a factor which does not explain the differential expression seen in this thesis chapter as samples were paired from the same individual.

Four distinct alternative spliced IRF5 isoforms have been identified in human primary plasmacytoid dendritic cells, with and additional two in human primary peripheral blood mononuclear cells (Mancl et al. 2005). Three of these isoforms have distinct insertion/deletion

patterns in exon 6 at the 3' end (Mancl et al. 2005). This study of human mononuclear cells of the innate immune system revealed distinct cell type-specific expression and dissimilar functions in interferon induction of the spliced isoforms (Mancl et al. 2005).

In the future it will be increasingly important to collate transcriptomic data from multiple studies in order to improve data sets and to make them freely available (Bijnens et al. 2006). The ultimate aim would be the identification of classification gene sets which would offer insight into the potential diagnostic and therapeutic strategies in atherosclerotic disease (Tabibiazar et al. 2005).

6.6 PROTEOMICS

The proteome is defined as all proteins expressed in a cell, tissue or organism (Bagnato et al. 2007). Proteomics, the analysis of a proteome, can detect proteins that are associated with a disease by measuring their levels of expression between control and disease states (You et al. 2003). Two dimensional electrophoresis (2DE) combined with protein identification by mass spectrometry allows for the analysis of hundreds to thousands of proteins at a time, including post-translational modifications (Martinez-Pinna et al. 2010). Proteomic studies have been carried out on both human artery carotid plaques and on atherosclerotic plasma samples (Martinez-Pinna et al. 2010). A recent review has looked into the proteomics of atherosclerosis (Didangelos et al. 2009). This included two relevant studies where proteomics was undertaken on human carotid atherosclerosis. Martin-Ventura *et al.* looked at 25 CEA specimens, comparing these to 36 control endarteries (Martin-Ventura et al. 2004). The endartery segments were used to condition protein-free medium, which was subsequently separated by 2-dimensional electrophoresis (DE) and subject to matrix-assisted laser desorption/ionisation- time of flight (MALDI-TOF) mass spectrometry. The main finding of this study was that heat shock protein (HSP)-27 secretion was significantly less in carotid atherosclerosis, and was barely detectable in the secretome of complicated plaques (determined histologically by the presence of rupture, intra-plaque haemorrhage and an important proportion of inflammatory cells).

You *et al.* took a proteomic approach to coronary atherosclerosis in ten diseased and seven normal individuals (You et al. 2003). 2D electrophoresis plates were directly visualised to compare diseased and normal specimens. Protein sequencing using mass spectrometry was performed on a protein spot which was shown to have higher levels of expression in the diseased sample. Proteomics identified that ferritin light chain was increased by 1.9 fold in

coronary artery disease. The mRNA expression level of ferritin light chain was investigated using PCR, but ferritin light chain was increased to a lesser extent than protein, highlighting the discrepancy often seen between mRNA and protein differences of the same analyte.

Lepedda *et al.* compared 19 histologically stable with 29 histologically unstable carotid plaques (Lepedda et al. 2009). Their criteria for plaque instability included the presence of a thin or fissured fibrous cap covering a foamy or necrotic core, and the presence of overt haemorrhage, ulceration or thrombosis. The CEA specimens were finely minced and extracted proteins were separated by 2DE, revealing 57 distinct spots representing 33 different proteins. MALDI-TOF MS. Compared to the stable plaques, unstable ones showed reduced abundance of the protective enzymes superoxide dismutase (SOD)-3, glutathione S-transferase (GST), HSP27, HSP20, annexin A10 and Rho guanosine 5'-diphosphate dissociation inhibitor (GDI).

Our group has undertaken proteomic analysis of smooth muscle cells (SMCs), which are key players in atherosclerosis (Full 2010). Carotid endarterectomies were collected from ten consenting patients (six symptomatic, four asymptomatic) and enzymatically digested as described in Section 4.4.1. SMCs were isolated from the resultant mixed cell population by negative selection using immunomagnetic beads (magnetic cell sorting, MACS, Miltenyi Biotech Ltd, Surrey, UK). Commercially available aortic medial SMCs from six healthy donors were purchased (Promocell, Heidelberg, Germany) as a non-diseased comparator. The cells were consistently used at passage number three. 2DE with digital image analysis (SameSpots, Non-linear Dynamics) and tandem mass spectrometry was used to detect changes in the proteome of atherosclerotic SMC. 2D gel image analysis revealed 29 proteins with a statistically significant difference in expression between medial and plaque SMC ($P<0.05$). Plaque SMC had decreased levels of mitochondrial protein ATP synthase subunit-beta but an increase in the oxidised form of peroxiredoxin-4, suggesting decreased mitochondrial function, possibly due to oxidative stress. Furthermore, differences in protein expression between SMC from symptomatic and asymptomatic patients were also found. Plaque SMC from symptomatic patients exhibited decreased levels of the anti-inflammatory protein Annexin I ($P<0.05$), compatible with pro-inflammatory behaviour. This data demonstrates that plaque-derived SMC are exposed to higher levels of oxidative stress compared to control SMC. Differences between SMC from symptomatic and asymptomatic patients appear to reflect pro-inflammatory changes associated with plaque instability.

Early proteomic studies in atherosclerosis failed to identify inflammatory cytokines which are involved in plaque inflammation raising the possibility that the extraction technique was poor

at identifying components which existed at low levels (Bagnato et al. 2007). Extraction of protein in samples and enriching for low abundant analytes (depleting potentially 'masking' high abundant entities such as albumin and haemoglobin) has previously been undertaken effectively in proteomics of aortic aneurysm tissue (Didangelos et al. 2010). Three human aortic samples were prepared with a phosphatase inhibitor mixture to inhibit proteinase activity and 25mM EDTA to inhibit metalloproteinases. Biochemical subfractionation comprised decellularisation to enrich scarce extracellular proteins, solubilisation and deglycosylation of extracellular membrane proteins and relative estimation of protein abundance before proteomic analysis. One dimensional electrophoresis was performed. Gel bands were excised in identical parallel positions across the lanes enabling each portion to be analysed separately by mass spectrometry (Didangelos et al. 2010). This is pertinent to atherosclerosis research, where the level of complexity is high, as individual components can be analysed separately and low level components can be unmasked. Proteomic and metabonomic studies in human atherosclerosis are summarised in Table 25.

Study Reference	Methodology	Sample Technique	Results	Analytes of Interest
(Chen et al. 2010)	Plasma metabonomics for biomarkers of atherosclerosis	Plasma from 16 subjects with stable atherosclerosis and 28 normal subjects	Development of atherosclerosis directly perturbed fatty acid metabolism	Palmitate was proposed as a phenotypic biomarker for the diagnosis of atherosclerosis
(Mayr et al. 2009)	Proteomics, metabonomics and immunomics on human atherosclerotic plaques	Human carotid atherosclerotic plaques from live subjects	Immunoglobilins are present within micro-particles derived from plaque macrophages	Anti-A antibodies (IgG, IgA, IgE), anti-carbohydrate antibodies and antibodies to oxidised LDL detected in plaques
(Bagnato et al. 2007)	Proteomics of human coronary atherosclerotic plaques	35 archival coronary vessels from 28 explanted hearts. Artery and plaque analysed separately	Distinct expression of 806 proteins. Selected 4 sub-groups for further analysis: extracellular; lipid binding; inflammatory; and apoptotic-cell	Periostin (cell migration), PEDF (expressed when cells are exposed to oxidised LDL), MFG-E8 (phagocytosis ligand), annexin1 (expressed by macrophages of foam cell phenotype, linked to apoptosis and phagocytosis)
(You et al. 2003)	Proteomics of coronary atherosclerosis	10 diseased and 7 normal coronary arteries from explanted hearts	Increased expression of ferritin light chain	May contribute to coronary artery disease by modulating oxidation of lipids within the vessel wall through generation of reactive oxygen species

Table 25 Summary of proteomic and metabolite profiling studies in human atherosclerosis

Ig, immunoglobulin; LDL, low density lipoprotein; MFG-E8, milk fat globule epidermal growth factor 8; PEDF, Pigment epithelium-derived factor.

6.7 PROTEOMICS METHODOLOGY

6.7.1 Study Design

Formal ethical approval (08/H0706/129) was obtained and all patients gave written fully informed consent for their participation in the study. This study design attempts to account for

biological heterogeneity in human samples: half the patients were male (n=6) and half female (n=6); half were symptomatic (n=6) and half asymptomatic (n=6) (Table 26). With regards to symptoms, only formal strokes were considered, defined as focal neurological events lasting for more than 24 hours pertaining to the anterior circulation of the cerebral hemisphere ipsilateral to the index carotid stenosis. As such transient ischaemic attack and amaurosis fugax were excluded, as were patients with atrial fibrillation from the symptomatic group where atrial thromboembolism may be a source of misdiagnosis.

Symptoms	Age (years)	Gender	Diabetes mellitus	Chronic obstructive pulmonary disease	Hypertension	Renal impairment	B-blockers	Aspirin	Angiotensin converting enzyme inhibitors	Statins
0	62	Male	1	0	1	0	0	1	1	1
0	70	Male	0	0	1	0	0	1	1	1
0	71	Male	0	0	1	0	0	1	1	1
0	80	Female	0	0	1	0	0	1	1	1
0	65	Female	0	1	1	0	0	1	0	1
0	69	Female	1	0	1	0	0	1	1	1
1	71	Male	0	0	1	0	0	1	1	0
1	76	Male	1	0	1	0	0	1	1	1
1	71	Male	0	0	1	1	0	1	1	1
1	84	Female	0	0	1	0	0	1	1	1
1	78	Female	0	0	1	0	0	1	1	0
1	71	Female	0	0	1	0	0	1	1	1

Table 26 Clinical characteristics of symptomatic and asymptomatic patients

6.7.2 Approach to Extraction for Proteomic Analysis

The proteomic studies described have used whole tissue (Martin-Ventura et al. 2004; Lepedda et al. 2009) or whole cell lysates, which are complex and rich in cellular proteins. These mask less abundant proteins, including proteins in the extracellular matrix (ECM), thus to date the vascular ECM and associated proteins are poorly defined. A novel approach to protein extraction has recently been described and employed in the context of human aortic tissue (Didangelos et al. 2010). This involves the sequential exposure of tissue to three solvents which extract protein from different tissue compartments. The initial salt extraction releases proteins and peptides bound loosely to ECM. The sodium dodecyl sulphate (SDS) step extracts cellular components. The use of guanidine at a low pH as been shown to solubilise vascular proteoglycans (Eisenstein et al. 1975). The salt extract holds particular interest as the proteins which are loosely bound to the ECM have the potential to contain putative biomarkers which may be translocated from the ECM compartment of the plaque into the arterial circulation.

6.7.3 Protein Extraction

Protein extraction was performed as previously described (Didangelos et al. 2010). Before extraction the tissue pieces were partially thawed and weighed. Approximately 150mg of tissue per plaque sample was immediately placed in ice-cold phosphate buffered saline (PBS) to remove frank blood and plasma contaminants. Commercially available protease and phosphatase inhibitor cocktails (Sigma-Aldrich) were included according to the manufacturer's instructions in order to inhibit broad-range proteinase activity. 25mM EDTA was added to ensure inhibition of metalloproteinases. While the tissue samples were immersed in the cold saline mixture, they were quickly diced with a scalpel into eight to ten smaller pieces. This was done to enhance:

- the initial removal of plasma contaminants; and
- the effective extraction of extracellular proteins.

The PBS mixture was changed a total of five times (approximately 30 mL total per sample). The diced samples were then incubated with 0.5 M NaCl, 10 mM Tris (pH 7.5), plus proteinase and phosphatase inhibitor cocktail and 25 mM EDTA. The volume of the buffer was adjusted to 10:1 of the tissue weight (*i.e.* 100 mg in 1 mL) and the samples were mildly vortexed for 4 hours at room temperature. The NaCl extracts were then desalted with centrifugation using desalting columns (Zeba Spin, Pierce Biotechnology). Following desalting the extracts were mixed with 100% acetone (5:1 volume ratio) at -20°C for 16 hours. Proteins were precipitated with centrifugation (16.000 x g for 45 minutes) and the pellets were dried and redissolved in deglycosylation buffer. Deglycosylation (removal of glycosaminoglycan side chains) of the salt extract was achieved in a 150 mM NaCl, 50 mM sodium acetate (pH 6.8) buffer supplemented with proteinase and phosphatase inhibitors and 10mM EDTA for 16 hours at 37°C. The deglycosylation enzymes (0.05 U) used (all purchased from Sigma-Aldrich) were:

- chondroitinase ABC from *Proteus vulgaris* (catalyzes the removal of polysaccharides containing 1→4-β-D-hexosaminyl and 1→3-β-D-glucuronosyl or 1→3-α-L iduronosyl linkages to disaccharides containing 4-deoxy-β-D-gluc-4-enuronosyl groups. It acts on chondroitin 4-sulfate, chondroitin 6-sulfate, and dermatan sulfate glycosaminoglycan side chains);
- keratanase from *Bacteroides fragillis* (cleaves internal 1→4-β-galactose linkages in unbranched, repeating poly-N-acetyl-lactosamine and keratan sulphate); and

- heparatinase II from *Flavobacterium heparinum* (cleaves heparan sulphate).

Following, deglycosylation the solutions were clarified again by centrifugation (16.000 x g for 10 minutes) in order to ensure that the samples were free of turbidity. Protein concentration was estimated by ultraviolet (UV) absorbance at 280 nm using extinction coefficient of 1.1 of 0.1% mg/mL solution calculated on the basis of the frequency of tyrosine and tryptophan which are the main UV absorbing amino acids at 280 nm in mammalian proteins (Zhuang et al. 2003).

6.7.4 Gelatinolytic Zymography

Gelatinolytic zymograms were used to detect the presence and activity of MMP2 and MMP9 in the 0.5 M NaCl extracts. Extract aliquots (20 μg of protein) were mixed with non-reducing sample buffer containing 100 mM Tris (pH 6.8) 40% glycerol, 0.2% SDS and 0.02% bromophenol blue and separated in 10% SDS-PAGE gels containing 0.5 mg/mL gelatin (Sigma-Aldrich). Pre-stained protein standards were run alongside the samples to allow molecular mass estimation of proteins (All Blue, Precision Plus, Bio-Rad Laboratories). To allow in-gel MMP activity, SDS was removed from the gels with three washes in a buffer containing 2% Triton X-100, 50 mM Tris (pH 7.4) and 200 mM NaCl for 45 minutes. Gels were then incubated for 16 hours to detect MMP9 or 36 hours to detect MMP2 at 37°C in a buffer containing 50mM Tris (pH 7.4), 200 mM NaCl and 10mM $CaCl_2$. Finally, gels were stained for 60 minutes with Coomassie Brilliant Blue (Sigma-Aldrich) and destained for 2 hours to visualise the MMPs.

6.7.5 Protein Gel Electrophoresis

The NaCl extracts were denatured and reduced in sample buffer containing 100 mM Tris (pH 6.8), 40% glycerol, 0.2% SDS, 2% beta-mercaptoethanol and 0.02% bromophenol blue, and boiled at 96°C for 10 minutes. 35 μg of protein per sample was loaded and separated on Bis-Tris discontinuous 4-12% polyacrylamide gradient gels (NuPage, Invitrogen). Pre-stained protein standards were run alongside the samples to allow molecular mass estimation of proteins (All Blue, Precision Plus, Bio-Rad Laboratories). Following electrophoresis, gels were silver stained (PlusOne Silver Staining Kit, GE Healthcare) (Figure 59). Silver staining was used to facilitate subsequent band excision to avoid cross-contamination with fainter gel bands, as Coomassie staining will preferably stain the abundant proteins hence fainter gel bands could be missed. The gel bands were excised in identical parallel positions across lanes and no "empty" gel pieces were left behind (Figure 60).

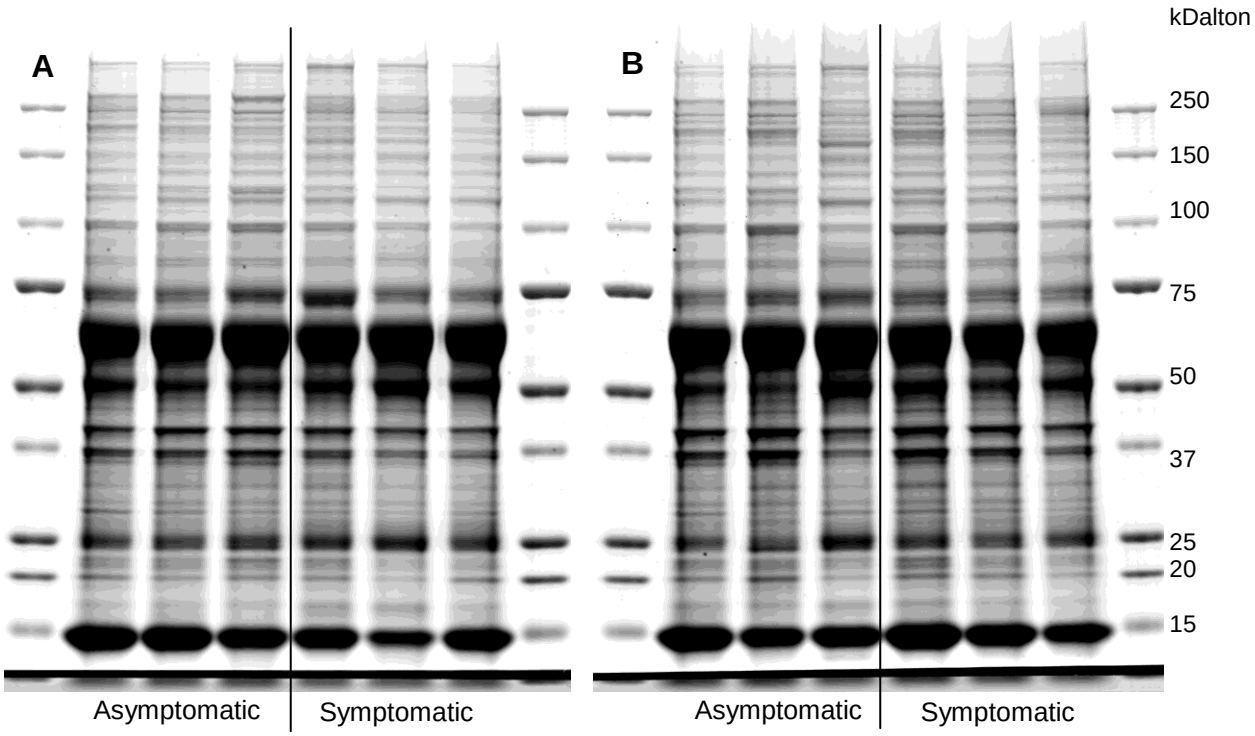


Figure 59 Salt extract protein gel electrophoresis

Salt extracts from carotid atherosclerotic plaques from male (A) and female (B) patients were separated on Bis-Tris discontinuous 4-12% polyacrylamide gradient gels (NuPage, Invitrogen) and silver stained.

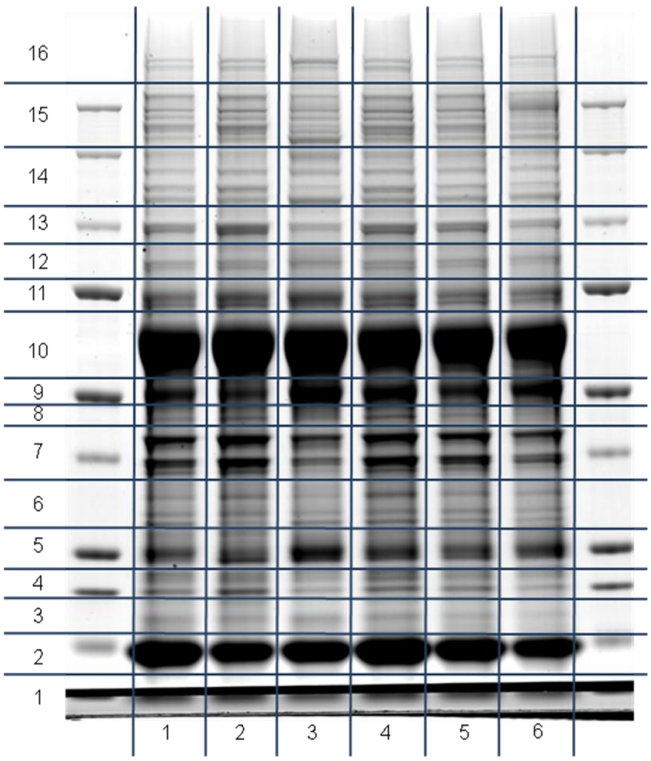


Figure 60 Salt extract protein gel band excision prior to trypsination

Each of the two proteins gels were fully sectioned into 96 pieces. The gel with separated salt extracts from female proteins is shown. Excision in identical parallel positions across lanes meant that no "empty" gel pieces were left behind.

6.7.6 Nanoflow Liquid Chromatography Tandem Mass Spectrometry

Subsequently, all gel bands were subjected to in-gel digestion with trypsin using an Investigator ProGest (Genomic Solutions) robotic digestion system. Tryptic peptides from the NaCl extract were separated on a nanoflow liquid chromatography (LC) system (Dionex UltiMate 3000, UK) and eluted with a 40 minute gradient (10-25% B in 35 minutes, 25-40% B in 5 minutes, 90% B in 10 minutes and 2% B in 30 minutes, where A = 2% acetonitrile [ACN], 0.1% formic acid in high performance liquid chromatography [HPLC] H_2O and B = 90% ACN, 0.1% formic acid in HPLC H_2O). The column (Dionex PepMap C18, 25 cm length, 75 μm internal diameter, 3 μm particle size) was coupled to a nanospray source (Picoview) using RePlay (Advion). After the direct LC-MS run, the flow was switched and the portion stored in the capillary of the RePlay device re-analyzed ('replay run') (Waanders et al. 2008). Spectra were collected from an ion-trap mass analyzer (LTQ Orbitrap XL, ThermoFisher Scientific) using full ion scan mode over the mass-to-charge (m/z) range 450-1600. Tandem mass spectrometry (MS/MS) was performed on the top six ions in each MS scan using the data-dependent acquisition mode with dynamic exclusion enabled. MS/MS

peaklists were generated by extract_msn.exe and matched to human database (UniProtKB/Swiss-Prot Release 14.6, 20333 protein entries) using SEQUEST v.28 (rev. 13), (Bioworks Browser 3.3.1 SP1, ThermoFisher Scientific) and X! Tandem (Version 2007.01.01.2). Carboxyamidomethylation of cysteine was chosen as fixed modification and oxidation of methionine as variable modification.

The mass tolerance was set at 1.5 atomic mass units (AMU) for the precursor ions and at 1.0 AMU for fragment ions. Two missed cleavages were allowed. Scaffold (version 2.0.5, Proteome Software Inc., Portland, OR) was used to calculate the spectral counts and to validate MS/MS based peptide and protein identifications (Keller et al. 2002; Nesvizhskii et al. 2003). According to the default values in the Scaffold software, the following peptide thresholds were applied: X! Tandem: -Log(Expect Scores) > 2.0, SEQUEST: deltaCn > 0.10 and XCorr > 2.5 (+2), 3.5 (+3) and 3.5 (+4). Peptide identifications were accepted if they could be established at greater than 95.0% probability as specified by the Peptide Prophet algorithm (Keller et al. 2002). Protein identifications were accepted if they could be established at greater than 99.0% probability (Nesvizhskii et al. 2003) with at least two independent peptides and a mass accuracy of ≤ 10 parts per million (ppm) of the precursor ion.

6.8 SALT EXTRACT PROTEOMICS RESULTS

There was a highly significant correlation between the number of assigned spectra in the first sample and the replay sample (linear regression, $r^2 = 0.9342$, $p < 0.0001$, Figure 61).

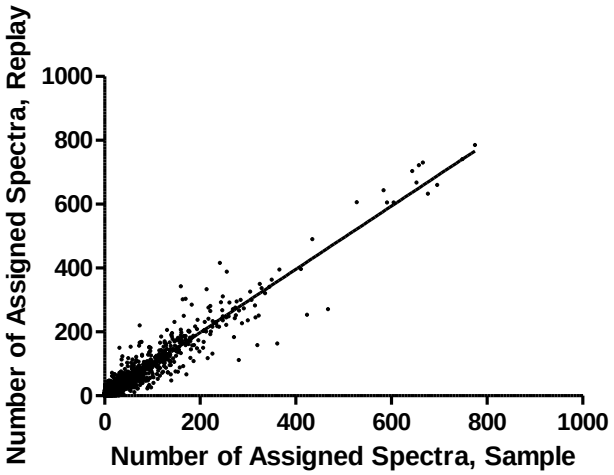


Figure 61 Comparison of assigned spectra in sample and replay of tandem mass spectrometry

Linear regression, $r^2 = 0.9342$, $p < 0.0001$.

Ion trap mass spectrometry of the atherosclerotic plaque salt extract identified 2,470 proteins. National Center for Biotechnology Information (NCBI) annotations were applied to all the proteins identified, and the proteins were categorised according to sub-categories of biological process, cellular compartment, and molecular function (Table 27).

Ontology Category	Process / Compartment / Function	Number of Indentified Proteins
Biological Process	Biological Adhesion	146
	Biological Regulation	937
	Cell Killing	8
	Cellular Process	1621
	Developmental Process	357
	Establishment of Localisation	370
	Growth	7
	Immune System Process	143
	Localisation	435
	Locomotion	42
	Metabolic Process	1028
	Multi-Organism Process	109
	Multi-Cellular Organismal Process	357
	Pigmentation	4
	Reproduction	44
	Reproductive Process	43
	Response to Stimulus	381
	Rhythmic Process	6
	Viral Reproduction	10
Cellular Compartment	Golgi Apparatus	106
	Cytoplasm	1099
	Cytoskeleton	296
	Endoplasmic Reticulum	78
	Endosome	40
	Extra-Cellular Region	352
	Intra-Cellular Organelle	1177
	Membrane	662
	Mitochondrion	89
	Nucleus	635
	Organelle Membrane	116
	Organelle Part	631
	Plasma Membrane	378
	Ribosome	43
Molecular Function	Anti-Oxidant Activity	21
	Auxilliary Transport Protein Activity	1
	Binding	1819
	Catalytic Activity	734
	Chemoattractant Activity	1
	Electron Carrier Activity	20
	Enzyme Regulator Activity	172
	Molecular Function	2005
	Molecular Transducer Activity	146
	Motor Activity	58
	Structural Molecule Activity	157
	Transcription Regulator Activity	124
	Translation Regulator Activity	33
	Transporter Activity	120

Table 27 Categorisation of the 2470 identified salt extract proteins

Categorisation is in accordance with National Center for Biotechnology Information (NCBI) annotation.

6.8.1 Analysis Based Upon Symptomatic Status

T-test revealed that the average number of spectra relating to 159 proteins were significantly different between symptomatic and asymptomatic atherosclerosis (Table 28). Principal components analysis revealed a clear separation of the samples based upon symptomatic status (Figure 62).

	Protein Name	Swiss-Prot Accession Name	Molecular Mass (kDa)	Unique Peptides (n)	Unique Spectra (n)	Coverage (%)	Average Spectra (n)		Average Spectra Asymptomatic versus Symptomatic	
							Asymptomatic	Symptomatic	T-Test P-Value	Fold Difference
Adhesion										
	Integrin beta-1	ITB1_HUMAN	75	1.8	1.8	3.8	5.7	2.0	0.0011	-2.8
Angiogenesis / Vasculogenesis										
	Thymidine phosphorylase	TYPH_HUMAN	51	1.6	1.6	3.9	2.0	3.7	0.018	1.8
*	Cysteine and glycine-rich protein 2	CSRP2_HUMAN	21	6.5	6.8	35.2	14.8	11.3	0.019	-1.3
*	Chloride intracellular channel protein 4	CLIC4_HUMAN	62	0.8	0.8	2.5	5.7	3.8	0.0075	-1.5
Binding										
	Fatty acid-binding protein, epidermal	FABP5_HUMAN	15	0.7	0.7	6.4	0.1	2.2	0.00037	26.0
*	Retinoblastoma-binding protein 6	RBBP6_HUMAN	81	0.6	0.6	1.1	0.3	1.1	0.022	3.3
*	Far upstream element-binding protein 2	FUBP2_HUMAN	20	1.6	1.6	10.4	0.5	1.0	0.048	2.0
*	Coronin-1A	COR1A_HUMAN	84	2.4	2.4	3.6	2.6	4.9	0.018	1.9
	Stress-70 protein, mitochondrial	GRP75_HUMAN	74	2.8	2.8	6.0	3.0	4.8	0.024	1.6
	Serotransferrin	TRFE_HUMAN	77	45.7	59.6	55.3	292.9	252.0	0.043	-1.2
	Vitamin D-binding protein	VTDB_HUMAN	68	0.7	0.7	1.8	22.0	18.5	0.018	-1.2
*	Phosphatidylethanolamine-binding protein 1	PEBP1_HUMAN	21	3.2	3.3	25.8	6.4	5.0	0.049	-1.3
	Insulin-like growth factor-binding protein 7	IBP7_HUMAN	42	4.9	6.5	14.9	17.3	13.4	0.033	-1.3
	Apolipoprotein D	APOD_HUMAN	76	0.5	0.5	0.7	9.4	6.8	0.037	-1.4
	Methyl-CpG-binding protein 2	MECP2_HUMAN	118	0.8	0.8	1.1	1.6	0.7	0.039	-2.4
*	Non-POU domain-containing octamer-binding protein	NONO_HUMAN	54	0.6	0.6	1.4	1.6	0.3	0.018	-6.3
Coagulation										
	Prothrombin	THRB_HUMAN	50	1.8	1.9	5.4	33.3	55.3	0.018	1.7
Collagen										
	Collagen alpha-1(XV) chain	COFA1_HUMAN	142	3.7	3.7	3.5	5.2	8.1	0.015	1.6
Cytoskeletal / Cytokinesis										
*	Dynein heavy chain 10, axonemal	DYH10_HUMAN	202	1.1	1.1	0.7	0.3	1.6	0.025	4.8
*	Neurofilament light polypeptide	NFL_HUMAN	29	2.4	2.4	13.3	0.9	2.5	0.0075	2.7
*	Cdc42-interacting protein 4	CIP4_HUMAN	53	7.0	9.4	18.6	0.7	1.8	0.018	2.6
	Keratin, type I cytoskeletal 18	K1C18_HUMAN	46	0.5	0.5	1.9	1.1	2.8	0.0063	2.6
	Radixin	RADI_HUMAN	51	2.7	2.7	6.3	0.2	0.4	0.024	2.5
*	T-complex protein 1 subunit eta	TCPH_HUMAN	124	3.0	3.0	3.5	0.6	1.3	0.017	2.3
*	Septin-9	SEPT9_HUMAN	124	2.8	2.8	2.9	0.9	1.8	0.013	2.0
	Vasodilator-stimulated phosphoprotein	VASP_HUMAN	42	1.0	1.0	3.5	1.1	1.9	0.031	1.8
*	Keratin, type II cytoskeletal 2 epidermal	K22E_HUMAN	65	2.7	2.8	5.5	3.2	5.5	0.035	1.7
*	Rootletin	CROCC_HUMAN	229	0.7	0.7	0.4	0.6	1.0	0.029	1.7
	Ezrin	EZRI_HUMAN	69	1.3	1.3	2.9	1.7	2.6	0.017	1.6
*	ADP-ribosylation factor 6	ARF6_HUMAN	83	0.9	0.9	1.4	2.3	3.3	0.048	1.5

	Protein Name	Swiss-Prot Accession Name	Molecular Mass (kDa)	Unique Peptides (n)	Unique Spectra (n)	Coverage (%)	Average Spectra (n)		Average Spectra Asymptomatic versus Symptomatic	
							Asymptomatic	Symptomatic	T-Test P-Value	Fold Difference
*	Actin-related protein 2/3 complex subunit 1B	ARC1B_HUMAN	73	0.6	0.6	1.3	5.0	7.2	0.048	1.4
	Moesin	MOES_HUMAN	13	0.9	1.1	9.5	25.8	30.4	0.0026	1.2
*	Talin-1	TLN1_HUMAN	47	11.3	13.5	33.9	154.3	124.5	0.027	-1.2
*	Actin, alpha cardiac muscle 1	ACTC_HUMAN	29	6.3	7.8	29.3	27.1	20.8	0.033	-1.3
	Calponin-1	CNN1_HUMAN	227	19.3	20.8	11.7	39.9	28.2	0.0074	-1.4
*	Spectrin alpha chain, brain	SPTA2_HUMAN	285	14.6	14.8	6.9	28.3	17.3	0.045	-1.6
*	Fermitin family homolog 2	FERM2_HUMAN	38	0.4	0.4	1.6	6.3	3.8	0.032	-1.7
	Myosin-11	MYH11_HUMAN	33	7.4	7.6	28.0	43.8	26.5	0.0074	-1.7
*	T-complex protein 1 subunit theta	TCPQ_HUMAN	19	0.7	0.7	3.6	4.9	2.9	0.017	-1.7
*	Spectrin beta chain, brain 1	SPTB2_HUMAN	275	10.2	10.4	5.2	19.8	11.2	0.016	-1.8
*	Microtubule-associated protein 1B	MAP1B_HUMAN	271	4.8	4.8	2.5	11.3	6.3	0.047	-1.8
	Myosin-10	MYH10_HUMAN	51	1.4	1.4	4.1	26.4	13.8	0.013	-1.9
*	Actin, gamma-enteric smooth muscle	ACTH_HUMAN	31	0.6	0.6	2.8	1.4	0.7	0.03	-2.1
*	Vinexin	VINEX_HUMAN	88	2.6	2.6	3.8	4.2	1.9	0.0011	-2.2
*	Annexin A11	ANX11_HUMAN	54	1.6	1.6	4.2	3.1	1.3	0.021	-2.3
*	Peptidyl-prolyl cis-trans isomerase H	PPIH_HUMAN	59	0.7	0.7	1.8	1.8	0.8	0.017	-2.3
*	Talin-2	TLN2_HUMAN	272	0.5	0.5	0.3	0.8	0.3	0.0014	-2.5
*	Dynein heavy chain 11, axonemal	DYH11_HUMAN	521	0.4	0.4	0.1	0.7	0.3	0.048	-2.7
*	Synaptopodin-2	SYNP2_HUMAN	52	0.6	0.6	2.0	1.4	0.5	0.039	-2.8
	Filamin-C	FLNC_HUMAN	291	3.3	3.3	1.9	6.8	2.3	0.00058	-2.9
	Sorbin and SH3 domain-containing protein 1	SRBS1_HUMAN	143	2.2	2.2	2.0	5.3	1.8	0.0079	-3.0
	Alpha-adducin	ADDA_HUMAN	202	0.6	0.6	0.5	1.4	0.4	0.022	-3.4
DNA Processing / Repair										
*	Dihydropyrimidine dehydrogenase [NADP+]	DPYD_HUMAN	111	0.6	0.6	0.8	0.1	1.8	0.0062	22.0
*	Replication factor C subunit 5	RFC5_HUMAN	34	0.9	0.9	3.6	0.3	0.9	0.012	2.8
*	ATP-dependent DNA helicase Q1	RECQ1_HUMAN	73	0.7	0.7	1.3	1.4	0.8	0.048	-1.9
	High mobility group protein B2	HMGB2_HUMAN	24	1.1	1.3	7.8	2.8	1.3	0.01	-2.2
*	Fanconi anemia group B protein	FANCB_HUMAN	98	0.4	0.4	0.7	1.1	0.1	0.044	-13.0
Energy Metabolism										
*	Hexokinase-3	HXK3_HUMAN	99	0.5	0.5	0.8	0.0	1.3	0.042	-
*	6-phosphofructokinase, liver type	K6PL_HUMAN	85	0.8	0.8	1.4	0.6	1.7	0.0036	2.9
*	UTP--glucose-1-phosphate uridylyltransferase	UGPA_HUMAN	57	1.2	1.2	3.0	0.8	2.1	0.036	2.5
*	ADP-ribosylation factor 1	ARF1_HUMAN (+1)	21	1.7	1.7	11.6	2.6	4.6	0.00045	1.8
*	L-lactate dehydrogenase A chain	LDHA_HUMAN	37	6.3	6.7	21.4	9.8	12.8	0.0061	1.3
*	ATP synthase subunit beta, mitochondrial	ATPB_HUMAN	57	4.5	4.8	11.0	8.7	5.9	0.033	-1.5
Enzyme / Enzyme Regulator										

	Protein Name	Swiss-Prot Accession Name	Molecular Mass (kDa)	Unique Peptides (n)	Unique Spectra (n)	Coverage (%)	Average Spectra (n)		Average Spectra Asymptomatic versus Symptomatic	
							Asymptomatic	Symptomatic	T-Test P-Value	Fold Difference
*	Aldose 1-epimerase	GALM_HUMAN	78	3.1	3.2	5.5	0.2	0.8	0.032	4.5
*	Mitogen-activated protein kinase 13	MK13_HUMAN	42	0.5	0.5	1.2	0.4	1.6	0.032	3.8
*	CMP-N-acetylneuraminate-poly-alpha-2,8-sialyltransferase	SIA8D_HUMAN	629	32.8	32.8	7.5	0.3	0.9	0.04	3.7
	Myeloperoxidase	PERM_HUMAN	70	12.8	13.7	26.7	2.2	6.8	0.018	3.2
*	N-acetyl-D-glucosamine kinase	NAGK_HUMAN	76	2.3	2.4	4.3	1.1	3.3	0.0024	3.1
*	Phospholipase DDHD2	DDHD2_HUMAN	14	4.9	5.1	43.3	0.4	1.1	0.015	2.6
	Matrix metalloproteinase-9	MMP9_HUMAN	229	10.8	10.8	7.0	2.7	6.8	0.013	2.6
*	Leukocyte elastase inhibitor	ILEU_HUMAN	36	3.6	5.4	15.5	2.9	4.3	0.046	1.5
	Calpain-1 catalytic subunit	CAN1_HUMAN	82	3.9	4.0	4.9	5.9	8.2	0.04	1.4
	Triosephosphate isomerase	TPIS_HUMAN	633	1.5	1.5	0.5	23.8	28.9	0.0089	1.2
	Alpha-enolase	ENOA_HUMAN	270	42.8	50.4	22.1	36.0	42.2	0.027	1.2
	Purine nucleoside phosphorylase	PNPH_HUMAN	18	1.0	1.0	7.9	6.6	5.3	0.028	-1.2
*	UDP-glucose:glycoprotein glucosyltransferase 1	UGGG1_HUMAN	47	1.0	1.0	3.1	1.3	0.8	0.036	-1.7
*	cAMP-dependent protein kinase type I-alpha regulatory subunit	KAP0_HUMAN	43	1.5	1.7	4.4	3.0	1.8	0.023	-1.7
	Integrin-linked protein kinase	ILK_HUMAN	43	1.0	1.0	5.6	6.0	3.0	0.024	-2.0
*	NADH-cytochrome b5 reductase 3	NB5R3_HUMAN	38	0.5	0.5	4.0	1.4	0.7	0.012	-2.1
	Kallistatin	KAIN_HUMAN	49	2.0	2.0	5.5	4.2	1.8	0.011	-2.3
*	Probable 2-oxoglutarate dehydrogenase E1 component DHKTD1, mitochondrial	DHTK1_HUMAN	103	0.6	0.6	0.9	1.1	0.4	0.02	-2.6
*	Glutathione S-transferase Mu 3	GSTM3_HUMAN	27	2.7	2.8	13.9	6.3	2.3	0.0015	-2.8
	Ubiquitin carboxyl-terminal hydrolase isozyme L1	UCHL1_HUMAN	25	1.2	1.4	8.2	2.8	0.9	0.026	-3.1
*	Omega-amidase NIT2	NIT2_HUMAN	236	0.4	0.4	0.3	1.3	0.4	0.03	-3.2
*	Glutathione S-transferase Mu 2	GSTM2_HUMAN	26	0.5	0.5	2.1	1.3	0.3	0.046	-3.8
GDP / GTP Associated										
	Ras GTPase-activating-like protein IQGAP1	IQGA1_HUMAN	189	22.0	22.5	15.6	49.0	59.7	0.0029	1.2
*	Rab GDP dissociation inhibitor beta	GDIB_HUMAN	51	7.6	7.7	19.4	16.3	9.8	0.0044	-1.7
*	Rab GDP dissociation inhibitor alpha	GDIA_HUMAN	78	2.7	2.8	4.9	2.9	1.8	0.013	-1.7
*	Rho guanine nucleotide exchange factor 11	ARHGB_HUMAN	168	0.7	0.7	0.9	1.3	0.4	0.043	-3.0
Glycoprotein										
	Lactotransferrin	TRFL_HUMAN	78	5.5	5.9	9.3	3.3	17.7	0.0046	5.4
	Fibronectin	FINC_HUMAN	263	42.0	53.4	23.6	168.7	242.3	0.0084	1.4
	Serum amyloid P-component	SAMP_HUMAN	25	7.9	9.4	29.2	60.0	45.6	0.026	-1.3
	Beta-2-glycoprotein 1	APOH_HUMAN	38	8.1	9.3	31.6	22.9	13.6	0.000024	-1.7
*	Thrombospondin-3	TSP3_HUMAN	104	1.0	1.0	1.3	1.8	0.9	0.014	-2.0
Inflammation										

	Protein Name	Swiss-Prot Accession Name	Molecular Mass (kDa)	Unique Peptides (n)	Unique Spectra (n)	Coverage (%)	Average Spectra (n)		Average Spectra Asymptomatic versus Symptomatic	
							Asymptomatic	Symptomatic	T-Test P-Value	Fold Difference
*	Mannan-binding lectin serine protease 2	MASP2_HUMAN	192	13.7	14.3	9.3	0.2	0.9	0.037	5.5
	Osteopontin	OSTP_HUMAN	35	1.8	1.8	6.7	5.5	16.6	0.0093	3.0
*	L-amino-acid oxidase	OXLA_HUMAN	63	0.8	0.8	1.3	0.7	2.0	0.0048	3.0
	Protein S100-A9	S10A9_HUMAN	41	2.7	3.2	9.2	3.8	8.8	0.048	2.3
	Scavenger receptor cysteine-rich type 1 protein M130	C163A_HUMAN	125	1.4	1.4	1.6	1.3	2.9	0.0051	2.2
*	Ig kappa chain V-IV region (Fragment)	KV401_HUMAN (+1)	13	2.0	2.5	19.7	4.2	7.9	0.013	1.9
*	Smad nuclear-interacting protein 1	SNIP1_HUMAN	46	1.1	1.1	4.2	2.9	5.5	0.00091	1.9
	Suppressor of cytokine signaling 6	SOCS6_HUMAN	60	1.1	1.1	3.2	1.8	2.9	0.037	1.6
*	Ig kappa chain V-III region VG (Fragment)	KV309_HUMAN	13	2.7	2.7	24.0	5.4	7.8	0.0071	1.4
*	Ig kappa chain V-III region HAH	KV312_HUMAN	81	0.6	0.6	1.4	11.9	15.8	0.015	1.3
*	Ig gamma-3 chain C region	IGHG3_HUMAN	30	2.0	2.1	9.7	110.2	140.2	0.014	1.3
*	Ig gamma-2 chain C region	IGHG2_HUMAN	43	2.2	2.2	6.6	33.7	37.5	0.046	1.1
*	SAM domain and HD domain-containing protein 1	SAMH1_HUMAN	72	1.6	1.6	3.0	3.2	2.1	0.044	-1.5
Intracellular Trafficking										
*	Sorting nexin-6	SNX6_HUMAN	70	0.8	0.8	2.1	1.8	1.1	0.036	-1.7
	Early endosome antigen 1	EEA1_HUMAN	515	0.9	0.9	0.3	2.5	1.0	0.025	-2.5
*	Sorting nexin-2	SNX2_HUMAN	58	1.6	1.6	4.0	3.9	1.3	0.0046	-3.1
*	AP-3 complex subunit sigma-1	AP3S1_HUMAN	22	0.4	0.4	2.2	0.8	0.3	0.033	-3.3
Mitosis										
	Kinesin-like protein KIF15	KIF15_HUMAN	28	2.8	3.4	15.4	0.3	1.7	0.041	6.7
Neural Cell Differentiation / Migration										
*	Glia maturation factor beta	GMFB_HUMAN	21	3.1	3.2	18.1	1.1	1.8	0.037	1.6
*	Neuroblast differentiation-associated protein AHNAK	AHNK_HUMAN	41	0.4	0.4	1.4	94.8	68.3	0.04	-1.4
*	Neuron navigator 1	NAV1_HUMAN	162	1.4	1.4	1.4	6.0	3.7	0.025	-1.6
Other										
*	NKAP-like protein	NKAPL_HUMAN	48	1.5	1.5	3.7	0.2	1.1	0.0063	6.5
*	Ankyrin repeat domain-containing protein 12	ANR12_HUMAN	43	5.1	5.2	17.3	0.2	0.8	0.03	5.0
*	Niban-like protein 1	NIBL1_HUMAN	13	2.1	2.9	25.2	0.6	2.0	0.048	3.4
*	Neurocalcin-delta	NCALD_HUMAN	22	0.5	0.5	3.1	0.3	0.9	0.032	2.8
	Epididymal secretory protein E1	NPC2_HUMAN	17	1.3	1.3	11.5	1.6	3.3	0.021	2.1
*	Protein FAM49B	FA49B_HUMAN	70	9.7	11.1	17.7	1.8	3.6	0.039	2.0
*	Glyoxalase domain-containing protein 4	GLOD4_HUMAN	60	2.5	2.5	5.4	0.9	1.8	0.017	1.9
*	Importin-5	IPO5_HUMAN	35	0.9	0.9	4.0	3.2	4.8	0.017	1.5
	78 kDa glucose-regulated protein	GRP78_HUMAN	72	10.4	11.5	20.0	17.4	21.6	0.02	1.2

	Protein Name	Swiss-Prot Accession Name	Molecular Mass (kDa)	Unique Peptides (n)	Unique Spectra (n)	Coverage (%)	Average Spectra (n)		Average Spectra Asymptomatic versus Symptomatic	
							Asymptomatic	Symptomatic	T-Test P-Value	Fold Difference
	Clathrin heavy chain 1	CLH1_HUMAN	17	1.0	1.0	6.6	31.3	23.6	0.037	-1.3
	Heat shock 70 kDa protein 1	HSP71_HUMAN	37	1.6	1.7	5.6	28.8	21.2	0.039	-1.4
	Tetranectin	TETN_HUMAN	23	5.7	6.5	30.2	17.3	11.8	0.011	-1.5
*	Forkhead-associated domain-containing protein 1	FHAD1_HUMAN	162	1.1	1.1	1.2	4.0	2.5	0.023	-1.6
*	Tumor protein D54	TPD54_HUMAN	22	1.3	1.3	6.3	3.8	2.1	0.043	-1.8
*	Huntingtin-associated protein 1	HAP1_HUMAN	9	1.2	1.2	18.4	1.4	0.8	0.028	-1.9
*	Tetratricopeptide repeat protein 39A	TT39A_HUMAN	177	0.8	0.8	0.6	1.8	0.9	0.036	-2.0
*	Layilin	LAYN_HUMAN	69	0.3	0.3	0.5	2.3	1.1	0.024	-2.2
*	Secernin-1	SCRN1_HUMAN	46	1.0	1.0	3.3	2.3	0.7	0.0017	-3.4
*	Olfactomedin-like protein 1	OLFL1_HUMAN	46	0.8	0.8	1.8	2.5	0.6	0.0056	-4.3
*	Thioredoxin-like protein 1	TXNL1_HUMAN	32	0.4	0.4	2.5	0.8	0.2	0.037	-4.5
Platelet										
	CD9 antigen	CD9_HUMAN	25	0.6	0.6	2.6	1.3	0.3	0.023	-4.0
Prohormone										
	Angiotensinogen	ANGT_HUMAN	53	2.4	2.4	6.2	4.8	3.1	0.011	-1.6
Proteosomal										
*	Proteasome subunit alpha type-1	PSA1_HUMAN	41	11.5	14.4	33.4	1.9	3.4	0.014	1.8
*	Proteasome subunit beta type-5	PSB5_HUMAN	28	1.7	2.3	8.7	3.8	2.7	0.049	-1.4
*	26S protease regulatory subunit 7	PRS7_HUMAN	49	1.5	1.5	4.0	2.9	1.8	0.044	-1.7
*	Proteasome subunit beta type-4	PSB4_HUMAN	29	1.0	1.0	4.8	1.9	1.0	0.043	-1.9
Redox										
*	Uncharacterized protein KIAA0467	K0467_HUMAN	32	3.3	3.3	13.7	1.7	4.2	0.028	2.5
Signalling										
*	Mitogen-activated protein kinase 11	MK11_HUMAN	41	0.5	0.5	1.0	0.4	1.5	0.032	3.6
*	14-3-3 protein eta	1433F_HUMAN	28	4.1	4.1	19.8	9.2	7.3	0.043	-1.3
*	14-3-3 protein zeta/delta	1433Z_HUMAN	160	0.7	0.7	0.8	9.4	7.5	0.041	-1.3
*	14-3-3 protein theta	1433T_HUMAN	28	3.0	3.6	15.8	7.9	4.8	0.00003	-1.7
*	Sorbin and SH3 domain-containing protein 2	SRBS2_HUMAN	65	1.0	1.0	2.9	10.4	2.8	0.013	-3.7
*	Ras-related protein Rab-23	RAB23_HUMAN	27	0.5	0.5	2.2	1.3	0.1	0.046	-15.0
Transcription										
*	Midasin	MDN1_HUMAN	27	11.2	13.8	49.8	0.9	2.8	0.0089	3.0
*	40S ribosomal protein S20	RS20_HUMAN	68	12.8	14.8	20.3	0.8	2.1	0.0026	2.8
*	40S ribosomal protein S16	RS16_HUMAN	16	0.9	0.9	6.7	0.8	1.9	0.005	2.3
*	60S ribosomal protein L30	RL30_HUMAN	13	1.7	1.7	21.0	2.0	4.4	0.021	2.2
*	Heterogeneous nuclear ribonucleoprotein G	HNRPG_HUMAN	40	1.2	1.2	4.3	2.3	3.8	0.031	1.7
*	60S ribosomal protein L23a	RL23A_HUMAN	278	1.1	1.1	0.7	1.8	2.8	0.028	1.6
	Polymerase I and transcript release factor	PTRF_HUMAN	25	2.0	2.1	11.8	15.6	10.4	0.03	-1.5

	Protein Name	Swiss-Prot Accession Name	Molecular Mass (kDa)	Unique Peptides (n)	Unique Spectra (n)	Coverage (%)	Average Spectra (n)		Average Spectra Asymptomatic versus Symptomatic	
							Asymptomatic	Symptomatic	T-Test P-Value	Fold Difference
*	60S ribosomal protein L10a	RL10A_HUMAN	42	0.5	0.5	2.4	4.4	2.3	0.03	-2.0
*	40S ribosomal protein S21	RS21_HUMAN	76	0.8	0.8	1.5	2.3	1.1	0.028	-2.1
*	Splicing factor 3B subunit 3	SF3B3_HUMAN	136	0.6	0.6	0.6	1.1	0.4	0.02	-2.6
*	Splicing factor, proline- and glutamine-rich	SFPQ_HUMAN	37	1.5	1.5	5.5	5.5	1.9	0.0024	-2.9

Table 28 Indentified proteins whose abundance within salt extracts is significantly different between symptomatic and asymptomatic carotid atherosclerosis

*Proteins identified by proteomic analysis of salt extracts which are significantly different between asymptomatic (n=6) and symptomatic (n=6) carotid atherosclerotic plaques. Total spectra (based upon two technical replicates for each sample) are shown separately for each of the two groups, with the T-test P-value and the fold difference in total spectra. * Proteins identified for the first time by proteomics in the context of atherosclerosis or the carotid artery*

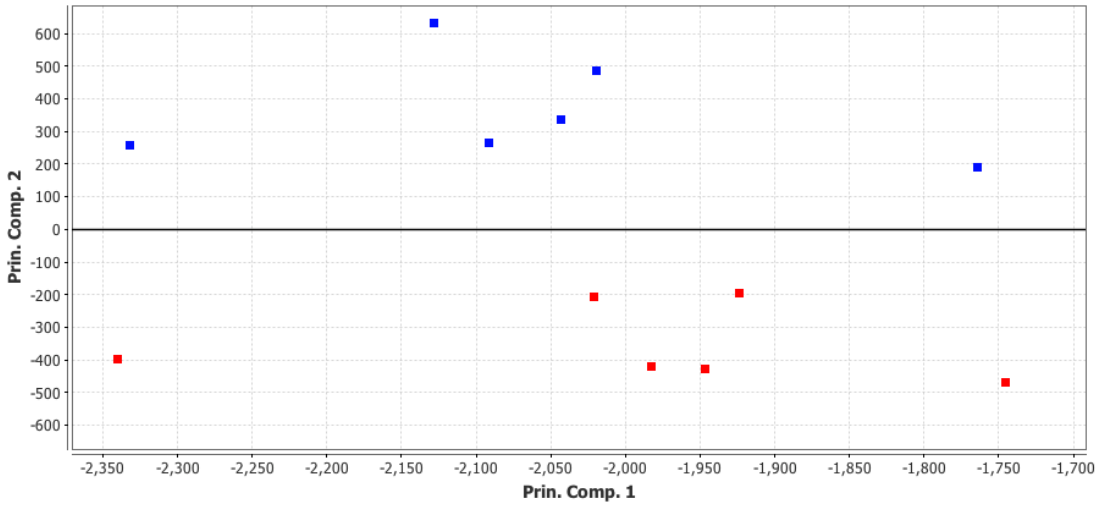


Figure 62 **Separation based on proteomic analysis of symptomatic and asymptomatic carotid atherosclerosis by 2-dimensional principal components analysis**

Excellent separation was observed between symptomatic (red) and asymptomatic (blue) samples in principal component (Prin. Comp.) 2.

6.8.2 Analysis Considering Gender

Analysing males and females separately, from the male carotid plaques there were 1,810 identified proteins of which 204 were significantly different in quantity considering symptomatic status In the female group 1,790 proteins were identified, with 90 significant differences Of the significant differences between symptomatic and asymptomatic in the gender sub-groups, only 11 proteins were significantly different in common in both male and female:

- 14-3-3 protein theta
- Apolipoprotein C-III
- Beta-2-glycoprotein 1
- Biliverdin reductase A
- Fatty acid-binding protein, epidermal
- Glutathione S-transferase Mu 3
- Latent-transforming growth factor beta-binding protein 2
- Neuron navigator 1
- Ras GTPase-activating-like protein IQGAP1
- Smad nuclear-interacting protein 1
- Sorting nexin-2

This prompted a comparison between females and males, at which point 332 significant differences were identified. Comparing asymptomatic males and females 221 differences emerged, and comparing symptomatic males and females 237 differences were seen.

6.8.3 Gelatinolytic Zymography Results and Validation

There was a significant difference in MMP9 activity between symptomatic and asymptomatic salt extracts (Figure 63A and B). This was also seen when comparing spectral counts between symptomatics and asymptomatics (Table 28). The significant correlation between MMP9 by zymography and tandem mass spectrometry (Figure 63C) serves to contribute to the validation of the dataset obtained through this proteomic analysis.

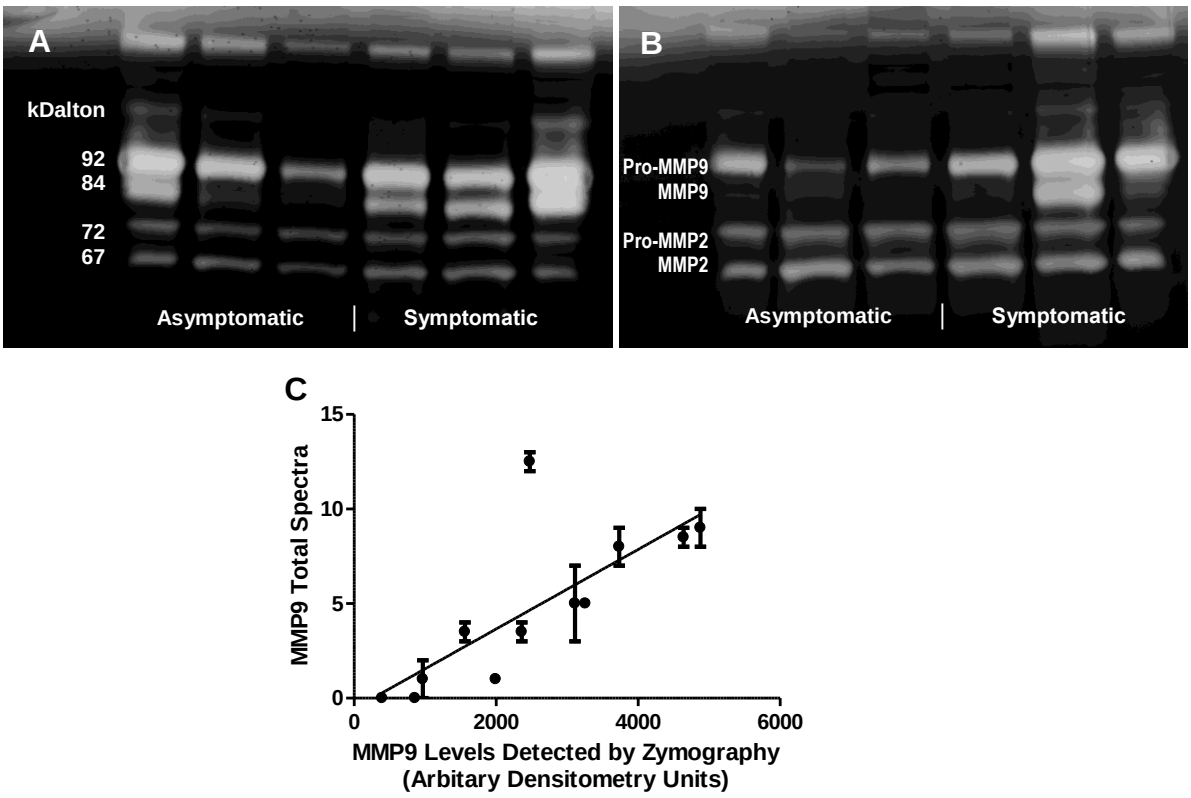


Figure 63 Salt extract gelatinolytic zymography – comparison with MMP9 spectra by tandem mass spectrometry

Total MMP9 levels by gelatine zymography (Males, A; Females, B), quantified by gel densitometry, significantly correlated with MMP9 spectral count as detected by tandem mass spectrometry (C; Linear regression, $r^2 = 0.5514$, $p < 0.0001$).

6.9 DISCUSSION

Proteomic analysis of the salt extract fraction from carotid atherosclerotic plaques identified 2,470 proteins implicated in 33 bio-molecular functions and having their origins previously

described in 14 different cellular compartments. There were 159 proteins which, based upon the number of assigned spectra, were significantly different between symptomatic and asymptomatic atherosclerosis. Of these, 8 did not feature in Pubmed, 119 had not been previously published in the context of "carotid", 112 not published in the context of "atherosclerosis", 132 not published in the context of "carotid AND atherosclerosis", and 108 not published in the context of "carotid OR atherosclerosis".

Osteopontin levels were significantly higher in the plaques from symptomatic compared with asymptomatic plaques in the salt extract. A recent study has confirmed that atherosclerotic plaques, in the carotid with validation in the femoral, are a source of biomarkers which make be predictive of future adverse cardiovascular events (de Kleijn et al. 2010). In particular, this large prospective study identified osteopontin by proteomics as a potential biomarker, subsequently confirming a hazard ratio of 3.8 in carotid plaques for the highest quartile compared with the lowest quartile for prediction of a composite cardiovascular endpoint. Epidermal fatty-acid binding protein (26-fold increased in symptomatic plaque salt extracts in this proteomic study) levels were found to be significantly higher in the plasma of patients with cardio-metabolic risk factors and also seen to be correlated with carotid intima-media thickness (Yeung et al. 2008; Yeung et al. 2009).

In addition to these two differentially abundant proteins which have previously been described in the context of atherosclerosis, a number of further novel 'candidate' proteins have been nominated as of potential interest. The glycolytic enzyme hexokinase 3 had no spectra detected in asymptomatic plaques, resulting in an 'infinite' fold change increase in symptomatic plaques. Mannan-binding lectin serine protease 2 showed a 5.5-fold increase in symptomatic atherosclerosis. This protein is known to have an important role in the activation of the compliment system via mannose-binding lectin. Mannan-binding lectin serine protease 2, after activation by auto-catalytic cleavage, cleaves C2 and C4 compliment pathway components leading to their activation and the subsequent formation of C3 convertase.

L-amino acid oxidase showed a 3-fold increase in symptomatic salt extracts. This protein is also known as interleukin 4 induced protein 1 and is considered to play an important role in lysosomal antigen processing and presentation. Smad nuclear-interacting protein 1 (SNIP1) was 1.9-fold higher in symptomatics than asymptomatics, and down-regulates NFκB signalling by competing with RELA for CREBBP/EP300 binding. SNIP1 has further been implicated in microRNA biogenesis, with microRNAs emerging as potentially important players in atherosclerosis development, progression and stability. SAM domain and HD domain-containing protein 1, which is also known as dendritic cell-derived IFNγ-induced

protein and monocyte protein 5, was 1.5-fold *decreased* in symptomatics It is a putative nuclease involved in the innate immune response by acting as a negative regulator of the cell-intrinsic antiviral response. Furthermore, it may play a role in mediating pro-inflammatory responses to TNFα signalling.

NKAP-like protein, for which little functional information exists, is 6.5-fold increased in symptomatic salt protein extracts. Mitogen-activated protein kinase (MAPK) 11 protein levels were 3.6-fold increased in symptomatic. Also known as MAPK p38β or stress-activated protein kinase 2, MAPK11 is implicated in a signal transduction pathway that is activated by changes in the osmolarity of the extracellular environment, by cytokines, or by environmental stress. Furthermore, it preferentially phosphorylates transcription factor ATF2. Monocyte / leukocyte elastase inhibitor, which is 1.5-fold increased in symptomatic, regulates the activity of the neutrophil proteases elastase, cathepsin G, proteinase-3, chymase, chymotrypsin, and kallikrein-3.

Of note, from the ten proteins highlighted in this discussion, two also featured in the list which was commonly differentially expressed when comparing symptomatic with asymptomatic extracts in the two gender groups: epidermal fatty-acid binding protein; and SNIP1.

6.9.1 Gender Differences in Protein Abundance

The difference between male and female atheromata supports the likely differences (biological heterogeneity) between male and female plaques, which also reflect the clinical differences. There are notable variations in the clinical behaviour of (particularly) asymptomatic plaques, with those in females considered by some as being more stable than those in males. This results in a higher number needed to treat (NNT) for significant asymptomatic female carotid stenosis (Halliday et al. 2004), which is reflected in the cost-per-quality-adjusted life year (QALY) for asymptomatic carotid endarterectomy being considerably more in young females (€311,133) than in young males (€34,557) (based on ACST data) (Henriksson et al. 2008). Gender medicine is an important and emerging field of study.

6.9.2 Limitations

Male and female samples were run on different gels. It is possible, although unlikely, that some of the differences seen between males and females could be attributed to them being run

on these different gels, and therefore analysed through the mass spectrometry process at slightly different times.

Luminex multi-analyte profiling (MAP) is more sensitive than mass spectrometry. This is evidenced by the lack of detection of a large number of analytes by mass spectrometry that were quantified by MAP. It is important at this point, however, to clarify the distinction that MAP of plaque cell culture supernatants detect *production* of proteins, *i.e.* the secretome (analogous in epidemiological terms to incidence of condition), whilst mass spectrometry of plaque tissue compartment fractions looks at the *presence* of protein at a particular timepoint (similar to prevalence).

6.10 LIPIDOMICS

According to the response-to-retention hypothesis, the binding of cholesterol containing lipoprotein particles to intimal proteoglycans is the central pathogenic process in atherogenesis (Williams and Tabas 1995). Once retained, lipoproteins are oxidised, accumulate in foam cells and provoke a cascade of immune-inflammatory processes, which drive the formation of atherosclerosis and ultimately define the propensity of the plaque to rupture. In most studies, the lipid content in plaques is visualised by oil red O staining. A more detailed characterisation, including the detection of single lipid species rather than lipid classes, may provide a better classification of atherosclerotic lesions with the goal of illuminating biology and discovering clinical biomarkers (Hu et al. 2009; Kim et al. 2010).

New mass spectrometry (MS) technologies allow the identification and quantification of hundreds of individual lipid species in complex biological samples and hold great promise to transform the profiling of atherosclerotic plaques (Gerszten and Wang 2008; Mayr 2008). For example, a recent study demonstrated that atherosclerotic lipids in murine lesions can be imaged by multiplex coherent anti-stokes Raman spectroscopy (Kim et al. 2010), however this method cannot identify individual lipid species. In another study (Manicke et al. 2009), desorption electrospray ionisation (DESI)-MS was used to image and identify 26 distinct lipid species in a single human plaque. However, a MS-based analysis comparing different human atherosclerotic lesions has not been reported to date.

To reveal a characteristic lipid signature for plaque vulnerability, the latest MS developments in lipidomics were harnessed to compare endarterectomy specimens from symptomatic and

asymptomatic patients, as well as stable and unstable areas within the same symptomatic lesion.

6.11 LIPIDOMICS METHODS

6.11.1 Clinical Samples

The study received Research Ethics Committee approval (08/H0706/129) and all patients gave their written informed consent. Carotid endarterectomy specimens were briefly rinsed with cold PBS to remove superficial blood, snap-frozen in liquid nitrogen and stored at -80°C. Eight carotid plaques from symptomatic patients were dissected into ruptured versus non-ruptured areas before freezing (Figure 64).

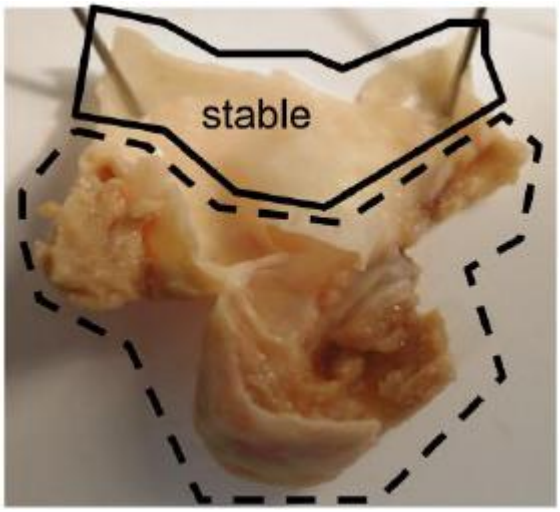


Figure 64 Macroscopic classification of unstable ruptured regions and stable areas within carotid plaques

Plaques from eight symptomatic patients were processed such that ruptured (lower dashed line region) were separated from areas of stable plaque or intimal thickening (upper solid line region).

6.11.2 Workflow Overview

Using QqQ-MS, two analyses were performed:

1. LESA, adapted for analysis of plaque lipids, allowed the direct extraction of molecules from tissue sections (Kertesz and Van Berkel 2010; Marshall et al. 2010); and
2. Shotgun lipidomics (Han and Gross 2003) was applied to endarterectomy tissue extracts.

The different scan options of a QqQ-MS can resolve isobaric lipids from different lipid subclasses and detect components, which would otherwise be masked by the presence of abundant lipid species. First a full MS scan in positive and negative ion mode was acquired. Then precursor ion (PI) and negative loss (NL) scans, characteristic for different lipid classes, unambiguously identify certain lipids by their characteristic MS/MS product ions.

6.11.3 Liquid Extraction Surface Analysis (LESA) Coupled to Nano-ESI-MS

A liquid extraction-based surface sampling device (Kertesz and Van Berkel 2010) was used to analyse lipids directly from tissue sections. Frozen human carotid plaque specimens were sectioned at 200 μm, without optimal cutting temperature (OCT) compound to avoid contamination with polyethylene glycol, using a rotary microtome (Microm HM560 cryostat, Thermo Scientific) and placed on electrostatically charged slides (Superfrost Plus, BDH), air dried for 15–30 min and analysed directly with a Advion TriVersa NanoMate system (Advion BioSciences Incorporated, Ithaca, NY) controlled by Chipsoft software (v8.1.0.928, Advion BioSciences) coupled to a triple quadrupole (QqQ)-MS (TSQ Vantage, Thermo Fisher Scientific, UK). The solvent extraction volume was 1.5 μL (chloroform/methanol/isopropanol 1:2:4 containing 7.5 mM ammonium acetate) and the dispensed volume was 1.0 μL. Solvents were sprayed through a 4.1-μm nozzle diameter chip (Advion BioSciences) at an ionisation voltage of 1.2 kV and a gas pressure of 0.3 psi. The first and third quadrupoles (mass resolution 0.7 Th) served as independent mass analysers while the second quadrupole was used as collision cell for tandem MS. The temperature of the ion transfer capillary was maintained at 150 °C. Full MS spectra and PI scans (argon was used as collision gas with a pressure of 1.0 mTorr) for cholesteryl esters (CEs) (PI 369.3) and phosphatidylcholine (PC) (PI 184.1) from different plaque sections were acquired over a period of 6 min.

6.11.4 Lipid Extraction

Lipids were extracted from endarterectomies specimens of greater than 25 mg wet weight using an adaptation of the Folch method (Folch et al. 1957). Tissue was pulverised with a pestle and mortar, or a ball-grinding method (Mikro Dismembrator, Sartorius). All subsequent steps were performed in glass vials that were thoroughly rinsed with water, methanol, and chloroform before use. 300 μL water (HPLC grade, Fisher Scientific), 2 mL methanol (HPLC grade, Fisher Scientific) and 4 mL chloroform (GLC-pesticide residue grade, Fisher Scientific) were added to each sample. The mixture was the vortexed for 10 min and centrifuged for 10 min at 3000 rpm. The supernatant was transferred, mixed with 1.2 mL water and vortexed for 10 min. After centrifugation at 1000 rpm for 5 min the lower organic phase was transferred into a new glass vial and 2 ml of chloroform/methanol/water (3:48:47)

was added. To extract any remaining lipids, the upper phase was washed with 2 mL chloroform and centrifuged for 5 min at 1000 rpm. The two organic phases were combined and split into aliquots corresponding to 50 mg of tissue. The organic solvent was evaporated and samples stored at -80°C.

6.11.5 Shotgun Lipidomics

Aliquots from tissue extracts were reconstituted in 500 µl chloroform/methanol 1:2 and further diluted 1:100 with chloroform/methanol/isopropanol 1:2:4 containing 7.5 mM ammonium acetate. Just prior to analysis, samples were centrifuged at 12,000 rpm for 2 min and analysed with a TriVersa NanoMate coupled to a QqQ-MS as described above. An ionisation voltage of 0.95 – 1.40 and a gas pressure of 1.25 psi was used (Graessler et al. 2009). Full MS spectra were acquired over a 1 min period of signal averaging in the profile mode in both positive and negative mode. The intensity of the full MS in positive mode was one magnitude higher than the one in negative ion mode.

For NL and PI scans the collision gas pressure (argon) was set at 1.0 mTorr, the collision energy was chosen depending on the classes of lipids. Spectra were automatically acquired with rolling scan events by a sequence subroutine operated under the Xcalibur software (Thermo, version 2.0.7). The different NL and PI scans were set according to previously published descriptions (Brugger et al. 1997; Han and Gross 2003; Han and Gross 2005).

The main classes of lipids in positive ion mode were:

- phosphatidylethanolamine (PE) / lyso-PE (lPE);
- phosphatidylserine (PS) / lyso-PS (lPS);
- cholesteryl ester (CE);
- triacylglycerol (TAG);
- phosphatidylcholine (PC) / lyso-PC (lPC); and
- sphingomyelin (SM)

The PI scan of the acetate ion of the PC species in the negative ion mode was used for the identification of PC-derived fatty acids. The same parent ion scan at 184.1 was used for the identification of SMs, but the nitrogen rule allowed a discrimination of these two lipid species. SMs with two nitrogen atoms appear at odd mass-to-charge (m/z) values, whereas PC-signals occur at even m/z values (Brugger et al. 1997). To further separate PCs from SMs, SMs were identified in negative ion mode by precursor ion scan at m/z 168.011. For lipid

quantification, 392 pmol of CE 19:0 (Avanti polar lipids, Alabaster, AL) was added to 100 µL of each sample as internal standard and analysed for 2 min using a PI scan at m/z 369.3. The coefficient of variation for these measurements was <10% in 58% (53%) of the analytes, 10% to 20% in 18% (28%) of the analytes, 20% to 40% in 5% (5%) of the analytes, and >40% in the remainder for intraday (interday) measurements. For quantification of PC, lPC and SM species 52 pmol PC(17:0/17:0), 46.4 pmol/µL lPC(19:0), and 61.2 pmol SM(d18:1/12:0) were added per 100 µL sample (all Avanti polar lipids) and analysed for 2 min using a PI scan at 184.1.

6.11.6 Data Processing

QqQ-MS data were analyzed with Xcalibur (version 2.0.7, ThermoFisher, USA). Lipid identification was based on their characteristic head groups and corresponding fatty acids or using the LipidMaps database and Lipid MS Predictor (v1.5) available at http://www.lipidmaps.org. For quantification, a peak list was generated and imported into LIMSA software (version 1.0) (Haimi et al. 2006) using the following settings:

- linear fit
- offset = 0
- peak full width at half maximum (fwhm) = 0.5
- sensitivity = 0.1

6.11.7 Nomenclature

We followed the designations and abbreviations recommended by the International Union of Pure and Applied Chemistry (IUPAC; http://www.chem.qmul.ac.uk/iupac/lipid). Glycero- and glycerophospholipids were named with shorthand notification and numbers separated by colons refer to carbon chain length and number of double bonds. The composition of the side chains for the glycero- and glycerophospholipids were not assigned and were used randomly for glycerolipids. For glycerophospholipids, the unsaturated fatty acid was set on *sn*-1 position and the saturated on *sn*-2. Sphingolipids are presented in the order of long-chain base and *N*-acyl substituent.

6.11.8 Statistical Analysis

Statistical analysis was performed using the Student's t-test or analysis of variance and Scheffe's post hoc test. A p value of <0.05 was considered significant. Principal components analysis (PCA) were performed in Matlab (2009a, The Mathworks Limited). Data were

normalised by expressing individual lipid intensities as percentage of accumulative intensities in each lipid class.

6.12 LIPIDOMICS RESULTS

6.12.1 Liquid Extraction Surface Analysis (LESA)

1.5 µL extraction solution was sufficient to provide a stable spray for over 10 min. The signals within the lipid relevant m/z range of 400 – 1000 in the full MS scan (Figure 65A) were comparable to the ones obtained from tissue extracts (Figure 65B).

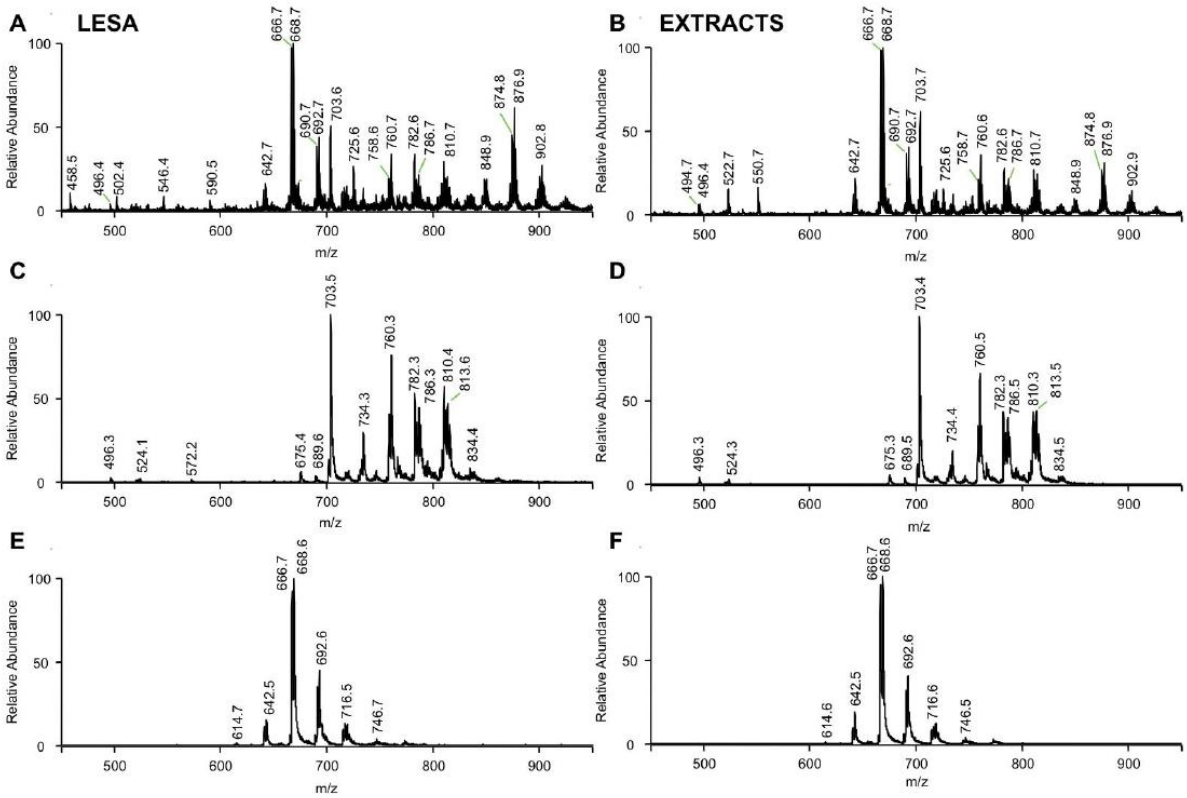


Figure 65 Liquid extraction surface analysis (LESA) compared to lipid extracts

The full MS in positive ion mode (A) and head group specific scans for PC (C, PI 184.1) and CE species (E, PI 369.3) from tissue sections of human endarterectomies. Note the similarity in peak numbers and signal intensities to tissue extracts (B, D, F). m/z, mass-to-charge.

Also, lipid class specific head group scans showed similar peaks and signal intensities (Figure 65C-F). Notably, lPC species within the m/z range of 490 – 540 were detected in tissue sections as well as extracts, confirming that these degradation products are present in human atherosclerotic plaques and not artefacts of the extraction method.

6.12.2 Identification of Plaque Lipids

Six scans were performed in positive ion mode and 14 in negative ion mode. The full MS scan between m/z 790 and 930 of endarterectomy samples was dominated by CE, SM, PC and TAG species. A comparison was made with lipidomic data from 3 radial artery specimens where TAGs accounted for the few prominent signals in the full MS. In total, 150 different lipid species were identified, of which 24 lipid species were detected in atherosclerotic plaques only (Table 29).

	Lipid species	m/z (positive ion mode)		Lipid species	m/z (positive ion mode)
lPS	lPS(20:0)	554.3	**CE**	CE(10:0)	558.5
PS	PS(38:5)	810.5		CE(14:0)	614.6
	PS(38:2)	816.5		CE(16:1)	640.6
lPC	lPC(14:0)	468.3		CE(18:3)	664.6
	lPC(O-16:0)	482.3		CE(18:1)	668.7
	lPC(O-18:0)	510.3		CE(22:6)	714.5
	lPC(18:2)	520.3		CE(22:5)	716.7
	lPC(22:5)	570.4		CE(22:4)	718.6
	lPC(22:4)	572.3		CE(22:3)	720.7
PC	PC(O-16:0/22:5)	794.5	**PE**	PE(38:3)	770.8
	PC(18:0/20:3)	812.7			
	Lipid species	**m/z (negative ion mode)**		**Lipid species**	**m/z (negative ion mode)**
SM	SM(d18:1/14:0)	709.7 + 733.4		SM(d18:0/15:0)	749.5
	SM(d18:1/15:0)	723.8 + 747.5			

Table 29 Lipid species found exclusively in atherosclerotic plaques

Of the 150 lipid species identified by lipidomics, 24 were found exclusively in carotid endarterectomy specimens and not in control radial artery samples. Nomenclature: (carbon chain length : number of double bonds); CE, cholesteryl ester; lPC, lysophosphatidylcholine; lPS, lysophosphatidylserine; PC, phatidylcholine; PE, phosphatidylethanolamine; PS, phosphatidylserine; SM, sphingomyelin; m/z, mass-to-charge.

Additional scans for acylcarnitine, phosphatidylinositol, phosphatidylinositol-phosphates, phosphatidylinositol (4,5) bisphosphate, sulfatides, acylCoA, ceramides and cerebrosides did not reveal strong signals for these lipid classes in shotgun lipidomics. In contrast, the signal intensities of the head group scans for CE differed by two orders of magnitude. For quantification, authentic standards were spiked into the samples. The average CE content was 23.8 mg/g in atherosclerotic plaques but 0.2 mg/g in control radial arteries (Figure 66A). As expected, oleic (18:1) and linoleic acid (18:2) were the most common fatty acids. The relative distribution of CEs identified in plaque and control arteries is depicted in Figure 66B.

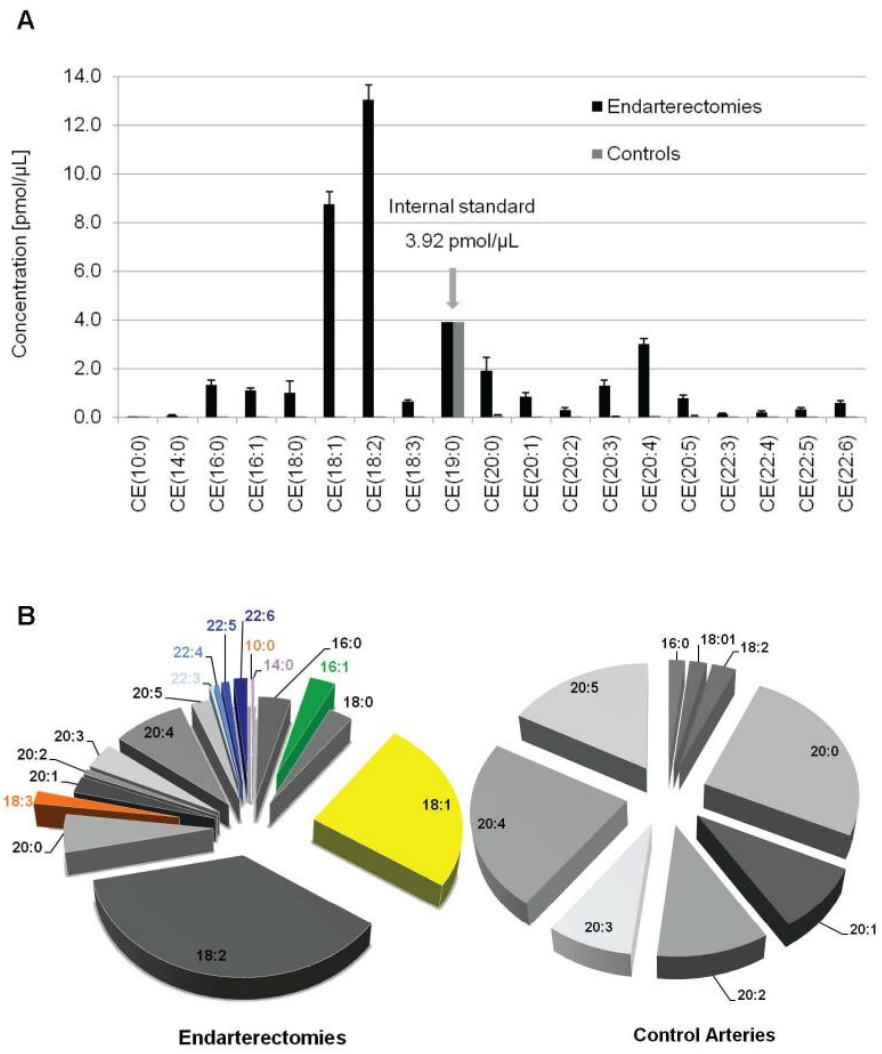


Figure 66 Cholesteryl ester species abundance differentially and exclusively found within atherosclerotic plaque compared with control artery

A. Quantification of cholesteryl ester (CE) species in plaque and control radial artery samples with CE(19:0) as internal standard. B. Relative distribution of CE in atherosclerotic plaques compared with control arteries. Plaque-specific CE species are highlighted in colour. Nomenclature: (carbon chain length : number of double bonds).

6.12.3 Comparison of Carotid Endarterectomy Samples

The lipid content of carotid endarterectomy samples from closely matched symptomatic and asymptomatic patients (n=6 per group, Table 26) was compared. PCA was performed to investigate the global variation of the patient samples in the metabolite space (Figure 67).

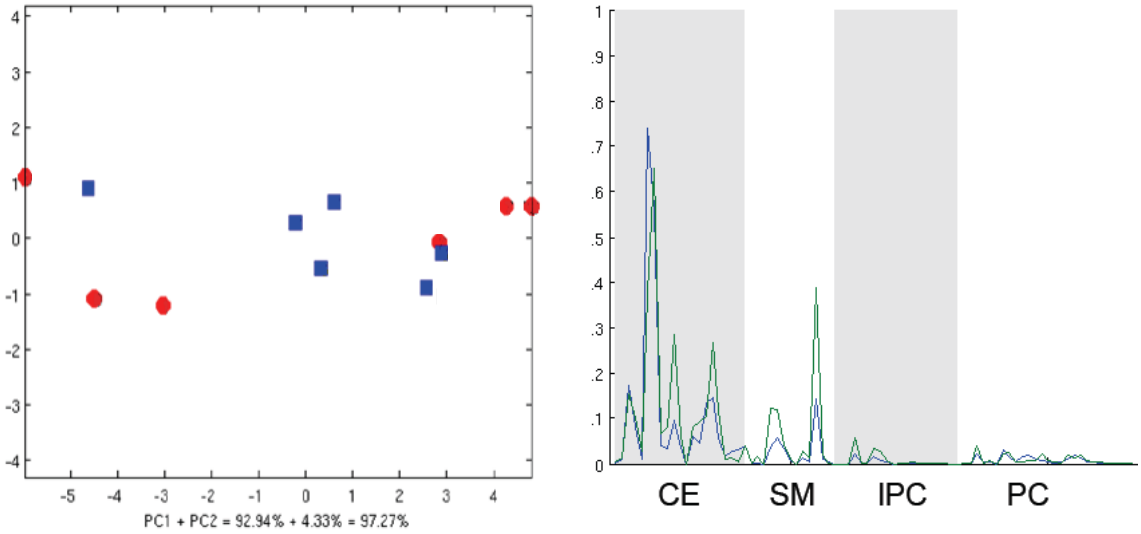


Figure 67 Principal components analysis for lipid profiles of symptomatic and asymptomatic patients

A. The red circles denote symptomatic patients; the blue squares denote asymptomatic patients. The first two principal components (PCs) capture 97% of the variance. B. The proportional magnitude of the first 2 PCs based on all measurements. The blue and green lines represent the mean value of the weights in symptomatic and asymptomatic plaques. Principal component analyses were biased towards cholecteryl esters (CE) with significant contributions from sphingomyelin (SMs), but the distance between symptomatic and asymptomatic patients was negligible. lPC, lysophosphatidylcholine; PC, phatidylcholine.

Given the heterogeneity of carotid endarterectomy samples, plaques excised from symptomatic and asymptomatic patients may share similar features. Thus, in another cohort of patients (Table 30), the stable area of the plaque/intimal thickening with no signs of rupture was excised from the unstable area, in which there was ulceration of the surface with or without thrombosis and/or macroscopic intra-plaque haemorrhage, thereby providing an internal control for each sample and minimising the effect of inter-patient variability.

Symptomatology	Age	Gender	DM	COPD	HTN	Renal failure	b-blockers	ACEI	Statins
Symptomatic	81	Male	No	No	Yes	No	No	No	Yes
Asymptomatic	70	Male	Yes	Yes	Yes	No	Yes	Yes	Yes
Symptomatic	54	Male	Yes	No	Yes	No	No	Yes	Yes
Symptomatic	76	Male	No	Yes	Yes	No	No	No	Yes
Symptomatic	79	Female	Yes	No	Yes	No	Yes	No	Yes
Symptomatic	73	Male	No	No	No	No	No	No	Yes (4 days)
Symptomatic	81	Male	No	No	Yes	No	Yes	Yes	Yes
Symptomatic	80	Female	Yes	No	Yes	Yes	No	Yes	Yes

Table 30 Clinical characteristics of patients whose plaques were divided into ruptured (unstable) and non-ruptured (stable) areas.

ACEI, angiotensin-converting enzyme inhibitor; ASA, acetyl salicylic acid (aspirin); COPD, chronic obstructive pulmonary disease; DM, diabetes mellitus; HTN, hypertension.

The 10 most differentially expressed species from 4 different lipid classes were sufficient to separate stable and unstable areas within the same lesion in PCA (Figure 68). No separation was obtained with individual lipid classes (Figure 69).

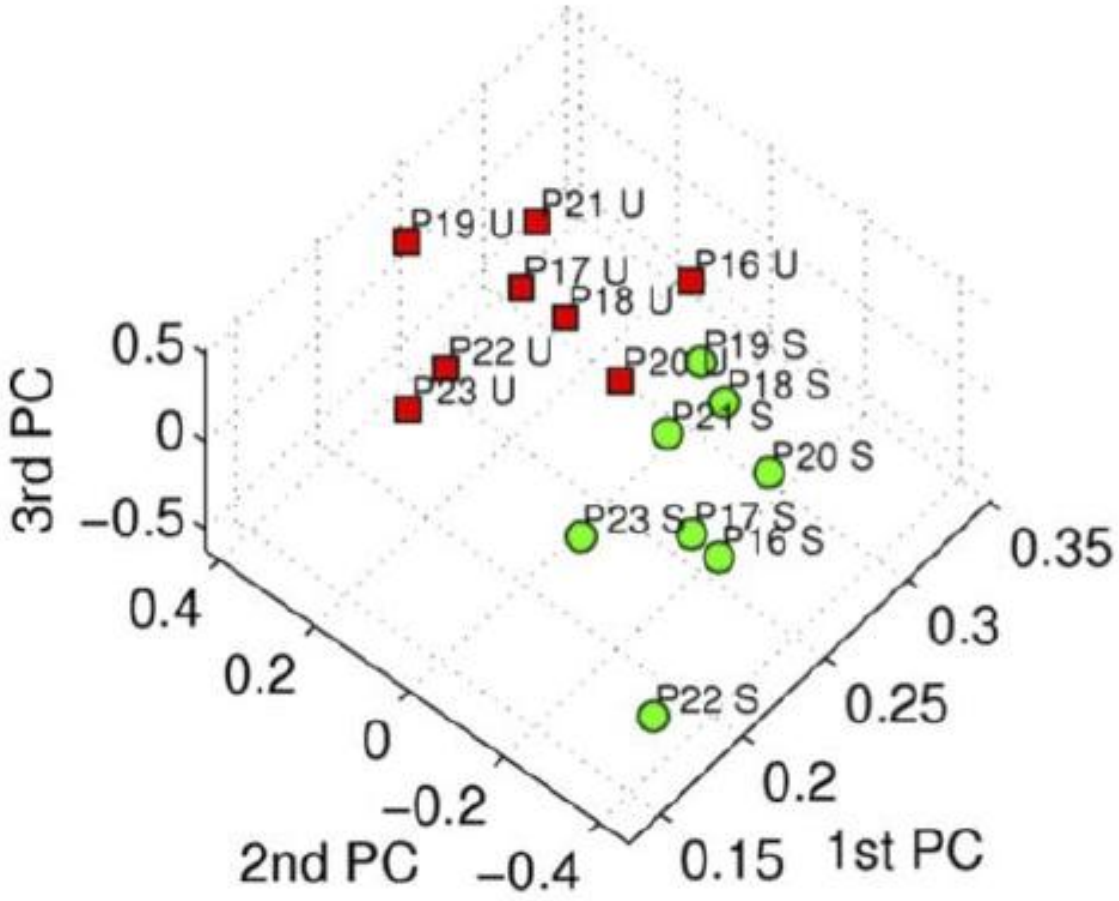


Figure 68 Principal components analysis of lipidomic data based upon top 10 differentially expressed species

PCA for lipid profiles of ruptured and non-ruptured areas of the same carotid atherosclerotic plaques (n=8). The green circles denote non-ruptured areas (S, stable) and the red squares ruptured areas (U, unstable) of the same lesion. A separation is seen.

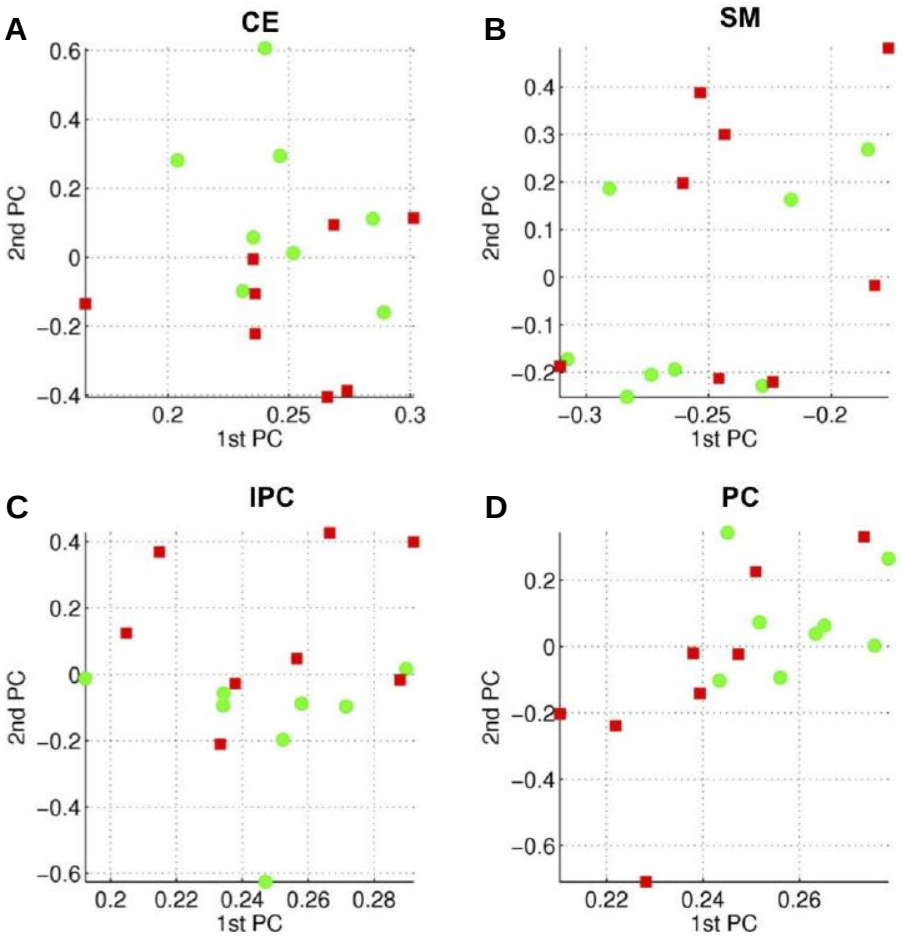


Figure 69 Principal components analysis of lipidomic data based upon lipid classes

PCA for lipid profiles of ruptured and non-ruptured areas of the same carotid atherosclerotic plaques (n=8). The green circles denote non-ruptured areas (stable) and the red squares ruptured areas (unstable) of the same lesion. No clear separation is observed based upon individual lipid classes: CE, cholesteryl esters (A); SM, sphingomyelin (B); lPC, lyso-phosphatidylcholine (C); or PC, phosphatidyl-choline (D).

6.12.4 Systems-Wide Analysis of Plaque Lipids

Lipid expression similarity in plaques from asymptomatic and symptomatic patients as well as in stable and unstable areas within the same lesion was inferred using Pearson correlation coefficients (PCC) and visualised as networks where nodes correspond to lipids and edges link correlated pairs ($PCC \geq 0.70$). Clusters of interlinked lipids were identified using an unbiased network clustering algorithm (Blondel et al. 2008). This systems-wide analysis revealed plaque-specific lipid signatures consisting of 19 lipid species in asymptomatic-symptomatic lesions (Figure 70A) and 12 lipid species in stable-unstable plaque areas (Figure 70B). There were 33 common lipid species that were differentially linked in the two networks (Figure 70). Unbiased network clustering (Blondel et al. 2008) demonstrated that lipid species belonging to the same class are more likely to be linked in the stable-unstable network (for example CE22:4, CE22:5 and CE22:6). These connectivity patterns were not observed in the asymptomatic-symptomatic network. Thus, the lipid composition as well as their connectivity change in atherosclerosis and may allow a differentiation between stable and unstable plaque areas.

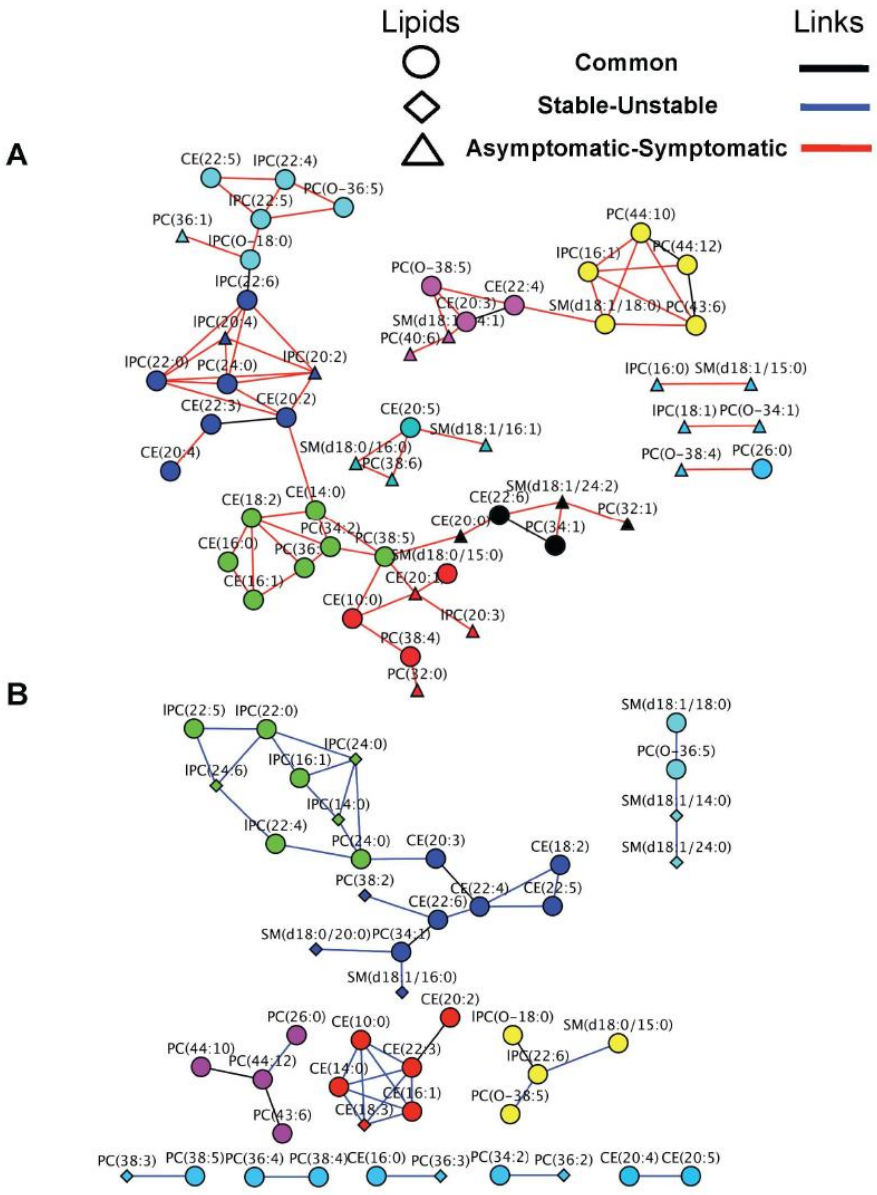


Figure 70 Systems-wide relationships between lipids involved in atherosclerosis

Lipid-lipid co-expression network where each node represents a lipid and each edge a correlation in expression between two lipid pairs. Only lipid pairs with Pearson correlation coefficient ≥ 0.70 were included in the network. Lipids and co-expressions specific for the asymptomatic-symptomatic phenotype are represented as triangles and red links, respectively (A). Lipids and co-expressions specific for stable-unstable network are represented as diamonds and blue links, respectively (B). Lipids and co-expressions common to both phenotypes are represented as circles and black edges, respectively. Lipid colours correspond to unique clusters, computed using an unbiased network clustering algorithm (Blondel et al. 2008).

6.13 LIPIDOMICS DISCUSSION

While lipids of human atherosclerotic plaques have previously been analysed, target-focused measurements restricted to individual lipid classes remain insufficient to reveal the global lipid imbalances in atherosclerosis. This study demonstrates the integration of advanced MS towards improved characterisation of the lipid composition in atherosclerosis. LESA allowed a rapid analysis of plaque lipids from tissue sections without time and labour-intensive sample preparation. This was the first time that LESA was used in combination with a QqQ instrument for lipid profiling. Notably, LESA provided similar signals and signal intensities as shotgun proteomics of chloroform/methanol extracts. For quantification, lipid extracts were spiked with class specific internal standards. Since only a single standard per lipid class is required, the shotgun lipidomics approach is less expensive compared to other lipid analysis techniques. Specificity is achieved by characteristic headgroup scans. In total, 150 lipid species were identified in this study, making it the most comprehensive lipid analysis of human atherosclerotic lesions to date.

6.13.1 Lipids in Atherosclerosis

The lipid classes accounting for the major differences between endarterectomy specimens and control radial artery tissue were CE, lPC and SM. Cholesterol within the vasculature accumulates as CE, either as a droplet in the cytosol or in lysosomes (Shio et al. 1979). Infiltrating LDL-particles contain a CE-rich core with linoleic acid (18:2) as the most abundant polyunsaturated fatty acid (Mallat et al. 1999b). The intimate relationship of plasma lipids, vascular matrix and CE deposits in the arterial wall is well documented (Suarna et al. 1995; Brown et al. 1997; Witting et al. 1999). Currently, knowledge at the biological level is mostly related to the classes of lipids rather than the bioactivity of single lipid species within the classes (Hu et al. 2009). Yet, the composition of the classes is likely to be an important atherogenic factor, *i.e.* LDL particles enriched with monounsaturated cholesteryl oleate (CE18:1) are typically larger and appear to be more active in binding to arterial proteoglycans, thereby favouring retention and subsequent formation of early atherosclerotic lesions (Degirolamo et al. 2009). In comparison, LDL particles enriched with polyunsaturated cholesteryl linoleate (CE18:2) are thought to be less atherogenic. Consistent with previous reports (Rapp et al. 1983), CE(18:2) was the major CE species in atherosclerosis and the relative distribution of most CEs was comparable to results obtained by thin layer chromatography, providing independent validation of the quantitative accuracy of the approach taken in this study. The sensitivity of shotgun lipidomics, however, allowed the identification of additional CE species as well as other lipid classes, such as lPCs (a by-product of LDL oxidation and formed by the enzymes phospholipase A1, phospholipase A2

or lecithin:cholesterol acyltransferase) and SMs (an ubiquitous component of cell membranes and of the LDL surface). Moreover, a simple, rapid macroscopic method of classification based on the definitions of plaque progression and instability (Stary et al. 1995a) was used to differentiate ruptured (unstable) versus non-ruptured (stable) segments of the same plaque as previously reported (Papaspyridonos et al. 2006; Papaspyridonos et al. 2008). In this homogenous cohort, the lipidomics approach was most successful and provided insights in the lipid heterogeneity within atherosclerotic lesions. Several lipids were reduced in regions with evidence of rupture and one could envisage that leakage of plaque-related lipid products into the circulation may constitute a better marker for plaque burden and vulnerability than total cholesterol levels and plasma lipoproteins.

6.13.2 Systems-Wide Network Analysis

The post-genomic shift in paradigm from reductionism to systems-wide network inference acknowledges the fact that biological systems are pleiotropic and interconnected (Barabasi and Oltvai 2004). Similarly, systemic relationships between lipid classes in atherosclerotic lesions are important for understanding genotype-phenotype relationships (Dreze et al. 2009) and working towards a lipid signature for risk prediction, early diagnosis, and personalised treatment of this disease. Previous studies enabled only a partial analysis of plaque lipids and mainly focused on LDL (Carpenter et al. 1994; Carpenter et al. 1995; Brown et al. 1997; Upston et al. 2002), cholesterol and its derivatives (Carpenter et al. 1993; Upston et al. 2002). There are also publications about individual lipid classes in atherosclerotic plaques, *i.e.* on isoprostanes (Mallat et al. 1999b), lPCs (Thukkani et al. 2003), and oxidised PCs (Davis et al. 2008), but no comprehensive comparison between diseased arteries across different lipid classes has been performed to date.

DESI-MS has recently been applied to atherosclerotic plaque tissue (Manicke et al. 2009). As proof-of principle, lipid profiling was performed on a single human plaque in positive and negative ion mode and 26 lipid species were identified. The shotgun lipidomic approach used in this study identified all of the 26 lipids except SM 22:0. Moreover, 16 of the 26 lipids in the former study were present in control arteries and were therefore not plaque-specific. Using a network approach, it was demonstrated that homogeneous lipid clusters were identified in the stable-unstable network and that sampling differentially expressed species across lipid classes improves the separation by PCA.

6.13.3 Clinical Relevance

While lipids of human atherosclerotic plaques have previously been analysed, target-focused measurements restricted to individual lipid classes remain insufficient to reveal the global lipid imbalances in atherosclerosis. A liquid extraction-based surface sampling device has been adapted for the analysis of plaque lipids from tissue sections. For quantification, shotgun lipidomics was performed on lipid extracts using the different scan options of a triple quadrupole mass spectrometer. In total, 150 lipid species from 9 different classes were identified, of which 24 were exclusive to atherosclerotic plaques. A comparison of 28 carotid endarterectomy specimens revealed lipid signatures of symptomatic compared with asymptomatic lesions, as well as stable and unstable plaque areas. This is the most comprehensive analysis of plaque lipids to date and highlights the importance of measuring individual lipid species rather than lipid classes to obtain insights into the lipid heterogeneity within atherosclerotic lesions.

6.13.4 Study Limitations

While MS has proven a valuable tool for comparative lipid analysis, minor components like signalling molecules (sphingosine-1-phosphate (Levkau 2008) or isoprostanes) remain undetected and not all the lipids identified can be reliably quantified due to low abundance. Also, modified lipids with alterations in the characteristic head groups as well as free cholesterol and other species, which do not readily ionise by ESI, are not detected in this analysis. Importantly, LESA only provides a qualitative comparison of plaque lipids. For quantification, lipids have to be extracted and spiked with authentic standards.

6.13.5 Conclusions

This study is the most comprehensive MS analysis of the lipid content in human atherosclerotic plaque to date. An in-depth comparison of the lipid composition in different atherosclerotic plaques combined with systems-wide network analysis unravelled plaque-specific lipid signatures. In future, these advanced technologies may be exploited for diagnostic purposes or as a platform for drug screening.

6.14 INTRODUCTION TO METABOLIC PROFILING

Metabolic profiling is defined as "the quantitative measurement of the dynamic multiparametric metabolic response of living systems to pathophysiological stimuli or genetic modification" (Nicholson et al. 1999). Combined with multivariate statistical methods, metabolic profiling via high-resolution spectroscopy provides a powerful tool for discovering novel biomarkers for disease diagnosis (Brindle et al. 2002) and prognosis (Clayton et al. 2006) as well as pharmaceutical targets, which could also pave the way for more individualised diagnostics and treatment schedules (Nicholson et al. 2005; Clayton et al. 2006). The potential application spectrum of the metabolic profiling approach is broad, due to advances in the analytical platforms employed, for example the introduction of cryoprobes in nuclear magnetic resonance (NMR), high resolution mass spectrometers (MS) and ultra performance liquid chromatography (UPLC) (Coen et al. 2008). These have enhanced the potential coverage of the metabolome. Further, recent statistical developments, allowing data integration of different analytical matrices, have provided new insights in gene (Nicholson et al. 2002) and enzyme function (Saghatelian et al. 2004; Tagore et al. 2009) studies and could potentially lead to cost reduction in the drug development pipeline (Nicholson et al. 2005), for example, by improving mechanistic understanding of drug toxicity (Nicholson et al. 2005; Clayton et al. 2006).

Screening of biological samples, such as biofluids, cells or tissues is usually performed as a first stage towards obtaining biomarker/metabolic pathway information relating to disease. This is done in order to obtain a global overview on the low-molecular weight metabolic composition and changes due to disease. Therefore, various spectroscopic techniques are employed (Nicholson et al. 2005; Martin et al. 2007; Holmes et al. 2008), such as NMR spectroscopy (Beckonert et al. 2007; Beckonert et al. 2010), UPLC-MS (De Vos et al. 2007; Want et al. 2010), mass spectrometry coupled to gas chromatography (GC-MS) (Lisec et al. 2006), and less frequently capillary electrophoresis (Hirai et al. 2005).

It has been shown that metabolic profiling of tissue, and/or of the biofluids that interact with the tissue of interest, delivers clinically and biologically significant results (Schmidt 2004). Consequently, metabolic profiling techniques are now being applied to homogenised or even intact tissues, as well as biofluids (Beckonert et al. 2007; Beckonert et al. 2010; Masson et al. 2010; Want et al. 2010). However, since with this approach the significant parameter of spatial distribution of the biomolecules through the tissue is disregarded, new screening techniques for untargeted determination of biomolecules in a manner that incorporates the

spatial distribution have been considered (Bunch et al. 2004; McDonnell and Heeren 2007; Trim et al. 2008b; Trim et al. 2010).

6.14.1 Metabolic Profiling in Atherosclerosis

There have been two contemporaneous reviews on the subject of metabolic profiling in atherosclerosis (Goonewardena et al. 2010; Martinez-Pinna et al. 2010). It is clear from these that, to date, there have been a limited number of such studies and that even fewer interrogate human samples, in particular human atherosclerosis tissue.

Chen *et al.* collected plasma from those with stable atherosclerosis and compared it with plasma from normal individuals. They found evidence of perturbed fatty acid metabolism in atherosclerosis, including differential levels of palmitate, which was confirmed as a phenotypic biomarker for the clinical diagnosis of atherosclerosis (Chen et al. 2010). Martinez-Pinna *et al.* identified multiple metabolites which were significantly modified associated with insulin resistance, correlating with metabolic syndrome (Martinez-Pinna et al. 2010) (Table 25). Mayr *et al.* used a combination of proteomics, metabolomics and immunomics to analyse microparticles derived from human atherosclerotic plaques (Mayr et al. 2009). They found that immunoglobulins present within the microparticles were derived from plaque macrophages. Plaque antibodies were different to circulating antibodies in the plasma as they recognise carbohydrate antigens including blood group antigen A.

6.14.2 Objectives

The objectives of this study were to investigate the utility of metabolic profiling in the context of human carotid atherosclerosis in separating plaque tissue responsible for recent focal neurological symptoms and tissue from asymptomatic individuals.

6.15 METABOLIC PROFILING METHODOLOGY

6.15.1 Biological Sample Characteristics and Handling

Ten patients (five asymptomatic and five recently symptomatic) consented to the collection of their atherosclerotic plaque at carotid endarterectomy surgery (Table 31). With regards to symptoms, only formal strokes were considered, defined as focal neurological events lasting for more than 24 hours pertaining to the anterior circulation of the cerebral hemisphere ipsilateral to the index carotid stenosis. As such transient ischaemic attack and amaurosis fugax were excluded, as were patients with atrial fibrillation from the symptomatic group where atrial thromboembolism may be a source of misdiagnosis. These diseased intimal

arterial segments were retrieved, snap frozen in liquid nitrogen and stored at -80°C for batch processing.

The endarterectomy specimens were processed as shown in Figure 71. For each specimen, two samples were obtained, each of which would have sequential aqueous (polar) and organic extraction of metabolites allowing for analysis of two biological replicates per sample.

Sample	Symptoms	Age (years)	Gender	Ischaemic heart disease	Peripheral arterial disease	Hypertension	Diabetes mellitus	Smoking history	Plasma creatinine (µmol/L)	Plasma C-reactive protein (mg/L)	Carotid Stenosis (%)	Statin use	Antiplatelet use	Time from symptoms to surgery (days)
V1248	0	67	M	1	0	1	0	1	77	15	85-90	1	1	-
V1370	0	78	M	1	0	1	0	0	142	-	85-90	1	1	-
V1412	0	69	M	0	0	1	0	1	73	1	>90	1	1	-
V1430	0	91	M	0	0	0	0	0	102	10.2	75-80	0	0	-
V1452	0	74	M	1	1	1	1	0	99	9.1	85	1	1	-
V1431	1	72	M	0	0	1	0	0	118	4.4	70	1	1	12
V1437	1	78	M	1	1	1	0	0	75	21.7	70	1	1	6
V1445	1	59	M	1	0	1	0	1	66	8.5	95	1	0	3
V1446	1	78	F	1	0	1	0	0	75	-	>95	1	1	6
V1448	1	75	M	0	1	1	0	0	115	14.7	95	1	1	6

Table 31 Characteristics of the individuals included in the metabolite profiling study

Demographic, clinical and pharmacotherapeutic information relating to the subjects included in the study. F, female; M, male.

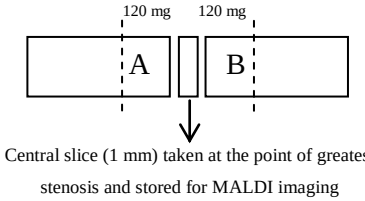


Figure 71 Processing of carotid atherosclerotic plaque for metabolic profiling with storage of tissue for future mass spectroscopy imaging

Frozen samples had a central slice of 1 mm in thickness at the point of greatest stenosis removed and stored in a labelled well of a 12-well culture plate which was returned to -80°C for future mass spectroscopy imaging. The areas of tissue flanking the central area (A and B) were cut and weighed to a target mass of 120 mg for each of these two biological replicate samples. It was aimed that sample weights should be within ±5% of each other.

6.15.2 Metabolite Extraction – Aqueous (Polar)

Tissue samples of 120 mg to which was added 1.5 mL methanol : water solution (1:1) (methanol HPLC gradient grade, Fisher; water LC-MS grade, Fluka). These samples were frozen on dry ice and loaded onto a bead beater (Bertin Technologies, Precellys 24, 1 mm zirconium beads, 6500 Hz, 40 seconds, 2 + 2 cycles separated by cooling on dry ice). Centrifugation (Biofuge Pico, Heraeus) at 13,000 rpm for 10 minutes, followed by aliquoting of supernatant into Eppendorf tubes (300 µL x4). 70 µL of each aqueous sample was combined to generate a 'quality control' (QC), which was mixed and split into aliquots (300 µL x4). Samples were spun on a vacuum concentrator for 160 minutes (Eppendorf Concentrator Plus, 45°C, V-AQ mode). Samples were then stored at -40°C for analysis.

6.15.3 Metabolite Extraction – Organic

Following decanting of supernatant from centrifuged aqueous samples, 1.5 mL dichloromethane (DCM, CH_2Cl_2) : methanol (3:1) (methanol HPLC gradient grade, Fisher; DCM HPLC grade, Sigma-Aldrich) was added and the samples were frozen on dry ice and re-loaded onto the bead beater (2 cycles). Centrifugation at 13,000 rpm for 20 minutes, followed by aliquoting of organic phase supernatant into glass tubes (200 µL x4). 50 µL of each aqueous sample was combined to generate a QC, which was mixed and split into aliquots (200 µL x4). Samples were allowed to evaporate at room temperature in an extractor hood overnight. Samples were then stored at -40°C for analysis.

6.15.4 Metabolite Profiling

Both aqueous and organic extracts were subject to metabolic profiling by NMR and UPLC-MS.

6.15.5 Nuclear Magnetic Resonance

NMR analyses were run using a Bruker 600 MHz spectrometer. For the aqueous phase analysis, extracts were resuspended in deuterium oxide (D2O) and Nuclear Overhauser effect spectroscopy (NOESY) and Carr-Purcell-Meiboom-Gill (CPMG) sequences were employed. Organic phase extracts were resuspended in Chloroform-D and run with a standard sequence. Spectra were subjected to phasing, calibration, baseline correction, alignment and normalisation. Principal components analysis (PCA) was performed with unit variance scaling in Matlab (The MathWorks Incorporated) programming language using a script developed in-house in the Department of Biomolecular Medicine at Imperial College London.

6.15.6 Nuclear Overhauser Effect Spectroscopy – NOESY

The Overhauser effect is the transfer of spin polarisation from one spin population to another via cross-relaxation. In NOESY, the nuclear Overhauser effect between nuclear spins is used to establish correlations. Hence the cross-peaks in the resulting two-dimensional spectrum connect resonances from spins that are spatially close.

6.15.7 Carr-Purcell-Meiboom-Gill – CPMG

The Carr-Purcell (CP) sequence is a spin-echo pulse sequence consisting of a 90 radiofrequency pulse followed by an echo train induced by successive 180 pulses. CP is designed to measure the T2 relaxation time in the presence of diffusion and magnetic field inhomogeneity. CPMG is an improved modification of the CP sequence. In the CP sequence, a constant flip-angle deviation from the nominal 180 results in errors accumulated throughout the echo train and in concomitant under-estimation of the T2 relaxation time. In contrast, CPMG partially corrects this error in every second echo, due to application of the initial 90 pulse and the subsequent 180 pulses with a defined phase difference of 90 in the rotating frame of reference. As a side effect, all echo signals in the CPMG experiment have the same phase, whereas signal phase alternates in successive echoes of the CP sequence.

6.15.8 Ultra Performance Liquid Chromatography Mass Spectrometry – UPLC-MS

UPLC separation was carried out on an Acquity UPLC system (Waters Ltd) using a HSS T3 C18 column. The mass spectrometer used was quadrupole-time of flight (Q-TOF) Premier

(Waters MS Technologies). Metabolic features were extracted from the UPLC-MS spectra. PCA was performed with unit variance scaling using SIMCA-P+ 11.5 (Umetrics) software.

6.15.9 Unit Variance and Pareto Scaling

Scaling is employed when variables are on different scales. As PCA is scale-dependent, scaling can be achieved by applying a scaling weight to each variable. Unit variance (UV) applies a scaling weight of 1/standard deviation (SD) for each variable, *i.e.* dividing each variable by its SD, whilst Pareto scaling uses the √(SD) as the scaling factor.

6.16 METABOLIC PROFILING RESULTS

In terms of time from symptoms to surgery in the symptomatic group, the times were: 3 days; 6 days; 6 days; 6 days; and 12 days. Spectroscopy by NMR and UPLC-MS generated high quality spectra (Figure 72).

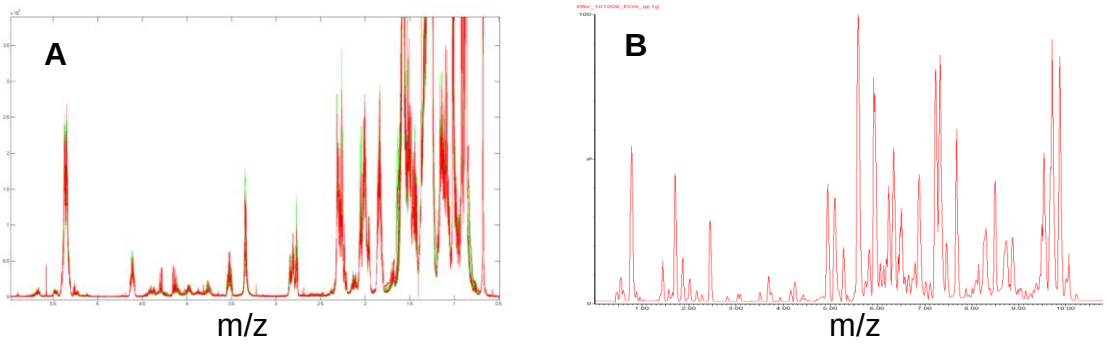


Figure 72 Representative NMR and UPLC-MS spectra

NMR (A) and UPLC-MS (B) spectra from analysis of the organic extract of atherosclerotic plaque. m/z, mass/charge ratio.

6.16.1 Results of NMR PCA

PCA from aqueous (Figure 73A) and organic phase (Figure 73B) extracts analysed using NMR did not provide clear separation between the symptomatic and asymptomatic groups. The organic phase NMR PCA presented a clear group comprising two samples with both their biological replicates (Figure 73B).

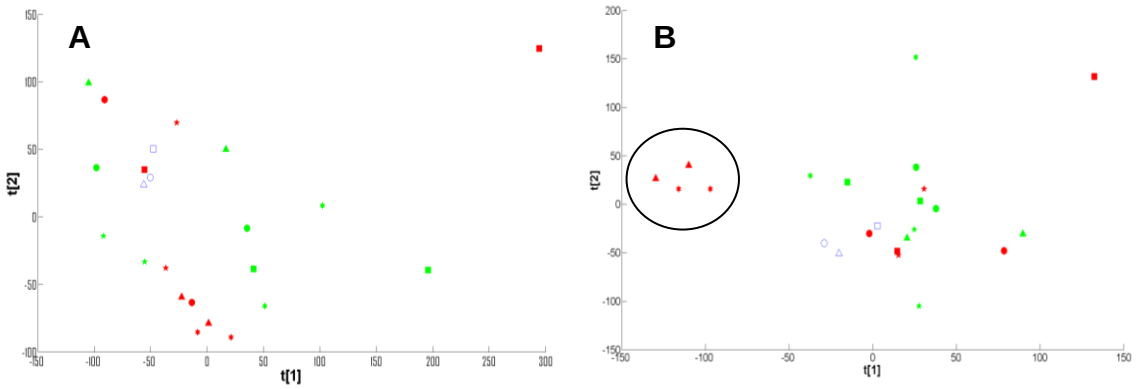


Figure 73 Results of NMR PCA

PCA scores plot of NMR analysis of aqueous extracts (CPMG sequence, A) and organic extracts (normal sequence, B). Unit variance scaling was applied to the data. Biological replicates are represented by the same marker. Green makers represent samples from the asymptomatic patients, red markers samples from symptomatic patients, and blue markers are pooled (QC) samples used for stability testing at 0 hours, 24 hours and 72 hours. No clear separation was seen, however with regards the organic phase NMR, a clear group comprising two samples with both their biological replicates was observed (circled), separated in PC t[1].

Results of UPLC-MS PCA

PCA from the organic phase positive mode UPLC-MS data provided good separation between the two groups (Figure 74). At least one of the two biological replicates was represented in the cluster of symptomatic samples.

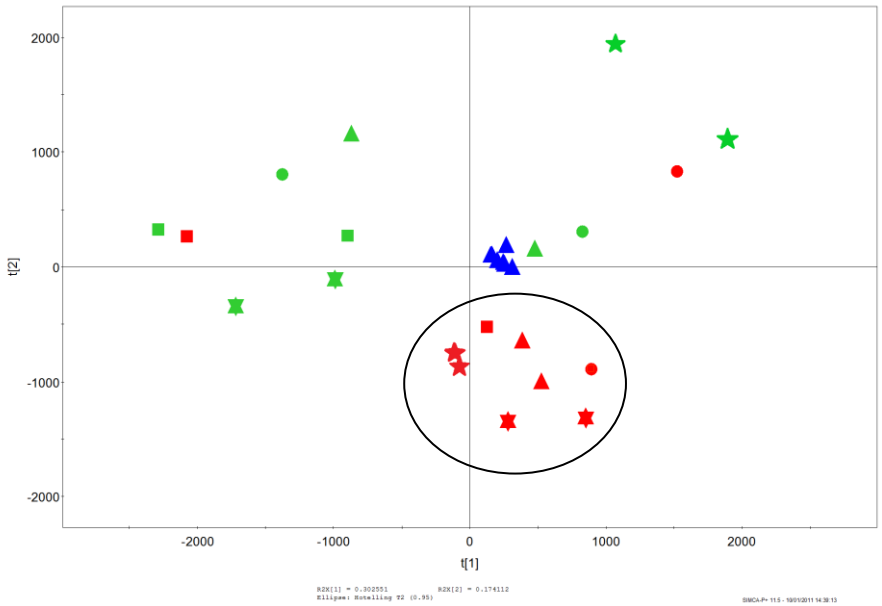


Figure 74 Results of organic UPLC-MS PCA

PCA scores plot of the organic phase positive mode UPLC-MS analysis. Data were Pareto scaled. Biological replicates are represented by the same marker. Green makers represent samples from the asymptomatic patients, red markers samples from symptomatic patients, and blue markers are pooled (QC) samples used for stability testing. Tight clustering of the QC samples indicate good system stability. There is clustering of symptomatic samples seen (circled), with at least one sample from each symptomatic pair located within the symptomatic cluster.

6.17 Metabolite Profiling Discussion

Metabolic differences can be seen between symptomatic and asymptomatic patients. It is evident that UPLC-MS of the organic extract is able to generate a metabolite 'signature' which can separate samples from symptomatic from samples derived from asymptomatic atherosclerotic plaques. This finding is in line with the separation seen in the lipidomic study and it is plausible that the analytes allowing for separation in this study are the metabolites of the lipids which are differentially abundant in the lipidomic analysis (Section 6.12). It has been proposed that the integration of metabonomic data with that from other techniques in molecular biology, such as those seen in this chapter and other areas of this thesis, is feasible (Lindon et al. 2006). Such an integrative approach would be necessary to support or refute this suggestion.

The times from symptoms to carotid endarterectomy (hence sample collection) are relatively short (median 6 days). To this end, when examining time from symptoms on the PCA plots, this did not result in any change in interpretation.

It would be useful to localise organic metabolites of differential abundance to particular areas within the plaque according to the metabolite mass / charge ratio (m/z). Applications of imaging techniques that can deliver chemical profiles related to organ or tissue topography have recently been demonstrated for metabolic profiling approaches (Bunch et al. 2004; Burrell et al. 2007; Trim et al. 2008a; Trim et al. 2008b). Mass spectrometry imaging (MSI) techniques appear to possess what is needed for metabolite *in situ* screening. There are several techniques proposed for MSI. However, matrix-assisted laser desorption/ionisation (MALDI)-MSI appears to be a dominating presence over the past few years. MALDI-MSI is currently under development in the Department of Biomolecular Medicine at Imperial (Figure 75). Samples from the plaques analysed in this experiment have been stored for this purpose and will be scrutinised by this 'virtual histology' technique once optimised.

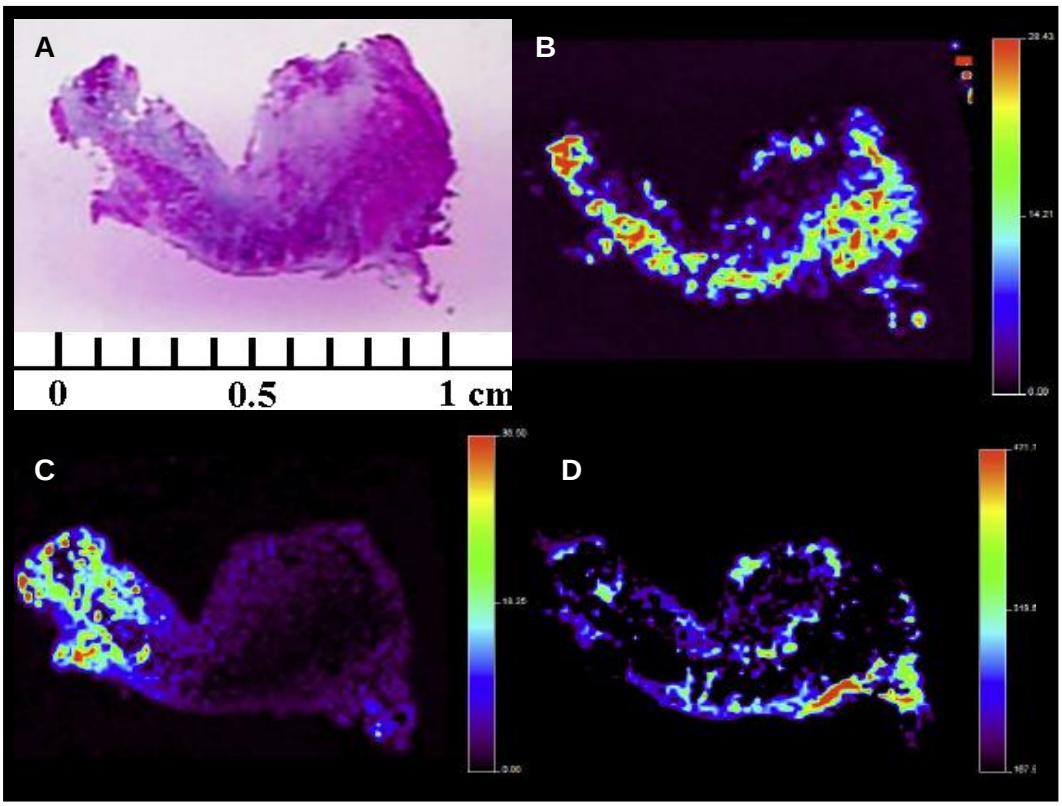


Figure 75 An example of MALDI mass spectroscopy imaging

A. Eosin stained aortic heart valve leaflet (12 µm thickness). B-D. MALDI mass spectroscopy images of the same leaflet, showing the localisation of three different metabolites in different areas of the leaflet based upon mass / charge ratio.

7 PLASMA LYSOZYME AS A PUTATIVE BIOMARKER IN CAROTID ATHEROSCLEROSIS

7.1 INTRODUCTION

Arterial plasma of patients with three vessel coronary disease with those with no coronary arterial disease on angiography has previously been compared (Abdul-Salam et al. 2010). Through the use of surface-enhanced laser desorption/ionisation–time-of-flight mass spectrometry (SELDI-TOF MS) proteomics, the level of a 14.7 kDa protein was found to be significantly raised. This protein was isolated and identified as the glycoside hydrolase enzyme lysozyme. The measurement of arterial plasma lysozyme levels in 197 patients with varying degrees of coronary atherosclerosis, using a cutoff value of 1.5 μg/mL, enabled the investigators to distinguish patients with one or more significantly involved coronary arteries, with 86% sensitivity and 93% specificity (Abdul-Salam et al. 2010). As such, arterial plasma lysozyme has emerged as a candidate biomarker of atherosclerotic burden, reflecting the amount of stenosing atheroma.

7.1.1 Aim

This study aimed to assess the utility of plasma lysozyme in the context of carotid atherosclerosis.

7.2 METHOD

7.2.1 Study Subjects

The study received research ethics committee approval (08/H0707/146). We recruited consecutive subjects who were due to undergo carotid endarterectomy for primary atherosclerotic stenosis of the carotid bifurcation from the vascular surgery clinics of a tertiary referral centre during a 6 month period between February 2009 and August 2009. All participants were greater than 18 years of age and gave written informed consent. The symptomatic status of the subjects with carotid stenosis was decided by a neurovascular multi-disciplinary team; subjects were considered symptomatic if symptoms consistent with stroke, TIA or amaurosis fugax had occurred in the neurovascular territory of a carotid stenosis in the four months prior to enrolment.

Additionally, age-matched control subjects were enrolled comprising two groups. Patients undergoing coronary angiography and found to have entirely normal coronary vessels were enrolled to act as arterial plasma controls. Individuals with no evidence of carotid atherosclerosis bilaterally on duplex ultrasound assessment volunteered to act as venous plasma controls.

7.2.2 Sample Collection and Processing

For subjects undergoing carotid endarterectomy whole arterial blood was collected from a radial artery cannula, sited in the arm contralateral to the operated carotid artery for the purpose of intra-operative continuous blood pressure monitoring, prior to the administration of any drugs. A group of these patients for carotid endarterectomy, along with matched control individuals without carotid disease, also had whole venous blood collected by venipuncture of a peripheral vein. Patients for coronary angiography had whole arterial blood collected from their femoral or radial artery interventional access sheath prior to contrast or drug administration – only samples from patients with normal coronary arteries were included in this study. Published evidence supports that, in the absence of detectable coronary atherosclerosis, subjects have a low likelihood of carotid disease (Craven et al. 1990).

For both arterial and venous samples, 3 ml of whole blood was collected in tubes containing 5.4 mg K2 EDTA (BD Vacutainer, New Jersey) Samples were transported on ice prior to centrifugation for 5 minutes at 1000 x g at 4°C. Aliquots of plasma were stored at -80°C.

Atherosclerotic plaques were collected from the patients undergoing carotid endarterectomy, immediately snap frozen in liquid nitrogen and stored at -80°C.

7.2.3 Lysozyme Analysis

The concentration of lysozyme in plasma and atherosclerotic plaque extracts was measured at using Enzyme-Linked Immunosorbent Assay (ELISA, Biomedical Technologies, Stoughton, Massachusetts) according to manufacturer's instructions. Zymography (EnzChek, Invitrogen Ltd, Paisley, UK) was used to quantify enzymatic activity of plaque lysozyme.

7.2.4 Statistical Analysis

Data was analysed with Prism (version 5.02, GraphPad Software, California). Where data was normally distributed, parametric tests were used. Non-parametric statistics were used for data which was not normally distributed. All tests used were 2-tailed and a p-value less than 0.05 was considered statistically significant.

7.3 RESULTS

A total of 54 subjects with carotid stenosis were enrolled. Of these 54 patients 28 also had venous plasma analysis. Venous plasma was analysed from 13 aged-matched controls and arterial plasma from 31 individuals with normal coronary angiograms. The characteristics of all groups are shown in Table 32. The groups were well matched in terms of sum of carotid

stenoses, demographic – particularly the proportion of patients with known ischaemic heart disease and peripheral arterial disease – clinical and pharmacotherapeutic parameters. The control group had a significantly higher total cholesterol level than the patients with carotid stenosis.

Parameter	Carotid Stenosis (*n* = 54)	Control Subjects	
		Arterial (*n* = 31)	Venous (*n* = 13)
Age (years)	69 (64.5 – 75)	57 (49 – 66)	60 (58 – 68.5)
Male gender	18 (33%)	14 (45%)	4 (31%)
Ischaemic heart disease	3 (6%)	N.A.	1 (8%)
Peripheral arterial disease	9 (17%)	0 (0%)	0 (0%)
Hypertension	38 (70%)	3 (10%)	2 (15%)
Diabetes mellitus	10 (19%)	6 (19%)	2 (15%)
Smoking history	29 (54%)	7 (23%)	6 (46%)
Plasma creatinine (µmol/L)	85 (76 – 102)	80 (70 – 94)	-
Statin use	50 (93%)	13 (42%)	2 (15%)
Antiplatelet use	46 (85%)	14 (45%)	-
Symptomatic carotid stenosis	26 (48%) (13 CVA, 10 TIA, 3 AmFu)	N.A.	N.A.
Sum of carotid stenoses (%)	118 (98 – 136)	N.A.	N.A.
Plasma C-reactive protein (mg/L)	2.3 (2.0 – 5.2)	-	-
Plasma total cholesterol (mmol/L)	4.20 (3.53 – 4.78)	5.51 * (4.28 – 5.95)	-

Table 32 Characteristics of the study groups

*Demographic, clinical and pharmacotherapeutic information relating to the three groups of subjects included in the study. Age, sum of stenoses, plasma C-reactive protein, plasma total cholesterol, and time from symptoms to plasma collection are presented as median (inter-quartile range). AmFu, amaurosis fugax; CVA, cerebrovascular accident; N.A., not applicable; TIA, transient ischaemic attack. * Mann Whitney test, P = 0.0118.*

7.3.1 Plasma Lysozyme

Plasma lysozyme levels were not normally distributed. Arterial plasma lysozyme levels were significantly higher in patients with carotid stenosis than controls with normal coronary angiograms (median 6.5 µg/mL versus 1.3 µg/mL, Mann Whitney test $p<0.0001$, Figure 76A). Receiver operator characteristic (ROC) curve analysis (Figure 76B) gave an area under the curve (AUC) of 0.88 (Table 33).

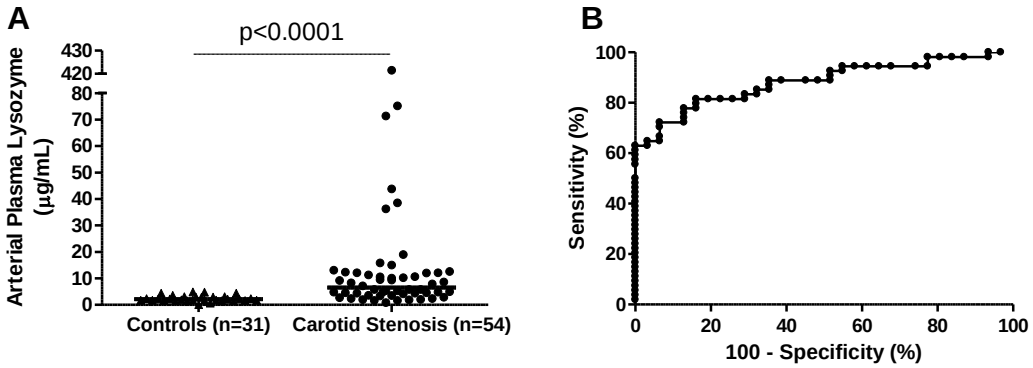


Figure 76 Arterial plasma lysozyme for carotid stenosis versus controls

A. Distribution of arterial plasma lysozyme levels in patients with carotid stenosis and controls. Median levels are shown as bars. B. Receiver operator characteristic curve analysis area under the curve is 0.88.

Plasma Lysozyme	Area under the curve	Lysozyme cut off (µg/mL)	Sensitivity (%)	Specificity (%)
Arterial, carotid stenosis versus controls	0.88	4.85	65	97
Venous, carotid stenosis versus controls	0.88	2.00	79	92
Arterial, carotid stenosis, symptomatic versus asymptomatic	0.69	12.8	35	96

Table 33 Receiver operator characteristic analysis results

Summary of receiver operator characteristic analyses for plasma lysozyme.

Venous plasma lysozyme levels were significantly higher in patients with carotid stenosis than the control group (median 3.2 µg/mL versus 1.2 µg/mL, p=0.0001, Mann Whitney test, Figure 77A). ROC curve analysis (Figure 77B) gave an AUC of 0.88 (Table 33). There was no significant correlation between arterial and venous plasma lysozyme levels (Spearman r=-0.3110, p=0.1072, Figure 77C). Venous plasma lysozyme levels were on the whole approximately half those seen in arterial plasma.

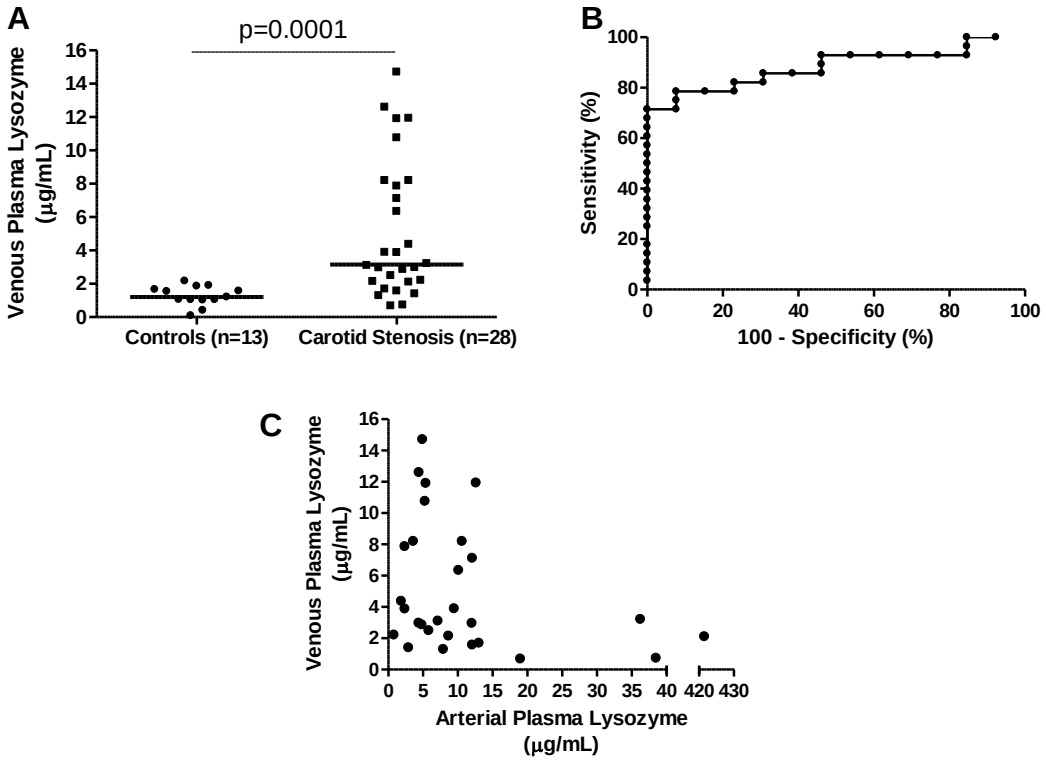


Figure 77 Venous plasma lysozyme for carotid stenosis versus controls

A. Distribution of venous plasma lysozyme levels in patients with carotid stenosis and controls. Median levels are shown as bars. B. Receiver operator characteristic curve analysis area under the curve is 0.88. C. There is no significant relationship between venous and arterial plasma lysozyme levels in patients with carotid stenosis. Spearman r=-0.3110, p=0.1072.

Arterial plasma lysozyme levels from patients with carotid stenosis were examined for their relationship to a number of key clinical, demographic and pharmacotherapeutic parameters (Table 34). Arterial plasma lysozyme was identified as being significantly higher in symptomatic patients with carotid stenosis than asymptomatic patients (median 10.4 µg/mL versus 5.1 µg/mL, p=0.0161, Figure 78A). There were a subgroup of symptomatic patients (n=6) seen to have very high arterial plasma lysozyme levels (>30 µg/mL) (Table 35). These results were confirmed on repeat analysis.

Parameter		*n*	Median Arterial Plasma Lysozyme (µg/mL)	Test Statistics
Age		54	-	Spearman r=-0.1324 p=0.3397
Gender	Male	36	7.749	Mann Whitney p=0.5819
	Female	18	5.832	
Ischaemic heart disease	Yes	13	5.299	Mann Whitney p=0.4979
	No	41	7.160	
Peripheral arterial disease	Yes	9	4.582	Mann Whitney p=0.3777
	No	45	8.337	
Hypertension	Yes	38	6.496	Mann Whitney p=0.3018
	No	16	7.251	
Diabetes mellitus	Yes	10	8.240	Mann Whitney p=0.2952
	No	44	6.469	
Smoking history	Yes	29	8.337	Mann Whitney p=0.5847
	No	25	5.414	
Plasma creatinine (µmol/L)		54	-	Spearman r=0.1941 p=0.1596
Statin use	Yes	50	6.496	Mann Whitney p=0.5971
	No	4	6.541	
Antiplatelet use	Yes	46	6.496	Mann Whitney p=0.6006
	No	8	6.875	
Sum of carotid stenoses (%)		54	-	Spearman r=0.02712 p=0.8532
Plasma C-reactive protein (mg/L)		54	-	Spearman r=0.04632 p=0.7394
Plasma total cholesterol (mmol/L)		54	-	Spearman r=-0.1097 p=0.6100
Symptomatic	Yes	26	10.39	**Mann Whitney p=0.0161**
	No	28	5.149	
Time from last symptom to plasma collection (days)		26	-	Spearman r=0.1544 p=0.4714

Table 34 Arterial plasma lysozyme and its relationship with demographic, clinical and pharmacotherapeutic parameters

There was a significant difference in arterial plasma lysozyme level between symptomatic and asymptomatic patients with carotid stenosis. No significant relationship was observed when assessing arterial plasma lysozyme level against other parameters.

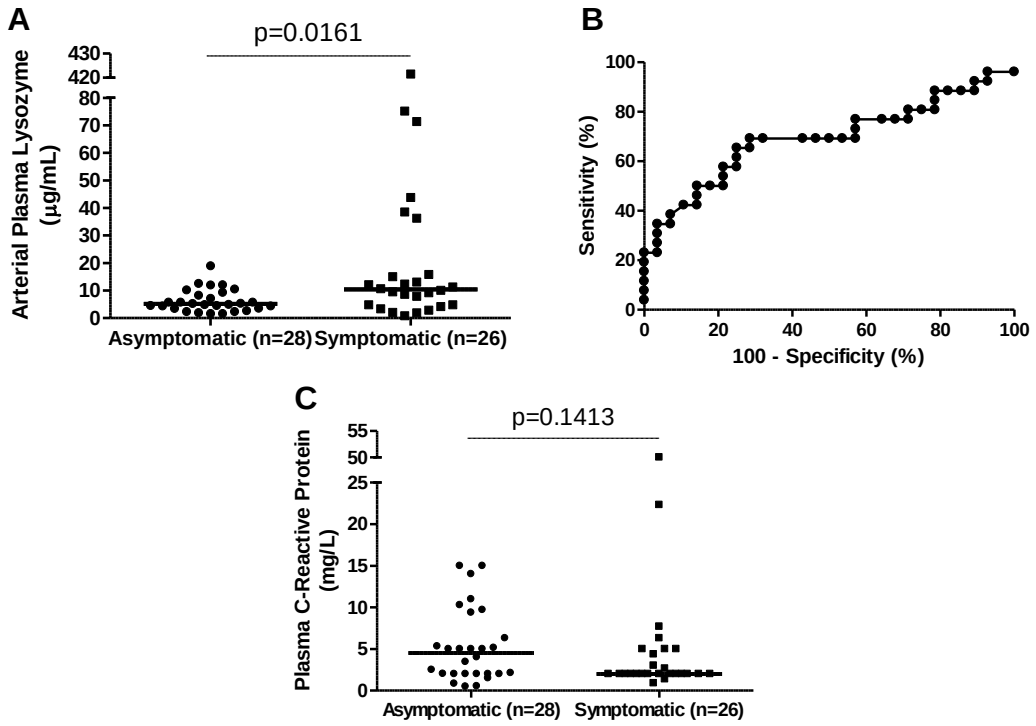


Figure 78 Arterial plasma lysozyme levels and symptomatic status

A. Distribution of arterial plasma lysozyme levels in patients with asymptomatic and symptomatic carotid stenosis. Median levels are shown as bars. A subgroup of symptomatic patients (n=6) displayed very high arterial plasma lysozyme levels (>30 µg/mL). B. Receiver operator characteristic curve analysis area under the curve is 0.69. C. There was no significant difference in the plasma C-reactive protein levels of these patients. Median levels are shown as bars.

Parameter	Patient 1	Patient 2	Patient 3	Patient 4	Patient 5	Patient 6
Arterial Plasma Lysozyme (µg/mL)	421.55	75.15	71.38	43.80	38.51	36.26
Age (years)	63	58	65	66	63	78
Gender	Male	Male	Male	Male	Male	Male
Ischaemic heart disease	0	0	1	0	0	0
Peripheral arterial disease	1	0	0	0	0	0
Hypertension	0	0	1	1	1	1
Diabetes mellitus	1	0	1	0	0	0
Smoking history	1	1	0	0	1	1
Plasma creatinine (µmol/L)	78	103	92	98	77	1501
Statin use	1	1	1	1	1	1
Antiplatelet use	1	0	1	1	1	0
Carotid symptoms	CVA (right hemi-paresis)	CVA (right hemi-paresis)	CVA (right hemi-paresis)	CVA (dysphasia, dysphagia)	TIA (right hemi-paresis)	TIA (left hemi-paresis)
Sum of carotid stenoses (%)	88	128	149	120	121	113
Symptomatic carotid stenosis (%)	Left (50)	Left (85-90)	Left (77)	Left (90)	Left (95-99)	Right (90-95)
Plasma C-reactive protein (mg/L)	2	2	2	2	2	50

Table 35 Characteristics of the six patients with high arterial plasma lysozyme levels

Six patients had arterial plasma lysozyme levels of >30 µg/mL. All of these patients were symptomatic, male and were on statin therapy. CVA, cerebrovascular accident; TIA, transient ischaemic attack.

There was no significant relationship between the other parameters examined and arterial plasma lysozyme level, including time since symptoms in the symptomatic subgroup, sum of carotid stenoses, statin use and self-reported history of ischaemic heart disease or peripheral arterial disease.

ROC curve analysis (Figure 78B) gave an AUC of 0.69 (Table 33). Comparing symptomatic and asymptomatic carotid stenosis, there was no significant difference in plasma C-reactive protein (CRP) levels (Figure 78C).

7.3.2 Carotid Atherosclerotic Plaque Lysozyme

Lysozyme concentration within seven carotid plaques was quantified (Table 36). Per unit wet weight, lysozyme ranged from 0.02 to 0.22 µg/mg (median 0.06 µg/mg). Per unit protein, this equated to 0.62 to 4.30 µg/mg (median 1.3 µg/mg). In all cases, plaque lysozyme activity was below the assay detection limit.

Symptomatic Status	Wet Weight (g)	Lysozyme per unit Wet Weight (µg/g)	Lysozyme per unit Protein (µg/mg)	Lysozyme Activity (U/mL)
Symptomatic	0.1257	62	1.278	0.000
Symptomatic	0.1558	129	2.953	0.000
Symptomatic	0.2206	51	1.209	0.000
Symptomatic	0.2960	32	1.139	0.000
Symptomatic	0.4402	22	0.622	0.000
Asymptomatic	0.0572	152	3.083	0.000
Asymptomatic	0.0832	216	4.298	0.000

Table 36 Carotid atherosclerotic plaque lysozyme analysis

Summary of results obtained from the analysis of carotid atherosclerotic plaque for lysozyme levels and enzymatic activity.

7.4 DISCUSSION

These results demonstrate that lysozyme levels in both arterial and venous plasma are significantly elevated in patients with carotid stenosis compared with control individuals. It has been shown for the first time that arterial plasma lysozyme levels are significantly higher in those with symptomatic compared with asymptomatic atherosclerosis. Furthermore, the presence of significant quantities of lysozyme within human atherosclerotic plaque has been confirmed, and shown to be inactive.

It is known that risk of cardiovascular and cerebrovascular events is determined not only by extent of disease, but by disease activity (Falk et al. 1995; Topol and Nissen 1995; Nicolaides et al. 2005).

In keeping with the finding in patients with coronary arterial disease (Abdul-Salam et al. 2010), there was no significant correlation between arterial and venous plasma lysozyme levels.

Previous work has demonstrated that, in the context of atherosclerosis, circulating lysozyme is largely inactive (Abdul-Salam et al. 2010). The finding in this study that lysozyme is found in carotid atherosclerotic tissue in significant concentration but that this lysosyme is inactive supports the hypothesis that the discriminatory arterial plasma lysozyme seen in individuals with arterial disease originates from such plaque. Naito and colleagues have previously

reported that whilst circulating monocytes enclose active lysozyme, in a rabbit model of atherosclerosis plaque-derived foam cells contain inactivated lysozyme (Naito et al. 1997). It has been postulated that foam cell myeloperoxidase catalyzes the production of hypochlorous acid which inactivates lysozyme (Schaffner et al. 1980; Naito et al. 1997; Heinecke 1999). In both experimental and human atherosclerosis, monocyte-macrophage and foam cell numbers are related to the development and destabilisation of atherosclerosis. It is noteworthy to mention at this point that the proteomic analysis of the salt extract of atherosclerotic plaques identified that myeloperoxidase levels were significantly higher in symptomatic than asymptomatic carotids (Table 28). This supports the inactivation of lysozyme by macrophages in symptomatic atherosclerosis which has been proposed (Abdul-Salam et al. 2010).

Low density lipoprotein (LDL)-associated lysozyme has recently been linked to the atherogenic properties of LDL found in type 2 diabetes and the metabolic syndrome (Pettersson et al. 2010). Patients with diabetes have also been shown to have increased levels of leukocyte-associated lysozyme than those without diabetes in the context of both acute myocardial infarction and unstable angina (Chavan et al. 2007). Importantly, the proportion of patients with known ischaemic heart disease and diabetes among the study population was not significantly different between those who were symptomatic and asymptomatic. There was no significant effect of statin use on lysozyme levels.

The fact that there was not significant relationship between total carotid stenosis and lysozyme levels may be explained by the fact that the all patients with carotid stenosis had a considerable burden of disease (median 118% combined stenosis).

A number of circulating biomarkers of atherosclerosis have been investigated, including CRP (CCGC 2011), matrix metalloproteinases, and pregnancy-associated plasma protein A (Alsheikh-Ali et al. 2010). To date, these have not been adopted into routine clinical practice. CRP levels were not significantly different between symptomatic and asymptomatic patients in this study. A circulating marker of atherosclerosis is eagerly sought. CRP has shown considerable promise but has not entered the clinical arena in this context. The data presented suggests that lysozyme is more sensitive than CRP in detecting unstable plaque. However, the specificity of lysozyme in identifying unstable plaque may be an important benefit.

The fact that there was no significant relationship between arterial plasma lysozyme and time from symptoms to sample collection may reflect the global instability of atherosclerosis across all arterial territories in individuals who have experienced a cerebrovascular event.

The reason for very high arterial lysozyme levels in symptomatic individuals may be explained by higher macrophage numbers in symptomatic plaques or greater release of lysozyme into the arterial circulation by ruptured plaques. It is hypothesised that circulating fragments from unstable plaques may be collected from the arterial line and be reflected as high lysozyme levels.

When patients with coronary arterial disease were studied (Abdul-Salam et al. 2010) there were no patients with the levels measured in this study. Although the patients in previous study had chronic stable without acute coronary events, it is unlikely that none of these had unstable disease.

Large scale studies are ongoing investigating the utility of lysozyme in coronary atherosclerosis. It is hoped that the results from this and the present study will support the use of plasma lysozyme as part of a multi-modal atherosclerosis risk stratification strategy, in terms of both extent and vulnerability of disease. This would facilitate the prioritisation, investigation and treatment of individuals with cardiovascular and cerebrovascular risk factors.

7.4.1 Limitations

Meaningful comparison between venous and plaque samples from symptomatic and asymptomatic individuals was precluded due to the small number of samples analysed in these groups.

7.4.2 Conclusions

This study demonstrates that arterial and venous plasma lysozyme levels are significantly higher in patients with carotid stenosis. Among the symptomatic group, there is a subgroup of patients with dramatically raised levels in their arterial plasma. The potential of arterial plasma lysozyme as a specific test for instability in atherosclerosis, either alone or as part of a multi-modal approach to risk stratification, warrants further investigation.

8 FINAL DISCUSSION

Risk stratification in patients with carotid stenosis is a clinical challenge and priority, as it bears implications for treatment or the timing of treatment. To date our risk stratification strategy has (formally and informally) considered age, life expectancy and quality of life, but has otherwise focused on structural features of the plaque. Time frame is important in that we need to explore when a stroke may occur in relation to a patient's life expectancy. For this reason, demographic and clinical parameters are considered, *i.e.* is this carotid stenosis likely to be responsible for a stroke in this individual's lifetime? ACST showed that half of patients with significant carotid stenosis aged 75 years or older die within five years from unrelated causes, hence the benefits of carotid intervention were lost (Halliday et al. 2004).

Plaque density, assessed by echogenicity on duplex ultrasound, has been shown to predict ipsilateral ischaemic stroke (Polak et al. 1998; Gronholdt et al. 2001; Mathiesen et al. 2001), however hazard ratios have not been sufficient to warrant translation into clinical practice. The mainstay structural predictor is degree of luminal stenosis as reported by the landmark European (ECST 1991) and North American (NASCET 1991) trials, but it is important to remember that these studied symptomatic individuals.

Therefore, even after the application of evidence-based current best practice, there remains a cohort of young individuals with significant asymptomatic carotid stenosis who face a 'number needed to treat' of 16 to prevent a stroke over 5 years; this prophylactic procedure itself carries a risk of stroke of up to 5%. Functional imaging and biomarkers offer the opportunity to explore plaque biology non-invasively, in vivo, and facilitate the selection of high-risk asymptomatic carotid stenoses warranting intervention. This need to risk stratify carotid atherosclerosis is 'bilateral': not only is there a desire to highlight high risk asymptomatic disease, but robust risk stratification could allow identification of symptomatic stenosis which is unlikely to be responsible for future cerebrovascular events. This approach facilitates informed decision making to benefit individual patients, but also has health economic implications when considering the allocation of health resources and reducing the overall burden of stroke and atherosclerosis in other arterial territories. With regards the latter, it has emerged that features of carotid atherosclerosis vulnerability are associated with global cardiovascular risk (Staub et al. 2010).

There has been a recent strong interest in functional imaging to investigate the biology of atherosclerosis. The results of the work on CEUS and PET/CTA have shown that functional imaging reflects plaque biological attributes. With regards PET/CTA, the ability to discriminate between symptomatic and asymptomatic atherosclerosis was enhanced when the functional parameter (PET) was combined with the structural aspects (CT). This underlines

the opportunities that a multi-modal or hybrid approach to imaging can offer (Sanz and Fayad 2008; Rudd et al. 2009). From a practical point of view it is unlikely that PET/CT will be translational into large-scale clinical use, owing to issues of acceptability, radiation dose, timing with regards radio-isotope half-life necessitating on-site cyclotron facility with clinical grade radio-pharmaceutical capabilities, and the costs thereof. There is the opportunity, however, that PET/CT may be harnessed as a research tool for the *in vivo* examination of plaque biology. The development of bespoke tracers targeted to ligands of interest would allow assessment of the *in vivo* discriminatory and predictive power of that ligand for future cerebrovascular events, both alone and when combined with the structural components of the imaging. An example of this would be determination of M1 burden using a CCR7 (Martinez et al. 2006) targeting compound, or even assessment of M1:M2 balance by combining this with CD206 quantification.

Such targeting is possible in the context of CEUS (Leong-Poi et al. 2005). However, it has been demonstrated that LP-CEUS employing untargeted microbubbles is able to reflect key biological features related to plaque vulnerability, namely inflammation (Owen et al. 2010), angiogenesis and matrix degradation. D-CEUS, an assessment of microvascular volume, may also be undertaken alongside LP-CEUS to complete the 'CEUS score' and offer greater discrimination between symptomatic and asymptomatic atherosclerosis. CEUS is a refinement of the current carotid duplex ultrasound assessment, building on a modality of investigation which is acceptable to patients and uses existing imaging infrastructure. Duplex assessment of stenosis, based upon velocity criteria (Oates et al. 2009), with or without measurement of plaque echolucency, provides the structural part of the hybrid structural-functional examination. CEUS is being developed for potential clinical use through prospective study to see whether CEUS measurements can predict future cerebrovascular events (Section 9.1).

Targets for imaging, as well as informing about pathogenesis and therapeutic strategies, are elucidated though the study of cellular and molecular biology. The activation of the innate immune system is central to atherosclerosis development, progression, rupture and the resulting sequelae. Considering the multi-step paradigm of macrophage activation recently proposed (Gordon and Martinez 2010) and the theory of a 'spectrum' of activation (Mosser and Edwards 2008), macrophage phenotype may be polarised to towards injurious and pro-inflammatory ('classical'; M1) or resolving, healing and regulatory ('alternative'; M2). The path of activation is determined by exposure to cytokines and chemokines microenvironmental. Examination of this microenvironment in human atherosclerosis with the aim of determining the predominant macrophage phenotype had not been previously

undertaken. In addition to showing a cytokine, chemokine and MMP pattern consistent with there being more M1 than M2-type macrophages in symptomatic compared with asymptomatic, the differentially abundant analytes feature in the 'differentiation', 'priming' and 'resolution' stages of the paradigm (Figure 5). The novel finding of CCL20 in atherosclerotic plaque and, in the context of an M1-type cytokine 'signature' pointed towards Th17/IL17 signalling, a feature of other inflammatory conditions (Hirota et al. 2007), a hypothesis which was supported by the listing of IL17 signalling as a key canonical pathway by bioinformatic analysis undertaken.

Ingenuity pathway analysis also highlighted 'Role of Pattern Recognition Receptors in Recognition of Bacteria and Viruses' and 'Activation of IRF by Cytosolic Pattern Recognition Receptors'. This is in line with important studies which link danger-associated molecular pattern (DAMP) activation of pattern-recognition receptors (PRRs), including TLRs and NLRs and the inflammasome pathway in generation of pro-inflammatory cytokines (Duewell et al. 2010). Furthermore exon-level transcriptomic analysis has shown that stenosing atherosclerosis, as compared with intimal thickening, has differential expression and splicing of IRF5, a transcription factor downstream of TLRs (Watters et al. 2007; Kawai and Akira 2010) and which has been shown to be important in human M1 macrophage polarisation (Krausgruber et al. 2011). The increased expression of IRF5 in stenosing plaque compared with intimal thickening also supports an interferon-gene expression signature in advanced atherosclerosis (Mancl et al. 2005; Cunninghame Graham et al. 2007), which was seen in the multi-analyte profiling analysis of symptomatic atheroma cell culture supernatants.

The concept of atherosclerosis as a passive accumulation of lipid in the arterial wall is considered outdated and has been superseded by an acute acknowledgement of the role played by inflammation in this most active of conditions (Ross 1999). Lipids, including cholesterol crystals, have been shown to activate PRRs (Duewell et al. 2010) and hence been implicated as endogenous ligands triggering the innate immune response. The finding by lipidomic analysis that the lipid profile of undiseased artery differs from that of atherosclerosis, and that stable and unstable areas of atherosclerosis may be separated by principal components analysis (PCA) is in keeping with lipids contributing to the pro-inflammatory drive within the plaque. Cholesteryl esters (CEs), a lipid class which contributed to the difference between the lipid profiles with advancing arterial disease, are a manifestation of vascular cholesterol found as lysosomal or cytosolic droplets (Shio et al. 1979) as would be seen in the foam cell macrophage phenotype. The importance of the lipidic compartment of atherosclerosis is once again seen in the results of the metabolic profiling, with PCA of the organic fraction showing

clustering of symptomatic plaques and separation of this cluster from asymptomatic atherosclerosis.

In addition to the results of multi-analyte profiling ('secretomics'), transcriptomics, lipidomics and metabonomics, proteomics identified almost 2,500 proteins, 159 of which differed significantly between symptomatic and asymptomatic atherosclerosis, and a large proportion of these found to be new to carotid atherosclerosis research. Interestingly, comparing male and females showed a greater degree of difference in protein abundance than based upon symptomatic status. The latter may contribute to the difference in clinical behaviour between carotid plaques in male and female individuals (Halliday et al. 2004). The utility of a systems biology approach, at multiple levels in the biological synthetic pathway, with human atherosclerosis tissue as the research substrate has been shown in separating early from advanced, and stable from unstable atherosclerosis. The role of bioinformatics in the analysis and interpretation of the large amount of data generated is evident. Furthermore, systems biology, as an exploratory tool, has been useful in the generation of hypotheses for further investigation. Beyond analyte identification and validation of findings, the 'omics' have been able to generate putative biomarkers of atherosclerosis burden for confirmation in clinical studies (Abdul-Salam et al. 2010).

Lysosyme, initially identified by MALDI-TOF mass spectrometry in plasma samples from patients with angiographically proven coronary artery disease, was measured in patients with carotid stenosis. The lysozyme measured is thought to be inactivated by foam cell myeloperoxidase (Schaffner et al. 1980), hence reflecting inflammation. Proteomic analysis revealed that myeloperoxidase levels were significantly higher in the salt extracts of symptomatic compared with asymptomatic atherosclerosis. Both arterial and venous plasma lysozyme levels were greater in patients with carotid stenosis than controls, and arterial plasma lysozyme was able to distinguish based on symptomatic status. Arterial plasma lysozyme ROC AUC for symptomatic status was 0.69 and was driven by a sub-group of symptomatic patients with very high levels. Although it is hoped that a single circulating biomarker will be sufficient to identify high risk individuals, it is more likely that a panel of uncorrelated molecules (Gerszten and Wang 2008). Similarly, the approach to risk stratification should be holistic, accounting for clinical factors, imaging features and circulating biomarkers, as well as patient choice and perception of risk.

These findings support the use of hybrid structural-functional imaging, and the utility and use of a systems biology approach in identifying significantly different and biologically relevant variations in atherosclerosis tissue, and in hypothesis generation for further study. The data

presented concurs with recent reports in the literature which link the lipidic/organic component of atherosclerosis with the generation of a pro-inflammatory plaque microenvironment prone to lesion development, instability and the complications thereof. The importance of innate immunity has been highlighted with the demonstration of a predominance of M1 macrophage polarisation and evidence of Th17/IL17 signalling in unstable atherosclerosis. It is hoped that this work will contribute to the ongoing refinement of multi-factorial risk stratification in carotid atherosclerosis.

8.1 CONCLUDING COMMENTS

- ^{11}C-PK11195 PET allowed the non-invasive detection and quantification of intraplaque inflammation in patients with carotid stenoses and, when combined with CTA provided an integrated assessment of plaque structure, composition and biological activity. ^{11}C-PK11195 PET/CT distinguished between recently symptomatic vulnerable plaques and asymptomatic plaques with a high positive predictive value.
- D-CEUS and LP-CEUS (at a cut-off of zero) was able to distinguish symptomatic and asymptomatic plaques. The utility in distinguishing based upon symptomatic status was improved by combining both techniques to achieve a carotid CEUS 'score'.
- Atheroma cell culture and supernatant MAP revealed that symptomatic human atherosclerotic carotid disease is associated with a cytokine, chemokine pattern consistent with the predominance of pro-inflammatory M1-type macrophage polarisation.
- IFNγ signatures are observed, including the novel finding of CCL20 with its significant elevation in symptomatic atherosclerosis.
- MAP of supernatants from patients who had undergone ipsilateral carotid LP-CEUS revealed significantly higher levels of interleukin 6, MMP1 and MMP3, as well as greater CD68 (macrophages) and CD31 (neovascularisation) immunopositivity by quantitative immunohistochemistry, in those with high (≥0) compared with low (<0) LP-CEUS signal. This suggests that LP-CEUS was able to reflect plaque biological attributes associated with unstable atherosclerosis.
- Transcriptomic analysis was able to able to clearly separate stenosing plaque and intimal thickening, as well as unstable and stable atherosclerosis based on messenger RNA profile, and was also able to generate a hypothesis based upon the finding of differential expression and alternative splicing of IRF5 between stenosing plaque and intimal thickening.
- Proteomic analysis of the salt extract fraction from carotid atherosclerotic plaques identified 2,470 proteins implicated in 33 bio-molecular functions and having their origins

previously described in 14 different cellular compartments. There were 159 proteins which, based upon the number of assigned spectra, were significantly different between symptomatic and asymptomatic atherosclerosis.

- Through lipidomic analysis, 150 lipid species from 9 different classes were identified, of which 24 were exclusive to atherosclerotic plaques. A comparison of 28 carotid endarterectomy specimens revealed lipid signatures of symptomatic compared with asymptomatic lesions, as well as stable and unstable plaque areas.
- Metabolite profiling by LC-MS analysis of organic plaque extract was able to separate symptomatic from asymptomatic atherosclerosis.
- These findings support the utility and use of a systems biology approach in indentifying significantly different and biologically relevant variations in atherosclerosis tissue, and in hypothesis generation for further study.
- The data supports recent reports in the literature which link the lipidic/organic component of atherosclerosis with the generation of a pro-inflammatory plaque microenvironment prone to lesion development, instability and the complications thereof.
- Levels of arterial and venous plasma lysozyme (initially identified as a candidate biomarker by proteomic analysis) were seen to distinguish individuals with carotid atherosclerosis from matched control subjects. Furthermore, arterial plasma lysozyme levels were significantly higher in patients with symptomatic than asymptomatic carotid stenosis.
- It is unlikely that, in the near future at least, a single modality will alone be adequate in the risk stratification of asymptomatic carotid stenosis. However, it is hoped that a refined multi-factorial approach will be developed using clinical, structural and functional imaging, and biochemical parameters; this may take the form of an effective and validated scoring system.

9 FUTURE WORK

9.1 Future Directions for Contrast Enhanced Ultrasound

9.1.1 Contrast Ultrasound for Stroke Prediction (CUSP)

As part of the ongoing validation of the CEUS in carotid risk stratification, ethical approval has been granted and funding obtained for a prospective study in asymptomatic carotid stenosis. This will allow exploration of the natural history of the CEUS signal by rescanning at annual intervals, including looking at the effect of pharmacotherapies, such as statin usage, on signal change. Primarily, evidence as regards the utility of CEUS signal upon entry into the study to predict outcomes will be generated. This Contrast Ultrasound for Stroke Prediction (CUSP) study (http://www1.imperial.ac.uk/surgeryandcancer/divisionofsurgery/clinical_themes/vascular/research/cusp/) aims to follow asymptomatic carotid stenosis patients for up to 2 years (Figure 79).

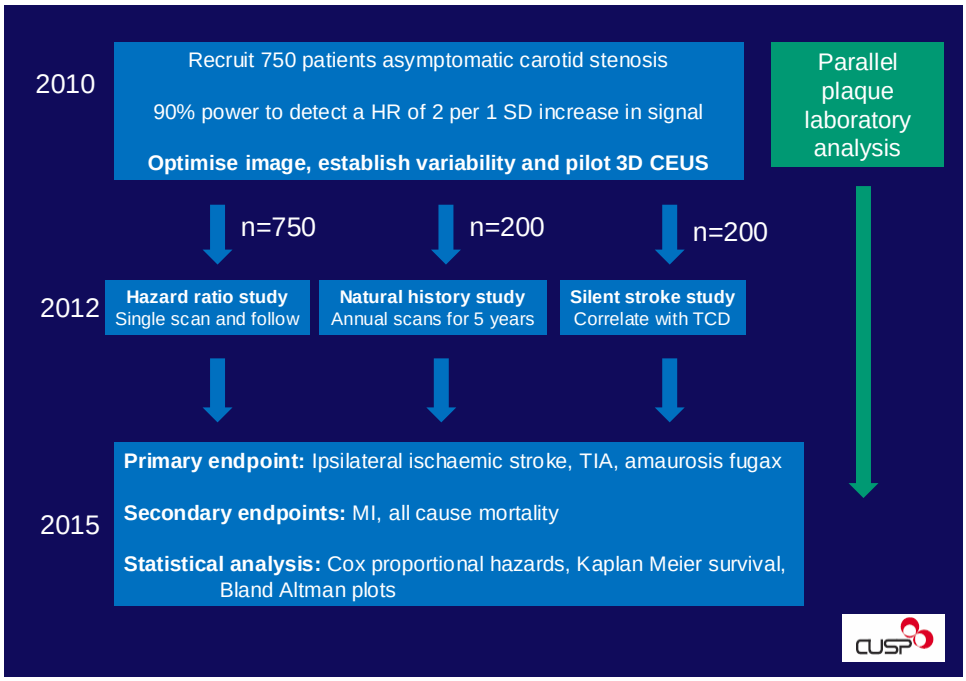


Figure 79 Contrast Ultrasound for Stroke Prediction (CUSP) study design

3D CEUS, 3-dimensional contrast enhanced ultrasound; HR, hazard ratio; MI, myocardial infarction; SD, standard deviation; TCD, trans-cranial Doppler; TIA, transient ischaemic attack.

The results of the CUSP study will confirm the signal cut off when deciding which asymptomatic patients to intervene on. This cut off may then be employed in a randomised trial to see if intervening on patients based upon CEUS signal can alter overall morbidity and mortality in asymptomatic carotid stenosis.

9.1.2 3-Dimensional Contrast Enhanced Ultrasound

The carotid plaque has been imaged in 3-dimensions (3D) with unenhanced ultrasound (Landry et al. 2004; Nanayakkara et al. 2009). The development of contrast modes on high frequency 3D transducers offers the opportunity to image carotid plaques in their entirety during a single microbubble acquisition. This potentially addresses two issues: out of plane motion for which there is no solution in 2-dimensional (2D) CEUS bar the exclusion of affected frames; and the false assumption that the single slice imaged by 2D CEUS is representative of the entire inhomogeneous plaque. As it is practically impossible to select the same plaque slice for imaging over two sessions using 2D CEUS, 3D imaging should improve reproducibility and monitoring of therapy. As described in the CUSP study design (Figure 79), it is planned that 3D CEUS will be piloted. There are a number of platforms and probe designs for consideration. The GE Logiq E9 system allows a static 3D acquisition (Figure 80), hence may be appropriate for LP-CEUS. Philips are developing matrix probes which allow real-time simultaneous multiple plane imaging.

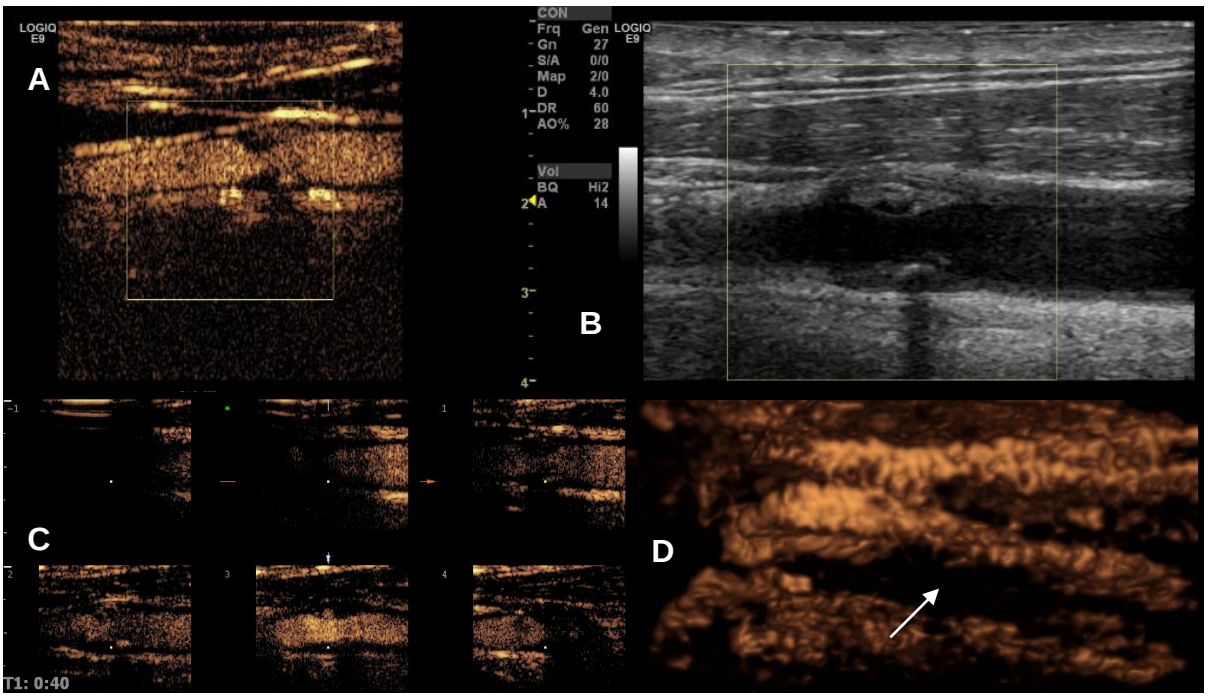


Figure 80 3-dimensional contrast enhanced ultrasound

Using a GE Logiq E9 system 2-dimensional contrast enhanced (A) and B mode (B) imaging is demonstrated. 3-dimensional contrast enhanced ultrasound represented as multiple longitudinal sections 1 mm apart (C) or as a rendered reconstruction (D) of cylindrical carotid lumen with plaque shown as a filling defect (arrow).

9.1.3 Advances in Microbubble Technology

Smaller microbubbles may have the facility to more readily enter the vasa vasorum, be retained by activated endothelium, and phagocytosed by macrophages. Furthermore, microbubbles need to be developed with increased longevity and stability, including stability to standard low MI imaging. Current microbubbles are used as blood pool agents because, for all intents and purposes, they remain in the vascular space. However, over time they have been shown to be *passively* taken up by macrophages, such as Kupffer cells in the liver, with the rate of phagocytosis being a function of their shell's constituents (Yanagisawa et al. 2007). Conjugation of microbubbles with ligands creates the possibility of *actively* targeting to specific molecules accessible from the vascular space. Microbubbles containing sialyl-Lewis X have been used to bind selectins (Villanueva et al. 2007). Kaufmann *et al* have quantified vascular inflammatory changes occurring at different stages of murine atherosclerosis utilising microbubbles targeted to vascular cell adhesion molecule-1 (VCAM-1) (Kaufmann et al. 2007). Similarly, microbubbles have been surface conjugated with the disintegrin echistatin which binds to α_V- and $\alpha_5\beta_1$-integrins expressed by the endothelium of neovessels (Leong-Poi et al. 2005). These tailored microbubbles have been used to assess endogenous and fibroblast growth factor-2-induced therapeutic neovascularisation in a rodent model of hindlimb ischaemia. Such molecular imaging with targeted microbubbles offers the possibility of early pharmacodynamic readouts for drugs in development, assisting drug discovery in the field of vascular inflammation.

9.1.4 Combining Diagnosis and Therapeutic Drug Delivery

In addition to imaging, microbubbles may have a future role in enhancing selectivity for delivery of therapeutics. Ultrasound itself can improve uptake of drugs by causing cavitation in the local cell membrane or increasing capillary permeability, but the energy levels required to do so exceed safety limits (Tinkov et al. 2008). However, by using ultrasound to destroy microbubbles (ultrasound targeted microbubble destruction (UTMD)) the amount of energy required to create these local pores is reduced to within acceptable limits. Moreover, if microbubbles are loaded with a drug of interest, either on their surface or within the shell, UTMD can further improve the selectivity of the drug delivery system (Tsutsui et al. 2004a; Tsutsui et al. 2004c; Tinkov et al. 2008).

9.2 Future Work in Molecular and Cellular Characterisation of Atherosclerosis

I hope to be involved in ongoing work within our group in relation to characterising, at a molecular and cellular level, advanced and unstable atherosclerosis. To take forward the

results generated by multi-analyte profiling, I will be examining mRNA expression in carotid plaque tissue from the same CEA specimens as those for atheroma cell culture and Luminex. This will employ microfluidic card arrays with TaqMan probes (Applied Biosystems) to examine a bespoke panel of 95 transcripts described as distinguishing M1 and M2 macrophages in humans (Martinez et al. 2006; Krausgruber et al. 2011). These arrays also include IRF5 which will allow examination of the role of this transcription factor in the context of our MAP findings. It will also serve to contribute to the validation of the differential expression of IRF5 in advanced atherosclerosis by exon-level analysis. Further validation of the different splice variants using probes specific to the different isoforms will also be necessary, as will validation of other key analytes found to be differentially expressed or spliced on the candidate list. The transcriptomic data will be subject to Ingenuity Pathway Analysis in a fashion similar to the MAP data to highlight the top canonical pathways involved in atherosclerosis progression on a broader transcriptional scale.

It is also hoped that the utility of proteomic analysis will be supported by validation of the candidate proteins by Western blotting and immunohistochemistry. The analysis of guanidine extracts of the plaque extracellular matrix and, subsequently, the complicated SDS extracts from in intracellular compartment will allow dissection of the mechanisms underlying plaque progression and destabilising in increments of increasing complexity; the SDS extracts are likely to require separation on two-dimensional gels prior to analysis in view of the expected protein mix.

In addition to optimising and undertaking MALDI-MS imaging to localise metabolites of interest within atherosclerotic plaque sections in a process akin to ‘virtual histology’, data generated by LC-MS of the aqueous metabolite extract will also be analysed. Subsequent to this there will be a period of metabolite identification. The transition of this technology into the arena of biomarkers will be taken by examining biofluids (plasma and urine) in the same manner as the plaque tissue metabolite extracts. The analysis to date has informed that, in this context, LC-MS appears to have a better ability to discriminate than NMR spectroscopy.

REFERENCES

Abdul-Salam, V. B., P. Ramrakha, U. Krishnan, D. R. Owen, J. Shalhoub, A. H. Davies, T. Y. Tang, J. H. Gillard, J. J. Boyle, M. R. Wilkins and R. J. Edwards (2010). "Identification and assessment of plasma lysozyme as a putative biomarker of atherosclerosis." *Arterioscler Thromb Vasc Biol* **30**(5): 1027-33.

ACAS (1995). "Endarterectomy for asymptomatic carotid artery stenosis. Executive Committee for the Asymptomatic Carotid Atherosclerosis Study." *JAMA* **273**(18): 1421-8.

Adamson, J., A. Beswick and S. Ebrahim (2004). "Is stroke the most common cause of disability?" *J Stroke Cerebrovasc Dis* **13**(4): 171-7.

Ahmed, R. M., J. P. Harris, C. S. Anderson, V. Makeham and G. M. Halmagyi (2010). "Carotid endarterectomy for symptomatic, but "haemodynamically insignificant" carotid stenosis." *Eur J Vasc Endovasc Surg* **40**(4): 475-82.

Ahn, Y. T., B. Huang, L. McPherson, C. Clayberger and A. M. Krensky (2007). "Dynamic interplay of transcriptional machinery and chromatin regulates "late" expression of the chemokine RANTES in T lymphocytes." *Mol Cell Biol* **27**(1): 253-66.

Alpern-Elran, H., N. Morog, F. Robert, G. Hoover, N. Kalant and S. Brem (1989). "Angiogenic activity of the atherosclerotic carotid artery plaque." *J Neurosurg* **70**(6): 942-5.

Alsheikh-Ali, A. A., G. D. Kitsios, E. M. Balk, J. Lau and S. Ip (2010). "The vulnerable atherosclerotic plaque: scope of the literature." *Ann Intern Med* **153**(6): 387-95.

Ancuta, P., R. Rao, A. Moses, A. Mehle, S. Shaw, F. Luscinskas and D. Gabuzda (2003). "Fractalkine preferentially mediates arrest and migration of CD16+ monocytes." *J Exp Med* **197**(12): 1701-7.

Archacki, S. and Q. Wang (2004). "Expression profiling of cardiovascular disease." *Hum Genomics* **1**(5): 355-70.

Archacki, S. R., G. Angheloiu, X. L. Tian, F. L. Tan, N. DiPaola, G. Q. Shen, C. Moravec, S. Ellis, E. J. Topol and Q. Wang (2003). "Identification of new genes differentially expressed in coronary artery disease by expression profiling." *Physiol Genomics* **15**(1): 65-74.

Archacki, S. R. and Q. K. Wang (2006). "Microarray analysis of cardiovascular diseases." *Methods Mol Med* **129**: 1-13.

Archie, J. P. (2010). "Comments regarding 'Carotid endarterectomy for symptomatic, but "haemodynamically insignificant" carotid stenosis'." *Eur J Vasc Endovasc Surg* **40**(4): 483-4.

Ardans, J. A., A. P. Economou, J. M. Martinson, Jr., M. Zhou and L. M. Wahl (2002). "Oxidized low-density and high-density lipoproteins regulate the production of matrix metalloproteinase-1 and -9 by activated monocytes." *J Leukoc Biol* **71**(6): 1012-8.

Asea, A., M. Rehli, E. Kabingu, J. A. Boch, O. Bare, P. E. Auron, M. A. Stevenson and S. K. Calderwood (2002). "Novel signal transduction pathway utilized by extracellular HSP70: role of toll-like receptor (TLR) 2 and TLR4." *J Biol Chem* **277**(17): 15028-34.

Ashida, K., K. Miyazaki, E. Takayama, H. Tsujimoto, M. Ayaori, T. Yakushiji, N. Iwamoto, A. Yonemura, K. Isoda, H. Mochizuki, H. Hiraide, M. Kusuhara and F. Ohsuzu (2005). "Characterization of the expression of TLR2 (toll-like receptor 2) and TLR4 on circulating monocytes in coronary artery disease." *J Atheroscler Thromb* **12**(1): 53-60.

Auffray, C., M. H. Sieweke and F. Geissmann (2009). "Blood monocytes: development, heterogeneity, and relationship with dendritic cells." *Annu Rev Immunol* **27**: 669-92.

Averkiou, M., M. Lampaskis, K. Kyriakopoulou, D. Skarlos, G. Klouvas, C. Strouthos and E. Leen (2010). "Quantification of tumor microvascularity with respiratory gated contrast enhanced ultrasound for monitoring therapy." *Ultrasound Med Biol* **36**(1): 68-77.

Bae, Y. S., J. H. Lee, S. H. Choi, S. Kim, F. Almazan, J. L. Witztum and Y. I. Miller (2009). "Macrophages generate reactive oxygen species in response to minimally oxidized low-density lipoprotein: toll-like receptor 4- and spleen tyrosine kinase-dependent activation of NADPH oxidase 2." *Circ Res* **104**(2): 210-8, 21p following 218.

Bagnato, C., J. Thumar, V. Mayya, S. I. Hwang, H. Zebroski, K. P. Claffey, C. Haudenschild, J. K. Eng, D. H. Lundgren and D. K. Han (2007). "Proteomics analysis of human coronary atherosclerotic plaque: a feasibility study of direct tissue proteomics by liquid chromatography and tandem mass spectrometry." *Mol Cell Proteomics* **6**(6): 1088-102.

Banati, R. B., G. W. Goerres, R. Myers, R. N. Gunn, F. E. Turkheimer, G. W. Kreutzberg, D. J. Brooks, T. Jones and J. S. Duncan (1999). "[11C](R)-PK11195 positron emission tomography imaging of activated microglia in vivo in Rasmussen's encephalitis." *Neurology* **53**(9): 2199-203.

Banati, R. B., J. Newcombe, R. N. Gunn, A. Cagnin, F. Turkheimer, F. Heppner, G. Price, F. Wegner, G. Giovannoni, D. H. Miller, G. D. Perkin, T. Smith, A. K. Hewson, G. Bydder, G. W. Kreutzberg, T. Jones, M. L. Cuzner and R. Myers (2000). "The peripheral benzodiazepine binding site in the brain in multiple sclerosis: quantitative in vivo imaging of microglia as a measure of disease activity." *Brain* **123 (Pt 11)**: 2321-37.

Bar-Or, A., R. K. Nuttall, M. Duddy, A. Alter, H. J. Kim, I. Ifergan, C. J. Pennington, P. Bourgoin, D. R. Edwards and V. W. Yong (2003). "Analyses of all matrix metalloproteinase members in leukocytes emphasize monocytes as major inflammatory mediators in multiple sclerosis." *Brain* **126**(Pt 12): 2738-49.

Barabasi, A. L. and Z. N. Oltvai (2004). "Network biology: understanding the cell's functional organization." *Nat Rev Genet* **5**(2): 101-13.

Bassand, J. P., C. W. Hamm, D. Ardissino, E. Boersma, A. Budaj, F. Fernandez-Aviles, K. A. Fox, D. Hasdai, E. M. Ohman, L. Wallentin and W. Wijns (2007). "Guidelines for the diagnosis and treatment of non-ST-segment elevation acute coronary syndromes." *Eur Heart J* **28**(13): 1598-660.

Beckonert, O., M. Coen, H. C. Keun, Y. Wang, T. M. Ebbels, E. Holmes, J. C. Lindon and J. K. Nicholson (2010). "High-resolution magic-angle-spinning NMR spectroscopy for metabolic profiling of intact tissues." *Nat Protoc* **5**(6): 1019-32.

Beckonert, O., H. C. Keun, T. M. Ebbels, J. Bundy, E. Holmes, J. C. Lindon and J. K. Nicholson (2007). "Metabolic profiling, metabolomic and metabonomic procedures for NMR spectroscopy of urine, plasma, serum and tissue extracts." *Nat Protoc* **2**(11): 2692-703.

Ben-Haim, S., E. Kupzov, A. Tamir and O. Israel (2004). "Evaluation of 18F-FDG uptake and arterial wall calcifications using 18F-FDG PET/CT." *J Nucl Med* **45**(11): 1816-21.

Bendeck, M. P., N. Zempo, A. W. Clowes, R. E. Galardy and M. A. Reidy (1994). "Smooth muscle cell migration and matrix metalloproteinase expression after arterial injury in the rat." *Circ Res* **75**(3): 539-45.

Biasi, G. M., A. Froio, E. B. Diethrich, G. Deleo, S. Galimberti, P. Mingazzini, A. N. Nicolaides, M. Griffin, D. Raithel, D. B. Reid and M. G. Valsecchi (2004). "Carotid plaque echolucency increases the risk of stroke in carotid stenting: the Imaging in Carotid Angioplasty and Risk of Stroke (ICAROS) study." *Circulation* **110**(6): 756-62.

Biasucci, L. M., A. Vitelli, G. Liuzzo, S. Altamura, G. Caligiuri, C. Monaco, A. G. Rebuzzi, G. Ciliberto and A. Maseri (1996). "Elevated levels of interleukin-6 in unstable angina." *Circulation* **94**(5): 874-7.

Bijnens, A. P., E. Lutgens, T. Ayoubi, J. Kuiper, A. J. Horrevoets and M. J. Daemen (2006). "Genome-wide expression studies of atherosclerosis: critical issues in methodology, analysis, interpretation of transcriptomics data." *Arterioscler Thromb Vasc Biol* **26**(6): 1226-35.

Biller, J., W. M. Feinberg, J. E. Castaldo, A. D. Whittemore, R. E. Harbaugh, R. J. Dempsey, L. R. Caplan, T. F. Kresowik, D. B. Matchar, J. F. Toole, J. D. Easton, H. P. Adams, Jr., L. M. Brass, R. W. Hobson, 2nd, T. G. Brott and L. Sternau (1998). "Guidelines for carotid endarterectomy: a statement for healthcare professionals from a Special Writing Group of the Stroke Council, American Heart Association." *Circulation* **97**(5): 501-9.

Biragyn, A., P. A. Ruffini, C. A. Leifer, E. Klyushnenkova, A. Shakhov, O. Chertov, A. K. Shirakawa, J. M. Farber, D. M. Segal, J. J. Oppenheim and L. W. Kwak (2002). "Toll-like receptor 4-dependent activation of dendritic cells by beta-defensin 2." *Science* **298**(5595): 1025-9.

Bird, J. L., D. Izquierdo-Garcia, J. R. Davies, J. H. Rudd, K. C. Probst, N. Figg, J. C. Clark, P. L. Weissberg, A. P. Davenport and E. A. Warburton (2010). "Evaluation of translocator protein quantification as a tool for characterising macrophage burden in human carotid atherosclerosis." *Atherosclerosis* **210**(2): 388-91.

Bjorkbacka, H., V. V. Kunjathoor, K. J. Moore, S. Koehn, C. M. Ordija, M. A. Lee, T. Means, K. Halmen, A. D. Luster, D. T. Golenbock and M. W. Freeman (2004). "Reduced atherosclerosis in MyD88-null mice links elevated serum cholesterol levels to activation of innate immunity signaling pathways." *Nat Med* **10**(4): 416-21.

Bland, J. M. and D. G. Altman (1986). "Statistical methods for assessing agreement between two methods of clinical measurement." *Lancet* **1**(8476): 307-10.

Blondel, V. B., J. L. Guillaume, R. Lambiotte and E. Lefebvre (2008). "Fast unfolding of communities in large networks." *J Stat Mech* **2008**: P10008.

Bongartz, G., S. Golding and A. Jurik (2004). "European Guidelines for Multislice Computed Tomography: Appendix C. Funded by the European Commission."

Bonita, R. and R. Beaglehole (1988). "Recovery of motor function after stroke." *Stroke* **19**(12): 1497-500.

Boring, L., J. Gosling, M. Cleary and I. F. Charo (1998). "Decreased lesion formation in CCR2-/- mice reveals a role for chemokines in the initiation of atherosclerosis." *Nature* **394**(6696): 894-7.

Bouhlel, M. A., B. Derudas, E. Rigamonti, R. Dievart, J. Brozek, S. Haulon, C. Zawadzki, B. Jude, G. Torpier, N. Marx, B. Staels and G. Chinetti-Gbaguidi (2007). "PPARgamma activation primes human monocytes into alternative M2 macrophages with anti-inflammatory properties." *Cell Metab* **6**(2): 137-43.

Boule, M. W., C. Broughton, F. Mackay, S. Akira, A. Marshak-Rothstein and I. R. Rifkin (2004). "Toll-like receptor 9-dependent and -independent dendritic cell activation by chromatin-immunoglobulin G complexes." *J Exp Med* **199**(12): 1631-40.

Boyle, J. J. (1997). "Association of coronary plaque rupture and atherosclerotic inflammation." *J Pathol* **181**(1): 93-9.

Boyle, J. J., H. A. Harrington, E. Piper, K. Elderfield, J. Stark, R. C. Landis and D. O. Haskard (2009). "Coronary intraplaque hemorrhage evokes a novel atheroprotective macrophage phenotype." *Am J Pathol* **174**(3): 1097-108.

Bracco (2005). SonoVue. Summary of Product Characteristics.

Braestrup, C. and R. F. Squires (1977). "Specific benzodiazepine receptors in rat brain characterized by high-affinity (3H)diazepam binding." *Proc Natl Acad Sci U S A* **74**(9): 3805-9.

Braunersreuther, V., A. Zernecke, C. Arnaud, E. A. Liehn, S. Steffens, E. Shagdarsuren, K. Bidzhekov, F. Burger, G. Pelli, B. Luckow, F. Mach and C. Weber (2007). "Ccr5 but not Ccr1 deficiency reduces development of diet-induced atherosclerosis in mice." *Arterioscler Thromb Vasc Biol* **27**(2): 373-9.

Briard, E., S. S. Zoghbi, F. G. Simeon, M. Imaizumi, J. P. Gourley, H. U. Shetty, S. Lu, M. Fujita, R. B. Innis and V. W. Pike (2009). "Single-step high-yield radiosynthesis and evaluation of a sensitive 18F-labeled ligand for imaging brain peripheral benzodiazepine receptors with PET." *J Med Chem* **52**(3): 688-99.

Brindle, J. T., H. Antti, E. Holmes, G. Tranter, J. K. Nicholson, H. W. Bethell, S. Clarke, P. M. Schofield, E. McKilligin, D. E. Mosedale and D. J. Grainger (2002). "Rapid and

noninvasive diagnosis of the presence and severity of coronary heart disease using 1H-NMR-based metabonomics." *Nat Med* **8**(12): 1439-44.

Broekhuizen, L. N., H. L. Mooij, J. J. Kastelein, E. S. Stroes, H. Vink and M. Nieuwdorp (2009). "Endothelial glycocalyx as potential diagnostic and therapeutic target in cardiovascular disease." *Curr Opin Lipidol* **20**(1): 57-62.

Brown, A. J., S. L. Leong, R. T. Dean and W. Jessup (1997). "7-Hydroperoxycholesterol and its products in oxidized low density lipoprotein and human atherosclerotic plaque." *J Lipid Res* **38**(9): 1730-45.

Brugger, B., G. Erben, R. Sandhoff, F. T. Wieland and W. D. Lehmann (1997). "Quantitative analysis of biological membrane lipids at the low picomole level by nano-electrospray ionization tandem mass spectrometry." *Proc Natl Acad Sci U S A* **94**(6): 2339-44.

Bunch, J., M. R. Clench and D. S. Richards (2004). "Determination of pharmaceutical compounds in skin by imaging matrix-assisted laser desorption/ionisation mass spectrometry." *Rapid Commun Mass Spectrom* **18**(24): 3051-60.

Burns, K., F. Martinon and J. Tschopp (2003). "New insights into the mechanism of IL-1beta maturation." *Curr Opin Immunol* **15**(1): 26-30.

Burrell, M., C. Earnshaw and M. Clench (2007). "Imaging Matrix Assisted Laser Desorption Ionization Mass Spectrometry: a technique to map plant metabolites within tissues at high spatial resolution." *J Exp Bot* **58**(4): 757-63.

Canat, X., P. Carayon, M. Bouaboula, D. Cahard, D. Shire, C. Roque, G. Le Fur and P. Casellas (1993a). "Distribution profile and properties of peripheral-type benzodiazepine receptors on human hemopoietic cells." *Life Sci* **52**(1): 107-18.

Canat, X., A. Guillaumont, M. Bouaboula, C. Poinot-Chazel, J. M. Derocq, P. Carayon, G. LeFur and P. Casellas (1993b). "Peripheral benzodiazepine receptor modulation with phagocyte differentiation." *Biochem Pharmacol* **46**(3): 551-4.

Cappendijk, V. C., K. B. Cleutjens, S. Heeneman, G. W. Schurink, R. J. Welten, A. G. Kessels, R. J. van Suylen, M. J. Daemen, J. M. van Engelshoven and M. E. Kooi (2004). "In vivo detection of hemorrhage in human atherosclerotic plaques with magnetic resonance imaging." *J Magn Reson Imaging* **20**(1): 105-10.

Caro, C. G. (2009). "Discovery of the role of wall shear in atherosclerosis." *Arterioscler Thromb Vasc Biol* **29**(2): 158-61.

Carpenter, K. L., S. E. Taylor, J. A. Ballantine, B. Fussell, B. Halliwell and M. J. Mitchinson (1993). "Lipids and oxidised lipids in human atheroma and normal aorta." *Biochim Biophys Acta* **1167**(2): 121-30.

Carpenter, K. L., S. E. Taylor, C. van der Veen, B. K. Williamson, J. A. Ballantine and M. J. Mitchinson (1995). "Lipids and oxidised lipids in human atherosclerotic lesions at different stages of development." *Biochim Biophys Acta* **1256**(2): 141-50.

Carpenter, K. L., G. M. Wilkins, B. Fussell, J. A. Ballantine, S. E. Taylor, M. J. Mitchinson and D. S. Leake (1994). "Production of oxidized lipids during modification of low-density lipoprotein by macrophages or copper." *Biochem J* **304 (Pt 2)**: 625-33.

Cavusoglu, E., C. Eng, V. Chopra, L. T. Clark, D. J. Pinsky and J. D. Marmur (2007). "Low plasma RANTES levels are an independent predictor of cardiac mortality in patients referred for coronary angiography." *Arterioscler Thromb Vasc Biol* **27**(4): 929-35.

CCGC (2011). "Association between C reactive protein and coronary heart disease: mendelian randomisation analysis based on individual participant data." *BMJ* **342**: d548.

Celletti, F. L., J. M. Waugh, P. G. Amabile, A. Brendolan, P. R. Hilfiker and M. D. Dake (2001). "Vascular endothelial growth factor enhances atherosclerotic plaque progression." *Nat Med* **7**(4): 425-9.

Chabaud, M., G. Page and P. Miossec (2001). "Enhancing effect of IL-1, IL-17, and TNF-alpha on macrophage inflammatory protein-3alpha production in rheumatoid arthritis: regulation by soluble receptors and Th2 cytokines." *J Immunol* **167**(10): 6015-20.

Chambers, B. R. and G. A. Donnan (2005). "Carotid endarterectomy for asymptomatic carotid stenosis." *Cochrane Database Syst Rev*(4): CD001923.

Chase, A. J., M. Bond, M. F. Crook and A. C. Newby (2002). "Role of nuclear factor-kappa B activation in metalloproteinase-1, -3, and -9 secretion by human macrophages in vitro and rabbit foam cells produced in vivo." *Arterioscler Thromb Vasc Biol* **22**(5): 765-71.

Chavan, V., N. Patil and N. D. Karnik (2007). "Study of leukocytic hydrolytic enzymes in patients with acute stage of coronary heart disease." *Indian J Med Sci* **61**(2): 73-82.

Chen, X., L. Liu, G. Palacios, J. Gao, N. Zhang, G. Li, J. Lu, T. Song, Y. Zhang and H. Lv (2010). "Plasma metabolomics reveals biomarkers of the atherosclerosis." *J Sep Sci* **33**(17-18): 2776-83.

Chen, Y. X., Y. Nakashima, K. Tanaka, S. Shiraishi, K. Nakagawa and K. Sueishi (1999). "Immunohistochemical expression of vascular endothelial growth factor/vascular permeability factor in atherosclerotic intimas of human coronary arteries." *Arterioscler Thromb Vasc Biol* **19**(1): 131-9.

Cheng, C., D. Tempel, R. van Haperen, H. C. de Boer, D. Segers, M. Huisman, A. J. van Zonneveld, P. J. Leenen, A. van der Steen, P. W. Serruys, R. de Crom and R. Krams (2007). "Shear stress-induced changes in atherosclerotic plaque composition are modulated by chemokines." *J Clin Invest* **117**(3): 616-26.

Cheng, C., D. Tempel, R. van Haperen, A. van der Baan, F. Grosveld, M. J. Daemen, R. Krams and R. de Crom (2006). "Atherosclerotic lesion size and vulnerability are determined by patterns of fluid shear stress." *Circulation* **113**(23): 2744-53.

Cheng, N., R. He, J. Tian, P. Ye and R. Ye (2008). "Cutting edge: TLR2 is a functional receptor for acute-phase serum amyloid A." *J Immunol* **181**(1): 22-6.

Chevrel, G., P. Garnero and P. Miossec (2002). "Addition of interleukin 1 (IL1) and IL17 soluble receptors to a tumour necrosis factor alpha soluble receptor more effectively reduces the production of IL6 and macrophage inhibitory protein-3alpha and increases that of collagen in an in vitro model of rheumatoid synoviocyte activation." *Ann Rheum Dis* **61**(8): 730-3.

Chinetti-Gbaguidi, G., M. Baron, M. A. Bouhlel, J. Vanhoutte, C. Copin, Y. Sebti, B. Derudas, T. Mayi, G. Bories, A. Tailleux, S. Haulon, C. Zawadzki, B. Jude and B. Staels (2011). "Human Atherosclerotic Plaque Alternative Macrophages Display Low Cholesterol Handling but High Phagocytosis Because of Distinct Activities of the PPAR{gamma} and LXRα Pathways." *Circ Res*.

Chinetti, G., J. C. Fruchart and B. Staels (2000). "Peroxisome proliferator-activated receptors (PPARs): nuclear receptors at the crossroads between lipid metabolism and inflammation." *Inflamm Res* **49**(10): 497-505.

Choi, S., R. Harkewicz, J. Lee, A. Boullier, F. Almazan, A. Li, J. Witztum, Y. Bae and Y. Miller (2009). "Lipoprotein accumulation in macrophages via toll-like receptor-4-dependent fluid phase uptake." *Circ Res* **104**(12): 1355-63.

Clayton, T. A., J. C. Lindon, O. Cloarec, H. Antti, C. Charuel, G. Hanton, J. P. Provost, J. L. Le Net, D. Baker, R. J. Walley, J. R. Everett and J. K. Nicholson (2006). "Pharmaco-metabonomic phenotyping and personalized drug treatment." *Nature* **440**(7087): 1073-7.

Coen, M., E. Holmes, J. C. Lindon and J. K. Nicholson (2008). "NMR-based metabolic profiling and metabonomic approaches to problems in molecular toxicology." *Chem Res Toxicol* **21**(1): 9-27.

Cole, J. E., E. Georgiou and C. Monaco (2010). "The Expression and Functions of Toll-Like Receptors in Atherosclerosis." *Mediators of Inflammation*.

Cole, J. E., T. J. Navin, A. J. Cross, M. E. Goddard, L. Alexopoulou, A. T. Mitra, A. H. Davies, R. A. Flavell, M. Feldmann and C. Monaco (2011). "From the Cover: Unexpected protective role for Toll-like receptor 3 in the arterial wall." *Proc Natl Acad Sci U S A* **108**(6): 2372-7.

Coli, S., M. Magnoni, G. Sangiorgi, M. M. Marrocco-Trischitta, G. Melisurgo, A. Mauriello, L. Spagnoli, R. Chiesa, D. Cianflone and A. Maseri (2008). "Contrast-enhanced ultrasound imaging of intraplaque neovascularization in carotid arteries: correlation with histology and plaque echogenicity." *J Am Coll Cardiol* **52**(3): 223-30.

Combadiere, C., S. Potteaux, J. L. Gao, B. Esposito, S. Casanova, E. J. Lee, P. Debre, A. Tedgui, P. M. Murphy and Z. Mallat (2003). "Decreased atherosclerotic lesion formation in CX3CR1/apolipoprotein E double knockout mice." *Circulation* **107**(7): 1009-16.

Combadiere, C., S. Potteaux, M. Rodero, T. Simon, A. Pezard, B. Esposito, R. Merval, A. Proudfoot, A. Tedgui and Z. Mallat (2008). "Combined inhibition of CCL2, CX3CR1, and CCR5 abrogates Ly6C(hi) and Ly6C(lo) monocytosis and almost abolishes atherosclerosis in hypercholesterolemic mice." *Circulation* **117**(13): 1649-57.

Cordeiro-da-Silva, A., J. Tavares, N. Araujo, F. Cerqueira, A. Tomas, P. Kong Thoo Lin and A. Ouaissi (2004). "Immunological alterations induced by polyamine derivatives on murine splenocytes and human mononuclear cells." *Int Immunopharmacol* **4**(4): 547-56.

Correll, P. H., A. Iwama, S. Tondat, G. Mayrhofer, T. Suda and A. Bernstein (1997). "Deregulated inflammatory response in mice lacking the STK/RON receptor tyrosine kinase." *Genes Funct* **1**(1): 69-83.

Cosgrove, D. (2006). "Ultrasound contrast agents: an overview." *Eur J Radiol* **60**(3): 324-30.

Coste, A., M. Dubourdeau, M. D. Linas, S. Cassaing, J. C. Lepert, P. Balard, S. Chalmeton, J. Bernad, C. Orfila, J. P. Seguela and B. Pipy (2003). "PPARgamma promotes mannose receptor gene expression in murine macrophages and contributes to the induction of this receptor by IL-13." *Immunity* **19**(3): 329-39.

Craven, T. E., J. E. Ryu, M. A. Espeland, F. R. Kahl, W. M. McKinney, J. F. Toole, M. R. McMahan, C. J. Thompson, G. Heiss and J. R. Crouse, 3rd (1990). "Evaluation of the associations between carotid artery atherosclerosis and coronary artery stenosis. A case-control study." *Circulation* **82**(4): 1230-42.

Crawford, E. S., M. E. DeBakey, H. E. Garrett and J. Howell (1966). "Surgical treatment of occlusive cerebrovascular disease." *Surg Clin North Am* **46**(4): 873-84.

Crea, F. and F. Andreotti (2009). "The unstable plaque: a broken balance." *Eur Heart J* **30**(15): 1821-3.

Cunninghame Graham, D. S., H. Manku, S. Wagner, J. Reid, K. Timms, A. Gutin, J. S. Lanchbury and T. J. Vyse (2007). "Association of IRF5 in UK SLE families identifies a variant involved in polyadenylation." *Hum Mol Genet* **16**(6): 579-91.

Danilkovitch, A. and E. J. Leonard (1999). "Kinases involved in MSP/RON signaling." *J Leukoc Biol* **65**(3): 345-8.

Davies, A. H., I. J. Franklin, J. Shalhoub and A. Thapar (2010a). "Refining selection for revascularisation in asymptomatic carotid stenosis is the key. Rapid Response to: Is there a role for revascularisation in asymptomatic carotid stenosis? No." *British Medical Journal*.

Davies, J. R., D. Izquierdo-Garcia, J. H. Rudd, N. Figg, H. K. Richards, J. L. Bird, F. I. Aigbirhio, A. P. Davenport, P. L. Weissberg, T. D. Fryer and E. A. Warburton (2010b). "FDG-PET can distinguish inflamed from non-inflamed plaque in an animal model of atherosclerosis." *Int J Cardiovasc Imaging* **26**(1): 41-8.

Davies, M. J., P. D. Richardson, N. Woolf, D. R. Katz and J. Mann (1993). "Risk of thrombosis in human atherosclerotic plaques: role of extracellular lipid, macrophage, and smooth muscle cell content." *Br Heart J* **69**(5): 377-81.

Davis, B., G. Koster, L. J. Douet, M. Scigelova, G. Woffendin, J. M. Ward, A. Smith, J. Humphries, K. G. Burnand, C. H. Macphee and A. D. Postle (2008). "Electrospray ionization mass spectrometry identifies substrates and products of lipoprotein-associated phospholipase A2 in oxidized human low density lipoprotein." *J Biol Chem* **283**(10): 6428-37.

Dawson, T. C., W. A. Kuziel, T. A. Osahar and N. Maeda (1999). "Absence of CC chemokine receptor-2 reduces atherosclerosis in apolipoprotein E-deficient mice." *Atherosclerosis* **143**(1): 205-11.

de Boer, O. J., A. C. van der Wal, P. Teeling and A. E. Becker (1999). "Leucocyte recruitment in rupture prone regions of lipid-rich plaques: a prominent role for neovascularization?" *Cardiovasc Res* **41**(2): 443-9.

de Kleijn, D. P., F. L. Moll, W. E. Hellings, G. Ozsarlak-Sozer, P. de Bruin, P. A. Doevendans, A. Vink, L. M. Catanzariti, A. H. Schoneveld, A. Algra, M. J. Daemen, E. A. Biessen, W. de Jager, H. Zhang, J. P. de Vries, E. Falk, S. K. Lim, P. J. van der Spek, S. K. Sze and G. Pasterkamp (2010). "Local atherosclerotic plaques are a source of prognostic biomarkers for adverse cardiovascular events." *Arterioscler Thromb Vasc Biol* **30**(3): 612-9.

De Vos, R. C., S. Moco, A. Lommen, J. J. Keurentjes, R. J. Bino and R. D. Hall (2007). "Untargeted large-scale plant metabolomics using liquid chromatography coupled to mass spectrometry." *Nat Protoc* **2**(4): 778-91.

de Weert, T. T., M. Ouhlous, E. Meijering, P. E. Zondervan, J. M. Hendriks, M. R. van Sambeek, D. W. Dippel and A. van der Lugt (2006). "In vivo characterization and quantification of atherosclerotic carotid plaque components with multidetector computed tomography and histopathological correlation." *Arterioscler Thromb Vasc Biol* **26**(10): 2366-72.

Debakey, M. E., E. S. Crawford, D. A. Cooley, G. C. Morris, Jr., H. E. Garret and W. S. Fields (1965). "Cerebral Arterial Insufficiency: One to 11-Year Results Following Arterial Reconstructive Operation." *Ann Surg* **161**: 921-45.

Degirolamo, C., G. S. Shelness and L. L. Rudel (2009). "LDL cholesteryl oleate as a predictor for atherosclerosis: evidence from human and animal studies on dietary fat." *J Lipid Res* **50 Suppl**: S434-9.

Devlin, C. M., G. Kuriakose, E. Hirsch and I. Tabas (2002). "Genetic alterations of IL-1 receptor antagonist in mice affect plasma cholesterol level and foam cell lesion size." *Proc Natl Acad Sci U S A* **99**(9): 6280-5.

Dewberry, R., H. Holden, D. Crossman and S. Francis (2000). "Interleukin-1 receptor antagonist expression in human endothelial cells and atherosclerosis." *Arterioscler Thromb Vasc Biol* **20**(11): 2394-400.

Didangelos, A., D. Simper, C. Monaco and M. Mayr (2009). "Proteomics of acute coronary syndromes." *Curr Atheroscler Rep* **11**(3): 188-95.

Didangelos, A., X. Yin, K. Mandal, M. Baumert, M. Jahangiri and M. Mayr (2010). "Proteomics characterization of extracellular space components in the human aorta." *Mol Cell Proteomics* **9**(9): 2048-62.

Dijkmans, P. A., C. A. Visser and O. Kamp (2005). "Adverse reactions to ultrasound contrast agents: is the risk worth the benefit?" *Eur J Echocardiogr* **6**(5): 363-6.

Doyle, B. and N. Caplice (2007). "Plaque neovascularization and antiangiogenic therapy for atherosclerosis." *J Am Coll Cardiol* **49**(21): 2073-80.

Dreze, M., B. Charloteaux, S. Milstein, P. O. Vidalain, M. A. Yildirim, Q. Zhong, N. Svrzikapa, V. Romero, G. Laloux, R. Brasseur, J. Vandenhaute, M. Boxem, M. E. Cusick, D. E. Hill and M. Vidal (2009). "'Edgetic' perturbation of a C. elegans BCL2 ortholog." *Nat Methods* **6**(11): 843-9.

Duewell, P., H. Kono, K. J. Rayner, C. M. Sirois, G. Vladimer, F. G. Bauernfeind, G. S. Abela, L. Franchi, G. Nunez, M. Schnurr, T. Espevik, E. Lien, K. A. Fitzgerald, K. L. Rock, K. J. Moore, S. D. Wright, V. Hornung and E. Latz (2010). "NLRP3 inflammasomes are required for atherogenesis and activated by cholesterol crystals." *Nature* **464**(7293): 1357-61.

Dunmore, B. J., M. J. McCarthy, A. R. Naylor and N. P. Brindle (2007). "Carotid plaque instability and ischemic symptoms are linked to immaturity of microvessels within plaques." *J Vasc Surg* **45**(1): 155-9.

Eastcott, H. H. G., G. W. Pickering and C. Rob (1954). "Reconstruction of internal carotid artery in a patient with intermittent attacks of hemiplegia." *Lancet* **2**: 994–996.

ECST (1991). "MRC European Carotid Surgery Trial: interim results for symptomatic patients with severe (70-99%) or with mild (0-29%) carotid stenosis. European Carotid Surgery Trialists' Collaborative Group." *Lancet* **337**(8752): 1235-43.

Edfeldt, K., J. Swedenborg, G. Hansson and Z. Yan (2002). "Expression of toll-like receptors in human atherosclerotic lesions: a possible pathway for plaque activation." *Circulation* **105**(10): 1158-61.

Eid, R. E., D. A. Rao, J. Zhou, S. F. Lo, H. Ranjbaran, A. Gallo, S. I. Sokol, S. Pfau, J. S. Pober and G. Tellides (2009). "Interleukin-17 and interferon-gamma are produced concomitantly by human coronary artery-infiltrating T cells and act synergistically on vascular smooth muscle cells." *Circulation* **119**(10): 1424-32.

Einstein, A. J., K. W. Moser, R. C. Thompson, M. D. Cerqueira and M. J. Henzlova (2007). "Radiation dose to patients from cardiac diagnostic imaging." *Circulation* **116**(11): 1290-305.

Eisenstein, R., S. E. Larsson, K. E. Kuettner, N. Sorgente and V. C. Hascal (1975). "The ground substance of the arterial wall. Part 1. Extractability of glycosaminoglycans and the isolation of a proteoglycan from bovine aorta." *Atherosclerosis* **22**(1): 1-17.

el-Barghouty, N., G. Geroulakos, A. Nicolaides, A. Androulakis and V. Bahal (1995). "Computer-assisted carotid plaque characterisation." *Eur J Vasc Endovasc Surg* **9**(4): 389-93.

el-Barghouty, N., A. Nicolaides, V. Bahal, G. Geroulakos and A. Androulakis (1996a). "The identification of the high risk carotid plaque." *Eur J Vasc Endovasc Surg* **11**(4): 470-8.

El-Barghouty, N. M., T. Levine, S. Ladva, A. Flanagan and A. Nicolaides (1996b). "Histological verification of computerised carotid plaque characterisation." *Eur J Vasc Endovasc Surg* **11**(4): 414-6.

Elhage, R., J. Jawien, M. Rudling, H. G. Ljunggren, K. Takeda, S. Akira, F. Bayard and G. K. Hansson (2003). "Reduced atherosclerosis in interleukin-18 deficient apolipoprotein E-knockout mice." *Cardiovasc Res* **59**(1): 234-40.

ESCT (1998). "Randomised trial of endarterectomy for recently symptomatic carotid stenosis: final results of the MRC European Carotid Surgery Trial (ECST)." *Lancet* **351**(9113): 1379-87.

Faber, B. C., K. B. Cleutjens, R. L. Niessen, P. L. Aarts, W. Boon, A. S. Greenberg, P. J. Kitslaar, J. H. Tordoir and M. J. Daemen (2001). "Identification of genes potentially involved in rupture of human atherosclerotic plaques." *Circ Res* **89**(6): 547-54.

Fabunmi, R. P., G. K. Sukhova, S. Sugiyama and P. Libby (1998). "Expression of tissue inhibitor of metalloproteinases-3 in human atheroma and regulation in lesion-associated cells: a potential protective mechanism in plaque stability." *Circ Res* **83**(3): 270-8.

Fadok, V. A., D. L. Bratton, A. Konowal, P. W. Freed, J. Y. Westcott and P. M. Henson (1998). "Macrophages that have ingested apoptotic cells in vitro inhibit proinflammatory cytokine production through autocrine/paracrine mechanisms involving TGF-beta, PGE2, and PAF." *J Clin Invest* **101**(4): 890-8.

Falk, E., P. K. Shah and V. Fuster (1995). "Coronary plaque disruption." *Circulation* **92**(3): 657-71.

Fernandez, A. Z. (2008). "Peroxisome proliferator-activated receptors in the modulation of the immune/inflammatory response in atherosclerosis." *PPAR Res* **2008**: 285842.

Filis, K. A., F. R. Arko, B. L. Johnson, Pipinos, II, E. J. Harris, C. t. Olcott and C. K. Zarins (2002). "Duplex ultrasound criteria for defining the severity of carotid stenosis." *Ann Vasc Surg* **16**(4): 413-21.

Fleiner, M., M. Kummer, M. Mirlacher, G. Sauter, G. Cathomas, R. Krapf and B. C. Biedermann (2004). "Arterial neovascularization and inflammation in vulnerable patients: early and late signs of symptomatic atherosclerosis." *Circulation* **110**(18): 2843-50.

Fleming, T. J., C. O'HUigin and T. R. Malek (1993). "Characterization of two novel Ly-6 genes. Protein sequence and potential structural similarity to alpha-bungarotoxin and other neurotoxins." *J Immunol* **150**(12): 5379-90.

Florian, J. A., J. R. Kosky, K. Ainslie, Z. Pang, R. O. Dull and J. M. Tarbell (2003). "Heparan sulfate proteoglycan is a mechanosensor on endothelial cells." *Circ Res* **93**(10): e136-42.

Folch, J., M. Lees and G. H. Sloane Stanley (1957). "A simple method for the isolation and purification of total lipides from animal tissues." *J Biol Chem* **226**(1): 497-509.

Forough, R., N. Koyama, D. Hasenstab, H. Lea, M. Clowes, S. T. Nikkari and A. W. Clowes (1996). "Overexpression of tissue inhibitor of matrix metalloproteinase-1 inhibits vascular smooth muscle cell functions in vitro and in vivo." *Circ Res* **79**(4): 812-20.

Fraser, A. G. and F. D. Dunstan (2010). "On the impossibility of being expert." *BMJ* **341**: c6815.

Fu, S., H. Zhao, J. Shi, A. Abzhanov, K. Crawford, L. Ohno-Machado, J. Zhou, Y. Du, W. P. Kuo, J. Zhang, M. Jiang and J. G. Jin (2008). "Peripheral arterial occlusive disease: global gene expression analyses suggest a major role for immune and inflammatory responses." *BMC Genomics* **9**: 369.

Fujimura, Y., P. M. Hwang, H. Trout Iii, L. Kozloff, M. Imaizumi, R. B. Innis and M. Fujita (2008a). "Increased peripheral benzodiazepine receptors in arterial plaque of patients with atherosclerosis: An autoradiographic study with [(3)H]PK 11195." *Atherosclerosis*.

Fujimura, Y., P. M. Hwang, H. Trout Iii, L. Kozloff, M. Imaizumi, R. B. Innis and M. Fujita (2008b). "Increased peripheral benzodiazepine receptors in arterial plaque of patients with atherosclerosis: an autoradiographic study with [(3)H]PK 11195." *Atherosclerosis* **201**(1): 108-11.

Full, L., C. Ruisanchez and C. Monaco (2009). "The inextricable link between atherosclerosis and prototypical inflammatory diseases rheumatoid arthritis and systemic lupus erythematosus." *Arthritis Res Ther* **11**(2): 217.

Full, L. E. (2010). Proteomic Characterisation of Vascular Smooth Muscle Cells in Atherosclerosis. *Cytokine Biology of Atherosclerosis, Kennedy Institute of Rheumatology*. London, Imperial College London. **PhD**.

Funk, J., K. Feingold, A. Moser and C. Grunfeld (1993). "Lipopolysaccharide stimulation of RAW 264.7 macrophages induces lipid accumulation and foam cell formation." *Atherosclerosis* **98**(1): 67-82.

Galis, Z. S., M. Muszynski, G. K. Sukhova, E. Simon-Morrissey, E. N. Unemori, M. W. Lark, E. Amento and P. Libby (1994a). "Cytokine-stimulated human vascular smooth muscle cells synthesize a complement of enzymes required for extracellular matrix digestion." *Circ Res* **75**(1): 181-9.

Galis, Z. S., G. K. Sukhova, M. W. Lark and P. Libby (1994b). "Increased expression of matrix metalloproteinases and matrix degrading activity in vulnerable regions of human atherosclerotic plaques." *J Clin Invest* **94**(6): 2493-503.

Gautier, E. L., C. Jakubzick and G. J. Randolph (2009). "Regulation of the migration and survival of monocyte subsets by chemokine receptors and its relevance to atherosclerosis." *Arterioscler Thromb Vasc Biol* **29**(10): 1412-8.

Geiringer, E. (1951). "Intimal vascularization and atherosclerosis." *J Pathol Bacteriol* **63**(2): 201-11.

Geissmann, F., S. Gordon, D. A. Hume, A. M. Mowat and G. J. Randolph (2010a). "Unravelling mononuclear phagocyte heterogeneity." *Nat Rev Immunol* **10**(6): 453-60.

Geissmann, F., S. Jung and D. R. Littman (2003). "Blood monocytes consist of two principal subsets with distinct migratory properties." *Immunity* **19**(1): 71-82.

Geissmann, F., M. G. Manz, S. Jung, M. H. Sieweke, M. Merad and K. Ley (2010b). "Development of monocytes, macrophages, and dendritic cells." *Science* **327**(5966): 656-61.

Geng, H., H. Lu, L. Zhang, H. Zhang, L. Zhou, H. Wang and R. Zhong (2006). "Increased expression of Toll like receptor 4 on peripheral-blood mononuclear cells in patients with coronary arteriosclerosis disease." *Clin Exp Immunol* **143**(2): 269-73.

Gerber, J. S. and D. M. Mosser (2001). "Reversing lipopolysaccharide toxicity by ligating the macrophage Fc gamma receptors." *J Immunol* **166**(11): 6861-8.

Gerszten, R. E. and T. J. Wang (2008). "The search for new cardiovascular biomarkers." *Nature* **451**(7181): 949-52.

Giannoni, M. F., E. Vicenzini, M. Citone, M. C. Ricciardi, L. Irace, A. Laurito, L. F. Scucchi, V. Di Piero, B. Gossetti, A. Mauriello, L. G. Spagnoli, G. L. Lenzi and F. B. Valentini (2009). "Contrast carotid ultrasound for the detection of unstable plaques with neoangiogenesis: a pilot study." *Eur J Vasc Endovasc Surg* **37**(6): 722-7.

Glass, C. K. and J. L. Witztum (2001). "Atherosclerosis. the road ahead." *Cell* **104**(4): 503-16.

Glatz, T., I. Stock, M. Nguyen-Ngoc, P. Gohlke, T. Herdegen, J. Culman and Y. Zhao (2010). "Peroxisome-proliferator-activated receptors gamma and peroxisome-proliferator-activated receptors beta/delta and the regulation of interleukin 1 receptor antagonist expression by pioglitazone in ischaemic brain." *J Hypertens* **28**(7): 1488-97.

Gleissner, C. A., I. Shaked, K. M. Little and K. Ley (2010). "CXC chemokine ligand 4 induces a unique transcriptome in monocyte-derived macrophages." *J Immunol* **184**(9): 4810-8.

Goonewardena, S. N., L. E. Prevette and A. A. Desai (2010). "Metabolomics and atherosclerosis." *Curr Atheroscler Rep* **12**(4): 267-72.

Gordon, S. (2003). "Alternative activation of macrophages." *Nat Rev Immunol* **3**(1): 23-35.

Gordon, S. (2007). "The macrophage: past, present and future." *Eur J Immunol* **37 Suppl 1**: S9-17.

Gordon, S. and F. O. Martinez (2010). "Alternative activation of macrophages: mechanism and functions." *Immunity* **32**(5): 593-604.

Gordon, S. and P. R. Taylor (2005). "Monocyte and macrophage heterogeneity." *Nat Rev Immunol* **5**(12): 953-64.

Grabner, R., K. Lotzer, S. Dopping, M. Hildner, D. Radke, M. Beer, R. Spanbroek, B. Lippert, C. A. Reardon, G. S. Getz, Y. X. Fu, T. Hehlgans, R. E. Mebius, M. van der Wall, D. Kruspe, C. Englert, A. Lovas, D. Hu, G. J. Randolph, F. Weih and A. J. Habenicht (2009). "Lymphotoxin beta receptor signaling promotes tertiary lymphoid organogenesis in the aorta adventitia of aged ApoE-/- mice." *J Exp Med* **206**(1): 233-48.

Graebe, M., S. F. Pedersen, L. Borgwardt, L. Hojgaard, H. Sillesen and A. Kjaer (2009). "Molecular pathology in vulnerable carotid plaques: correlation with [18]-fluorodeoxyglucose positron emission tomography (FDG-PET)." *Eur J Vasc Endovasc Surg* **37**(6): 714-21.

Graessler, J., D. Schwudke, P. E. Schwarz, R. Herzog, A. Shevchenko and S. R. Bornstein (2009). "Top-down lipidomics reveals ether lipid deficiency in blood plasma of hypertensive patients." *PLoS One* **4**(7): e6261.

Graham, R. R., S. V. Kozyrev, E. C. Baechler, M. V. Reddy, R. M. Plenge, J. W. Bauer, W. A. Ortmann, T. Koeuth, M. F. Gonzalez Escribano, B. Pons-Estel, M. Petri, M. Daly, P. K. Gregersen, J. Martin, D. Altshuler, T. W. Behrens and M. E. Alarcon-Riquelme (2006). "A common haplotype of interferon regulatory factor 5 (IRF5) regulates splicing and expression and is associated with increased risk of systemic lupus erythematosus." *Nat Genet* **38**(5): 550-5.

Graham, R. R., C. Kyogoku, S. Sigurdsson, I. A. Vlasova, L. R. Davies, E. C. Baechler, R. M. Plenge, T. Koeuth, W. A. Ortmann, G. Hom, J. W. Bauer, C. Gillett, N. Burtt, D. S. Cunninghame Graham, R. Onofrio, M. Petri, I. Gunnarsson, E. Svenungsson, L. Ronnblom, G. Nordmark, P. K. Gregersen, K. Moser, P. M. Gaffney, L. A. Criswell, T. J. Vyse, A. C. Syvanen, P. R. Bohjanen, M. J. Daly, T. W. Behrens and D. Altshuler (2007). "Three functional variants of IFN regulatory factor 5 (IRF5) define risk and protective haplotypes for human lupus." *Proc Natl Acad Sci U S A* **104**(16): 6758-63.

Granada, J. F. and S. B. Feinstein (2008). "Imaging of the vasa vasorum." *Nat Clin Pract Cardiovasc Med* **5 Suppl 2**: S18-25.

Grant, E. G., C. B. Benson, G. L. Moneta, A. V. Alexandrov, J. D. Baker, E. I. Bluth, B. A. Carroll, M. Eliasziw, J. Gocke, B. S. Hertzberg, S. Katanick, L. Needleman, J. Pellerito, J. F. Polak, K. S. Rholl, D. L. Wooster and R. E. Zierler (2003). "Carotid artery stenosis: gray-scale and Doppler US diagnosis--Society of Radiologists in Ultrasound Consensus Conference." *Radiology* **229**(2): 340-6.

Gray-Weale, A. C., J. C. Graham, J. R. Burnett, K. Byrne and R. J. Lusby (1988). "Carotid artery atheroma: comparison of preoperative B-mode ultrasound appearance with carotid endarterectomy specimen pathology." *J Cardiovasc Surg (Torino)* **29**(6): 676-81.

Grogan, J. K., W. E. Shaalan, H. Cheng, B. Gewertz, T. Desai, G. Schwarze, S. Glagov, L. Lozanski, A. Griffin, M. Castilla and H. S. Bassiouny (2005). "B-mode ultrasonographic characterization of carotid atherosclerotic plaques in symptomatic and asymptomatic patients." *J Vasc Surg* **42**(3): 435-41.

Gronholdt, M. L., B. G. Nordestgaard, J. Bentzon, B. M. Wiebe, J. Zhou, E. Falk and H. Sillesen (2002). "Macrophages are associated with lipid-rich carotid artery plaques, echolucency on B-mode imaging, and elevated plasma lipid levels." *J Vasc Surg* **35**(1): 137-45.

Gronholdt, M. L., B. G. Nordestgaard, T. V. Schroeder, S. Vorstrup and H. Sillesen (2001). "Ultrasonic echolucent carotid plaques predict future strokes." *Circulation* **104**(1): 68-73.

Gronholdt, M. L., B. G. Nordestgaard, B. M. Wiebe, J. E. Wilhjelm and H. Sillesen (1998). "Echo-lucency of computerized ultrasound images of carotid atherosclerotic plaques are associated with increased levels of triglyceride-rich lipoproteins as well as increased plaque lipid content." *Circulation* **97**(1): 34-40.

Gronholdt, M. L., B. M. Wiebe, H. Laursen, T. G. Nielsen, T. V. Schroeder and H. Sillesen (1997). "Lipid-rich carotid artery plaques appear echolucent on ultrasound B-mode images and may be associated with intraplaque haemorrhage." *Eur J Vasc Endovasc Surg* **14**(6): 439-45.

Gu, L., Y. Okada, S. K. Clinton, C. Gerard, G. K. Sukhova, P. Libby and B. J. Rollins (1998). "Absence of monocyte chemoattractant protein-1 reduces atherosclerosis in low density lipoprotein receptor-deficient mice." *Mol Cell* **2**(2): 275-81.

Guillot, L., V. Balloy, F. X. McCormack, D. T. Golenbock, M. Chignard and M. Si-Tahar (2002). "Cutting edge: the immunostimulatory activity of the lung surfactant protein-A involves Toll-like receptor 4." *J Immunol* **168**(12): 5989-92.

Gupta, S., A. M. Pablo, X. Jiang, N. Wang, A. R. Tall and C. Schindler (1997). "IFN-gamma potentiates atherosclerosis in ApoE knock-out mice." *J Clin Invest* **99**(11): 2752-61.

Haghighat, A., D. Weiss, M. K. Whalin, D. P. Cowan and W. R. Taylor (2007). "Granulocyte colony-stimulating factor and granulocyte macrophage colony-stimulating factor exacerbate atherosclerosis in apolipoprotein E-deficient mice." *Circulation* **115**(15): 2049-54.

Haimi, P., A. Uphoff, M. Hermansson and P. Somerharju (2006). "Software tools for analysis of mass spectrometric lipidome data." *Anal Chem* **78**(24): 8324-31.

Halliday, A., M. Harrison, E. Hayter, X. Kong, A. Mansfield, J. Marro, H. Pan, R. Peto, J. Potter, K. Rahimi, A. Rau, S. Robertson, J. Streifler and D. Thomas (2010). "10-year stroke prevention after successful carotid endarterectomy for asymptomatic stenosis (ACST-1): a multicentre randomised trial." *Lancet* **376**(9746): 1074-84.

Halliday, A., A. Mansfield, J. Marro, C. Peto, R. Peto, J. Potter and D. Thomas (2004). "Prevention of disabling and fatal strokes by successful carotid endarterectomy in patients without recent neurological symptoms: randomised controlled trial." *Lancet* **363**(9420): 1491-502.

Halvorsen, B., E. Heggen, T. Ueland, C. Smith, W. J. Sandberg, J. K. Damas, K. Otterdal, S. Tonstad and P. Aukrust (2010). "Treatment with the PPARgamma agonist rosiglitazone downregulates interleukin-1 receptor antagonist in individuals with metabolic syndrome." *Eur J Endocrinol* **162**(2): 267-73.

Hamilton, J. A. (1993). "Rheumatoid arthritis: opposing actions of haemopoietic growth factors and slow-acting anti-rheumatic drugs." *Lancet* **342**(8870): 536-9.

Hamilton, J. A. (2008). "Colony-stimulating factors in inflammation and autoimmunity." *Nat Rev Immunol* **8**(7): 533-44.

Han, X. and R. W. Gross (2003). "Global analyses of cellular lipidomes directly from crude extracts of biological samples by ESI mass spectrometry: a bridge to lipidomics." *J Lipid Res* **44**(6): 1071-9.

Han, X. and R. W. Gross (2005). "Shotgun lipidomics: electrospray ionization mass spectrometric analysis and quantitation of cellular lipidomes directly from crude extracts of biological samples." *Mass Spectrom Rev* **24**(3): 367-412.

Hansson, G. K. (2005). "Inflammation, atherosclerosis, and coronary artery disease." *N Engl J Med* **352**(16): 1685-95.

Hansson, G. K. (2008). "Atherosclerosis An immune disease: The Anitschkov Lecture 2007." *Atherosclerosis*: 1-9.

Haque, S., H. Mirjafari and I. N. Bruce (2008). "Atherosclerosis in rheumatoid arthritis and systemic lupus erythematosus." *Curr Opin Lipidol* **19**(4): 338-43.

Harrington, L. E., R. D. Hatton, P. R. Mangan, H. Turner, T. L. Murphy, K. M. Murphy and C. T. Weaver (2005). "Interleukin 17-producing CD4+ effector T cells develop via a lineage distinct from the T helper type 1 and 2 lineages." *Nat Immunol* **6**(11): 1123-32.

Hashimoto, S., T. Suzuki, H. Y. Dong, N. Yamazaki and K. Matsushima (1999). "Serial analysis of gene expression in human monocytes and macrophages." *Blood* **94**(3): 837-44.

Hausleiter, J., T. Meyer, F. Hermann, M. Hadamitzky, M. Krebs, T. C. Gerber, C. McCollough, S. Martinoff, A. Kastrati, A. Schomig and S. Achenbach (2009). "Estimated radiation dose associated with cardiac CT angiography." *JAMA* **301**(5): 500-7.

Hayward, J. K., A. H. Davies and P. M. Lamont (1995). "Carotid plaque morphology: a review." *Eur J Vasc Endovasc Surg* **9**(4): 368-74.

Heckemann, R. A., D. O. Cosgrove, M. J. Blomley, R. J. Eckersley, C. J. Harvey and Y. Mine (2000). "Liver lesions: intermittent second-harmonic gray-scale US can increase conspicuity with microbubble contrast material-early experience." *Radiology* **216**(2): 592-6.

Heilbronn, L. K. and L. V. Campbell (2008). "Adipose tissue macrophages, low grade inflammation and insulin resistance in human obesity." *Curr Pharm Des* **14**(12): 1225-30.

Heinecke, J. W. (1999). "Mechanisms of oxidative damage by myeloperoxidase in atherosclerosis and other inflammatory disorders." *J Lab Clin Med* **133**(4): 321-5.

Heller, E. A., E. Liu, A. M. Tager, Q. Yuan, A. Y. Lin, N. Ahluwalia, K. Jones, S. L. Koehn, V. M. Lok, E. Aikawa, K. J. Moore, A. D. Luster and R. E. Gerszten (2006). "Chemokine CXCL10 promotes atherogenesis by modulating the local balance of effector and regulatory T cells." *Circulation* **113**(19): 2301-12.

Henriksson, M., F. Lundgren and P. Carlsson (2008). "Cost-effectiveness of endarterectomy in patients with asymptomatic carotid artery stenosis." *Br J Surg* **95**(6): 714-20.

Herman, M. P., G. K. Sukhova, P. Libby, N. Gerdes, N. Tang, D. B. Horton, M. Kilbride, R. E. Breitbart, M. Chun and U. Schonbeck (2001). "Expression of neutrophil collagenase (matrix metalloproteinase-8) in human atheroma: a novel collagenolytic pathway suggested by transcriptional profiling." *Circulation* **104**(16): 1899-904.

Hetzel, M., D. Walcher, M. Grub, H. Bach, V. Hombach and N. Marx (2003). "Inhibition of MMP-9 expression by PPARgamma activators in human bronchial epithelial cells." *Thorax* **58**(9): 778-83.

Hiltunen, M. O., T. T. Tuomisto, M. Niemi, J. H. Brasen, T. T. Rissanen, P. Toronen, I. Vajanto and S. Yla-Herttuala (2002). "Changes in gene expression in atherosclerotic plaques analyzed using DNA array." *Atherosclerosis* **165**(1): 23-32.

Hirai, M. Y., M. Klein, Y. Fujikawa, M. Yano, D. B. Goodenowe, Y. Yamazaki, S. Kanaya, Y. Nakamura, M. Kitayama, H. Suzuki, N. Sakurai, D. Shibata, J. Tokuhisa, M. Reichelt, J. Gershenzon, J. Papenbrock and K. Saito (2005). "Elucidation of gene-to-gene and metabolite-to-gene networks in arabidopsis by integration of metabolomics and transcriptomics." *J Biol Chem* **280**(27): 25590-5.

Hirota, K., H. Yoshitomi, M. Hashimoto, S. Maeda, S. Teradaira, N. Sugimoto, T. Yamaguchi, T. Nomura, H. Ito, T. Nakamura, N. Sakaguchi and S. Sakaguchi (2007). "Preferential recruitment of CCR6-expressing Th17 cells to inflamed joints via CCL20 in rheumatoid arthritis and its animal model." *J Exp Med* **204**(12): 2803-12.

Hoebe, K., P. Georgel, S. Rutschmann, X. Du, S. Mudd, K. Crozat, S. Sovath, L. Shamel, T. Hartung, U. Zähringer and B. Beutler (2005). "CD36 is a sensor of diacylglycerides." *Nature* **433**(7025): 523-7.

Hoksbergen, A. W., D. A. Legemate, D. T. Ubbink and M. J. Jacobs (2000). "Collateral variations in circle of willis in atherosclerotic population assessed by means of transcranial color-coded duplex ultrasonography." *Stroke* **31**(7): 1656-60.

Holbrook, M. and C. E. Skilbeck (1983). "An activities index for use with stroke patients." *Age Ageing* **12**(2): 166-70.

Holmes, E., I. D. Wilson and J. K. Nicholson (2008). "Metabolic phenotyping in health and disease." *Cell* **134**(5): 714-7.

Holvoet, P., P. C. Davey, D. De Keyzer, M. Doukouré, E. Deridder, M.-L. Bochaton-Piallat, G. Gabbiani, E. Beaufort, K. Bishay, N. Andrieux, N. Benhabilès and G. Marguerie (2006). "Oxidized low-density lipoprotein correlates positively with toll-like receptor 2 and interferon regulatory factor-1 and inversely with superoxide dismutase-1 expression: studies in hypercholesterolemic swine and THP-1 cells." *Arterioscler Thromb Vasc Biol* **26**(7): 1558-65.

Howarth, S. P., T. Y. Tang, R. Trivedi, R. Weerakkody, U. K.-I. J, M. E. Gaunt, J. R. Boyle, Z. Y. Li, S. R. Miller, M. J. Graves and J. H. Gillard (2009). "Utility of USPIO-enhanced MR imaging to identify inflammation and the fibrous cap: a comparison of symptomatic and asymptomatic individuals." *Eur J Radiol* **70**(3): 555-60.

Hu, C., R. van der Heijden, M. Wang, J. van der Greef, T. Hankemeier and G. Xu (2009). "Analytical strategies in lipidomics and applications in disease biomarker discovery." *J Chromatogr B Analyt Technol Biomed Life Sci* **877**(26): 2836-46.

Ingersoll, M. A., R. Spanbroek, C. Lottaz, E. L. Gautier, M. Frankenberger, R. Hoffmann, R. Lang, M. Haniffa, M. Collin, F. Tacke, A. J. Habenicht, L. Ziegler-Heitbrock and G. J. Randolph (2010). "Comparison of gene expression profiles between human and mouse monocyte subsets." *Blood* **115**(3): e10-9.

Inzitari, D., M. Eliasziw, P. Gates, B. L. Sharpe, R. K. Chan, H. E. Meldrum and H. J. Barnett (2000). "The causes and risk of stroke in patients with asymptomatic internal-carotid-artery stenosis. North American Symptomatic Carotid Endarterectomy Trial Collaborators." *N Engl J Med* **342**(23): 1693-700.

Ishida, B. Y., P. J. Blanche, A. V. Nichols, M. Yashar and B. Paigen (1991). "Effects of atherogenic diet consumption on lipoproteins in mouse strains C57BL/6 and C3H." *J Lipid Res* **32**(4): 559-68.

Ishii, N., T. Matsumura, H. Kinoshita, K. Fukuda, H. Motoshima, T. Senokuchi, S. Nakao, A. Tsutsumi, S. Kim-Mitsuyama, T. Kawada, M. Takeya, N. Miyamura, T. Nishikawa and E. Araki (2010). "Nifedipine induces peroxisome proliferator-activated receptor-gamma activation in macrophages and suppresses the progression of atherosclerosis in apolipoprotein E-deficient mice." *Arterioscler Thromb Vasc Biol* **30**(8): 1598-605.

James, M. L., S. Selleri and M. Kassiou (2006). "Development of ligands for the peripheral benzodiazepine receptor." *Curr Med Chem* **13**(17): 1991-2001.

Jayasooriya, G. S., J. Shalhoub, A. Thapar and A. H. Davies (2011). "Patient preference survey in the management of asymptomatic carotid stenosis." *J Vasc Surg*.

Johnson, J. L. and A. C. Newby (2009). "Macrophage heterogeneity in atherosclerotic plaques." *Curr Opin Lipidol* **20**(5): 370-8.

Johnson, J. L., G. B. Sala-Newby, Y. Ismail, C. M. Aguilera and A. C. Newby (2008). "Low tissue inhibitor of metalloproteinases 3 and high matrix metalloproteinase 14 levels defines a subpopulation of highly invasive foam-cell macrophages." *Arterioscler Thromb Vasc Biol* **28**(9): 1647-53.

Jones, H. A., S. O. Valind, I. C. Clark, G. E. Bolden, T. Krausz, J. B. Schofield, A. R. Boobis and C. Haslett (2002). "Kinetics of lung macrophages monitored in vivo following particulate challenge in rabbits." *Toxicol Appl Pharmacol* **183**(1): 46-54.

Junqueira, L. C., G. Bignolas and R. R. Brentani (1979). "Picrosirius staining plus polarization microscopy, a specific method for collagen detection in tissue sections." *Histochem J* **11**(4): 447-55.

Kadl, A., A. K. Meher, P. R. Sharma, M. Y. Lee, A. C. Doran, S. R. Johnstone, M. R. Elliott, F. Gruber, J. Han, W. Chen, T. Kensler, K. S. Ravichandran, B. E. Isakson, B. R. Wamhoff and N. Leitinger (2010). "Identification of a novel macrophage phenotype that develops in response to atherogenic phospholipids via Nrf2." *Circ Res* **107**(6): 737-46.

Kakkos, S. K., M. Sabetai, T. Tegos, J. Stevens, D. Thomas, M. Griffin, G. Geroulakos and A. N. Nicolaides (2009). "Silent embolic infarcts on computed tomography brain scans and risk of ipsilateral hemispheric events in patients with asymptomatic internal carotid artery stenosis." *J Vasc Surg* **49**(4): 902-9.

Kamari, Y., A. Shaish, S. Shemesh, E. Vax, I. Grosskopf, S. Dotan, M. White, E. Voronov, C. A. Dinarello, R. N. Apte and D. Harats (2011). "Reduced atherosclerosis and inflammatory cytokines in apolipoprotein-E-deficient mice lacking bone marrow-derived interleukin-1alpha." *Biochem Biophys Res Commun* **405**(2): 197-203.

Kariko, K., H. Ni, J. Capodici, M. Lamphier and D. Weissman (2004). "mRNA is an endogenous ligand for Toll-like receptor 3." *J Biol Chem* **279**(13): 12542-50.

Kaufmann, B. A., J. M. Sanders, C. Davis, A. Xie, P. Aldred, I. J. Sarembock and J. R. Lindner (2007). "Molecular imaging of inflammation in atherosclerosis with targeted ultrasound detection of vascular cell adhesion molecule-1." *Circulation* **116**(3): 276-84.

Kawai, T. and S. Akira (2010). "The role of pattern-recognition receptors in innate immunity: update on Toll-like receptors." *Nat Immunol* **11**(5): 373-84.

Kawakami, A., M. Osaka, M. Aikawa, S. Uematsu, S. Akira, P. Libby, K. Shimokado, F. M. Sacks and M. Yoshida (2008). "Toll-like receptor 2 mediates apolipoprotein CIII-induced monocyte activation." *Circ Res* **103**(12): 1402-9.

Keller, A., A. I. Nesvizhskii, E. Kolker and R. Aebersold (2002). "Empirical statistical model to estimate the accuracy of peptide identifications made by MS/MS and database search." *Anal Chem* **74**(20): 5383-92.

Kertesz, V. and G. J. Van Berkel (2010). "Fully automated liquid extraction-based surface sampling and ionization using a chip-based robotic nanoelectrospray platform." *J Mass Spectrom* **45**(3): 252-60.

Kerwin, W., A. Hooker, M. Spilker, P. Vicini, M. Ferguson, T. Hatsukami and C. Yuan (2003). "Quantitative magnetic resonance imaging analysis of neovasculature volume in carotid atherosclerotic plaque." *Circulation* **107**(6): 851-6.

Khallou-Laschet, J., A. Varthaman, G. Fornasa, C. Compain, A. T. Gaston, M. Clement, M. Dussiot, O. Levillain, S. Graff-Dubois, A. Nicoletti and G. Caligiuri (2010). "Macrophage plasticity in experimental atherosclerosis." *PLoS One* **5**(1): e8852.

Kietselaer, B. L., C. P. Reutelingsperger, G. A. Heidendal, M. J. Daemen, W. H. Mess, L. Hofstra and J. Narula (2004). "Noninvasive detection of plaque instability with use of radiolabeled annexin A5 in patients with carotid-artery atherosclerosis." *N Engl J Med* **350**(14): 1472-3.

Kim, S., H. Takahashi, W. W. Lin, P. Descargues, S. Grivennikov, Y. Kim, J. L. Luo and M. Karin (2009). "Carcinoma-produced factors activate myeloid cells through TLR2 to stimulate metastasis." *Nature* **457**(7225): 102-6.

Kim, S. H., E. S. Lee, J. Y. Lee, B. S. Lee, J. E. Park and D. W. Moon (2010). "Multiplex coherent anti-stokes Raman spectroscopy images intact atheromatous lesions and

concomitantly identifies distinct chemical profiles of atherosclerotic lipids." *Circ Res* **106**(8): 1332-41.

Kim, S. R., K. S. Lee, H. S. Park, S. J. Park, K. H. Min, S. M. Jin and Y. C. Lee (2005). "Involvement of IL-10 in peroxisome proliferator-activated receptor gamma-mediated anti-inflammatory response in asthma." *Mol Pharmacol* **68**(6): 1568-75.

Kim, T. K., B. I. Choi, H. S. Hong, B. Y. Choi and J. K. Han (2000). "Improved imaging of hepatic metastases with delayed pulse inversion harmonic imaging using a contrast agent SH U 508A: preliminary study." *Ultrasound Med Biol* **26**(9): 1439-44.

Kim, T. W., M. Febbraio, P. Robinet, B. Dugar, D. Greene, A. Cerny, E. Latz, R. Gilmour, K. Staschke, G. Chisolm, P. L. Fox, P. E. Dicorleto, J. D. Smith and X. Li (2011). "The Critical Role of IL-1 Receptor-Associated Kinase 4-Mediated NF-{kappa}B Activation in Modified Low-Density Lipoprotein-Induced Inflammatory Gene Expression and Atherosclerosis." *J Immunol* **186**(5): 2871-80.

Kinahan, P. E. and J. G. Rogers (1989). "Analytic 3D image reconstruction using all detected events." *IEEE Trans Nucl Sci* **36**: 964-8.

Kirii, H., T. Niwa, Y. Yamada, H. Wada, K. Saito, Y. Iwakura, M. Asano, H. Moriwaki and M. Seishima (2003). "Lack of interleukin-1beta decreases the severity of atherosclerosis in ApoE-deficient mice." *Arterioscler Thromb Vasc Biol* **23**(4): 656-60.

Kodaira, Y., S. K. Nair, L. E. Wrenshall, E. Gilboa and J. L. Platt (2000). "Phenotypic and functional maturation of dendritic cells mediated by heparan sulfate." *J Immunol* **165**(3): 1599-604.

Koenig, W. and N. Khuseyinova (2007). "Biomarkers of atherosclerotic plaque instability and rupture." *Arterioscler Thromb Vasc Biol* **27**(1): 15-26.

Koga, M., H. Kai, H. Yasukawa, S. Kato, T. Yamamoto, Y. Kawai, K. Kusaba, Y. Seki, M. Kai, K. Egashira, Y. Kataoka and T. Imaizumi (2007a). "Postnatal blocking of interferon-gamma function prevented atherosclerotic plaque formation in apolipoprotein E-knockout mice." *Hypertens Res* **30**(3): 259-67.

Koga, M., H. Kai, H. Yasukawa, T. Yamamoto, Y. Kawai, S. Kato, K. Kusaba, M. Kai, K. Egashira, Y. Kataoka and T. Imaizumi (2007b). "Inhibition of progression and stabilization of plaques by postnatal interferon-gamma function blocking in ApoE-knockout mice." *Circ Res* **101**(4): 348-56.

Kono, Y., S. P. Pinnell, C. B. Sirlin, S. R. Sparks, B. Georgy, W. Wong and R. F. Mattrey (2004). "Carotid arteries: contrast-enhanced US angiography--preliminary clinical experience." *Radiology* **230**(2): 561-8.

Koutouzis, M., A. Nomikos, S. Nikolidakis, V. Tzavara, V. Andrikopoulos, N. Nikolaou, C. Barbatis and Z. S. Kyriakides (2007). "Statin treated patients have reduced intraplaque angiogenesis in carotid endarterectomy specimens." *Atherosclerosis* **192**(2): 457-63.

Kozyrev, S. V. and M. E. Alarcon-Riquelme (2007). "The genetics and biology of Irf5-mediated signaling in lupus." *Autoimmunity* **40**(8): 591-601.

Kraaijeveld, A. O., S. C. de Jager, W. J. de Jager, B. J. Prakken, S. R. McColl, I. Haspels, H. Putter, T. J. van Berkel, L. Nagelkerken, J. W. Jukema and E. A. Biessen (2007). "CC chemokine ligand-5 (CCL5/RANTES) and CC chemokine ligand-18 (CCL18/PARC) are specific markers of refractory unstable angina pectoris and are transiently raised during severe ischemic symptoms." *Circulation* **116**(17): 1931-41.

Krausgruber, T., K. Blazek, T. Smallie, S. Alzabin, H. Lockstone, N. Sahgal, T. Hussell, M. Feldmann and I. A. Udalova (2011). "IRF5 promotes inflammatory macrophage polarization and T(H)1-T(H)17 responses." *Nat Immunol* **12**(3): 231-8.

Kreider, T., R. M. Anthony, J. F. Urban, Jr. and W. C. Gause (2007). "Alternatively activated macrophages in helminth infections." *Curr Opin Immunol* **19**(4): 448-53.

Kropholler, M. A., R. Boellaard, E. H. Elzinga, C. J. van der Laken, K. Maruyama, R. W. Kloet, A. E. Voskuyl, B. A. Dijkmans and A. A. Lammertsma (2009). "Quantification of (R)-[11C]PK11195 binding in rheumatoid arthritis." *Eur J Nucl Med Mol Imaging* **36**(4): 624-31.

Kuwahata, S., S. Fujita, K. Orihara, S. Hamasaki, R. Oba, H. Hirai, K. Nagata, S. Ishida, T. Kataoka, N. Oketani, H. Ichiki, Y. Iriki, K. Saihara, H. Okui, Y. Ninomiya and C. Tei (2009). "High expression level of Toll-like receptor 2 on monocytes is an important risk factor for arteriosclerotic disease." *Atherosclerosis*.

Kuwana, M., Y. Okazaki, H. Kodama, K. Izumi, H. Yasuoka, Y. Ogawa, Y. Kawakami and Y. Ikeda (2003). "Human circulating CD14+ monocytes as a source of progenitors that exhibit mesenchymal cell differentiation." *J Leukoc Biol* **74**(5): 833-45.

Kuziel, W. A., T. C. Dawson, M. Quinones, E. Garavito, G. Chenaux, S. S. Ahuja, R. L. Reddick and N. Maeda (2003). "CCR5 deficiency is not protective in the early stages of atherogenesis in apoE knockout mice." *Atherosclerosis* **167**(1): 25-32.

Laitinen, I., P. Marjamaki, K. Nagren, V. J. Laine, I. Wilson, P. Leppanen, S. Yla-Herttuala, A. Roivainen and J. Knuuti (2009). "Uptake of inflammatory cell marker [11C]PK11195 into mouse atherosclerotic plaques." *Eur J Nucl Med Mol Imaging* **36**(1): 73-80.

Lamare, F., R. Hinz, O. Gaemperli, F. Pugliese, J. C. Mason, T. Spinks, P. G. Camici and O. E. Rimoldi (2010). "Detection and quantification of large vessel inflammation with [11C]-(R)-PK11195 PET/CT." *J Nucl Med* **[In print]**.

Landry, A., J. D. Spence and A. Fenster (2004). "Measurement of carotid plaque volume by 3-dimensional ultrasound." *Stroke* **35**(4): 864-9.

Langheinrich, A. C., M. Kampschulte, T. Buch and R. M. Bohle (2007). "Vasa vasorum and atherosclerosis - Quid novi?" *Thromb Haemost* **97**(6): 873-9.

Leadbetter, E., I. Rifkin, A. Hohlbaum, B. Beaudette, M. Shlomchik and A. Marshak-Rothstein (2002). "Chromatin-IgG complexes activate B cells by dual engagement of IgM and Toll-like receptors." *Nature* **416**(6881): 603-7.

Lee, J. G., E. J. Lim, D. W. Park, S. H. Lee, J. R. Kim and S. H. Baek (2008). "A combination of Lox-1 and Nox1 regulates TLR9-mediated foam cell formation." *Cell Signal* **20**(12): 2266-75.

Leen, E., S. J. Moug and P. Horgan (2004). "Potential impact and utilization of ultrasound contrast media." *Eur Radiol* **14 Suppl 8**: P16-24.

Leong-Poi, H., J. Christiansen, P. Heppner, C. W. Lewis, A. L. Klibanov, S. Kaul and J. R. Lindner (2005). "Assessment of endogenous and therapeutic arteriogenesis by contrast ultrasound molecular imaging of integrin expression." *Circulation* **111**(24): 3248-54.

Lepedda, A. J., A. Cigliano, G. M. Cherchi, R. Spirito, M. Maggioni, F. Carta, F. Turrini, C. Edelstein, A. M. Scanu and M. Formato (2009). "A proteomic approach to differentiate histologically classified stable and unstable plaques from human carotid arteries." *Atherosclerosis* **203**(1): 112-8.

Lesnik, P., C. A. Haskell and I. F. Charo (2003). "Decreased atherosclerosis in CX3CR1-/- mice reveals a role for fractalkine in atherogenesis." *J Clin Invest* **111**(3): 333-40.

Levkau, B. (2008). "Sphingosine-1-phosphate in the regulation of vascular tone: a finely tuned integration system of S1P sources, receptors, and vascular responsiveness." *Circ Res* **103**(3): 231-3.

Li, M., D. F. Carpio, Y. Zheng, P. Bruzzo, V. Singh, F. Ouaaz, R. M. Medzhitov and A. A. Beg (2001). "An essential role of the NF-kappa B/Toll-like receptor pathway in induction of inflammatory and tissue-repair gene expression by necrotic cells." *J Immunol* **166**(12): 7128-35.

Liapis, C. D., P. R. Bell, D. Mikhailidis, J. Sivenius, A. Nicolaides, J. Fernandes e Fernandes, G. Biasi and L. Norgren (2009). "ESVS guidelines. Invasive treatment for carotid stenosis: indications, techniques." *Eur J Vasc Endovasc Surg* **37**(4 Suppl): 1-19.

Libby, P., P. M. Ridker and A. Maseri (2002). "Inflammation and atherosclerosis." *Circulation* **105**(9): 1135-43.

Lindner, J. R., M. P. Coggins, S. Kaul, A. L. Klibanov, G. H. Brandenburger and K. Ley (2000a). "Microbubble persistence in the microcirculation during ischemia/reperfusion and inflammation is caused by integrin- and complement-mediated adherence to activated leukocytes." *Circulation* **101**(6): 668-75.

Lindner, J. R., P. A. Dayton, M. P. Coggins, K. Ley, J. Song, K. Ferrara and S. Kaul (2000b). "Noninvasive imaging of inflammation by ultrasound detection of phagocytosed microbubbles." *Circulation* **102**(5): 531-8.

Lindon, J. C., E. Holmes and J. K. Nicholson (2006). "Metabonomics techniques and applications to pharmaceutical research & development." *Pharm Res* **23**(6): 1075-88.

Lisec, J., N. Schauer, J. Kopka, L. Willmitzer and A. R. Fernie (2006). "Gas chromatography mass spectrometry-based metabolite profiling in plants." *Nat Protoc* **1**(1): 387-96.

Liu, X., T. Ukai, H. Yumoto, M. Davey, S. Goswami, F. C. Gibson and C. A. Genco (2008). "Toll-like receptor 2 plays a critical role in the progression of atherosclerosis that is independent of dietary lipids." *Atherosclerosis* **196**(1): 146-54.

Liu, Y., J. M. Cousin, J. Hughes, J. Van Damme, J. R. Seckl, C. Haslett, I. Dransfield, J. Savill and A. G. Rossi (1999). "Glucocorticoids promote nonphlogistic phagocytosis of apoptotic leukocytes." *J Immunol* **162**(6): 3639-46.

Liuzzo, G., D. J. Angiolillo, A. Buffon, V. Rizzello, C. Colizzi, F. Ginnetti, L. M. Biasucci and A. Maseri (2001a). "Enhanced response of blood monocytes to in vitro lipopolysaccharide-challenge in patients with recurrent unstable angina." *Circulation* **103**(18): 2236-41.

Liuzzo, G., A. N. Vallejo, S. L. Kopecky, R. L. Frye, D. R. Holmes, J. J. Goronzy and C. M. Weyand (2001b). "Molecular fingerprint of interferon-gamma signaling in unstable angina." *Circulation* **103**(11): 1509-14.

Loftus, I. M., A. R. Naylor, S. Goodall, M. Crowther, L. Jones, P. R. Bell and M. M. Thompson (2000). "Increased matrix metalloproteinase-9 activity in unstable carotid plaques. A potential role in acute plaque disruption." *Stroke* **31**(1): 40-7.

Loke, P., M. G. Nair, J. Parkinson, D. Guiliano, M. Blaxter and J. E. Allen (2002). "IL-4 dependent alternatively-activated macrophages have a distinctive in vivo gene expression phenotype." *BMC Immunol* **3**: 7.

Lopez, A. D., C. D. Mathers, M. Ezzati, D. T. Jamison and C. J. Murray (2006). "Global and regional burden of disease and risk factors, 2001: systematic analysis of population health data." *Lancet* **367**(9524): 1747-57.

Lortat-Jacob, H., A. Grosdidier and A. Imberty (2002). "Structural diversity of heparan sulfate binding domains in chemokines." *Proc Natl Acad Sci U S A* **99**(3): 1229-34.

Lovett, J. K., J. N. Redgrave and P. M. Rothwell (2005). "A critical appraisal of the performance, reporting, and interpretation of studies comparing carotid plaque imaging with histology." *Stroke* **36**(5): 1091-7.

Macchi, C., C. Catini, C. Federico, M. Gulisano, P. Pacini, F. Cecchi, L. Corcos and E. Brizzi (1996). "Magnetic resonance angiographic evaluation of circulus arteriosus cerebri (circle of Willis): a morphologic study in 100 human healthy subjects." *Ital J Anat Embryol* **101**(2): 115-23.

Mach, F., A. Sauty, A. S. Iarossi, G. K. Sukhova, K. Neote, P. Libby and A. D. Luster (1999). "Differential expression of three T lymphocyte-activating CXC chemokines by human atheroma-associated cells." *J Clin Invest* **104**(8): 1041-50.

Mackaness, G. B. (1964). "The Immunological Basis of Acquired Cellular Resistance." *J Exp Med* **120**: 105-20.

Madan, M. and S. Amar (2008). "Toll-like receptor-2 mediates diet and/or pathogen associated atherosclerosis: proteomic findings." *PLoS ONE* **3**(9): e3204.

Magnoni, M., S. Coli, M. M. Marrocco-Trischitta, G. Melisurgo, D. De Dominicis, D. Cianflone, R. Chiesa, S. B. Feinstein and A. Maseri (2009). "Contrast-enhanced ultrasound imaging of periadventitial vasa vasorum in human carotid arteries." *Eur J Echocardiogr* **10**(2): 260-4.

Malarstig, A., S. Sigurdsson, P. Eriksson, G. Paulsson-Berne, U. Hedin, L. Wallentin, A. Siegbahn, A. Hamsten and A. C. Syvanen (2008). "Variants of the interferon regulatory factor 5 gene regulate expression of IRF5 mRNA in atherosclerotic tissue but are not associated with myocardial infarction." *Arterioscler Thromb Vasc Biol* **28**(5): 975-82.

Mallat, Z., S. Besnard, M. Duriez, V. Deleuze, F. Emmanuel, M. F. Bureau, F. Soubrier, B. Esposito, H. Duez, C. Fievet, B. Staels, N. Duverger, D. Scherman and A. Tedgui (1999a). "Protective role of interleukin-10 in atherosclerosis." *Circ Res* **85**(8): e17-24.

Mallat, Z., T. Nakamura, J. Ohan, G. Leseche, A. Tedgui, J. Maclouf and R. C. Murphy (1999b). "The relationship of hydroxyeicosatetraenoic acids and F-2-isoprostanes to plaque instability in human carotid atherosclerosis." *Journal of Clinical Investigation* **103**(3): 421-427.

Mallat, Z., S. Taleb, H. Ait-Oufella and A. Tedgui (2009). "The role of adaptive T cell immunity in atherosclerosis." *J Lipid Res* **50 Suppl**: S364-9.

Mancl, M. E., G. Hu, N. Sangster-Guity, S. L. Olshalsky, K. Hoops, P. Fitzgerald-Bocarsly, P. M. Pitha, K. Pinder and B. J. Barnes (2005). "Two discrete promoters regulate the alternatively spliced human interferon regulatory factor-5 isoforms. Multiple isoforms with distinct cell type-specific expression, localization, regulation, and function." *J Biol Chem* **280**(22): 21078-90.

Manicke, N. E., M. Nefliu, C. Wu, J. W. Woods, V. Reiser, R. C. Hendrickson and R. G. Cooks (2009). "Imaging of lipids in atheroma by desorption electrospray ionization mass spectrometry." *Anal Chem* **81**(21): 8702-7.

Mantovani, A., C. Garlanda and M. Locati (2009). "Macrophage diversity and polarization in atherosclerosis: a question of balance." *Arterioscler Thromb Vasc Biol* **29**(10): 1419-23.

Mantovani, A., A. Sica, S. Sozzani, P. Allavena, A. Vecchi and M. Locati (2004). "The chemokine system in diverse forms of macrophage activation and polarization." *Trends Immunol* **25**(12): 677-86.

Marechal, X., R. Favory, O. Joulin, D. Montaigne, S. Hassoun, B. Decoster, F. Zerimech and R. Neviere (2008). "Endothelial glycocalyx damage during endotoxemia coincides with microcirculatory dysfunction and vascular oxidative stress." *Shock* **29**(5): 572-6.

Mariathasan, S. and D. M. Monack (2007). "Inflammasome adaptors and sensors: intracellular regulators of infection and inflammation." *Nat Rev Immunol* **7**(1): 31-40.

Markus, H. S., A. King, M. Shipley, R. Topakian, M. Cullinane, S. Reihill, N. M. Bornstein and A. Schaafsma (2010). "Asymptomatic embolisation for prediction of stroke in the Asymptomatic Carotid Emboli Study (ACES): a prospective observational study." *Lancet Neurol* **9**(7): 663-71.

Marshall, P., V. Toteu-Djomte, P. Bareille, H. Perry, G. Brown, M. Baumert and K. Biggadike (2010). "Correlation of skin blanching and percutaneous absorption for glucocorticoid receptor agonists by matrix-assisted laser desorption ionization mass spectrometry imaging and liquid extraction surface analysis with nanoelectrospray ionization mass spectrometry." *Anal Chem* **82**(18): 7787-94.

Martin-Ventura, J. L., M. C. Duran, L. M. Blanco-Colio, O. Meilhac, A. Leclercq, J. B. Michel, O. N. Jensen, S. Hernandez-Merida, J. Tunon, F. Vivanco and J. Egido (2004). "Identification by a differential proteomic approach of heat shock protein 27 as a potential marker of atherosclerosis." *Circulation* **110**(15): 2216-9.

Martin, F. P., M. E. Dumas, Y. Wang, C. Legido-Quigley, I. K. Yap, H. Tang, S. Zirah, G. M. Murphy, O. Cloarec, J. C. Lindon, N. Sprenger, L. B. Fay, S. Kochhar, P. van Bladeren, E. Holmes and J. K. Nicholson (2007). "A top-down systems biology view of microbiome-mammalian metabolic interactions in a mouse model." *Mol Syst Biol* **3**: 112.

Martinez-Pinna, R., C. Barbas, L. M. Blanco-Colio, J. Tunon, P. Ramos-Mozo, J. A. Lopez, O. Meilhac, J. B. Michel, J. Egido and J. L. Martin-Ventura (2010). "Proteomic and metabolomic profiles in atherothrombotic vascular disease." *Curr Atheroscler Rep* **12**(3): 202-8.

Martinez, F. O., S. Gordon, M. Locati and A. Mantovani (2006). "Transcriptional profiling of the human monocyte-to-macrophage differentiation and polarization: new molecules and patterns of gene expression." *J Immunol* **177**(10): 7303-11.

Martinez, F. O., A. Sica, A. Mantovani and M. Locati (2008). "Macrophage activation and polarization." *Front Biosci* **13**: 453-61.

Martinon, F., A. Mayor and J. Tschopp (2009). "The inflammasomes: guardians of the body." *Annu Rev Immunol* **27**: 229-65.

Martinovic, I., N. Abegunewardene, M. Seul, M. Vosseler, G. Horstick, M. Buerke, H. Darius and S. Lindemann (2005). "Elevated monocyte chemoattractant protein-1 serum levels in patients at risk for coronary artery disease." *Circ J* **69**(12): 1484-9.

Marx, N., A. Imhof, J. Froehlich, L. Siam, J. Ittner, G. Wierse, A. Schmidt, W. Maerz, V. Hombach and W. Koenig (2003). "Effect of rosiglitazone treatment on soluble CD40L in patients with type 2 diabetes and coronary artery disease." *Circulation* **107**(15): 1954-7.

Mas, J. L., L. Trinquart, D. Leys, J. F. Albucher, H. Rousseau, A. Viguier, J. P. Bossavy, B. Denis, P. Piquet, P. Garnier, F. Viader, E. Touze, P. Julia, M. Giroud, D. Krause, H. Hosseini, J. P. Becquemin, G. Hinzelin, E. Houdart, H. Henon, J. P. Neau, S. Bracard, Y. Onnient, R. Padovani and G. Chatellier (2008). "Endarterectomy Versus Angioplasty in Patients with Symptomatic Severe Carotid Stenosis (EVA-3S) trial: results up to 4 years from a randomised, multicentre trial." *Lancet Neurol* **7**(10): 885-92.

Masson, P., A. C. Alves, T. M. Ebbels, J. K. Nicholson and E. J. Want (2010). "Optimization and evaluation of metabolite extraction protocols for untargeted metabolic profiling of liver samples by UPLC-MS." *Anal Chem* **82**(18): 7779-86.

Mathiesen, E. B., K. H. Bonaa and O. Joakimsen (2001). "Echolucent plaques are associated with high risk of ischemic cerebrovascular events in carotid stenosis: the tromso study." *Circulation* **103**(17): 2171-5.

Matsui, T., T. Akahoshi, R. Namai, A. Hashimoto, Y. Kurihara, M. Rana, A. Nishimura, H. Endo, H. Kitasato, S. Kawai, K. Takagishi and H. Kondo (2001). "Selective recruitment of CCR6-expressing cells by increased production of MIP-3 alpha in rheumatoid arthritis." *Clin Exp Immunol* **125**(1): 155-61.

Matter, C. M., M. T. Wyss, P. Meier, N. Spath, T. von Lukowicz, C. Lohmann, B. Weber, A. Ramirez de Molina, J. C. Lacal, S. M. Ametamey, G. K. von Schulthess, T. F. Luscher, P. A. Kaufmann and A. Buck (2006). "18F-choline images murine atherosclerotic plaques ex vivo." *Arterioscler Thromb Vasc Biol* **26**(3): 584-9.

Mauriello, A., G. M. Sangiorgi, R. Virmani, S. Trimarchi, D. R. Holmes, Jr., F. D. Kolodgie, D. G. Piepgras, G. Piperno, D. Liotti, J. Narula, P. Righini, A. Ippoliti and L. G. Spagnoli (2010). "A pathobiologic link between risk factors profile and morphological markers of carotid instability." *Atherosclerosis* **208**(2): 572-80.

Mayerl, C., M. Lukasser, R. Sedivy and H. Niederegger (2006). "Atherosclerosis research from past to present—on the track of two pathologists with opposing views, Carl von Rokitansky and Rudolf Virchow." *Virchows Archiv*.

Mayr, M. (2008). "Metabolomics: ready for the prime time?" *Circ Cardiovasc Genet* **1**(1): 58-65.

Mayr, M., D. Grainger, U. Mayr, A. S. Leroyer, G. Leseche, A. Sidibe, O. Herbin, X. Yin, A. Gomes, B. Madhu, J. R. Griffiths, Q. Xu, A. Tedgui and C. M. Boulanger (2009). "Proteomics, metabolomics, and immunomics on microparticles derived from human atherosclerotic plaques." *Circ Cardiovasc Genet* **2**(4): 379-88.

McCarthy, M. J., I. M. Loftus, M. M. Thompson, L. Jones, N. J. London, P. R. Bell, A. R. Naylor and N. P. Brindle (1999a). "Angiogenesis and the atherosclerotic carotid plaque: an association between symptomatology and plaque morphology." *J Vasc Surg* **30**(2): 261-8.

McCarthy, M. J., I. M. Loftus, M. M. Thompson, L. Jones, N. J. London, P. R. Bell, A. R. Naylor and N. P. Brindle (1999b). "Vascular surgical society of great britain and ireland: angiogenesis and the atherosclerotic carotid plaque: association between symptomatology and plaque morphology." *Br J Surg* **86**(5): 707-8.

McDonnell, L. A. and R. M. Heeren (2007). "Imaging mass spectrometry." *Mass Spectrom Rev* **26**(4): 606-43.

McLaren, J. E. and D. P. Ramji (2009). "Interferon gamma: a master regulator of atherosclerosis." *Cytokine Growth Factor Rev* **20**(2): 125-35.

Medzhitov, R. (2001). "Toll-like receptors and innate immunity." *Nat Rev Immunol* **1**(2): 135-45.

Medzhitov, R., P. Preston-Hurlburt and C. A. Janeway, Jr. (1997). "A human homologue of the Drosophila Toll protein signals activation of adaptive immunity." *Nature* **388**(6640): 394-7.

Merino, A., P. Buendia, A. Martin-Malo, P. Aljama, R. Ramirez and J. Carracedo (2011). "Senescent CD14+CD16+ Monocytes Exhibit Proinflammatory and Proatherosclerotic Activity." *J Immunol* **186**(3): 1809-15.

Merkkola, P., H. Tulla, A. Ronkainen, V. Soppi, A. Oksala, T. Koivisto and M. Hippelainen (2006). "Incomplete circle of Willis and right axillary artery perfusion." *Ann Thorac Surg* **82**(1): 74-9.

Methe, H., J. Kim, S. Kofler, M. Weis, M. Nabauer and J. Koglin (2005). "Expansion of circulating Toll-like receptor 4-positive monocytes in patients with acute coronary syndrome." *Circulation* **111**(20): 2654-61.

Methe, H. and M. Weis (2007). "Atherogenesis and inflammation--was Virchow right?" *Nephrology Dialysis Transplantation*.

Michelsen, K. S., M. H. Wong, P. K. Shah, W. Zhang, J. Yano, T. M. Doherty, S. Akira, T. B. Rajavashisth and M. Arditi (2004). "Lack of Toll-like receptor 4 or myeloid differentiation factor 88 reduces atherosclerosis and alters plaque phenotype in mice deficient in apolipoprotein E." *Proc Natl Acad Sci USA* **101**(29): 10679-84.

Midwood, K., S. Sacre, A. M. Piccinini, J. Inglis, A. Trebaul, E. Chan, S. Drexler, N. Sofat, M. Kashiwagi, G. Orend, F. Brennan and B. Foxwell (2009). "Tenascin-C is an endogenous activator of Toll-like receptor 4 that is essential for maintaining inflammation in arthritic joint disease." *Nat Med* **15**(7): 774-80.

Miller, A. M., D. L. Asquith, A. J. Hueber, L. A. Anderson, W. M. Holmes, A. N. McKenzie, D. Xu, N. Sattar, I. B. McInnes and F. Y. Liew (2010). "Interleukin-33 induces protective effects in adipose tissue inflammation during obesity in mice." *Circ Res* **107**(5): 650-8.

Miller, A. M., D. Xu, D. L. Asquith, L. Denby, Y. Li, N. Sattar, A. H. Baker, I. B. McInnes and F. Y. Liew (2008). "IL-33 reduces the development of atherosclerosis." *J Exp Med* **205**(2): 339-46.

Miller, Y. I., S. H. Choi, P. Wiesner, L. Fang, R. Harkewicz, K. Hartvigsen, A. Boullier, A. Gonen, C. J. Diehl, X. Que, E. Montano, P. X. Shaw, S. Tsimikas, C. J. Binder and J. L. Witztum (2011). "Oxidation-specific epitopes are danger-associated molecular patterns recognized by pattern recognition receptors of innate immunity." *Circ Res* **108**(2): 235-48.

Miller, Y. I., S. Viriyakosol, C. J. Binder, J. R. Feramisco, T. N. Kirkland and J. L. Witztum (2003). "Minimally modified LDL binds to CD14, induces macrophage spreading via TLR4/MD-2, and inhibits phagocytosis of apoptotic cells." *J Biol Chem* **278**(3): 1561-8.

Miller, Y. I., S. Viriyakosol, D. S. Worrall, A. Boullier, S. Butler and J. L. Witztum (2005). "Toll-like receptor 4-dependent and -independent cytokine secretion induced by minimally oxidized low-density lipoprotein in macrophages." *Arterioscler Thromb Vasc Biol* **25**(6): 1213-9.

Mofidi, R., T. B. Crotty, P. McCarthy, S. J. Sheehan, D. Mehigan and T. V. Keaveny (2001). "Association between plaque instability, angiogenesis and symptomatic carotid occlusive disease." *Br J Surg* **88**(7): 945-50.

Molloy, K. J., M. M. Thompson, J. L. Jones, E. C. Schwalbe, P. R. Bell, A. R. Naylor and I. M. Loftus (2004). "Unstable carotid plaques exhibit raised matrix metalloproteinase-8 activity." *Circulation* **110**(3): 337-43.

Monaco, C., E. Andreakos, S. Kiriakidis, C. Mauri, C. Bicknell, B. Foxwell, N. Cheshire, E. Paleolog and M. Feldmann (2004). "Canonical pathway of nuclear factor kappa B activation selectively regulates proinflammatory and prothrombotic responses in human atherosclerosis." *Proc Natl Acad Sci U S A* **101**(15): 5634-9.

Monaco, C., S. M. Gregan, T. J. Navin, B. M. Foxwell, A. H. Davies and M. Feldmann (2009). "Toll-like receptor-2 mediates inflammation and matrix degradation in human atherosclerosis." *Circulation* **120**(24): 2462-9.

Moreno, P. R., E. Falk, I. F. Palacios, J. B. Newell, V. Fuster and J. T. Fallon (1994). "Macrophage infiltration in acute coronary syndromes. Implications for plaque rupture." *Circulation* **90**(2): 775-8.

Moreno, P. R., K. R. Purushothaman, V. Fuster, D. Echeverri, H. Truszczynska, S. K. Sharma, J. J. Badimon and W. N. O'Connor (2004). "Plaque neovascularization is increased in ruptured atherosclerotic lesions of human aorta: implications for plaque vulnerability." *Circulation* **110**(14): 2032-8.

Moreno, P. R., K. R. Purushothaman, M. Sirol, A. P. Levy and V. Fuster (2006a). "Neovascularization in human atherosclerosis." *Circulation* **113**(18): 2245-52.

Moreno, P. R., K. R. Purushothaman, E. Zias, J. Sanz and V. Fuster (2006b). "Neovascularization in human atherosclerosis." *Curr Mol Med* **6**(5): 457-77.

Mosmann, T. (1983). "Rapid colorimetric assay for cellular growth and survival: application to proliferation and cytotoxicity assays." *J Immunol Methods* **65**(1-2): 55-63.

Mosser, D. M. and J. P. Edwards (2008). "Exploring the full spectrum of macrophage activation." *Nat Rev Immunol* **8**(12): 958-69.

Motoyama, S., M. Sarai, H. Harigaya, H. Anno, K. Inoue, T. Hara, H. Naruse, J. Ishii, H. Hishida, N. D. Wong, R. Virmani, T. Kondo, Y. Ozaki and J. Narula (2009). "Computed tomographic angiography characteristics of atherosclerotic plaques subsequently resulting in acute coronary syndrome." *J Am Coll Cardiol* **54**(1): 49-57.

Moulin, D., A. Bianchi, S. Boyault, S. Sebillaud, M. Koufany, M. Francois, P. Netter, J. Y. Jouzeau and B. Terlain (2005). "Rosiglitazone induces interleukin-1 receptor antagonist in interleukin-1beta-stimulated rat synovial fibroblasts via a peroxisome proliferator-activated receptor beta/delta-dependent mechanism." *Arthritis Rheum* **52**(3): 759-69.

Moulton, K. S. (2006). "Angiogenesis in atherosclerosis: gathering evidence beyond speculation." *Curr Opin Lipidol* **17**(5): 548-55.

Moulton, K. S., K. Vakili, D. Zurakowski, M. Soliman, C. Butterfield, E. Sylvin, K. M. Lo, S. Gillies, K. Javaherian and J. Folkman (2003). "Inhibition of plaque neovascularization reduces macrophage accumulation and progression of advanced atherosclerosis." *Proc Natl Acad Sci U S A* **100**(8): 4736-41.

Mulivor, A. W. and H. H. Lipowsky (2002). "Role of glycocalyx in leukocyte-endothelial cell adhesion." *Am J Physiol Heart Circ Physiol* **283**(4): H1282-91.

Mullick, A. E., P. S. Tobias and L. K. Curtiss (2005). "Modulation of atherosclerosis in mice by Toll-like receptor 2." *J Clin Invest* **115**(11): 3149-56.

Naghavi, M., P. Libby, E. Falk, S. W. Casscells, S. Litovsky, J. Rumberger, J. J. Badimon, C. Stefanadis, P. Moreno, G. Pasterkamp, Z. Fayad, P. H. Stone, S. Waxman, P. Raggi, M. Madjid, A. Zarrabi, A. Burke, C. Yuan, P. J. Fitzgerald, D. S. Siscovick, C. L. de Korte, M. Aikawa, K. E. Juhani Airaksinen, G. Assmann, C. R. Becker, J. H. Chesebro, A. Farb, Z. S. Galis, C. Jackson, I. K. Jang, W. Koenig, R. A. Lodder, K. March, J. Demirovic, M. Navab, S. G. Priori, M. D. Rekhter, R. Bahr, S. M. Grundy, R. Mehran, A. Colombo, E. Boerwinkle, C. Ballantyne, W. Insull, Jr., R. S. Schwartz, R. Vogel, P. W. Serruys, G. K. Hansson, D. P. Faxon, S. Kaul, H. Drexler, P. Greenland, J. E. Muller, R. Virmani, P. M. Ridker, D. P. Zipes, P. K. Shah and J. T. Willerson (2003). "From vulnerable plaque to vulnerable patient: a call for new definitions and risk assessment strategies: Part I." *Circulation* **108**(14): 1664-72.

Nahrendorf, M., F. K. Swirski, E. Aikawa, L. Stangenberg, T. Wurdinger, J. L. Figueiredo, P. Libby, R. Weissleder and M. J. Pittet (2007). "The healing myocardium sequentially mobilizes two monocyte subsets with divergent and complementary functions." *J Exp Med* **204**(12): 3037-47.

Naito, M., H. Nomura, T. Esaki and A. Iguchi (1997). "Characteristics of macrophage-derived foam cells isolated from atherosclerotic lesions of rabbits." *Atherosclerosis* **135**(2): 241-7.

Nakaya, H., B. D. Summers, A. C. Nicholson, A. M. Gotto, Jr., D. P. Hajjar and J. Han (2009). "Atherosclerosis in LDLR-knockout mice is inhibited, but not reversed, by the PPARgamma ligand pioglitazone." *Am J Pathol* **174**(6): 2007-14.

Nanayakkara, N. D., B. Chiu, A. Samani, J. D. Spence, J. Samarabandu, G. Parraga and A. Fenster (2009). "Nonrigid registration of three-dimensional ultrasound and magnetic resonance images of the carotid arteries." *Med Phys* **36**(2): 373-85.

Nandalur, K. R., E. Baskurt, K. D. Hagspiel, C. D. Phillips and C. M. Kramer (2005). "Calcified carotid atherosclerotic plaque is associated less with ischemic symptoms than is noncalcified plaque on MDCT." *AJR Am J Roentgenol* **184**(1): 295-8.

Nanney, L. B., A. Skeel, J. Luan, S. Polis, A. Richmond, M. H. Wang and E. J. Leonard (1998). "Proteolytic cleavage and activation of pro-macrophage-stimulating protein and upregulation of its receptor in tissue injury." *J Invest Dermatol* **111**(4): 573-81.

Narula, J. and H. W. Strauss (2007). "The popcorn plaques." *Nat Med* **13**(5): 532-4.

NASCET (1991). "Beneficial effect of carotid endarterectomy in symptomatic patients with high-grade carotid stenosis. North American Symptomatic Carotid Endarterectomy Trial Collaborators." *N Engl J Med* **325**(7): 445-53.

Nathan, C. (2008). "Metchnikoff's Legacy in 2008." *Nat Immunol* **9**(7): 695-8.

Naylor, A. R. (2007). "Time is brain!" *Surgeon* **5**(1): 23-30.

Naylor, A. R., P. A. Gaines and P. M. Rothwell (2009). "Who benefits most from intervention for asymptomatic carotid stenosis: patients or professionals?" *Eur J Vasc Endovasc Surg* **37**(6): 625-32.

Nesvizhskii, A. I., A. Keller, E. Kolker and R. Aebersold (2003). "A statistical model for identifying proteins by tandem mass spectrometry." *Anal Chem* **75**(17): 4646-58.

Newby, A. C., S. J. George, Y. Ismail, J. L. Johnson, G. B. Sala-Newby and A. C. Thomas (2009). "Vulnerable atherosclerotic plaque metalloproteinases and foam cell phenotypes." *Thromb Haemost* **101**(6): 1006-11.

Nicholson, J. K., J. Connelly, J. C. Lindon and E. Holmes (2002). "Metabonomics: a platform for studying drug toxicity and gene function." *Nat Rev Drug Discov* **1**(2): 153-61.

Nicholson, J. K., E. Holmes and I. D. Wilson (2005). "Gut microorganisms, mammalian metabolism and personalized health care." *Nat Rev Microbiol* **3**(5): 431-8.

Nicholson, J. K., J. C. Lindon and E. Holmes (1999). "'Metabonomics': understanding the metabolic responses of living systems to pathophysiological stimuli via multivariate statistical analysis of biological NMR spectroscopic data." *Xenobiotica* **29**(11): 1181-9.

Nicolaides, A. N., S. K. Kakkos, M. Griffin, M. Sabetai, S. Dhanjil, T. Tegos, D. J. Thomas, A. Giannoukas, G. Geroulakos, N. Georgiou, S. Francis, E. Ioannidou and C. J. Dore (2005). "Severity of asymptomatic carotid stenosis and risk of ipsilateral hemispheric ischaemic events: results from the ACSRS study." *Eur J Vasc Endovasc Surg* **30**(3): 275-84.

Nicolaides, A. N., E. G. Shifrin, A. Bradbury, S. Dhanjil, M. Griffin, G. Belcaro and M. Williams (1996). "Angiographic and duplex grading of internal carotid stenosis: can we overcome the confusion?" *J Endovasc Surg* **3**(2): 158-65.

Nieuwdorp, M., M. C. Meuwese, H. L. Mooij, M. H. van Lieshout, A. Hayden, M. Levi, J. C. Meijers, C. Ince, J. J. Kastelein, H. Vink and E. S. Stroes (2009). "Tumor necrosis factor-alpha inhibition protects against endotoxin-induced endothelial glycocalyx perturbation." *Atherosclerosis* **202**(1): 296-303.

Nishina, P., J. Wang, W. Toyofuku, F. Kuypers, B. Ishida and B. Paigen (1993). "Atherosclerosis and plasma and liver lipids in nine inbred strains of mice." *Lipids* **28**(7): 599-605.

Oalmann, M. C., R. W. Palmer, M. A. Guzman and J. P. Strong (1980). "Sudden death, coronary heart disease, atherosclerosis and myocardial lesions in young men." *Am J Epidemiol* **112**(5): 639-49.

Oates, C. P., A. R. Naylor, T. Hartshorne, S. M. Charles, T. Fail, K. Humphries, M. Aslam and P. Khodabakhsh (2009). "Joint recommendations for reporting carotid ultrasound investigations in the United Kingdom." *Eur J Vasc Endovasc Surg* **37**(3): 251-61.

Odegaard, J. I., R. R. Ricardo-Gonzalez, M. H. Goforth, C. R. Morel, V. Subramanian, L. Mukundan, A. Red Eagle, D. Vats, F. Brombacher, A. W. Ferrante and A. Chawla (2007). "Macrophage-specific PPARgamma controls alternative activation and improves insulin resistance." *Nature* **447**(7148): 1116-20.

Oiknine, J. and M. Aviram (1992). "Increased susceptibility to activation and increased uptake of low density lipoprotein by cholesterol-loaded macrophages." *Arterioscler Thromb* **12**(6): 745-53.

Okamura, Y., M. Watari, E. S. Jerud, D. W. Young, S. T. Ishizaka, J. Rose, J. C. Chow and J. F. Strauss, 3rd (2001). "The extra domain A of fibronectin activates Toll-like receptor 4." *J Biol Chem* **276**(13): 10229-33.

Owen, D. R., J. Shalhoub, S. Miller, T. Gauthier, O. Doryforou, A. H. Davies and E. L. Leen (2010). "Inflammation within carotid atherosclerotic plaque: assessment with late-phase contrast-enhanced US." *Radiology* **255**(2): 638-44.

Packard, R. R., A. H. Lichtman and P. Libby (2009). "Innate and adaptive immunity in atherosclerosis." *Semin Immunopathol* **31**(1): 5-22.

Page, G., S. Lebecque and P. Miossec (2002). "Anatomic localization of immature and mature dendritic cells in an ectopic lymphoid organ: correlation with selective chemokine expression in rheumatoid synovium." *J Immunol* **168**(10): 5333-41.

Palframan, R. T., S. Jung, G. Cheng, W. Weninger, Y. Luo, M. Dorf, D. R. Littman, B. J. Rollins, H. Zweerink, A. Rot and U. H. von Andrian (2001). "Inflammatory chemokine transport and presentation in HEV: a remote control mechanism for monocyte recruitment to lymph nodes in inflamed tissues." *J Exp Med* **194**(9): 1361-73.

Papantchev, V., S. Hristov, D. Todorova, E. Naydenov, A. Paloff, D. Nikolov, A. Tschirkov and W. Ovtscharoff (2007). "Some variations of the circle of Willis, important for cerebral protection in aortic surgery--a study in Eastern Europeans." *Eur J Cardiothorac Surg* **31**(6): 982-9.

Papaspyridonos, M., E. McNeill, J. P. de Bono, A. Smith, K. G. Burnand, K. M. Channon and D. R. Greaves (2008). "Galectin-3 is an amplifier of inflammation in atherosclerotic plaque progression through macrophage activation and monocyte chemoattraction." *Arterioscler Thromb Vasc Biol* **28**(3): 433-40.

Papaspyridonos, M., A. Smith, K. G. Burnand, P. Taylor, S. Padayachee, K. E. Suckling, C. H. James, D. R. Greaves and L. Patel (2006). "Novel candidate genes in unstable areas of human atherosclerotic plaques." *Arterioscler Thromb Vasc Biol* **26**(8): 1837-44.

Passlick, B., D. Flieger and H. W. Ziegler-Heitbrock (1989). "Identification and characterization of a novel monocyte subpopulation in human peripheral blood." *Blood* **74**(7): 2527-34.

Pasterkamp, G., A. H. Schoneveld, D. J. Hijnen, D. P. de Kleijn, H. Teepen, A. C. van der Wal and C. Borst (2000). "Atherosclerotic arterial remodeling and the localization of macrophages and matrix metalloproteases 1, 2 and 9 in the human coronary artery." *Atherosclerosis* **150**(2): 245-53.

Peeters, W., W. E. Hellings, D. P. de Kleijn, J. P. de Vries, F. L. Moll, A. Vink and G. Pasterkamp (2009). "Carotid atherosclerotic plaques stabilize after stroke: insights into the natural process of atherosclerotic plaque stabilization." *Arterioscler Thromb Vasc Biol* **29**(1): 128-33.

Pettersson, C., H. Karlsson, M. Stahlman, T. Larsson, B. Fagerberg, M. Lindahl, O. Wiklund, J. Boren and L. Fogelstrand (2010). "LDL-associated apolipoprotein J and lysozyme are associated with atherogenic properties of LDL found in type 2 diabetes and the metabolic syndrome." *J Intern Med*.

Polak, J. F., L. Shemanski, D. H. O'Leary, D. Lefkowitz, T. R. Price, P. J. Savage, W. E. Brant and C. Reid (1998). "Hypoechoic plaque at US of the carotid artery: an independent risk factor for incident stroke in adults aged 65 years or older. Cardiovascular Health Study." *Radiology* **208**(3): 649-54.

Potteaux, S., C. Combadiere, B. Esposito, S. Casanova, R. Merval, P. Ardouin, J. L. Gao, P. M. Murphy, A. Tedgui and Z. Mallat (2005). "Chemokine receptor CCR1 disruption in bone marrow cells enhances atherosclerotic lesion development and inflammation in mice." *Mol Med* **11**(1-12): 16-20.

Potteaux, S., C. Combadiere, B. Esposito, C. Lecureuil, H. Ait-Oufella, R. Merval, P. Ardouin, A. Tedgui and Z. Mallat (2006). "Role of bone marrow-derived CC-chemokine receptor 5 in the development of atherosclerosis of low-density lipoprotein receptor knockout mice." *Arterioscler Thromb Vasc Biol* **26**(8): 1858-63.

Puchtler, H., F. S. Waldrop and L. S. Valentine (1973). "Polarization microscopic studies of connective tissue stained with picro-sirius red FBA." *Beitr Pathol* **150**(2): 174-87.

Pugliese, F., O. Gaemperli, A. R. Kinderlerer, F. Lamare, J. Shalhoub, A. H. Davies, O. E. Rimoldi, J. C. Mason and P. G. Camici (2010). "Imaging of Vascular Inflammation with [11C]-PK11195 and PET/CT Angiography." *J Am Coll Cardiol* **56**(8): 653-661.

Quinones, M. P., H. G. Martinez, F. Jimenez, C. A. Estrada, M. Dudley, O. Willmon, H. Kulkarni, R. L. Reddick, G. Fernandes, W. A. Kuziel, S. K. Ahuja and S. S. Ahuja (2007). "CC chemokine receptor 5 influences late-stage atherosclerosis." *Atherosclerosis* **195**(1): e92-103.

Raes, G., R. Van den Bergh, P. De Baetselier, G. H. Ghassabeh, C. Scotton, M. Locati, A. Mantovani and S. Sozzani (2005). "Arginase-1 and Ym1 are markers for murine, but not human, alternatively activated myeloid cells." *J Immunol* **174**(11): 6561; author reply 6561-2.

Raisanen-Sokolowski, A., T. Glysing-Jensen, J. Koglin and M. E. Russell (1998). "Reduced transplant arteriosclerosis in murine cardiac allografts placed in interferon-gamma knockout recipients." *Am J Pathol* **152**(2): 359-65.

Randi, A. M., E. Biguzzi, F. Falciani, P. Merlini, S. Blakemore, E. Bramucci, S. Lucreziotti, M. Lennon, E. M. Faioni, D. Ardissino and P. M. Mannucci (2003). "Identification of differentially expressed genes in coronary atherosclerotic plaques from patients with stable or unstable angina by cDNA array analysis." *J Thromb Haemost* **1**(4): 829-35.

Rapp, J. H., W. E. Connor, D. S. Lin, T. Inahara and J. M. Porter (1983). "Lipids of human atherosclerotic plaques and xanthomas: clues to the mechanism of plaque progression." *J Lipid Res* **24**(10): 1329-35.

Reiter, M., R. A. Bucek, I. Effenberger, J. Boltuch, W. Lang, R. Ahmadi, E. Minar and M. Schillinger (2006). "Plaque echolucency is not associated with the risk of stroke in carotid stenting." *Stroke* **37**(9): 2378-80.

Ridker, P. M., E. Danielson, F. A. Fonseca, J. Genest, A. M. Gotto, Jr., J. J. Kastelein, W. Koenig, P. Libby, A. J. Lorenzatti, J. G. MacFadyen, B. G. Nordestgaard, J. Shepherd, J. T. Willerson and R. J. Glynn (2008). "Rosuvastatin to prevent vascular events in men and women with elevated C-reactive protein." *N Engl J Med* **359**(21): 2195-207.

Ridker, P. M., N. Rifai, M. Pfeffer, F. Sacks, S. Lepage and E. Braunwald (2000). "Elevation of tumor necrosis factor-alpha and increased risk of recurrent coronary events after myocardial infarction." *Circulation* **101**(18): 2149-53.

Robertson, J. T. (1998). "Carotid endarterectomy: a saga of clinical science, personalities, and evolving technology: the Willis lecture." *Stroke* **29**(11): 2435-41.

Rockman, C. and T. Riles (2010). "Carotid artery disease: selecting the appropriate asymptomatic patient for intervention." *Perspect Vasc Surg Endovasc Ther* **22**(1): 30-7.

Roffi, M. (2010). "Is there a role for revascularisation in asymptomatic carotid stenosis? Yes." *BMJ* **341**: c4898.

Romero, J. R., A. Beiser, S. Seshadri, E. J. Benjamin, J. F. Polak, R. S. Vasan, R. Au, C. DeCarli and P. A. Wolf (2009). "Carotid artery atherosclerosis, MRI indices of brain ischemia, aging, and cognitive impairment: the Framingham study." *Stroke* **40**(5): 1590-6.

Rominger, A., T. Saam, S. Wolpers, C. C. Cyran, M. Schmidt, S. Foerster, K. Nikolaou, M. F. Reiser, P. Bartenstein and M. Hacker (2009). "18F-FDG PET/CT identifies patients at

risk for future vascular events in an otherwise asymptomatic cohort with neoplastic disease." *J Nucl Med* **50**(10): 1611-20.

Ross, R. (1999). "Atherosclerosis--an inflammatory disease." *N Engl J Med* **340**(2): 115-26.

Rossi, L., I. Lapini, A. Magi, G. Pratesi, M. Lavitrano, G. M. Biasi, R. Pulli, C. Pratesi, R. Abbate and B. Giusti (2010). "Carotid artery disease: novel pathophysiological mechanisms identified by gene-expression profiling of peripheral blood." *Eur J Vasc Endovasc Surg* **40**(5): 549-58.

Rothenbacher, D., S. Muller-Scholze, C. Herder, W. Koenig and H. Kolb (2006). "Differential expression of chemokines, risk of stable coronary heart disease, and correlation with established cardiovascular risk markers." *Arterioscler Thromb Vasc Biol* **26**(1): 194-9.

Rothwell, P. M., M. Eliasziw, S. A. Gutnikov, A. J. Fox, D. W. Taylor, M. R. Mayberg, C. P. Warlow and H. J. Barnett (2003a). "Analysis of pooled data from the randomised controlled trials of endarterectomy for symptomatic carotid stenosis." *Lancet* **361**(9352): 107-16.

Rothwell, P. M., S. A. Gutnikov and C. P. Warlow (2003b). "Reanalysis of the final results of the European Carotid Surgery Trial." *Stroke* **34**(2): 514-23.

Rudd, J. H., F. Hyafil and Z. A. Fayad (2009). "Inflammation imaging in atherosclerosis." *Arterioscler Thromb Vasc Biol* **29**(7): 1009-16.

Rudd, J. H., K. S. Myers, S. Bansilal, J. Machac, C. A. Pinto, C. Tong, A. Rafique, R. Hargeaves, M. Farkouh, V. Fuster and Z. A. Fayad (2008). "Atherosclerosis inflammation imaging with 18F-FDG PET: carotid, iliac, and femoral uptake reproducibility, quantification methods, and recommendations." *J Nucl Med* **49**(6): 871-8.

Rudd, J. H., K. S. Myers, S. Bansilal, J. Machac, A. Rafique, M. Farkouh, V. Fuster and Z. A. Fayad (2007). "(18)Fluorodeoxyglucose positron emission tomography imaging of atherosclerotic plaque inflammation is highly reproducible: implications for atherosclerosis therapy trials." *J Am Coll Cardiol* **50**(9): 892-6.

Rudd, J. H., E. A. Warburton, T. D. Fryer, H. A. Jones, J. C. Clark, N. Antoun, P. Johnstrom, A. P. Davenport, P. J. Kirkpatrick, B. N. Arch, J. D. Pickard and P. L. Weissberg (2002). "Imaging atherosclerotic plaque inflammation with [18F]-fluorodeoxyglucose positron emission tomography." *Circulation* **105**(23): 2708-11.

Sabetai, M. M., T. J. Tegos, A. N. Nicolaides, S. Dhanjil, G. J. Pare and J. M. Stevens (2000). "Reproducibility of computer-quantified carotid plaque echogenicity: can we overcome the subjectivity?" *Stroke* **31**(9): 2189-96.

Saederup, N., L. Chan, S. A. Lira and I. F. Charo (2008). "Fractalkine deficiency markedly reduces macrophage accumulation and atherosclerotic lesion formation in CCR2-/- mice: evidence for independent chemokine functions in atherogenesis." *Circulation* **117**(13): 1642-8.

Saghatelian, A., S. A. Trauger, E. J. Want, E. G. Hawkins, G. Siuzdak and B. F. Cravatt (2004). "Assignment of endogenous substrates to enzymes by global metabolite profiling." *Biochemistry* **43**(45): 14332-9.

Sanz, J. and Z. A. Fayad (2008). "Imaging of atherosclerotic cardiovascular disease." *Nature* **451**(7181): 953-7.

Saren, P., H. G. Welgus and P. T. Kovanen (1996). "TNF-alpha and IL-1beta selectively induce expression of 92-kDa gelatinase by human macrophages." *J Immunol* **157**(9): 4159-65.

Schaar, J. A., J. E. Muller, E. Falk, R. Virmani, V. Fuster, P. W. Serruys, A. Colombo, C. Stefanadis, S. Ward Casscells, P. R. Moreno, A. Maseri and A. F. van der Steen (2004). "Terminology for high-risk and vulnerable coronary artery plaques. Report of a meeting on the vulnerable plaque, June 17 and 18, 2003, Santorini, Greece." *Eur Heart J* **25**(12): 1077-82.

Schaefer, L., A. Babelova, E. Kiss, H. J. Hausser, M. Baliova, M. Krzyzankova, G. Marsche, M. F. Young, D. Mihalik, M. Gotte, E. Malle, R. M. Schaefer and H. J. Grone (2005).

"The matrix component biglycan is proinflammatory and signals through Toll-like receptors 4 and 2 in macrophages." *J Clin Invest* **115**(8): 2223-33.

Schaffner, T., K. Taylor, E. J. Bartucci, K. Fischer-Dzoga, J. H. Beeson, S. Glagov and R. W. Wissler (1980). "Arterial foam cells with distinctive immunomorphologic and histochemical features of macrophages." *Am J Pathol* **100**(1): 57-80.

Scheibner, K., M. Lutz, S. Boodoo, M. Fenton, J. Powell and M. Horton (2006). "Hyaluronan fragments act as an endogenous danger signal by engaging TLR2." *J Immunol* **177**(2): 1272-81.

Schirmer, S. H., J. O. Fledderus, A. M. van der Laan, T. C. van der Pouw-Kraan, P. D. Moerland, O. L. Volger, J. M. Baggen, M. Bohm, J. J. Piek, A. J. Horrevoets and N. van Royen (2009). "Suppression of inflammatory signaling in monocytes from patients with coronary artery disease." *J Mol Cell Cardiol* **46**(2): 177-85.

Schlitt, A., G. H. Heine, S. Blankenberg, C. Espinola-Klein, J. F. Dopheide, C. Bickel, K. J. Lackner, M. Iz, J. Meyer, H. Darius and H. J. Rupprecht (2004). "CD14+CD16+ monocytes in coronary artery disease and their relationship to serum TNF-alpha levels." *Thromb Haemost* **92**(2): 419-24.

Schmidt, C. (2004). "Metabolomics takes its place as latest up-and-coming "omic" science." *J Natl Cancer Inst* **96**(10): 732-4.

Schneider, P. A. and A. R. Naylor (2010a). "Asymptomatic carotid artery stenosis--medical therapy alone versus medical therapy plus carotid endarterectomy or stenting." *J Vasc Surg* **52**(2): 499-507.

Schneider, P. A. and A. R. Naylor (2010b). "Transatlantic debate. Asymptomatic carotid artery stenosis--medical therapy alone versus medical therapy plus carotid endarterectomy or stenting." *Eur J Vasc Endovasc Surg* **40**(2): 274-81.

Schoneveld, A., I. Hoefer, J. Sluijter, J. Laman, D. de Kleijn and G. Pasterkamp (2008). "Atherosclerotic lesion development and Toll like receptor 2 and 4 responsiveness." *Atherosclerosis* **197**(1): 95-104.

Schoneveld, A. H., M. M. Oude Nijhuis, B. van Middelaar, J. D. Laman, D. P. de Kleijn and G. Pasterkamp (2005). "Toll-like receptor 2 stimulation induces intimal hyperplasia and atherosclerotic lesion development." *Cardiovasc Res* **66**(1): 162-9.

Schutyser, E., S. Struyf and J. Van Damme (2003). "The CC chemokine CCL20 and its receptor CCR6." *Cytokine Growth Factor Rev* **14**(5): 409-26.

Schwartz, S. M., Z. S. Galis, M. E. Rosenfeld and E. Falk (2007). "Plaque rupture in humans and mice." *Arterioscler Thromb Vasc Biol* **27**(4): 705-13.

Scotton, C. J., F. O. Martinez, M. J. Smelt, M. Sironi, M. Locati, A. Mantovani and S. Sozzani (2005). "Transcriptional profiling reveals complex regulation of the monocyte IL-1 beta system by IL-13." *J Immunol* **174**(2): 834-45.

Seimon, T. A., M. J. Nadolski, X. Liao, J. Magallon, M. Nguyen, N. T. Feric, M. L. Koschinsky, R. Harkewicz, J. L. Witztum, S. Tsimikas, D. Golenbock, K. J. Moore and I. Tabas (2010). "Atherogenic lipids and lipoproteins trigger CD36-TLR2-dependent apoptosis in macrophages undergoing endoplasmic reticulum stress." *Cell Metab* **12**(5): 467-82.

Seo, D., T. Wang, H. Dressman, E. E. Herderick, E. S. Iversen, C. Dong, K. Vata, C. A. Milano, F. Rigat, J. Pittman, J. R. Nevins, M. West and P. J. Goldschmidt-Clermont (2004). "Gene expression phenotypes of atherosclerosis." *Arterioscler Thromb Vasc Biol* **24**(10): 1922-7.

Shah, F., P. Balan, M. Weinberg, V. Reddy, R. Neems, M. Feinstein, J. Dainauskas, P. Meyer, M. Goldin and S. B. Feinstein (2007). "Contrast-enhanced ultrasound imaging of atherosclerotic carotid plaque neovascularization: a new surrogate marker of atherosclerosis?" *Vasc Med* **12**(4): 291-7.

Shalhoub, J. and A. H. Davies (2010). Identification of 'high-risk' carotid stenosis. *Vascular and Endovascular Surgery Highlights 2009-10*. A. H. Davies. Oxford, Health Press Limited**:** 19-27.

Shapiro, S. D., E. J. Campbell, D. K. Kobayashi and H. G. Welgus (1990). "Immune modulation of metalloproteinase production in human macrophages. Selective

pretranslational suppression of interstitial collagenase and stromelysin biosynthesis by interferon-gamma." *J Clin Invest* **86**(4): 1204-10.

Shi, W., N. J. Wang, D. M. Shih, V. Z. Sun, X. Wang and A. J. Lusis (2000). "Determinants of atherosclerosis susceptibility in the C3H and C57BL/6 mouse model: evidence for involvement of endothelial cells but not blood cells or cholesterol metabolism." *Circ Res* **86**(10): 1078-84.

Shinohara, M., K. Hirata, T. Yamashita, T. Takaya, N. Sasaki, R. Shiraki, T. Ueyama, N. Emoto, N. Inoue, M. Yokoyama and S. Kawashima (2007). "Local overexpression of toll-like receptors at the vessel wall induces atherosclerotic lesion formation: synergism of TLR2 and TLR4." *Arterioscler Thromb Vasc Biol* **27**(11): 2384-91.

Shio, H., N. J. Haley and S. Fowler (1979). "Characterization of Lipid-Laden Aortic-Cells from Cholesterol-Fed Rabbits .3. Intracellular-Localization of Cholesterol and Cholesteryl Ester." *Laboratory Investigation* **41**(2): 160-167.

Shiraki, R., N. Inoue, S. Kobayashi, J. Ejiri, K. Otsui, T. Honjo, M. Takahashi, K. Hirata, M. Yokoyama and S. Kawashima (2006). "Toll-like receptor 4 expressions on peripheral blood monocytes were enhanced in coronary artery disease even in patients with low C-reactive protein." *Life Sci* **80**(1): 59-66.

Sidhu, P. S. and P. L. Allan (1997). "Ultrasound assessment of internal carotid artery stenosis." *Clin Radiol* **52**(9): 654-8.

Sidhu, P. S., P. L. Allan, F. Cattin, D. O. Cosgrove, A. H. Davies, D. D. Do, S. Karakagil, J. Langholz, D. A. Legemate, A. Martegani, J. B. Llull, C. Pezzoli and A. Spinazzi (2006). "Diagnostic efficacy of SonoVue, a second generation contrast agent, in the assessment of extracranial carotid or peripheral arteries using colour and spectral Doppler ultrasound: a multicentre study." *Br J Radiol* **79**(937): 44-51.

Sigurdsson, S., G. Nordmark, H. H. Goring, K. Lindroos, A. C. Wiman, G. Sturfelt, A. Jonsen, S. Rantapaa-Dahlqvist, B. Moller, J. Kere, S. Koskenmies, E. Widen, M. L. Eloranta, H. Julkunen, H. Kristjansdottir, K. Steinsson, G. Alm, L. Ronnblom and A. C. Syvanen (2005). "Polymorphisms in the tyrosine kinase 2 and interferon regulatory factor 5 genes are associated with systemic lupus erythematosus." *Am J Hum Genet* **76**(3): 528-37.

Sluijter, J. P., W. P. Pulskens, A. H. Schoneveld, E. Velema, C. F. Strijder, F. Moll, J. P. de Vries, J. Verheijen, R. Hanemaaijer, D. P. de Kleijn and G. Pasterkamp (2006). "Matrix metalloproteinase 2 is associated with stable and matrix metalloproteinases 8 and 9 with vulnerable carotid atherosclerotic lesions: a study in human endarterectomy specimen pointing to a role for different extracellular matrix metalloproteinase inducer glycosylation forms." *Stroke* **37**(1): 235-9.

Sluimer, J. C., N. Kisters, K. B. Cleutjens, O. L. Volger, A. J. Horrevoets, L. H. van den Akker, A. P. Bijnens and M. J. Daemen (2007). "Dead or alive: gene expression profiles of advanced atherosclerotic plaques from autopsy and surgery." *Physiol Genomics* **30**(3): 335-41.

Smiley, S. T., J. A. King and W. W. Hancock (2001). "Fibrinogen stimulates macrophage chemokine secretion through toll-like receptor 4." *J Immunol* **167**(5): 2887-94.

Smith, E., K. M. Prasad, M. Butcher, A. Dobrian, J. K. Kolls, K. Ley and E. Galkina (2010). "Blockade of interleukin-17A results in reduced atherosclerosis in apolipoprotein E-deficient mice." *Circulation* **121**(15): 1746-55.

Smith, J. D., E. Trogan, M. Ginsberg, C. Grigaux, J. Tian and M. Miyata (1995). "Decreased atherosclerosis in mice deficient in both macrophage colony-stimulating factor (op) and apolipoprotein E." *Proc Natl Acad Sci U S A* **92**(18): 8264-8.

Southgate, K. M., M. Fisher, A. P. Banning, V. J. Thurston, A. H. Baker, R. P. Fabunmi, P. H. Groves, M. Davies and A. C. Newby (1996). "Upregulation of basement membrane-degrading metalloproteinase secretion after balloon injury of pig carotid arteries." *Circ Res* **79**(6): 1177-87.

Spence, J. D. (2010). "Is there a role for revascularisation in asymptomatic carotid stenosis? No." *BMJ* **341**: c4900.

Stary, H. C., A. B. Chandler, R. E. Dinsmore, V. Fuster, S. Glagov, W. Insull, Jr., M. E. Rosenfeld, C. J. Schwartz, W. D. Wagner and R. W. Wissler (1995a). "A definition of advanced types of atherosclerotic lesions and a histological classification of atherosclerosis. A report from the Committee on Vascular Lesions of the Council on Arteriosclerosis, American Heart Association." *Arterioscler Thromb Vasc Biol* **15**(9): 1512-31.

Stary, H. C., A. B. Chandler, R. E. Dinsmore, V. Fuster, S. Glagov, W. Insull, Jr., M. E. Rosenfeld, C. J. Schwartz, W. D. Wagner and R. W. Wissler (1995b). "A definition of advanced types of atherosclerotic lesions and a histological classification of atherosclerosis. A report from the Committee on Vascular Lesions of the Council on Arteriosclerosis, American Heart Association." *Circulation* **92**(5): 1355-74.

Staub, D., M. B. Patel, A. Tibrewala, D. Ludden, M. Johnson, P. Espinosa, B. Coll, K. A. Jaeger and S. B. Feinstein (2010). "Vasa vasorum and plaque neovascularization on contrast-enhanced carotid ultrasound imaging correlates with cardiovascular disease and past cardiovascular events." *Stroke* **41**(1): 41-7.

Steinman, R. M. and J. Idoyaga (2010). "Features of the dendritic cell lineage." *Immunol Rev* **234**(1): 5-17.

Sternberg, E. M. (2006). "Neural regulation of innate immunity: a coordinated nonspecific host response to pathogens." *Nat Rev Immunol* **6**(4): 318-28.

Stewart, C. R., L. M. Stuart, K. Wilkinson, J. M. van Gils, J. Deng, A. Halle, K. J. Rayner, L. Boyer, R. Zhong, W. A. Frazier, A. Lacy-Hulbert, J. El Khoury, D. T. Golenbock and K. J. Moore (2010a). "CD36 ligands promote sterile inflammation through assembly of a Toll-like receptor 4 and 6 heterodimer." *Nat Immunol* **11**(2): 155-61.

Stewart, C. R., L. M. Stuart, K. Wilkinson, J. M. van Gils, J. Deng, A. Halle, K. J. Rayner, L. Boyer, R. Zhong, W. A. Frazier, A. Lacy-Hulbert, J. E. Khoury, D. T. Golenbock and K. J. Moore (2010b). "CD36 ligands promote sterile inflammation through assembly of a Toll-like receptor 4 and 6 heterodimer." *Nat Immunol* **11**(2): 155-61.

Stojakovic, M., R. Krzesz, A. H. Wagner and M. Hecker (2007). "CD154-stimulated GM-CSF release by vascular smooth muscle cells elicits monocyte activation--role in atherogenesis." *J Mol Med* **85**(11): 1229-38.

Straus, D. S. and C. K. Glass (2007). "Anti-inflammatory actions of PPAR ligands: new insights on cellular and molecular mechanisms." *Trends Immunol* **28**(12): 551-8.

Strauss-Ayali, D., S. M. Conrad and D. M. Mosser (2007). "Monocyte subpopulations and their differentiation patterns during infection." *J Leukoc Biol* **82**(2): 244-52.

Suarna, C., R. T. Dean, J. May and R. Stocker (1995). "Human atherosclerotic plaque contains both oxidized lipids and relatively large amounts of alpha-tocopherol and ascorbate." *Arterioscler Thromb Vasc Biol* **15**(10): 1616-24.

Swirski, F., P. Libby, E. Aikawa, P. Alcaide, F. Luscinskas, R. Weissleder and M. Pittet (2007). "Ly-6Chi monocytes dominate hypercholesterolemia-associated monocytosis and give rise to macrophages in atheromata." *J Clin Invest* **117**(1): 195-205.

Swirski, F. K., R. Weissleder and M. J. Pittet (2009). "Heterogeneous in vivo behavior of monocyte subsets in atherosclerosis." *Arterioscler Thromb Vasc Biol* **29**(10): 1424-32.

Sztajzel, R., S. Momjian, I. Momjian-Mayor, N. Murith, K. Djebaili, G. Boissard, M. Comelli and G. Pizolatto (2005). "Stratified gray-scale median analysis and color mapping of the carotid plaque: correlation with endarterectomy specimen histology of 28 patients." *Stroke* **36**(4): 741-5.

Tabas, I. (2010). "Macrophage death and defective inflammation resolution in atherosclerosis." *Nat Rev Immunol* **10**(1): 36-46.

Tabibiazar, R., R. A. Wagner, E. A. Ashley, J. Y. King, R. Ferrara, J. M. Spin, D. A. Sanan, B. Narasimhan, R. Tibshirani, P. S. Tsao, B. Efron and T. Quertermous (2005). "Signature patterns of gene expression in mouse atherosclerosis and their correlation to human coronary disease." *Physiol Genomics* **22**(2): 213-26.

Tacke, F., D. Alvarez, T. J. Kaplan, C. Jakubzick, R. Spanbroek, J. Llodra, A. Garin, J. Liu, M. Mack, N. van Rooijen, S. A. Lira, A. J. Habenicht and G. J. Randolph (2007).

"Monocyte subsets differentially employ CCR2, CCR5, and CX3CR1 to accumulate within atherosclerotic plaques." *J Clin Invest* **117**(1): 185-94.

Tagore, D. M., W. M. Nolte, J. M. Neveu, R. Rangel, L. Guzman-Rojas, R. Pasqualini, W. Arap, W. S. Lane and A. Saghatelian (2009). "Peptidase substrates via global peptide profiling." *Nat Chem Biol* **5**(1): 23-5.

Takaya, N., C. Yuan, B. Chu, T. Saam, H. Underhill, J. Cai, N. Tran, N. L. Polissar, C. Isaac, M. S. Ferguson, G. A. Garden, S. C. Cramer, K. R. Maravilla, B. Hashimoto and T. S. Hatsukami (2006). "Association between carotid plaque characteristics and subsequent ischemic cerebrovascular events: a prospective assessment with MRI--initial results." *Stroke* **37**(3): 818-23.

Taleb, S., M. Romain, B. Ramkhelawon, C. Uyttenhove, G. Pasterkamp, O. Herbin, B. Esposito, N. Perez, H. Yasukawa, J. Van Snick, A. Yoshimura, A. Tedgui and Z. Mallat (2009). "Loss of SOCS3 expression in T cells reveals a regulatory role for interleukin-17 in atherosclerosis." *J Exp Med* **206**(10): 2067-77.

Taleb, S., A. Tedgui and Z. Mallat (2008). "Regulatory T-cell immunity and its relevance to atherosclerosis." *J Intern Med* **263**(5): 489-99.

Taleb, S., A. Tedgui and Z. Mallat (2010). "Interleukin-17: friend or foe in atherosclerosis?" *Curr Opin Lipidol* **21**(5): 404-8.

Tang, T. Y., S. P. Howarth, S. R. Miller, M. J. Graves, U. K.-I. JM, R. A. Trivedi, Z. Y. Li, S. R. Walsh, A. P. Brown, P. J. Kirkpatrick, M. E. Gaunt and J. H. Gillard (2007). "Comparison of the inflammatory burden of truly asymptomatic carotid atheroma with atherosclerotic plaques contralateral to symptomatic carotid stenosis: an ultra small superparamagnetic iron oxide enhanced magnetic resonance study." *J Neurol Neurosurg Psychiatry* **78**(12): 1337-43.

Tang, T. Y., S. P. Howarth, S. R. Miller, M. J. Graves, A. J. Patterson, U. K.-I. JM, Z. Y. Li, S. R. Walsh, A. P. Brown, P. J. Kirkpatrick, E. A. Warburton, P. D. Hayes, K. Varty, J. R. Boyle, M. E. Gaunt, A. Zalewski and J. H. Gillard (2009). "The ATHEROMA (Atorvastatin Therapy: Effects on Reduction of Macrophage Activity) Study. Evaluation using ultrasmall superparamagnetic iron oxide-enhanced magnetic resonance imaging in carotid disease." *J Am Coll Cardiol* **53**(22): 2039-50.

Tawakol, A., R. Q. Migrino, G. G. Bashian, S. Bedri, D. Vermylen, R. C. Cury, D. Yates, G. M. LaMuraglia, K. Furie, S. Houser, H. Gewirtz, J. E. Muller, T. J. Brady and A. J. Fischman (2006). "In vivo 18F-fluorodeoxyglucose positron emission tomography imaging provides a noninvasive measure of carotid plaque inflammation in patients." *J Am Coll Cardiol* **48**(9): 1818-24.

Tedgui, A. and Z. Mallat (2006). "Cytokines in atherosclerosis: pathogenic and regulatory pathways." *Physiol Rev* **86**(2): 515-81.

Teupser, D., S. Pavlides, M. Tan, J. C. Gutierrez-Ramos, R. Kolbeck and J. L. Breslow (2004). "Major reduction of atherosclerosis in fractalkine (CX3CL1)-deficient mice is at the brachiocephalic artery, not the aortic root." *Proc Natl Acad Sci U S A* **101**(51): 17795-800.

Thomas, A. C., G. B. Sala-Newby, Y. Ismail, J. L. Johnson, G. Pasterkamp and A. C. Newby (2007). "Genomics of foam cells and nonfoamy macrophages from rabbits identifies arginase-I as a differential regulator of nitric oxide production." *Arterioscler Thromb Vasc Biol* **27**(3): 571-7.

Thukkani, A. K., J. McHowat, F. F. Hsu, M. L. Brennan, S. L. Hazen and D. A. Ford (2003). "Identification of alpha-chloro fatty aldehydes and unsaturated lysophosphatidylcholine molecular species in human atherosclerotic lesions." *Circulation* **108**(25): 3128-33.

Thygesen, K., J. S. Alpert and H. D. White (2007). "Universal definition of myocardial infarction." *Eur Heart J* **28**(20): 2525-38.

Tinkov, S., R. Bekeredjian, G. Winter and C. Coester (2008). "Microbubbles as ultrasound triggered drug carriers." *J Pharm Sci*.

Tobias, P. S., K. Soldau, L. Kline, J. D. Lee, K. Kato, T. P. Martin and R. J. Ulevitch (1993). "Cross-linking of lipopolysaccharide (LPS) to CD14 on THP-1 cells mediated by LPS-binding protein." *J Immunol* **150**(7): 3011-21.

Tomasi, G., P. Edison, A. Bertoldo, F. Roncaroli, P. Singh, A. Gerhard, C. Cobelli, D. J. Brooks and F. E. Turkheimer (2008). "Novel reference region model reveals increased microglial and reduced vascular binding of 11C-(R)-PK11195 in patients with Alzheimer's disease." *J Nucl Med* **49**(8): 1249-56.

Tontonoz, P., L. Nagy, J. G. Alvarez, V. A. Thomazy and R. M. Evans (1998). "PPARgamma promotes monocyte/macrophage differentiation and uptake of oxidized LDL." *Cell* **93**(2): 241-52.

Topol, E. J. and S. E. Nissen (1995). "Our preoccupation with coronary luminology. The dissociation between clinical and angiographic findings in ischemic heart disease." *Circulation* **92**(8): 2333-42.

Trim, P. J., S. J. Atkinson, A. P. Princivalle, P. S. Marshall, A. West and M. R. Clench (2008a). "Matrix-assisted laser desorption/ionisation mass spectrometry imaging of lipids in rat brain tissue with integrated unsupervised and supervised multivariant statistical analysis." *Rapid Commun Mass Spectrom* **22**(10): 1503-9.

Trim, P. J., M. C. Djidja, S. J. Atkinson, K. Oakes, L. M. Cole, D. M. Anderson, P. J. Hart, S. Francese and M. R. Clench (2010). "Introduction of a 20 kHz Nd:YVO4 laser into a hybrid quadrupole time-of-flight mass spectrometer for MALDI-MS imaging." *Anal Bioanal Chem* **397**(8): 3409-19.

Trim, P. J., C. M. Henson, J. L. Avery, A. McEwen, M. F. Snel, E. Claude, P. S. Marshall, A. West, A. P. Princivalle and M. R. Clench (2008b). "Matrix-assisted laser desorption/ionization-ion mobility separation-mass spectrometry imaging of vinblastine in whole body tissue sections." *Anal Chem* **80**(22): 8628-34.

Trivedi, R., U. K.-I. J and J. Gillard (2003). "Accumulation of ultrasmall superparamagnetic particles of iron oxide in human atherosclerotic plaque." *Circulation* **108**(19): e140; author reply e140.

Tsutsui, J. M., P. A. Grayburn, F. Xie and T. R. Porter (2004a). "Drug and gene delivery and enhancement of thrombolysis using ultrasound and microbubbles." *Cardiol Clin* **22**(2): 299-312, vii.

Tsutsui, J. M., F. Xie, M. Cano, J. Chomas, P. Phillips, S. J. Radio, J. Lof and T. R. Porter (2004b). "Detection of retained microbubbles in carotid arteries with real-time low mechanical index imaging in the setting of endothelial dysfunction." *J Am Coll Cardiol* **44**(5): 1036-46.

Tsutsui, J. M., F. Xie and R. T. Porter (2004c). "The use of microbubbles to target drug delivery." *Cardiovasc Ultrasound* **2**: 23.

Tureyen, K., R. Vemuganti, M. S. Salamat and R. J. Dempsey (2006). "Increased angiogenesis and angiogenic gene expression in carotid artery plaques from symptomatic stroke patients." *Neurosurgery* **58**(5): 971-7; discussion 971-7.

Unanue, E. R., D. I. Beller, J. Calderon, J. M. Kiely and M. J. Stadecker (1976). "Regulation of immunity and inflammation by mediators from macrophages." *Am J Pathol* **85**(2): 465-78.

Upston, J. M., X. Niu, A. J. Brown, R. Mashima, H. Wang, R. Senthilmohan, A. J. Kettle, R. T. Dean and R. Stocker (2002). "Disease stage-dependent accumulation of lipid and protein oxidation products in human atherosclerosis." *Am J Pathol* **160**(2): 701-10.

Urbanski, P. P., A. Lenos, J. C. Blume, V. Ziegler, B. Griewing, R. Schmitt, A. Diegeler and M. Dinkel (2008). "Does anatomical completeness of the circle of Willis correlate with sufficient cross-perfusion during unilateral cerebral perfusion?" *Eur J Cardiothorac Surg* **33**(3): 402-8.

van der Wal, A. C., A. E. Becker, C. M. van der Loos and P. K. Das (1994). "Site of intimal rupture or erosion of thrombosed coronary atherosclerotic plaques is characterized by an inflammatory process irrespective of the dominant plaque morphology." *Circulation* **89**(1): 36-44.

Van Ginderachter, J. A., K. Movahedi, G. Hassanzadeh Ghassabeh, S. Meerschaut, A. Beschin, G. Raes and P. De Baetselier (2006). "Classical and alternative activation of mononuclear phagocytes: picking the best of both worlds for tumor promotion." *Immunobiology* **211**(6-8): 487-501.

van Swieten, J. C., P. J. Koudstaal, M. C. Visser, H. J. Schouten and J. van Gijn (1988). "Interobserver agreement for the assessment of handicap in stroke patients." *Stroke* **19**(5): 604-7.

Varki, A. (2008). "Sialic acids in human health and disease." *Trends Mol Med* **14**(8): 351-60.

Veenman, L. and M. Gavish (2006). "The peripheral-type benzodiazepine receptor and the cardiovascular system. Implications for drug development." *Pharmacol Ther* **110**(3): 503-24.

Versteeg, D., I. E. Hoefer, A. H. Schoneveld, D. P. V. De Kleijn, E. Busser, C. Strijder, M. Emons, P. R. Stella, P. A. Doevendans and G. Pasterkamp (2008). "Monocyte toll-like receptor 2 and 4 responses and expression following percutaneous coronary intervention: association with lesion stenosis and fractional flow reserve." *Heart* **94**(6): 770-776.

Vicenzini, E., M. F. Giannoni, F. Benedetti-Valentini and G. L. Lenzi (2009). "Imaging of carotid plaque angiogenesis." *Cerebrovasc Dis* **27 Suppl 2**: 48-54.

Vicenzini, E., M. F. Giannoni, F. Puccinelli, M. C. Ricciardi, M. Altieri, V. Di Piero, B. Gossetti, F. B. Valentini and G. L. Lenzi (2007). "Detection of carotid adventitial vasa vasorum and plaque vascularization with ultrasound cadence contrast pulse sequencing technique and echo-contrast agent." *Stroke* **38**(10): 2841-3.

Villanueva, F. S., E. Lu, S. Bowry, S. Kilic, E. Tom, J. Wang, J. Gretton, J. J. Pacella and W. R. Wagner (2007). "Myocardial ischemic memory imaging with molecular echocardiography." *Circulation* **115**(3): 345-52.

Villarraga, H. R., D. A. Foley, B. C. Aeschbacher, K. W. Klarich and S. L. Mulvagh (1997). "Destruction of contrast microbubbles during ultrasound imaging at conventional power output." *J Am Soc Echocardiogr* **10**(8): 783-91.

Vink, A., A. H. Schoneveld, J. J. van der Meer, B. J. van Middelaar, J. P. Sluijter, M. B. Smeets, P. H. Quax, S. K. Lim, C. Borst, G. Pasterkamp and D. P. de Kleijn (2002). "In vivo evidence for a role of toll-like receptor 4 in the development of intimal lesions." *Circulation* **106**(15): 1985-90.

Virmani, R., A. P. Burke, A. Farb and F. D. Kolodgie (2006). "Pathology of the vulnerable plaque." *J Am Coll Cardiol* **47**(8 Suppl): C13-8.

Virmani, R., A. P. Burke, F. D. Kolodgie and A. Farb (2003). "Pathology of the thin-cap fibroatheroma: a type of vulnerable plaque." *J Interv Cardiol* **16**(3): 267-72.

Virmani, R., F. D. Kolodgie, A. P. Burke, A. Farb and S. M. Schwartz (2000). "Lessons from sudden coronary death: a comprehensive morphological classification scheme for atherosclerotic lesions." *Arterioscler Thromb Vasc Biol* **20**(5): 1262-75.

Virmani, R., F. D. Kolodgie, A. P. Burke, A. V. Finn, H. K. Gold, T. N. Tulenko, S. P. Wrenn and J. Narula (2005). "Atherosclerotic plaque progression and vulnerability to rupture: angiogenesis as a source of intraplaque hemorrhage." *Arterioscler Thromb Vasc Biol* **25**(10): 2054-61.

Waanders, L. F., R. Almeida, S. Prosser, J. Cox, D. Eikel, M. H. Allen, G. A. Schultz and M. Mann (2008). "A novel chromatographic method allows on-line reanalysis of the proteome." *Mol Cell Proteomics* **7**(8): 1452-9.

Wade, D. T. and C. Collin (1988). "The Barthel ADL Index: a standard measure of physical disability?" *Int Disabil Stud* **10**(2): 64-7.

Waldo, S. W., Y. Li, C. Buono, B. Zhao, E. M. Billings, J. Chang and H. S. Kruth (2008). "Heterogeneity of human macrophages in culture and in atherosclerotic plaques." *Am J Pathol* **172**(4): 1112-26.

Walker, K. W., G. A. Pantely and D. J. Sahn (1997). "Ultrasound-mediated destruction of contrast agents. Effect of ultrasound intensity, exposure, and frequency." *Invest Radiol* **32**(12): 728-34.

Walton, K. A., A. L. Cole, M. Yeh, G. Subbanagounder, S. R. Krutzik, R. L. Modlin, R. M. Lucas, J. Nakai, E. J. Smart, D. K. Vora and J. A. Berliner (2003a). "Specific phospholipid oxidation products inhibit ligand activation of toll-like receptors 4 and 2." *Arterioscler Thromb Vasc Biol* **23**(7): 1197-203.

Walton, K. A., X. Hsieh, N. Gharavi, S. Wang, G. Wang, M. Yeh, A. L. Cole and J. A. Berliner (2003b). "Receptors involved in the oxidized 1-palmitoyl-2-arachidonoyl-sn-glycero-3-phosphorylcholine-mediated synthesis of interleukin-8. A role for Toll-like receptor 4 and a glycosylphosphatidylinositol-anchored protein." *J Biol Chem* **278**(32): 29661-6.

Wang, S., M. Miura, Y. K. Jung, H. Zhu, E. Li and J. Yuan (1998). "Murine caspase-11, an ICE-interacting protease, is essential for the activation of ICE." *Cell* **92**(4): 501-9.

Wang, T. J., P. Gona, M. G. Larson, G. H. Tofler, D. Levy, C. Newton-Cheh, P. F. Jacques, N. Rifai, J. Selhub, S. J. Robins, E. J. Benjamin, R. B. D'Agostino and R. S. Vasan (2006). "Multiple biomarkers for the prediction of first major cardiovascular events and death." *N Engl J Med* **355**(25): 2631-9.

Want, E. J., I. D. Wilson, H. Gika, G. Theodoridis, R. S. Plumb, J. Shockcor, E. Holmes and J. K. Nicholson (2010). "Global metabolic profiling procedures for urine using UPLC-MS." *Nat Protoc* **5**(6): 1005-18.

Ware, J. H. (2006). "The limitations of risk factors as prognostic tools." *N Engl J Med* **355**(25): 2615-7.

Watters, T. M., E. F. Kenny and L. A. O'Neill (2007). "Structure, function and regulation of the Toll/IL-1 receptor adaptor proteins." *Immunol Cell Biol* **85**(6): 411-9.

Weber, C., K. U. Belge, P. von Hundelshausen, G. Draude, B. Steppich, M. Mack, M. Frankenberger, K. S. Weber and H. W. Ziegler-Heitbrock (2000). "Differential chemokine receptor expression and function in human monocyte subpopulations." *J Leukoc Biol* **67**(5): 699-704.

Weber, C., A. Zernecke and P. Libby (2008). "The multifaceted contributions of leukocyte subsets to atherosclerosis: lessons from mouse models." *Nat Rev Immunol* **8**(10): 802-15.

Welgus, H. G., E. J. Campbell, J. D. Cury, A. Z. Eisen, R. M. Senior, S. M. Wilhelm and G. I. Goldberg (1990). "Neutral metalloproteinases produced by human mononuclear phagocytes. Enzyme profile, regulation, and expression during cellular development." *J Clin Invest* **86**(5): 1496-502.

WHO (2009). Global Burden of Disease Study Operations Manual, Harvard University, University of Washington, Johns Hopkins University, University of Queensland, World Health Organization.

Wildgruber, M., H. Lee, A. Chudnovskiy, T. J. Yoon, M. Etzrodt, M. J. Pittet, M. Nahrendorf, K. Croce, P. Libby, R. Weissleder and F. K. Swirski (2009). "Monocyte subset dynamics in human atherosclerosis can be profiled with magnetic nano-sensors." *PLoS One* **4**(5): e5663.

Williams, K. J. and I. Tabas (1995). "The response-to-retention hypothesis of early atherogenesis." *Arterioscler Thromb Vasc Biol* **15**(5): 551-61.

Wilson, P. W. (2004). "CDC/AHA Workshop on Markers of Inflammation and Cardiovascular Disease: Application to Clinical and Public Health Practice: ability of inflammatory markers to predict disease in asymptomatic patients: a background paper." *Circulation* **110**(25): e568-71.

Wilson, S. R., P. N. Burns, D. Muradali, J. A. Wilson and X. Lai (2000). "Harmonic hepatic US with microbubble contrast agent: initial experience showing improved characterization of hemangioma, hepatocellular carcinoma, and metastasis." *Radiology* **215**(1): 153-61.

Wilson, S. R., L. D. Greenbaum and B. B. Goldberg (2009). "Contrast-enhanced ultrasound: what is the evidence and what are the obstacles?" *AJR Am J Roentgenol* **193**(1): 55-60.

Witting, P., K. Pettersson, A. M. Ostlund-Lindqvist, C. Westerlund, M. Wagberg and R. Stocker (1999). "Dissociation of atherogenesis from aortic accumulation of lipid

hydro(pero)xides in Watanabe heritable hyperlipidemic rabbits." *J Clin Invest* **104**(2): 213-20.

Wright, S. D., R. A. Ramos, P. S. Tobias, R. J. Ulevitch and J. C. Mathison (1990). "CD14, a receptor for complexes of lipopolysaccharide (LPS) and LPS binding protein." *Science* **249**(4975): 1431-3.

Xie, J. J., J. Wang, T. T. Tang, J. Chen, X. L. Gao, J. Yuan, Z. H. Zhou, M. Y. Liao, R. Yao, X. Yu, D. Wang, Y. Cheng, Y. H. Liao and X. Cheng (2010). "The Th17/Treg functional imbalance during atherogenesis in ApoE(-/-) mice." *Cytokine* **49**(2): 185-93.

Xiong, L., Y. B. Deng, Y. Zhu, Y. N. Liu and X. J. Bi (2009). "Correlation of carotid plaque neovascularization detected by using contrast-enhanced US with clinical symptoms." *Radiology* **251**(2): 583-9.

Xu, X. H., P. K. Shah, E. Faure, O. Equils, L. Thomas, M. C. Fishbein, D. Luthringer, X. P. Xu, T. B. Rajavashisth, J. Yano, S. Kaul and M. Arditi (2001). "Toll-like receptor-4 is expressed by macrophages in murine and human lipid-rich atherosclerotic plaques and upregulated by oxidized LDL." *Circulation* **104**(25): 3103-8.

Yajima, N., M. Takahashi, H. Morimoto, Y. Shiba, Y. Takahashi, J. Masumoto, H. Ise, J. Sagara, J. Nakayama, S. Taniguchi and U. Ikeda (2008). "Critical role of bone marrow apoptosis-associated speck-like protein, an inflammasome adaptor molecule, in neointimal formation after vascular injury in mice." *Circulation* **117**(24): 3079-87.

Yan, Z. Q. and G. K. Hansson (2007). "Innate immunity, macrophage activation, and atherosclerosis." *Immunol Rev* **219**: 187-203.

Yanagisawa, K., F. Moriyasu, T. Miyahara, M. Yuki and H. Iijima (2007). "Phagocytosis of ultrasound contrast agent microbubbles by Kupffer cells." *Ultrasound Med Biol* **33**(2): 318-25.

Yeung, D. C., Y. Wang, A. Xu, S. C. Cheung, N. M. Wat, D. Y. Fong, C. H. Fong, M. T. Chau, P. C. Sham and K. S. Lam (2008). "Epidermal fatty-acid-binding protein: a new circulating biomarker associated with cardio-metabolic risk factors and carotid atherosclerosis." *Eur Heart J* **29**(17): 2156-63.

Yeung, D. C., A. Xu, A. W. Tso, W. S. Chow, N. M. Wat, C. H. Fong, S. Tam, P. C. Sham and K. S. Lam (2009). "Circulating levels of adipocyte and epidermal fatty acid-binding proteins in relation to nephropathy staging and macrovascular complications in type 2 diabetic patients." *Diabetes Care* **32**(1): 132-4.

Yona, S. and S. Jung (2010). "Monocytes: subsets, origins, fates and functions." *Curr Opin Hematol* **17**(1): 53-9.

Yoshida, J., K. Ohmori, H. Takeuchi, K. Shinomiya, T. Namba, I. Kondo, H. Kiyomoto and M. Kohno (2005). "Treatment of ischemic limbs based on local recruitment of vascular endothelial growth factor-producing inflammatory cells with ultrasonic microbubble destruction." *J Am Coll Cardiol* **46**(5): 899-905.

You, S. A., S. R. Archacki, G. Angheloiu, C. S. Moravec, S. Rao, M. Kinter, E. J. Topol and Q. Wang (2003). "Proteomic approach to coronary atherosclerosis shows ferritin light chain as a significant marker: evidence consistent with iron hypothesis in atherosclerosis." *Physiol Genomics* **13**(1): 25-30.

Yunoki, K., T. Naruko, R. Komatsu, S. Ehara, N. Shirai, K. Sugioka, M. Nakagawa, C. Kitabayashi, Y. Ikura, A. Itoh, K. Kusano, T. Ohe, K. Haze, A. E. Becker and M. Ueda (2009). "Enhanced expression of haemoglobin scavenger receptor in accumulated macrophages of culprit lesions in acute coronary syndromes." *Eur Heart J* **30**(15): 1844-52.

Zavala, F., J. Haumont and M. Lenfant (1984). "Interaction of benzodiazepines with mouse macrophages." *Eur J Pharmacol* **106**(3): 561-6.

Zempo, N., R. D. Kenagy, Y. P. Au, M. Bendeck, M. M. Clowes, M. A. Reidy and A. W. Clowes (1994). "Matrix metalloproteinases of vascular wall cells are increased in balloon-injured rat carotid artery." *J Vasc Surg* **20**(2): 209-17.

Zernecke, A., E. A. Liehn, J. L. Gao, W. A. Kuziel, P. M. Murphy and C. Weber (2006). "Deficiency in CCR5 but not CCR1 protects against neointima formation in atherosclerosis-prone mice: involvement of IL-10." *Blood* **107**(11): 4240-3.

Zernecke, A. and C. Weber (2010). "Chemokines in the vascular inflammatory response of atherosclerosis." *Cardiovasc Res* **86**(2): 192-201.

Zhu, S. N., M. Chen, J. Jongstra-Bilen and M. I. Cybulsky (2009). "GM-CSF regulates intimal cell proliferation in nascent atherosclerotic lesions." *J Exp Med* **206**(10): 2141-9.

Zhuang, Y., F. Ma, J. Li-Ling, X. Xu and Y. Li (2003). "Comparative analysis of amino acid usage and protein length distribution between alternatively and non-alternatively spliced genes across six eukaryotic genomes." *Mol Biol Evol* **20**(12): 1978-85.

Ziegler-Heitbrock, H. W., G. Fingerle, M. Strobel, W. Schraut, F. Stelter, C. Schutt, B. Passlick and A. Pforte (1993). "The novel subset of CD14+/CD16+ blood monocytes exhibits features of tissue macrophages." *Eur J Immunol* **23**(9): 2053-8.

Ziegler-Heitbrock, L. (2007). "The CD14+ CD16+ blood monocytes: their role in infection and inflammation." *J Leukoc Biol* **81**(3): 584-92.

APPENDICES

APPENDIX 1 GRANTS, FELLOWSHIPS, PUBLICATIONS AND PRESENTATIONS

Research Fellowships and Grants

2008: Circulation Foundation Mary Davies Research Fellowship
Graham-Dixon Charitable Trust Research Grant (co-investigator)
European Society for Vascular Surgery Congress Travel Grant

2009: Stroke Association Grant (co-investigator)
Royal College of Surgeons of England / Rosetrees Trust Research Fellowship
Graham-Dixon Charitable Trust Research Grant
Peel Medical Research Trust

2010: Circulation Foundation Mary Davies Research Fellowship (co-investigator)
Graham-Dixon Charitable Trust Research Grant
European Society for Vascular Surgery Japan Congress Travel Grant

2011: Graham-Dixon Charitable Trust Research Grant (co-investigator)

Awards and Prizes

2008: Best Overall Scientific Presentation, Imperial College Surgical Symposium

2009: Glaxo Travelling Fellowship, Surgery Section, The Royal Society of Medicine
Best Overall Scientific Presentation, Imperial College Surgical Symposium

2010: MIA Prize, Surgery Section, The Royal Society of Medicine
Best Presentation, Winter Meeting, Surgery Section, The Royal Society of Medicine (co-author)

2011: Graham-Dixon Prize for Surgery

Related Journal Publications

Dholakia S, Shalhoub J, Ellis M, Davies AH
Letter to the Editor: An urgent access neurovascular clinic
Clinical Medicine 2009;**9(6)**:631

Lim CS, Shalhoub J, Gohel MS, Shepherd AC, Davies AH
Matrix Metalloproteinases in Vascular Disease – A Potential Therapeutic Target?
Current Vascular Pharmacology 2010;**8(1)**:75-85

Pugliese F, Gaemperli O, Kinderlerer AR, Lamare F, Shalhoub J, Davies AH, Rimoldi OE, Mason JC, Camici PG
Imaging of Vascular Inflammation With [(11)C]-PK11195 and Positron Emission Tomography/Computed Tomography Angiography
Journal of the American College of Cardiology 2010;**56(8)**:653-661

Lane TR, Shalhoub J, Perera R, Mehta A, Ellis MR, Sandison A, Davies AH Franklin IJ
Diagnosis and Surgical Management of Free Floating Thrombus Within the Carotid Artery
Vascular and Endovascular Surgery 2010;**44(7)**:586-593

Maruthappu M, Shalhoub J, Thapar A, Jayasooriya G, Franklin I, Davies AH
The Patients' Perspective of Carotid Endarterectomy
Vascular and Endovascular Surgery 2010;**44(7)**:529-534

Owen DR, Shalhoub J, Miller S, Gauthier T, Doryforou O, Davies AH, Leen EL
Inflammation within carotid atherosclerotic plaque: assessment with late-phase contrast-enhanced US
Radiology 2010;**255(2)**:638-644

Abdul-Salam VB, Ramrakha P, Krishnan U, Owen DR, Shalhoub J, Davies AH, Tang TY, Gillard JH, Boyle JJ, Wilkins MR, Edwards RJ
Identification and Assessment of Plasma Lysozyme as a Putative Biomarker of Atherosclerosis
Arteriosclerosis, Thrombosis, and Vascular Biology 2010;**30(5)**:1027-1033

Shalhoub J, Owen DRJ, Gauthier T, Monaco C, Leen ELS, Davies AH
The use of Contrast Enhanced Ultrasound in Carotid Arterial Disease
European Journal of Vascular and Endovascular Surgery 2010;**39(4)**:381-387

Miller S, Owen DR, Shalhoub J, Davies AH, Leen EL
Late-Phase Contrast-enhanced US to Assess Unstable Carotid Atherosclerotic Plaques
Radiology 2010;**257(2)**:589

Davies AH, Franklin IJ, Shalhoub J, Thapar A
Refining selection for revascularisation in asymptomatic carotid stenosis is the key. Rapid Response to: Is there a role for revascularisation in asymptomatic carotid stenosis? No
British Medical Journal 2010

Shalhoub J, Falck-Hansen MA, Davies AH, Monaco C
Innate Immunity and Monocyte-Macrophage Activation in Atherosclerosis
Journal of Inflammation 2011;**8(1)**:9

Stegemann C, Drozdov I, Shalhoub J, Humphries J, Ladroue C, Didangelos A, Baumert M, Allen M, Davies AH, Monaco C, Smith A, Xu Q, Mayr M
Comparative Lipidomics Profiling of Human Atherosclerotic Plaques
Circulation Cardiovascular Genetics 2011;**110**

Jayasooriya GS, Shalhoub J, Thapar A, Davies AH – *shared first authorship*
Patient preference survey in the management of asymptomatic carotid stenosis
Journal of Vascular Surgery 2011;**53(6)**:1466-1472

Bouri S, Thapar A, Shalhoub J, Jayasooriya G, Fernando A, Franklin IJ, Davies AH
Hypertension and the Post-carotid Endarterectomy Cerebral Hyperperfusion Syndrome
European Journal of Vascular and Endovascular Surgery 2011;**41(2)**:229-237

Malik Z, Shalhoub J, Hettige R, Davies AH
The Role of Endarterectomy and Stenting in the Management of Carotid Artery Stenosis: A 5-Year Delphi Survey
Vascular and Endovascular Surgery 2011;**45(1)**:15-21

Kasivisvanathan V, Shalhoub J, Lim CS, Shepherd AC, Thapar A, Davies AH
Hypoxia-Inducible Factor-1 in Arterial Disease: A Putative Therapeutic Target
Current Vascular Pharmacology 2011;**9(3)**:333-349

Jayasooriya GS, Thapar A, Shalhoub J, Davies AH
Silent Cerebral Events in Asymptomatic Carotid Stenosis
Journal of Vascular Surgery 2011;**54(1)**

Newbould RD, Owen DRJ, Shalhoub J, Brown AP, Gambarota G

Motion Sensitized Driven Equilibrium for Blood-Suppressed T2* Mapping
Manuscript accepted for publication by *Journal of Magnetic Resonance Imaging*

Shalhoub J, Monaco C, Owen DRJ, Gauthier T, Thapar A, Leen ELS, Davies AH
Late-Phase Contrast Enhanced Ultrasound Reflects Biological Features of Instability in Human Carotid Atherosclerosis
Second revision of manuscript under review by *Stroke*

Related Published Book Chapters

Shalhoub J, Davies AH
Identification of 'high-risk' carotid stenosis
Vascular and Endovascular Surgery Highlights 2009-10. Ed: Davies AH. Health Press (2010)

Shalhoub J, Owen DRJ, Leen ELS
Early evaluation by DCE-US of carotid inflammatory disease
In press: Systemic Vasculitis. Imaging Features
Eds. Hendaoui L, Stanson AW, Bouhaouala MH, Joffre F. Springer (2011)

Related Published Abstracts

Shalhoub J, Cross A, Allin D, Davies AH, Monaco C
Intra-plaque production of M1-type cytokines and matrix metalloproteinases differentiate stable from unstable carotid atherosclerosis
Atherosclerosis 2010;**213(1)**:e17-18

Gaemperli O, Shalhoub J, Owen D, Lamare F, Rimoldi OE, Davies AH, Camici PG
Imaging intraplaque inflammation in carotid atherosclerosis with 11C-PK11195 PET/CT
Circulation 2010;**122(21)** Suppl A12561

Stegemann C, Shalhoub J, Humphries J, Ladroue C, Davies AH , Monaco C, Smith A, Xu Q, Mayr M
Comparative lipidomic profiling of human atherosclerotic plaques
Circulation 2010;**122(21)** Suppl A20523

Gaemperli O, Shalhoub J, Owen D, Lamare F, Rimoldi OE, Davies AH, Camici PG
Imaging intraplaque inflammation in carotid atherosclerosis with 11C-PK11195 PET/CT
European Heart Journal 2010;**31** Suppl 1 Sep P2738:451

Shalhoub J, Cross A, Allin D, Essex D, Davies AH, Monaco C
Cytokine profiling in culture reveals a predominance of M1 macrophage polarisation in symptomatic carotid plaques
Heart 2010;**96(17)**:e23

Stegemann C, Shalhoub J, Jenkins J, Davies AH, Ladroue C, Monaco C, Smith A, Xu Q, Mayr M
Lipidomic profiling of human atherosclerotic plaques
Heart 2010;**96(17)**:e16

Shalhoub J, Owen DRJ, Monaco C, Leen ELS, Davies AH
Molecular Characterisation of Inflammation in Human Carotid Atherosclerosis by Multi-Analyte Profiling and Non-Invasive Imaging with Late-Phase Contrast Enhanced Ultrasound
Japanese Journal of Vascular Surgery 2010;**19(2)**:482

Shalhoub J, Owen DRJ, Monaco C, Leen ELS, Davies AH
Late phase contrast enhanced ultrasound identifies inflammation within human carotid atherosclerotic plaques
Annals of the Royal College of Surgeons of England 2010;**92(2)**:W1-2

Shalhoub J, Owen D, Miller S, Gauthier T, Doryforou O, Franklin I, Leen E, Davies A
Novel late-phase contrast-enhanced ultrasound to assess atherosclerotic plaques in humans
British Journal of Surgery 2010;**97** (S1):4

Lane TRA, Shalhoub J, Perera R, Mehta A, Ellis MR, Sandison A, Davies AH Franklin IJ
Diagnosis and surgical management of free-floating thrombus within the carotid artery
International Journal of Surgery 2010;**8(7)**:558

Malik Z, Shalhoub J, Hettige R, Davies AH
The role of endarterectomy and stenting in the management of carotid artery stenosis: a 5 year Delphi survey
International Journal of Surgery 2010;**8(7)**:541

Shalhoub J, Cross A, Allin DM, Franklin IJ, Monaco C Davies AH
Multi-analyte profiling and pathway analysis reveals a predominance of pro-inflammatory M1-type macrophage polarisation and evidence of IL17/Th17 signalling in symptomatic human carotid atherosclerosis

British Journal of Surgery 2011;**98** (S2):2

Shalhoub J, Gaemperli O, Owen DRG, Lamare F, Rimoldi OE, Camici PG, Davies AH
Imaging intraplaque inflammation in carotid atherosclerosis with 11C-PK11195 PET/CT
British Journal of Surgery 2011;**98** (S2):33

Shalhoub J, Cross A, Allin DM, Franklin IJ, Monaco C, Davies AH
Intra-plaque production of M1-type cytokines and matrix metalloproteinases differentiate stable from unstable carotid atherosclerosis
British Journal of Surgery 2011;**98** (S1):3

Related Research Presentations

Sritharan K, Navin T, Essex D, Shalhoub J, Monaco C, Davies AH
Matrix Metalloproteinases and Inflammation: plausible mediators of plaque instability & symptoms in carotid atherosclerotic disease

- Scientific poster, European Society for Vascular Surgery, Nice, France, September 2008

Monaco C, Gregan S, Navin T, Shalhoub J, Durante A, Franklin IJ, Foxwell B, Feldmann M, Davies AH
The key Toll-like receptor / Intereukin-1 signalling adaptor MyD88 regulates inflammatory mediators production in human atherosclerosis

- Scientific poster, European Society for Vascular Surgery, Nice, France, September 2008
- Oral presentation, Imperial College Surgical Symposium, London, October 2008 – *presented by myself and winner of best overall scientific presentation*

Shalhoub J, Monaco C, Davies AH
Carotid Research. Multi-Factorial Risk Stratification in Atherosclerotic Carotid Artery Stenosis

- Oral presentation, Royal Society of Medicine, Surgery Section, Winter Meeting, Tignes, France, January 2009

Shalhoub J, Owen DRJ, Miller S, Gauthier T, Doryforou O, Franklin IJF, Monaco C, Leen ELS, Davies AH

Novel Late Phase Contrast Enhanced Ultrasound to Assess Inflammation within the Carotid Atherosclerotic Plaque in Humans

- Oral presentation, Imperial College Surgical Symposium, London, September 2009 – *winner of best overall scientific presentation*
- Oral presentation, The Vascular Society of Great Britain and Ireland, Liverpool, November 2009 – *presented in the British Journal of Surgery Prize Session*
- Oral presentation, Royal Society of Medicine, London, December 2009 – *presented in the Norman Tanner Prize Session, runner up and winner of the Glaxo Travelling Fellowship*

Owen DRJ, Shalhoub J, Miller S, Gauthier T, Davies AH, Leen ELS

The Use of Contrast-enhanced Ultrasound to Detect Inflammation within the Carotid Atherosclerotic Plaque in Humans

- Oral presentation, Radiological Society of North America, Chicago, USA, December 2009
- Scientific poster, Medical Research Society, Royal College of Physicians, London, February 2010
- Oral presentation, European Congress of Radiology, Vienna, Austria, March 2010

Kasivisvanathan V, Shalhoub J, Lim CS, Shepherd AC, Davies AH

A Systematic Review: The Role of Hypoxia-Inducible Factor-1α in Arterial Disease

- Oral presentation, Royal Society of Medicine, Surgery Section, Winter Meeting, Tignes, France, January 2010 – *winner of best presentation*
- Poster presentation, Association of Surgeons in Training, Kingston upon Hull, March 2010

Shalhoub J, Cross A, Davies AH, Monaco C

Cytokine Profiling in Clinically Characterised Carotid Atherosclerosis

- Oral presentation, Innate Immune Signalling in Atherosclerosis (IMMUNATH), London, March 2010

Owen DR, Shalhoub J, Miller S, Gauthier T, Thapar A, Davies A, Leen E

Contrast enhanced ultrasound to quantify carotid intraplaque angiogensis: Reproducibility

- Oral presentation, European Congress of Radiology, Vienna, Austria, March 2010

Lane TRA, Shalhoub J, Perera R, Mehta A, Ellis MR, Sandison A, Davies AH Franklin IJ

Diagnosis and surgical management of free-floating thrombus within the carotid artery

- Poster presentation, Association of Surgeons in Training, Kingston upon Hull, March 2010

Malik Z, Shalhoub J, Hettige R, Davies AH

The role of endarterectomy and stenting in the management of carotid artery stenosis: a 5 year Delphi survey

- Poster presentation, Association of Surgeons in Training, Kingston upon Hull, March 2010
- Poster presentation, Student Research and Communication Conference, London, November 2010

Shalhoub J, Owen DRJ, Monaco C, Leen ELS, Davies AH

Molecular Characterisation of Inflammation in Human Carotid Atherosclerosis by Multi-Analyte Profiling and Non-Invasive Imaging with Late-Phase Contrast Enhanced Ultrasound.

- Poster presentation, 38th Annual Meeting of Japanese Society for Vascular Surgery, Omiya, Saitama, Japan, May 2010 – *Awarded European Society for Vascular Surgery Japan Congress Travel Grant*

Shalhoub J

Contrast ultrasound of the unstable plaque

- Oral presentation, British Heart Foundation Centre of Research Excellence Symposium, Vascular Biology and Arterial Inflammation, Imperial College London, June 2010

Shalhoub J, Cross A, Allin DM, Essex D, Davies AH, Monaco C

Cytokine Profiling in Culture Reveals a Predominance of M1 Macrophage Polarisation in Symptomatic Carotid Plaques

- Poster presentation, British Atherosclerosis Society/British Society for Cardiovascular Research/British Cardiovascular Society, Manchester, June 2010
- Poster presentation, British Heart Foundation Centre of Research Excellence Symposium, Vascular Biology and Arterial Inflammation, Imperial College London, June 2010
- Poster presentation, British Atherosclerosis Society, Oxford, September 2010

Stegemann C, Shalhoub J, Jenkins J, Davies AH, Ladroue C, Monaco C, Smith A, Xu Q,

Mayr M

Lipidomic Profiling of Human Atherosclerotic Plaques

- Poster presentation, British Atherosclerosis Society/British Society for Cardiovascular Research/British Cardiovascular Society, Manchester, June 2010
- Oral presentation, American Heart Association, Chicago, November 2010
- Poster presentation, London Vascular Biology Forum, London, December 2010

Gaemperli O, Shalhoub J, Owen D, Lamare F, Rimoldi OE, Davies AH, Camici PG

Imaging intraplaque inflammation in carotid atherosclerosis with ^{11}C-PK11195 PET/CT

- Poster presentation, European Society of Cardiology, Stockholm, Sweden, August 2010
- Oral presentation, American Heart Association, Chicago, November 2010

Shalhoub J

Microbubble Imaging of the Carotid Plaque

- Oral presentation, Molecular and Functional Imaging in Clinical Practice, British Institute of Radiology, London, October 2010

Shalhoub J

Towards Predicting Stroke

- Oral presentation, Surgical Futures, Royal College of Surgeons of England, London, October 2010 – http://www.rcseng.ac.uk/museums/events/audio-video-and-transcripts
- Oral presentation on behalf of the Royal College of Surgeons of England, Chichester Science Group, Sussex, March 2011 – *personal letter of thanks from Mr John Black PRCS (Eng)*

Shalhoub J, Cross A, Allin DM, Franklin IJ, Monaco C, Davies AH

Intra-plaque production of M1-type cytokines and matrix metalloproteinases differentiate stable from unstable carotid atherosclerosis

- Oral presentation, The Vascular Society of Great Britain and Ireland, Brighton, November 2010 – *presented in the Society of Academic and Research Surgery Session*

Davies AH, Shalhoub J, Thapar A, Owen DRJ, Leen ELS

Contrast Enhanced Ultrasound To Identify Asymptomatic Carotid Plaques At Risk For Causing A Stroke

- Oral presentation, 37th Veith Symposium, New York, November 2010

Jayasooriya G, Shalhoub J, Thapar A, Davies AH

Patient preference in the management of asymptomatic carotid stenosis

- Poster presentation, The Vascular Society of Great Britain and Ireland, Brighton, November 2010
- Poster presentation, Association of Surgeons in Training, Sheffield, April 2011

Maruthappu M, Shalhoub J, Thapar A, Jayasooriya G, Franklin I, Davies AH

The Patients' Perspective of Carotid Endarterectomy

- Accepted for poster presentation, Research in Clinical Practice, Oxford, November 2010
- Poster presentation, Association of Surgeons in Training, Sheffield, April 2011
- Poster presentation, Association of Surgeons of Great Britain and Ireland, Bournemouth, May 2011

Thapar A, Owen DRJ, Shalhoub J, Davies AH, Leen ELS

Carotid plaque risk stratification with contrast enhanced ultrasound

- Oral presentation, UK Stroke Forum, Glasgow, December 2010

Shalhoub J, Cross A, Davies AH, Monaco C

Multi-analyte profiling and pathway analysis reveals a predominance of pro-inflammatory M1-type macrophage polarisation and evidence of IL17/Th17 signalling in symptomatic human carotid atherosclerosis

- Oral presentation, Royal Society of Medicine, Surgery Section, London, December 2010 – *winner of the MIA Prize*
- Oral presentation, Imperial College London, Division of Surgery Research Afternoon, London, December 2010
- Oral presentation, Society of Academic and Research Surgery, Dublin, Ireland, January 2011 – *presented in the Patey Prize Session*

Shalhoub J, Gaemperli O, Owen D, Lamare F, Rimoldi OE, Davies AH, Camici PG

Imaging intraplaque inflammation in carotid atherosclerosis with ^{11}C-PK11195 PET/CT for risk stratification in carotid atherosclerosis

- Oral presentation, Royal Society of Medicine, Surgery Section, London, December 2010 – *presented in the Norman Tanner Prize Session*

- Oral presentation, Society of Academic and Research Surgery, Dublin, Ireland, January 2011

Vorkas PA, Shalhoub J, Monaco C, Want EJ, Lewis MR, Davies AH, Holmes E, Nicholson JK

Metabolic Profiling Strategies in Carotid Plaque Tissue

- Poster presentation, Surgical Metabonomics, St Mary's Hospital, London, January 2011

Shalhoub J

The "-Omic" Disciplines in Atherosclerosis Risk Stratification

- Oral presentation, Royal Society of Medicine, Surgery Section, Winter Meeting, Champoluc, Italy, January 2011

Shalhoub J, Monaco C, Owen DRJ, Gauthier T, Thapar A, Leen ELS, Davies AH

Late-Phase Contrast Enhanced Ultrasound Reflects Biological Features of Instability in Human Carotid Atherosclerosis

- Oral presentation, 16th European Symposium on Ultrasound Contrast Imaging, Rotterdam, The Netherlands, January 2011
- Accepted for electronic poster presentation, European Congress of Radiology, Vienna, Austria, March 2011

Shalhoub J, Cross A, Allin DM, Davies AH, Monaco C

Multi-Analyte Profiling in Human Carotid Atherosclerosis Uncovers Signatures of Interferon-γ Priming and Classical Macrophage Polarization in Unstable Plaques

- Poster presentation, AHA Arteriosclerosis, Thrombosis, and Vascular Biology, Chicago, USA, April 2011

Thapar A, Shalhoub J, Owen DRJ, Davies AH, Leen ELS

3D contrast enhanced ultrasound of carotid atherosclerosis

- Poster presentation, Association of Surgeons in Training, Sheffield, April 2011

Bouri S, Thapar A, Shalhoub J, Jayasooriya GS, Fernando A, Franklin IJ, Davies AH

Hypertension and the post-carotid endarterectomy cerebral hyperperfusion syndrome

- Poster presentation, Association of Surgeons in Training, Sheffield, April 2011
- Poster presentation, Association of Surgeons of Great Britain and Ireland,

Bournemouth, May 2011 – *e-Poster of Distinction*

Shalhoub J, Malik Z, Abdul-Salam VB, Edwards R, Davies AH

Investigation of plasma lysozyme as a putative biomarker in carotid atherosclerosis

- Poster presentation, Association of Surgeons in Training, Sheffield, April 2011

Jayasooriya GS, Thapar A, Shalhoub J, Davies AH

Silent cerebral events in asymptomatic carotid stenosis

- Poster presentation, Association of Surgeons in Training, Sheffield, April 2011
- Poster presentation, Association of Surgeons of Great Britain and Ireland, Bournemouth, May 2011

Shalhoub J, Thapar A, Franklin IJ, Jenkins IH, Davies AH

Acute Carotid Endarterectomy After Stroke Thrombolysis Appears Safe but Registry Data is Required

- Poster presentation, Association of Surgeons of Great Britain and Ireland, Bournemouth, May 2011